The manufacture of gas turbine compressor components by Metal Injection Moulding

Andrew D Russell

A thesis submitted in partial fulfilment of the requirements of
Edinburgh Napier University for the award of
Doctor of Philosophy

September 2015

DECLARATION

I hereby declare that the work presented in this thesis was solely carried out by myself at Edinburgh Napier University, Edinburgh, except where acknowledgements are made and that it has not been submitted for any other degree.

Andrew D Russell (Candidate)

September 2015

ABSTRACT

Gas turbine compressor components manufactured from nickel base alloys have traditionally been precision die forged in sequential thermo-mechanical processing operations in order to achieve the desired geometry and mechanical properties.

Metal Injection Moulding (MIM) is a competing three dimensional forming technology with proven applications in both the automotive and medical industries for producing industrial quantities of small, net shaped components. To date, the Metal Injection Moulding process has had limited exposure as a manufacturing process for gas turbine compressor components.

The aim of this research thesis is to establish if the Metal Injection Moulding process can be used to manufacture compressor components of equivalent mechanical properties to those manufactured by conventional processing methods.

In order to achieve this aim a rigorous program of metallurgical testing and analysis has been developed. The objectives of this program focus on determining the key material properties from each of the competing manufacturing processes. The methodology used to assess the merits of each process was based upon comparative back to back testing trials using both representative components and material test bars.

The test results demonstrate that while the mechanical properties of the Injection Moulded 718 alloy can be improved by subsequent thermo-mechanical processing, there remains however a significant deficit in the strength, ductility and creep properties compared to the wrought 718 alloy datum results.

The recommendations which have been made as a result of this research focus on improvements to the condition of supply of the powdered 718 alloy and to the controls associated with the Metal Injection Moulding process in order to minimise process variation. Standardisation of the mechanical testing methodology including the test piece geometry is also considered necessary in order to achieve a more meaningful comparison to published historical test data and allow wider industry corroboration of test results conducted in accordance with aerospace standards.

ACKNOWLEDGEMENTS

The author wishes to thank the following persons for their help, support and encouragement throughout the duration of this research project.

Dr Mike Barker, Mr Alan Davidson and Dr Neil Shearer, Edinburgh Napier University - for their support and technical guidance associated with the material characterisation and testing techniques utilised during this research.

Professor Martin Bache and Dr Gavin Stratford, Swansea Materials Research & Testing Ltd (SMaRT), Swansea University - for advice and access to Small Punch Testing capabilities.

Professor Iain Todd, Dr Fatos Derguti and Dr Albert Sidambe, University of Sheffield - for their assistance in the production of injection moulded test pieces.

Mr Colin High (Manufacturing Engineering Program Manager - Aerofoil Technology) for research funding and project guidance.

Dr Wayne Voice, European Space Agency - for encouraging me to expand my horizons and engage in materials research.

Finally, I would like to thank my family and friends for all the support they have provided, especially my partner Kim, for her encouragement and patience throughout this research.

LIST OF FIGURES **PAGE**

LIST OF FIGURES (continued) **PAGE**

LIST OF FIGURES (continued) **PAGE**

LIST OF FIGURES (continued) **PAGE**

LIST OF FIGURES (continued) **PAGE**

LIST OF FIGURES (continued) **PAGE**

LIST OF FIGURES (continued) **PAGE**

LIST OF FIGURES (continued) **PAGE**

LIST OF TABLES **PAGE**

LIST OF TABLES (continued) **PAGE**

LIST OF TABLES (continued) **PAGE**

LIST OF SYMBOLS AND ABBREVIATIONS

Symbols

A	Arithmetic mean
Al	Aluminium
θ	Angle
~	Approximately
Bi	Bismuth
B	Boron
GBP	British Pound sterling
C	Carbon
Cr	Chromium
Co	Cobalt
Cu	Copper
º	Degree
ºC	Degree Celsius
ɣ”	Gamma Double Prime
GHz	Gigahertz
Tg	Glass transition temperature
Ag	Gold
>	Greater than
He	Helium
pH	Hydrogen ion concentration
Fe	Iron
Pb	Lead
<	Less than
Mn	Manganese
µ	Micro
µm	Micrometre
Mo	Molybdenum
Ne	Neon
Ni	Nickel
Nb	Niobium
%	Percent
P	Phosphorus

LIST OF SYMBOLS AND ABBREVIATIONS (continued)

Symbols (continued)

σ	Standard deviation
S	Sulphur
Si	Silicon
Ta	Tantallum
Ti	Titanium
W	Tungsten
σ^2	Variance

LIST OF SYMBOLS AND ABBREVIATIONS (continued)

Abbreviations

2D	2 dimensional
3D	3 dimensional
/min	Per minute
AD	Anderson-Darling
AMS	Aerospace Material Specifications
App	Application
ASM	American Society for Metals
ASTM	American Society for Testing and Materials
At%	Atomic percent
atm	Atmosphere
BASF	Baden Aniline and Soda Factory
BC	Binder Constituents
BS	British Standards
BS EN ISO	British Standard European Norm International Standards Organisation
CEN	European Committee for Standardization
CI	Confidence Interval
CIM	Ceramic Injection Moulding
CIP	Carbonyl Iron Powder
cm	Centimetre
CT	Computer Tomography
D	Debinding
D	Diameter
D	Indentation
d	Depth of impression
DoE	Design of Experiments
EBQ	Economical batch quantity
EDAX	Energy Dispersive X-ray Analysis
EPMA	European Powder Metallurgy Association
ET	Elevated temperature
EU CoP	European Union Code of Practice
FCC	Face centered cubic
g	Grams

LIST OF SYMBOLS AND ABBREVIATIONS (continued)

Abbreviations (continued)

g/cm^3	Grams per centimetre cubed
g/mol	Grams per molecule
HBW	Hardness Brinell (tungsten)
HIP	Hot Isostatic Press
HRC	Hardness Rockwell C scale
hrs	Hours
HV	Hardness Vickers
I	Injection Moulding
ISO	International Organisation for Standardisation
kg	Kilogram
kN	Kilonewton
KPV	Key Process Variables
kv	Kilovolt
LVDT	Low Voltage Displacement Transducer
M	Mixing
MC	Mixed Carbides
micro	Microstructure
MIM	Metal Injection Moulding
min	Minimum
mins	Minutes
Misc	Miscellaneous
ml	Millilitre
mm	Millimetre
mm/s	Millimetres per second
MPa	Mega Pascal
MPIF	Metal Powder Industries Federation
N	Newtons
NDT	Non Destructive Testing
OEM	Original Equipment Manufacturer
Op	Operation
P	Powder
PE	Polyethylene

LIST OF SYMBOLS AND ABBREVIATIONS (continued)

Abbreviations (continued)

PEG	Polyethylene Glycol
PH	Precipitation hardened
PIM	Powder Injection Moulding
PMMA	Polymethyl Methacrylate
PP	Polypropylene
ppm	Part per million
PS	Proof Stress
psi	Pounds per square inch
Pub	Publication
PVOH	Polyvinyl Alcohol
Ref	Reference
RI	Refractive Index
RLM	Reflected Light Microscopy
rpm	Revolutions per minute
RT	Room Temperature
S	Sintering
S^{-1}	Seconds
SA	Stearic Acid
SD	Standard Deviation
SEM	Scanning Electron Microscope
SIM	Tech Singapore Institute for Manufacturing Technologies
SPC	Small Punch Creep
SPT	Small Punch Tensile
T/C	Thermocouple
TEM	Transmission Electron Microscope
Temp	Temperature
Tm	Melting Temperature
™	Trademark
uA	Microamps
US	United States
UTS	Ultimate Tensile Strength
VAR	Vacuum Arc Re-melting

LIST OF SYMBOLS AND ABBREVIATIONS (continued)

Abbreviations (continued)

VIM	Vacuum Induction Melting
vol	Volume
vol%	Volume percent
WIPO	World Intellectual Property Organisation
wppm	Weight part per million
wrt	Wrought
wt%	Weight percent
XRF	X-ray Fluorescence

CONTENTS **PAGE**

CHAPTER 1

INTRODUCTION

1. Introduction

1.1 Primary Aim

The primary aim of this research thesis is to determine the feasibility of utilising the Metal Injection Moulding (MIM) process for the manufacture of gas turbine compressor blades from 718 alloy in order to achieve a competitive manufacturing advantage.

The aim is driven by the generally accepted hypothesis that components manufactured from injection moulded 718 alloy will display equivalence in terms of metallurgical structure and mechanical properties to those manufactured from the conventional thermos-mechanical processing route which utilises wrought 718 alloy.

The research questions listed below have been derived in order to prove or disprove the accepted hypothesis.

Research questions:

- How similar or dissimilar are the structures and mechanical properties of fully heat treated 718 alloy as a consequence of fundamentally differing manufacturing methods?
- Can the metal injection moulding materials and processing techniques meet the anticipated application?
- Is the process capable of conforming to aerospace standards?

To address the research questions data sets will be created in order to capture the key material properties from both the conventional wrought 718 alloy test results and the competing Metal Injection Moulded 718 alloy test results.

The testing methodology employed to assess the merits of both manufacturing methods will be in accordance with agreed international testing standards where possible and where not practicable, local testing procedures will be employed. The testing will be of a comparative back to back nature using similar test piece geometries and standard test rigs.

The degree of association between the competing manufacturing methods will be assessed statistically using Minitab™ statistical software.

1.2 Objectives

In order to answer the key research questions and to fulfil the aim of this research, a comparative testing strategy has been formulated. The purpose of this strategy is to compare the material properties of the competing manufacturing methods by performing a series of back to back material evaluations on standardised test pieces and components in the fully heat treated condition.

The characterisation and testing strategy will incorporate the following key analysis features and other supporting evaluation techniques where appropriate:

- Elevated temperature tensile - wrought test pieces.
- Elevated temperature tensile - metal injection moulded test pieces.
- Metallographic evaluation - wrought test pieces.
- Metallographic evaluation - metal injection moulded test pieces.

Non-standard comparative 718 alloy test results derived from development components tested in accordance with European CEN Workshop Agreement 15627:2007 (Small Punch Test Methods for Metallic Materials).

- Small punch tensile - wrought component pieces.
- Small punch tensile - metal injection moulded component pieces.
- Small punch creep - wrought component pieces.
- Small punch creep - metal injection moulded component pieces.

The thesis literature review of published academic papers and associated documentation will be performed in order to acknowledge and challenge the current industry beliefs and to substantiate the strategic direction of this research thesis.

A historical review of published patents will be conducted which will complement the literature review process. The patent review will provide an insight into the commercial aspects of the research, and in addition to acknowledging the current patent landscape, will also identify any patenting opportunities which may arise as a result of the research thesis strategy and findings.

1.3 Introduction

The primary role of the modern gas turbine engine is to convert the energy derived from burning fuel into useable work. Gas turbine engines developed for aero applications accelerate air to produce thrust. Atmospheric air enters the engine fan section and then travels through the compressor via sequential stages of rotating blades and static vanes. The purpose of the compressor is to increase the pressure of the air as it travels through the core of the gas turbine. The compressed air is then mixed with fuel and ignited in the combustion chamber. Within the combustion chamber the chemical energy from the fuel is then converted into thermal energy before entry into the turbine. The role of the turbine is to extract the thermal energy from the gaseous combustion products and transmit the energy to power in order to drive the fan. The amount of thrust generated depends on the mass flow through the engine and the exit velocity of the gas. Figure 1 below illustrates the key sections of a typical gas turbine engine.

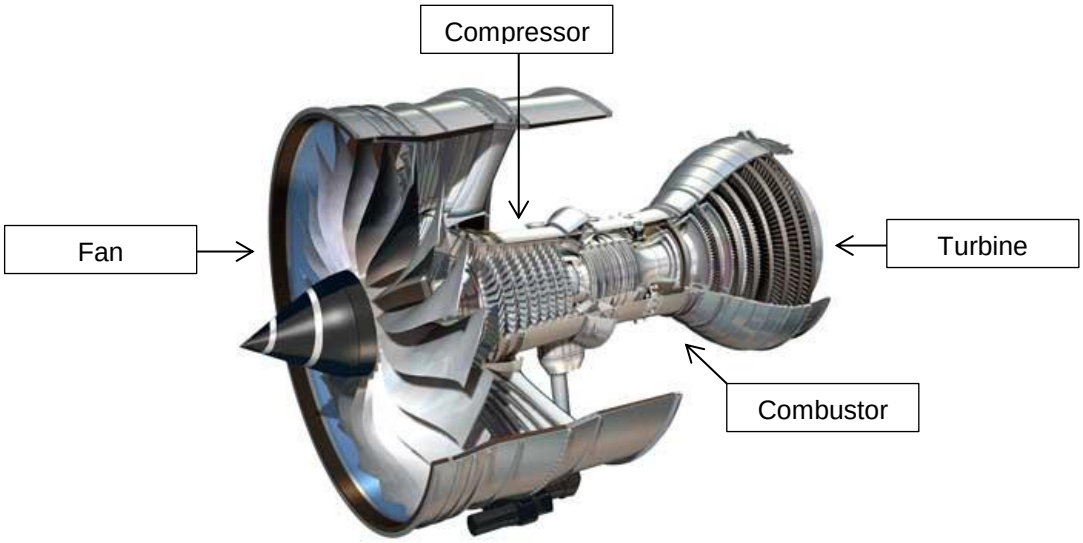

Figure 1: Gas Turbine Engine

Gas turbine propulsion technology has evolved considerably throughout the last 60 years. Advances in manufacturing processes and materials have contributed significantly towards the achievement of higher pressure ratios, increased turbine exit temperatures and improved engine cooling and sealing technologies. These contributions have been key milestones in the evolution of gas turbine technology leading to significant improvements in operational performance.

From a materials science perspective, the enabling technologies which have played a pivotal role in the evolution of the alloys adopted for the manufacture of gas turbine components, have been the development of both the vacuum induction melting (VIM) and vacuum arc re-melting (VAR) processing technologies. Prior to the advent of such technologies, the temperature capabilities of established iron based austenitic superalloys such as A286 were restricted to below 700ºC.
The improved raw material melting capabilities and refining methods provided by the VIM / VAR processes have accelerated the development of Nickel based superalloys. This enables better control over the elemental chemical composition of the alloy and also minimises the formation of impurities which had historically resulted in alloys exhibiting poor ductility. Nickel based superalloys such as 718 alloy have emerged from the 20th century as the most commonly used wrought superalloy in current use today amongst aero gas turbine suppliers.

718 alloy offers high temperature strength, creep and oxidation resistance. The ease by which components may be thermo-mechanically processed during hot forging operations offers considerable benefits to the utilisation of this superalloy. Table 1 and 2 below illustrate the typical chemical composition of 718 alloy and corresponding material properties.

Table 1: Nominal 718 Alloy Composition (wt%)

Element	Value	Element	Value
Carbon	C 0.020 to 0.08wt%	Cobalt	Co <=1.0wt%
Silicon	Si <=0.35wt%	Chromium	Cr 17.0 to 21.0wt%
Manganese	Mn <=0.35wt%	Copper	Cu <=0.2wt%
Phosphorus	P <=0.015wt%	Molybdenum	Mo 2.8 to 3.3wt%
Sulphur	S <=0.008wt%	Nickel	Ni 50 to 55wt%
Gold	Ag <=5wppm	Niobium+Tantallum	Nb+Ta 4.8 to 5.5wt%
Aluminium	Al 0.30 to 0.70wt%	Lead	Pb <=10wppm
Boron	B 20 to 60wppm	Titanium	Ti0.70 to 1.15wt%
Bismuth	Bi <=1wppm	Iron	Fe REMAINDER

Table 2: Industry Standard - Elevated Temperature (650ºC) Tensile Properties

UTS (MPa)	0.2% PS (MPa)	Elongation (%)	Reduction in area (%)
1000 minimum	860 minimum	10 minimum	18 minimum

From a metallurgical perspective, 718 alloy presents a face centred cubic (FCC) gamma matrix which is strengthened by the presence of solutes and precipitates. The constituents of 718 alloy can be classified broadly as solid solution formers, precipitation formers, carbide formers and surface stabilisers. The solid solution

formers increase the strength of the solution by increasing the resistance to the movement of dislocations. Elements such as cobalt, iron, chromium and molybdenum having atomic radii similar to nickel tend to partition easily in the FCC gamma matrix where they provide improved stability of the matrix. These elements are commonly accepted as solid solution strengtheners.

Elements such as aluminium, niobium, titanium and tantalum all have greater atomic radii and have a differing metallurgical effect on the structure and properties of the alloy. These elements tend towards the formation of ordered phases such as Ni_3 (Al Ta Ti). These compounds are often referred to as gamma prime. In superalloys such as 718 alloy and other nickel iron alloys with a high percentage of niobium, an ordered phase is present and is often referred to as gamma double prime. This phase has a body centred tetragonal structure. Gamma double prime is coherent with the gamma matrix and imparts local coherency strains. The kinetics associated with the formation of this product are very slow. The presence of gamma double prime and the associated reaction kinetics are one of the main reasons for the high temperature capability of the alloy. This phase has been found to coarsen above 650ºC leading to a deterioration in properties resulting in over ageing and a loss of mechanical properties. High coherency strains associated with gamma double prime. Carbon is known to combine with elements such as titanium and hafnium to form MC carbides.

Thermo-mechanical processing or longevity of service can degrade these carbides to $M_{23}C_6$ or M_6C. These carbides are known to migrate to the original austenitic gamma boundaries. The carbides tend to precipitate at grain boundaries and hence reduce the tendency for grain boundary sliding. Carbide formers (C, Cr, Mo, W, C, Nb, Ta, Ti) enhance the elevated temperature properties of the alloy by providing the ability to operate at elevated temperatures (0.6Tm of the absolute melting temperature) whilst maintaining key material properties such as tensile strength, creep strength and resistance to thermal and mechanical fatigue.

For the purpose of this research gas atomised 718 alloy powder was selected. The powder particle size (D90,16μm) was a compromise between powder cost and powder packing density. The selected powder alloy was readily obtainable with certified chemical composition, reflecting the current wrought production alloy.

1.3.1 Traditional Manufacturing Method

The manufacture of compressor aerofoil components has traditionally been achieved by successive thermo-mechanical precision die forming operations. This method of achieving the final geometry is generally accepted as being the most economical manufacturing method for industrial quantities of similar component types and imparts enhanced mechanical properties to the finished product. A typical manufacturing sequence is illustrated in Figure 2 below. The starting point is the slug of high quality wrought 718 alloy. As can be seen, several sequential thermo-mechanical processing operations are necessary in order to achieve the finished product.

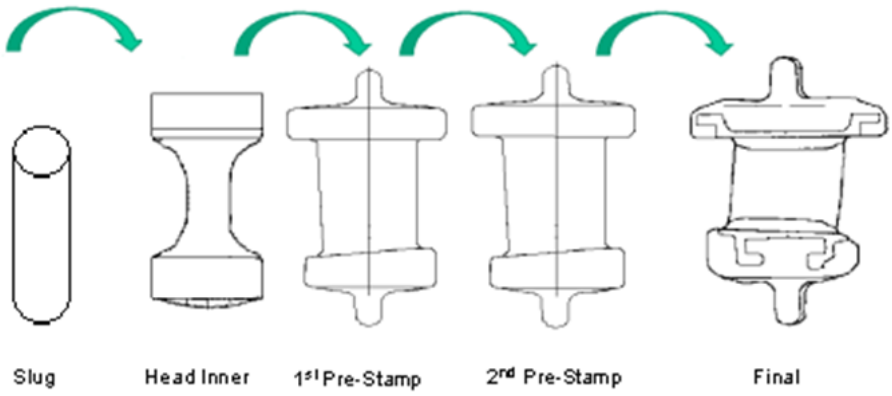

Figure 2: Precision Die Forging Process Sequence

At each of stage of the forming process considerable thermal energy and force is required in order to achieve the desired component geometry. Extrusion and heading operations are performed to redistribute the material prior to the pre-stamp and final stamping operations. The bulk of the hot forging operations are performed at temperatures in excess of 1080ºC in a controlled Argon / Hydrogen furnace atmosphere to minimise the formation of tenacious surface oxides. To avoid deleterious metallurgical defects being pressed into the main bulk of the component complex surface treatments are required. These treatments take place between thermo forming operations and adopt both mechanical and chemical methods. Aluminium oxide grit is used to remove both the residual forging lubricants and surface oxides from the components during the dry blasting process. Chemical machining is employed to equalise the part to part variation in component dimensions which is an integral part of the hot forging process during the

manufacture of production quantities of components. The inherent variation in component dimensions can be attributed to factors which are generally considered to be challenging or uneconomical to control during the manufacturing process, such as the consistent application of forging lubricants, variable material forging temperatures, variable component transfer times between the furnace hearth and the forging die. These variations have an effect on how the material ultimately flows in the die and are compounded by other external variables such a die wear and press functionality. In addition to equalising the dimensions of the forged component, chemical machining offers the opportunity to visually inspect the surface integrity of the forgings following both initial and final stamping operations. This operation ensures that there are no residual surface features present which could undermine the integrity of the component during service.

The manufacture of economical batch quantities (EBQ) of components varies considerably depending on the component forger. In determining the EBQ certain considerations require to be evaluated such as furnace and press set up times, shift patterns and the die life of sequential forming operations. The manufacture of compressor blades and vanes using the conventional forging process without automation is a relatively expensive process. The labour costs associated with the conventional forging process arise from the need to have a forging operative present throughout the salient parts of the process. These costs are associated with furnace loading, component transfer and component inspection activities. In addition to the direct labour costs associated closely with the manufacture of the product there are also overhead costs which contribute to the overall component cost. The overhead costs associated with the process result due to the consumption of electrical power, inert furnace gas and the management of both trade effluent waste and raw material waste.

Conventional precision die forging methods for the manufacture of aero compressor components are well established and understood. The motivation for conducting research into competing three dimensional forming techniques is driven by the requirement to deliver cost effective products to the customer through the adoption of lean manufacturing principles and processes.

1.3.2 Research Method of Manufacture

Metal Injection Moulding (MIM) is an established three dimensional forming technology whose origins can be traced to the ceramics industry and Ceramic Injection Moulding (CIM) applications. Today MIM has successfully achieved a presence in five key industry sectors, namely the automotive, medical, consumer, information technology and mechanical. In terms of tonnage of powdered materials supplied, the European automotive market is a clear leader in the quantity of materials used for automotive applications. Typical automotive components which are metal injection moulded in industrial quantities include rocker arm components, fuel injectors, cooling nozzles and turbo charger components. BASF are recognised to be among the market leaders for the supply of complete metal injection moulding solutions in terms of powdered alloys and associated chemicals to respective industry sectors. Figure 3 below illustrates a typical processing sequence.

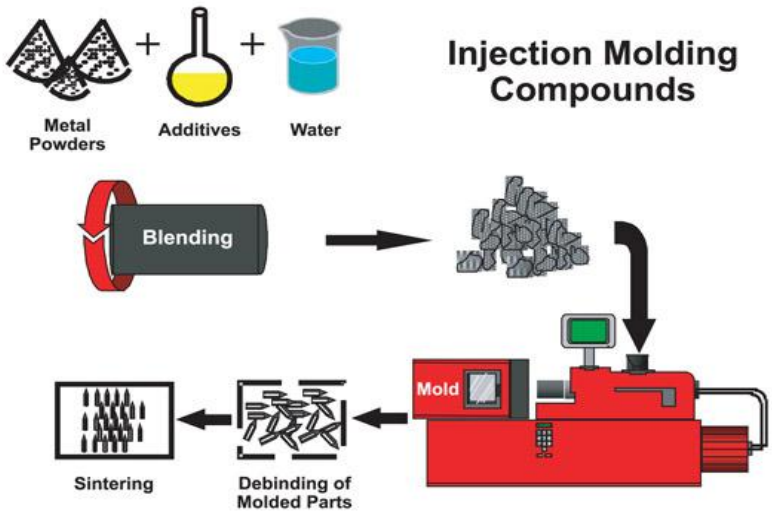

Figure 3: Metal Injection Moulding Processing Sequence

Typically the particulate material is mixed with a binder and then formed into the desired shape using conventional injection moulding capability. The ‘as moulded’ condition is referred to as being in the ‘green state’ and whilst having the desired geometry, is generally friable and weak. In order to achieve the desired properties the ‘green state’ body is then sintered. During the sintering process the binder volatilises and the particulate material particles fuse together thus producing a more structurally sound component. The MIM illustration above captures the typical key stages of the manufacturing process.

The manufacture and development of powdered MIM alloys are at an advanced stage and a wide variety of both ferrous and non-ferrous alloy are available commercially.

Powdered alloys are generally classified in terms of the powder particle shape and also the particle size distribution within the powder lot. Several industrial process are available for the production of powdered alloys, however the inert gas atomisation process is generally preferred for the production of spherical powder particles in order to minimise the amount of surface oxidation present on individual powder particles. In this type of process the alloy is induction melted in an inert atmosphere then fed through an atomising gas in a controlled manner. The resulting metallic particles are then classified by exposure to sieves of varying aperture size.

Metallic powders manufactured by the gas atomisation process vary in powder particle size. Powder particle sizes range from 5 to 40 microns.
Water atomisation processes are also available providing similar powder particle size ranges however the resulting particles are of a less uniform shape.

From a manufacturing perspective the ideal powder would have a mix of both large and small powder particles in order to obtain a high packing density. Inter particle friction and cohesion are key powder attributes as this minimises distortion of the moulded product following removal of the binder system. Hollow powder particles are undesirable as this has an effect on the final sintered density of the product. Metallic powders in the 5 to 40 micron particle size range are generally characterised using laser diffractometry / scattering techniques.

The metal injection moulding process is proven to be capable of producing high component volumes at a relatively low cost due to the net shape manufacturing capabilities of the process. As with any manufacturing process the resulting product output is a factor of the inherent variability of the process inputs. The key process variables associated with polymer injection moulding are well understood, however the application of the metal injection moulding process to the manufacture of aero compressor components is a less well documented process.

The critical success factors associated with this research thesis will be the ability to manufacture and test metal injection moulded products in order to demonstrate mechanical property equivalence to the established wrought 718 alloy. The testing will be conducted in accordance with aerospace testing standards.

CHAPTER 2

REVIEW OF PUBLISHED RESEARCH

2. Review of Published Research

2.1 Literature Review

The vision of employing the metal injection moulding process for the manufacture of gas turbine compressor components has been discussed in detail by Sikorski, Kraus and Müller (2006). The authors acknowledge the technological advances which have been achieved through the evolution of the gas turbine engine in recent decades as well as the commercial aspects and challenges facing modern airline operators. From an airline operators' perspective, reliability, safety and cost effectiveness are the key business metrices from which the success of the business can be measured. Airline operators strive to provide the customer with a safe and competitively priced product. These requirements put the onus on the gas turbine manufacturer to challenge the conventional manufacturing methods, materials and supply chains in order to deliver a competitively priced product to the marketplace.

The metal injection moulding process is a proven manufacturing route for the production of economical quantities of small thin walled components for both the automotive and the medical industries. In terms of application of the metal injection moulding process to the gas turbine compressor Sikorski, Kraus and Miller (2006) claim that the component geometry and size of compressor components are key attributes for the cost effective application of the process, and substantiate this claim by the manufacture of typical stator vane components in addition to the more complex stator vane assemblies. The stator vane assemblies utilise the sintering process as opposed to vacuum brazing techniques to achieve a joint between the individual vanes. This joining method can be adopted as an integral part of the metal injection moulding process and offers additional product cost savings due to the avoidance of supplementary joining technologies such as vacuum brazing in order to achieve the final component assembly. The metal injection moulding process used to manufacture the development components follows the typical processing steps which involve mixing the finely divided gas atomised metallic powder with a suitable binder and moulding the required component shape. Debinding takes place by either a solvent or a thermal processing operation followed by material consolidation by the sintering process. In recognition that the components will not present the same material density as the equivalent wrought product, an additional hot isostatic pressing operation has been introduced in order to achieve full material density.

The choice between applying the metal injection moulding technique to either a single stator vane and vane assembly or a corresponding rotor blade was made based upon the generally accepted view that the compressor vanes are subject to much lower operating stresses than the corresponding cantilever type rotor blades. Recognising the material types commonly used in the compressor section of the gas turbine as being titanium and nickel base alloy, the sample components have been manufactured from an undisclosed nickel base superalloy. The powdered superalloy has been manufactured by vacuum melting and subsequent gas atomisation of a high quality ingot of undisclosed nickel base superalloy in an inert argon atmosphere. The authors justify the selection of the nickel base superalloy capable of operating at temperatures up to 650ºC, over other possible titanium alloy alternatives for their research, by citing the increased susceptibility of titanium alloys to manufacturing imperfections.

The metal injection moulding technique is stated as being capable of delivering cost savings for the manufacture of compressor components due to the net shape manufacturing capabilities of the moulding process. The cost savings are calculated in both raw material and additionally in reduced machining costs. The strength of metal injection moulded materials is accepted as being greater than those produced by the casting process and almost approaching the values achieved from wrought forgings Davis *et al.* (2004). Whilst authors Sikorski, Kraus and Miller (2006) appear to have successfully created the compressor vane geometry by the metal injection moulding process, there is no test data available to support the mechanical properties from either the actual component parts or from representative test pieces. The authors recognise that testing is an integral part of the component and material substantiation process and do however allude to development engine testing taking place in the near future.

There are several factors from a manufacturing perspective which additionally require to be evaluated before a true cost analysis can be performed. Data gathered from conventional aerofoil forging techniques provides a broad analysis of the repeatability and the stability of the manufacturing process. Compressor aerofoil components manufactured by the metal injection moulding process are not at the same level of maturity as conventional manufacturing methods. As a consequence of this, there is no data available to define the levels of dimensional variation

between individual components or sequential batches of components. This level of information, coupled with reject rates from both surface and sub-surface component evaluation techniques would form a broader appreciation of the merits of the metal injection moulding process.

The objectives of the research conducted by Davis *et al*. (2004) focused on the comparison between wrought 718 alloy in the fully heat treated condition with metal injection moulded 718 master alloy test pieces in the fully heat treated condition. The gas atomised powder was air classified to a particle size of 90% minimum -22um. The powder was mixed using a proprietary binder and pelletised for moulding to form test bars. The test bars were produced by the injection moulding process. The mould incorporated a single injection cavity in accordance with the European Powder Metallurgy Association (EPMA) best practice. The test bars were manufactured having a length to diameter ration of 20 to 1. The test bar sintering process was performed at 1265ºC for one hour. Following completion of the sintering process, the pieces were furnace cooled to 600ºC followed by a forced gas quench using nitrogen. The sintering temperature of 1265ºC for one hour was selected as a result of preliminary trials. These earlier trials found the sintering at between 1260ºC and 1280ºC for times up to 4.5 hours resulted in inferior sinter densities and poor mechanical properties.

Following completion of the sintering process the test pieces were vacuum solution treated at 980ºC for one hour then subsequently aged. The ageing cycle was also performed in vacuum and consisted of a 2 stage process whereby the pieces were aged at 720ºC for 8 hours followed by an additional 8 hour exposure at 620ºC.

The mechanical properties of the fully heat treated master alloy test pieces were evaluated at ambient temperatures and elevated temperatures. The elevated temperature testing was conducted at 540ºC.

The test piece gauge lengths were not machined or polished prior to testing. No indication of the strain rates used during both room temperature or elevated temperature testing were indicated in the research publication. The master alloy tensile test results were compared with historical wrought data from ASM International Handbook Vol 1.

The test results presented by Davis *et al.* (2004) are summarised in Table 3 below for the elevated temperature aspects of the mechanical testing.

Table 3: Elevated Temperature (540ºC) Tensile Properties

Condition	Tensile Test Temp. (540ºC)	Ultimate Tensile Strength (MPa)	Proof Stress (0.2%)	Elongation (%)
Wrought	540	1275	1065	18
MIM (heat treated)	540	1027	895	4

In conclusion Davis *et al.* (2004) found that following the solution treatment and ageing heat treatment cycles, the microstructure of the injection moulded and sintered piece had significantly improved. In order to address the property deficit between wrought and metal injection moulded 718 alloy pieces, the authors have cited two possible reasons.

The surface condition of the injection moulded test pieces had not been modified in any way in terms of machining or polishing at the gauge length, so minor surface flaws and the sintered texture could have had an impact on the ductility of the pieces being tested. Examination of the fractured surfaces revealed the presence of large unreacted powder particles, the presence of which is likely to have an effect on the homogeneity of the alloy which has been reflected in the steeply inferior ductility results. No values were recorded for the reduction in area presumably because the decrease was so slight it would be out with the measurement capability of the testing instrumentation.

In addition to the testing results and analysis offered by authors Davis *et al*. (2004), it is worthwhile noting that mechanical testing performed in accordance with the aerospace series of both European and American standards require a much more controlled regime for the manufacture of test pieces to ensure that the material being tested is homogeneous throughout the section with minimal machining stresses being induced at the surface.

Tensile test piece specimens are subject to rigorous surface finish and visual inspection requirements to ensure that the test results are not influenced by either surface discontinuities, residual machining stresses or indeed tool indentations during the test piece manufacture.

Johnson *et al.* (2004) also conducted a similar evaluation of the tensile properties of a range of powdered alloys including 718 alloy. In all instances the powder loading factor was found to be approximately 65 vol% and the binder used was an undisclosed wax polymer system.

The test bars were sintered at 1260ºC in a vacuum furnace. Increasing the sintering time at this temperature from one to two hours was found to slightly increase the overall sintered density of the test piece, however both sintering conditions failed to achieve 100% density. The test bars do not appear to have received the standard solution treatment operation conducted at 980ºC for one hour, however there is objective evidence that regular 720ºC / 620ºC ageing cycle had been applied. The mechanical testing regime is not fully documented in terms of the temperature at which the tensile testing was performed, however the strain rate has been identified as being 2mm/min. The number of pieces tested by Johnson *et al.* (2004) has not been disclosed, however the range in mechanical test results provides the reader with an insight into the metallurgical uniformity of the pieces being tested. The mechanical testing equipment and testing methods were assumed to be consistent throughout the duration of the testing process. The range of ultimate tensile strengths were reported as being between 812 MPa and 1218 MPa with the yield strengths (presumed to have been conducted at 0.2%) ranging from 686 MPa to 995 MPa. In terms of sample ductility, values of between 3.3% and 17.4% were recorded. Research authors Johnson *et al*. (2004) offer no explanation for what would be considered an unacceptable scatter in material properties from a 718 alloy design perspective. No explanation of the possible causes of the variable test results or even acknowledgement that the test results are indeed variable has been recorded. The authors do however state that following hot isostatic pressing at 1190ºC and 1020 atm for 4 hours, the pieces achieved full specimen density and delivered mechanical properties slightly below the requirements stipulated in AMS5596 for wrought material. Due to the lack of test data this research has to be reviewed in isolation as there is insufficient documented test piece uniformity data or testing parameters to allow the test results to be compared among the wider testing community.

The mechanical properties of metal injection moulded 718 alloy were evaluated by Gulsoy *et al*. (2010). The researchers combined gas atomised 718 alloy powder with

a binder consisting of a mixture of paraffin wax, carnuba wax, stearic acid and polypropylene. The 718 alloy powder particle size was determined using a Malvern Mastersizer, D90 min -26.2µm. The powder loading at the injection stage was 62.5 vol%. The binder was removed during a 2 stage solvent / thermal method. The test samples were subsequently sintered at 1100ºC for 5 minutes and 1285ºC for 2 hours. Following the sintering operation the test pieces were solution treated at 980ºC for one hour in a vacuum atmosphere, followed by the standard 720ºC for 8 hours, furnace cooled to 620ºC for a further 8 hours and oil quenched. The 718 alloy samples achieved high sintered densities to a liquid phase sintering effect. The sintered density was reported as being 97.18%.

Mechanical testing was performed using a Zwick 2010 mechanical tester. The test pieces were injection moulded as standard tensile bars. The testing is assumed to have been conducted on unmachined pieces or in the as moulded and heat treated condition. The crosshead speed of 1mm/min over a gauge length of 25mm was employed. No specific standard was referenced for the production of the test pieces or the conduct of the mechanical test. The tensile testing cross head speed which was used to generate the mechanical test data was half the speed employed by Johnson *et al*. (2004) in which they stated their crosshead speed as being 2mm/min.

The mechanical property data generated by Gulsoy *et al.* (2010) is presented in a slightly different manner to previous researchers work. Previous researchers have endeavoured to compare the mechanical properties of metal injection moulded 718 alloy with a plethora of historical test data for the wrought 718 alloy in various forms and from various sources. The research conducted by Gulsoy *et al.* (2010) serves to initially compare the mechanical test data from metal injection moulded 718 alloy powder with other injection moulded alloy types, namely Ni 625 alloy and Nimonic 90 alloy. Metallurgical inspection of the 718 alloy microstructure following sintering and heat treatment operations found small amounts of micro porosity and oxides were found to be present at the grain boundaries.

The mechanical properties derived from the fully heat treated 718 alloy test pieces were found to present an ultimate tensile strength of 1065 MPa and an elongation of 6%. Test data for the 0.2% proof stress and the test piece reduction in area were not documented. The testing was assumed to have taken place at ambient

temperature. The authors conclude that the test results they have achieved are comparable with other published research for powdered alloys manufactured from Ni 718, Ni 625 and Nimonic 90. By comparison with casting and forging data for the same alloy type, the authors conclude that powder injection moulded superalloy samples have lower mechanical property values, but still suggest that the alloys could find uses in less critical applications.

Recent literature published by Sidambe *et al* (2013) finds the sintered density of 718 alloy to be approximately 98% following processing at 1270ºC for one hour. This is a similar density to that reported by Gulsoy *et al*. (2010). Near 100% density was achieved following hot isostatic pressing operations conducted at 1160ºC at a pressure of 103 MPa for 3 hours. The test pieces were subsequently solution treated at 968ºC for 3 hours, then furnace cooled to room temperature, followed by ageing at 730ºC for 8 hours, furnace cooled to 630ºC and subsequently aged for a further 8 hours in accordance with AMS5917 (Metal Injection Moulded Parts, Hot Isostatically Pressed). Mechanical testing was performed in accordance with ASTM E8 and ISO 6892. Test pieces were manufactured in accordance with MPIF guidelines for ambient temperature tensile testing and in accordance with BSEN ISO 6892 for elevated temperature (650ºC) testing. Testing was conducted in accordance with ASTM E8 and ISO 6892 respectively. In a similar pattern to a lot of published research, the researchers rely on a considerable amount of published historical data for comparisons being made between injection moulded test piece results and historical results for both cast and wrought products. This research publication has made clear references to the types of test piece being used and also the testing standards being employed for the generation of mechanical test data.

One of the most comprehensive publications which addresses the application of metal injection moulding for aerospace applications from both a technical and commercial perspective has recently been published. Ott and Peretti (2012) scoped a vendor research strategy which would determine by objective testing which metal injection moulding suppliers would be capable of developing into a credible supplier of injection moulded components manufactured from 718 alloy. The supplier evaluation was performed by requesting both square and round test bar materials with a target chemical composition which was typically chosen to reflect the current wrought standard. The chemical composition chosen was declared as Ni -18.1Cr -

2.9 Mo - 18 Fe - 5.4 Nb - 1Ti - 0.45 Al. The key research questions which would form the basis of this research were based upon determining the overall material quality and understanding the effects of surface finish and test piece geometry on the properties of the test pieces. Analysis was also conducted on the vendors products in order to assess the effects of process variation on the final delivered product. The authors note at the start of the research paper that although there are many suppliers of metal injection moulded 718 alloy, not all suppliers are able to meet aerospace requirements. This is a significant conclusion because although 718 alloy is used predominantly in the aero compressor section of the gas turbine engine, not all suppliers or testing facilities operate in accordance with aerospace standards and specifications.

From an aerospace perspective the authors recognised a number of considerations which require to be addressed for the successful application of the metal injection moulding process in the aerospace industry. Their approach is holistic, going beyond the manufacture and testing of sample pieces.

The first consideration is from a materials perspective and focuses on the microstructural repeatability and the stability of the subsequent mechanical properties. The need to identify and control the process variables associated with gas atomised powder, component geometry, injection moulding and other key manufacturing processes are identified as being paramount to the success and repeatability of the 718 alloy metal injection moulding process. The identification and mitigation of inclusion or anomaly effects requires to be addresses through inspection processes. The inspection processes could include both surface and sub-surface non-destructive testing techniques. This could be applied during the initial sample validation processes or routinely throughout the manufacturing process until process stability and repeatability has been established. Ott and Peretti (2012) also identify the need to closely control both chemistry and processing effects in order to minimise contamination effects such as prior powder particle boundary effects or other types of alloy contamination as a result of thermal processing such as sintering and hot isostatic processing. In addition to specific technical requirements consideration has also been made for the development of a robust supply chain with adherence to aerospace standard specifications.

From a technical perspective the authors note that the formation of significant oxide or nitride grain boundary films can have a detrimental effect on the strength and ductility of the alloy which would make it unacceptable for structural applications. Test pieces containing oxygen levels less than 500 wppm produced ductile results, while pieces containing greater than 2000 wppm oxygen showed significant ductility debits.

The heat treatment cycle chosen for test bars manufactured from 718 alloy as in accordance with AMS 5662 and consisted of 718ºC / 8hrs followed by a furnace cool at 55ºC to 621ºC / 8hrs. The test pieces were subsequently subjected to a hot isostatic pressing operation after which full density was achieved.

Mechanical test results from 2 differing test piece types were evaluated. One of the test pieces followed the recommendations of the MPIF and was tested in the as sintered and fully heat treated condition, including hot isostatic pressing. The other type of test piece offered a square section and was machined all over. Ott and Peretti (2012) concluded from their mechanical testing that test piece geometry and the surface finish of the test piece have an influence of the reported strength and ductility of the piece being tested. Other significant findings of their research were the influence of the oxygen content on the ductility of the material test piece being tested.

In terms of testing standards the authors recognise the wide variety of material specifications which are currently in circulation for use with 718 alloy. In terms of aerospace standards the authors find that several MPIF Standards, as well as ASTM B883 are not adequate for aerospace material properties and processing requirements. In order to address this anomaly AMS5917 (Metal Injection Moulding Nickel Based Alloy 718 Parts, Hot Isostatically Pressed, Solution Treated and Aged) was introduced, Ref Tables 4 and 5. The purpose of this standard is to address key acceptance criteria including ambient and elevated (650ºC) tensile testing. Tensile properties are documented for vendor specific processes. In addition, the standard also captures the requirement to address vendor specific powder anomalies such a metallurgical inclusions. The mechanical property requirements for metal injection moulding comparison purposes suggests the MIM materials exhibit strength of close

to 95% of wrought aerospace grade 718 alloy with ductility levels between cast and wrought 718 alloy.

Table 4: AMS5917 (2011) - Extract - Elevated Temperature (649ºC)

Tensile Test Temp.	Proof Stress (0.2%)	Ultimate Tensile Strength (MPa)	Elongation (%)	Reduction in area (%)
649ºC	827	931	6	6

The publication of AMS 5917 (2011) is a significant step in the evolution of the use of 718 alloy for gas turbine applications in the hot isostatically pressed conditions. In addition to specifying the specific chemical requirements of the powdered alloy, the standard provides clear mechanical property requirements for testing being performed at both room temperature and elevated temperatures (649ºC).

Also defined are the acceptance standards for mechanical testing, in process testing and equipment calibration.

Table 5: AMS5917 (2011) - Extract - Room Temperature

Tensile Test Temp.	Proof Stress (0.2%)	Ultimate Tensile Strength (MPa)	Elongation (%)	Reduction in area (%)
Ambient	1034	1241	6	8

The standard offers the following chemical composition. Compositional variations are in accordance with AMS2269 (2012). Ref Table 6 below.

Table 6: AMS2269 (2012) - Extract - Powder and Parts Composition

Element	Minimum	Maximum
Carbon(1)	-	0.08
Manganese	-	0.35
Silicon	-	0.35
Phosphorus	-	0.015
Sulphur	-	0.015
Chromium	17.00	21.00
Nickel	50.00	55.00
Molybdenum	2.80	3.30
Chromium	4.75	5.50
Titanium	0.65	1.15
Aluminium	0.20	0.80
Cobalt	-	1.0
Tantalum (2)	-	0.05
Boron	-	0.006
Copper	-	0.30
Lead (2)	-	0.0005 (5ppm)
Bismuth (2)	-	0.00003 (0.3ppm)
Nitrogen (1)	-	0.02
Oxygen (1)	-	0.06
Selenium (2)	-	0.0003 (3ppm)
Iron	remainder	-

The elements listed above are applicable to the powder and parts and are determined by wet chemical methods or where not applicable recognised best practice or recommended practice standards.

Element (1) - Test to be performed on components in the fully finished condition. This is a significant factor in the chemical composition specification because it recognises that the absorption of these elements can influence the mechanical properties of the alloy.

Element (2) - Test not required for routine testing.
These elements are considered to be trace elements, the levels of which are not likely to influence the metallurgy or properties of the alloy during normal manufacturing.

The powder method of manufacture, distribution and identification is given considerable attention. When a powder lot contains more than one powder heat, each powder heat must conform to the compositional requirements. A powder heat

is defined as the product of one melt and gas atomisation run. A powder lot is defined as purchased powder having a unique identification. A powder lot can consist of one or more powder heats, obviously providing the chemical composition of each heat is in accordance with the overall compositional specification.

In order to standardise the manufacturing route and the testing methodology being applied the following standards have been cited in AMS5917. The standards referenced below are not however the only standards which can provide a governance structure around the control of the metal injection moulding process for 718 alloy. The standard is applied to the assessment of components produced from manufacturing powder lots.

Chemical Composition	AMS5917 (2011), as per compositional table
Density	ASTM B311 (2013), minimum 8 g/cc
Tensile	ASTM E8 / E8M (2013), MPIM 50 standard
Grain size	ASTM E112 (2013), ASTM 5 of finer
Hardness	ASTM E18 (2014), 34-44HRC

Fluorescent penetrant inspection (customer requirements)

Radiographic inspection (customer requirements).

The control of thermal processing equipment used for sintering and heat treatment is conducted in accordance with AMS2750E Pyrometry requirements. The terminology used is referenced from ARP1917.

The specification requirements are specific to metal injection moulded products which are subsequently subjected to a hot isostatic processing technique. The standards referenced are a reflection on the geographic location of the researchers and provide a clear starting point for the standardised manufacture of components from 718 alloy, as opposed to AMS5662 which is the recognised global standard for aerospace grade wrought 718 alloy.

It is worth noting however that not all gas turbine manufacturers purchase and process wrought 718 alloy in accordance with AMS5662. Certain Original Equipment Manufacturers (OEM) have historically controlled the condition of supply of wrought products through internal materials quality procedures.

2.1.1 Literature Review Summary

In summary, in the last 10 years there has been considerable documented interest in the creation of powdered superalloy materials for the purpose of injection moulding complex component geometries. The challenges presented by adopting the metal injection moulding process for the manufacture of compressor components are complex due to the nature of the manufacturing process. A knowledge of polymeric materials, metallic materials, thermal processing and pyrometry are required in order to identify and stabilise the key process variables associated with the process.

The research to date has been undertaken by academic institutions, technology centres and in conjunction with key industry partners. The varying research methodologies which have been identified all contribute towards increased levels of process understanding. These contributions both corroborate the findings of prior published literature, in addition to providing a platform for further research and questioning.

Research which is specific to the application of the metal injection moulding process in the manufacture of gas turbine compressor components from powdered 718 alloy still presents a number of research opportunities. The details of which are listed below.

Test Piece Geometry

The effects of test piece geometry on the mechanical test results achieved at both ambient and elevated temperature requires further investigation in order to ascertain the degree of test result variation which can be attributed to the geometry of the pieces being tested. Typical test pieces can be seen in Figure 4. In addition to inter sample testing, there is also scope for a ‘round robin’ style of material testing analysis in order to establish the level of variation on both a national and international scale to recognised aerospace testing methodologies.

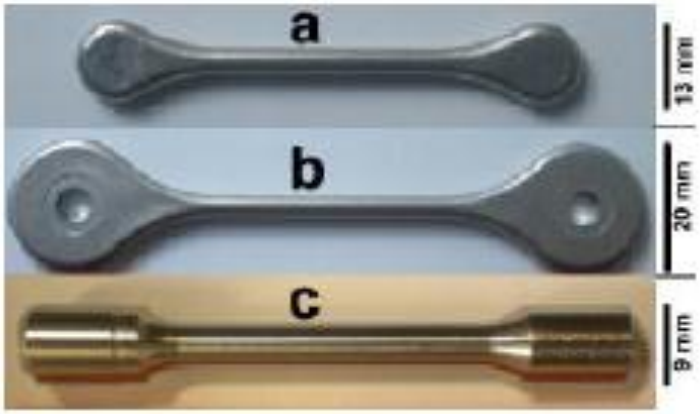

Figure 4: Test Sample Geometries

Test Piece Surface Condition

The surface condition of the test pieces is also an important factor, whether the test data is derived from unmachined 'as sintered and heat treated' samples or whether the data has been derived from fully homogeneous sections requires investigation. Heat treated unmachined test pieces often display many surface irregularities due to the powder particle size presenting an 'open' surface structure. The metallurgy of the fully heat treated test piece surface differs from the metallurgical structure at the centre of the test piece, resulting in a surface layer effect which can be detected after chemical etching. Ideally the test piece surface condition should match that of the component from which the mechanical test results are a representation.

Test Piece Type

In addition to tensile testing data offering UTS, 0.2%PS, Elongation and Reduction in Area values, there is also a need to correlate mechanical test data for other key properties associated with 718 alloy. Material classification techniques such as creep testing, fracture toughness and ambient temperature fatigue testing provide a much broader assimilation of the suitability of the powdered alloy for operation at elevated temperatures.

Component Dimensional Stability

The resulting change in component dimensions, following both debinding and sintering operations, are well documented. One area which is not particularly well documented is that of the variation in final component geometry following both sintering and heat treatment operations specific to compressor aerofoil geometries.

Wrought gas turbine compressor components often require additional cold working techniques to achieve dimensional conformity. It is recognised that since compressor aerofoil components are not 'designed to accommodate the metal injection moulding process'. Heat treatment and hot isostatic pressing techniques are likely to result in a certain amount of distortion, which some moulding suppliers correct by introducing a further coining operation. No data is available which describes the 'right first time' aspect of the process, when applied to the manufacture of compressor components. This is a key aspect of the commercial business case which is yet to be established and will depend on the geometry and complexity of the components being manufactured.

In recognition of the research which has been conducted historically and also the research opportunities available, this research thesis will address the research questions below.

- How similar or dissimilar are the mechanical properties of fully heat treated 718 Alloy as a consequence of radically differing manufacturing methods? Test data will be generated from both representative test bar specimens in addition to trial components. The test data will be a straight comparison between the properties of the injection moulded 718 alloy and the wrought aerospace equivalent 718 alloy.

  Test piece - Elevated Temperature (650ºC) comparative tensile testing utilising both wrought and metal injection moulded identical standardised test pieces in the fully machined condition.

  Test piece (hybrid method) - Elevated Temperature (650ºC) Hot isostatic pressing techniques will not be used in an attempt to achieve full material densification, however as an alternative, progressive thermo-mechanical processing operations will be adopted which will result in a hybrid manufacturing technique. Injection moulded test bars will be subject to progressive reductions in diameter.

  Component testing – Small Punch Tensile and Small Punch Creep tests will be performed on test pieces extracted from both wrought and injection

moulded components. The test pieces will be subjected to comparative testing for both wrought and injection moulded test pieces.

Hardness testing - Depending on the test piece thickness, either Brinell hardness testing or Vickers hardness testing will be performed on representative test pieces.

- How important is the feedstock quality and processing parameters to the integrity and repeatability of the process.

  This question will be addressed following the analysis of the mechanical test results.

This research strategy builds upon the already published data and in addition provides an insight into other material property values. The potential effects of test piece geometry and surface finish have been negated by the adoption of a standardised manufacture and testing approach. All component heat treatment operations will be performed in accordance with aerospace standards and associated temperature tolerances.

2.2 Patent Review

The purpose of conducting a Patent Map of the Metal Injection Moulding (MIM) process is to establish who the key process innovators are and also how the innovations relate to the design and manufacture of compressor aerofoil type components. The scope of the research was specific to the salient steps in the metal injection moulding process. As a starting point a spider chart of the process was created, as illustrated in Figure 5 below.

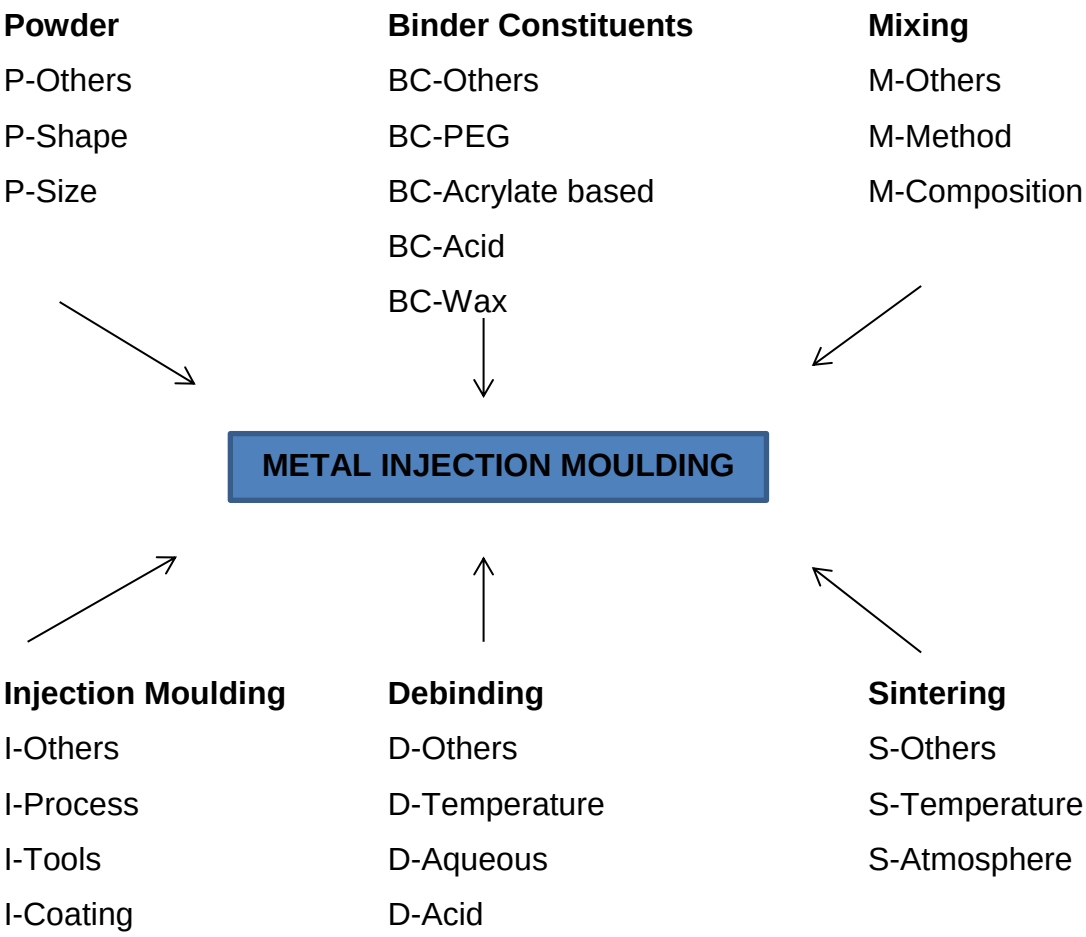

Figure 5: MIM Patent Search

The spider diagram above captures the key metal injection moulding processing steps and further sub divisions of each category are included for clarification and classification of the patent types. The Patent analysis was constructed over a 33 year period which enabled the construction of a time line from 1982 to 2015. The preceding Tables 7 to 12 detail the key process steps. The most relevant publications are highlighted.

2.2.1 MIM Patent Search – Powder

Table 7: Powder Patents

No	Granted Date	Publication Number	Patent Office	Company	Sub Category
16	24/05/1994	5314658	US Patent	AMAX Inc	P - Shape
19	**28/03/1995**	**5401292**	**US Patent**	**ISP Investments Inc**	**P - Others**
23	**31/12/1996**	**5590387**	**US Patent**	**Starck H C, GMBH & Co**	**P - Size**
51	**25/07/2002**	**0098106/A1**	**US Patent App**	**Japanese / Sagawa Masato / Nagata Hiroshi**	**P - Others**
59	19/06/2003	0110887/A1	US Patent App	Honeywell International Inc	P - Others
64	24/06/2004	0120841/A1	US Patent App	General Electric	P - Others
66	16/12/2004	0250653/A1	US Patent App	Southco Inc	P - Others
70	15/12/2005	0274222/A1	US Patent App	Taiwan Powder Technologies Co Ltd	P - Others
92	07/01/2010	0003157/A1	US Patent App	Starck H C GMBH	P - Size
96	**10/02/2011**	**0033334/A1**	**US Patent App**	**Geesthacht GKSS**	**P - Size**
97	**20/10/2011**	**0253815/A1**	**US Patent App**	**Rolls-Royce PLC**	**P - Shape**
100	31/05/2012	DE 10 2010 061 958 A1	Deutsches Patent	Rolls-Royce Deutschland Ltd	P - Others
103	20/09/2012	WO 2012/125113 A1	WIPO	O Wallinder / Y Hedberg / P Szakalos	P - Others
106	27/06/2013	CA 282 267	Canadian Intellectual Property Office	Hoganas AB (PUBL), SE	P - Others
108	08/05/2014	WO2014/068267	WIPO	Metalysis Limited	P - Size

Powders used for the metal injection moulding process are normally derived from either the gas atomisation or the water atomisation processes. Both processes provide powder particle sizes ranging from 6µm-40µm. The average particle size, the particle size distribution and the shape of the metal particles have an influence on the injection viscosity and also the homogeneity of the finished product.

There are currently a wide range of powder alloys available to the consumer. Sandvik are one of the leading powder manufacturers in the UK providing a range of gas atomised powder types. Typical alloy groups include

- Stainless steels
- Nickel base superalloys - Including 718 Alloy
- Cobalt alloys
- Specialist magnetic alloys
- Duplex stainless steels.

The key characteristics of gas atomised metal injection moulding Powders are

- Spherical Shape
- Low oxide / impurity levels
- Good flow and mixing characteristics
- Isotropic properties.

Recent powder specific inventions have focused on conditioning the “as received” metallic powder in order to produce particle sizes which are 100% less than 20µm. The conditioned powders (tungsten and molybdenum) are manufactured by the jet milling process to produce non spherical powder particles between 0.1µm and 10µm.

Evidence of further powder refinements can be found in US Patent 5401292, Japka (1995), Carbonyl Iron Powder (CIP) Premix Composition. The inventor used the arritar milling process to achieve a mixture of CIP and alloying material. The premix is prepared by intensive milling of the powder particles which reduces the particle size further and minimises segregation. The powder particle size ranges from 0.2µm to 7.0µm with a narrow particle size distribution.

Continuing with powder size refinements, US Patent 5590387, Schmidt *et al.*

(1996), resolves the powder agglomeration challenges associated with nanoscale particles (particles including powders whose average size is not more than 10µm. Nanodisperse materials are nanoscale powder particles dispersed in a carrier medium which can be a binder. The optimum result is achieved by modifying the particle surface by chemical compounds to maximise powder dispersion and achieve a high well dispersed solids content.

An alternative to powder injection moulding for net shaped components is identified in US Patent Application Publication 2002/0098106 A1, Sagawa, Watanabe and Nagata (2002). The powder compaction method relies upon a much smaller amount of binder by volume and subsequently benefits from a shorter debinding cycle in addition to the possible deleterious effects of carbon contamination and volatilisation during debinding. The powder is essentially introduced to the mould by an "air tapping" technique. The mould is then heated, without the application of force, to achieve the desired net shape.

Titanium alloy components manufactured by the MIM process have historically proved challenging due to the reactivity of titanium. US Patent Application Publication 2011/0033334 A1, Ferri and Ebel (2011), describes a method of manufacturing titanium or titanium alloy components using a homogeneous mixture of boron powder and titanium alloy in conjunction with an appropriate binder. The controlled nature of the vacuum sintering process and careful selection of binder minimises the absorption of elements such as Oxygen and Hydrogen and maintains the desirable properties of the alloy.

In addition to the well-established powder manufacturing methods such as gas atomisation, water atomisation and the carbonyl iron process for producing powders suitable for the MIM process, US Patent Application Publication 2011/0253815 A1, Voice (2011), reports a novel method of manufacturing powder by using one or more jets of liquid directed onto the surface of a solid material thereby causing the ablation of powder particles from the solid material. This method for the manufacture of powder is unique in that it is capable of cutting polyhedral grains from a solid material. The solid material could be titanium, a titanium alloy or an intermetallic compound such as gamma titanium aluminide. The liquid in which the powder particles are entrained is then collected and the

powder particles are separated from the liquid. Separation may be achieved by either the use of a settlement tank or by centrifugal means. Powder derived from this method can have a particle size in the region of 10-20µm.

The powder method of manufacture is tailored towards the production of titanium or titanium alloy powders. This method of powder production is relatively inexpensive compared to conventional methods such as gas atomisation and the plasma rotating electrode method.

2.2.2 MIM Patent Search – Binder

Table 8: Binder Patents

No	Granted Date	Publication Number	Patent Office	Company	Sub Category
6	26/03/1991	5002988	US Patent	Sanwa Chemical Industry	BC - Acid
10	14/01/1992	5080714	US Patent	Masakazu Achikita	BC - Acid
12	24/03/1992	5098942	US Patent	Fraunhofer Ges	BC - Polyethylene glycol
13	27/10/1992	5159007	US Patent	Idemitsu Petrochemical Co Ltd	BC - Others
14	19/10/1993	5254613	US Patent	Hoechst Aktiengesellschaft	BC - Wax
15	18/01/1994	5280086	US Patent	Sanyo Chemical Ltd Industries	BC - Others
17	10/01/1995	5380179	US Patent	Kawasaki Steel Corporation	BC - Acrylate based
18	14/03/1995	5397531	US Patent	Advanced Materials Technologies	BC - Wax
20	**06/06/1995**	**5421853**	**US Patent**	**Industrial Technology Research Institute**	**BC - Others**
36	18/04/2000	6051184	US Patent	Mold Research Co	BC - Acid
40	12/12/2000	6159265	US Patent	Dai-ichi Kogyo Seyaku Co	BC - Acrylate based
41	**09/01/2001**	**6171360/B1**	**US Patent**	**Yamaha Corporation**	**BC - Others**
45	**17/07/2001**	**6262150/B1**	**US Patent**	**Honeywell International Inc**	**BC - Others**
48	**06/12/2001**	**0049412/A1**	**US Patent App**	**Japanene Iijima Shinya / Seyama Yoshihiko**	**BC - Polyethylene glycol**
58	15/05/2003	0091456/A1	US Patent App	BASF AG	BC - Acrylate based
61	27/11/2003	0220424/A1	US Patent App	Apex Advanced Technologies LLC	BC-Others

2.2.2 MIM Patent Search – Binder (continued)

Table 8: Binder Patents (continued)

No	Granted Date	Publication Number	Patent Office	Company	Sub Category
69	**08/09/2005**	**0196312/A1**	**US Patent App**	**Batelle Memorial Institute**	**BC -Acid**
112	04/12/2014	WO 2014/ 191304 A1	WIPO	Damien Cartier	BC - Others

Binder selection is a crucial part of the metal injection moulding process. The exact composition of commercially available binders is undisclosed, however the main ingredients are frequently mixtures of organic compounds, namely waxes or synthetic polymers. The binders most commonly used in conjunction with metallic powders typically contain two or more polymeric materials and an oil or wax.

US Patent 5421853, Chen *et al* (1995) discloses an improved binder composition for use with metallic powder materials for the fabrication of precision components. The binder composition is comprised of a polymer having a relatively low solubility parameter and high crystallinity and a second polymer having a much higher solubility parameter combined with lower crystallinity and a third block copolymer containing blocks of the constituting monomers of the first and second polymers, or of monomers of respectively similar structures. The block copolymer enhances the miscibility of both the first and second polymer. The first and second binder constituents could be polypropylene/polymethyl methacrylate or polyethylene/polymethyl methacrylate.

US Patent 6171360 B1, Suzuki and Fukusima (2001), discloses further metal injection moulding binder improvements specifically related to an agar having average molecular weights in the range of 30,000 to 150,000. Agar is soluble in warm water and derived from seaweed. If the average molecular weight of the agar is less than 30,000 the green body has low strength and shape retention is difficult. The sintered product has poor dimensional stability. At the other end of the scale if the molecular weight of the agar is higher than 150,000 the agar has low decomposability and the sintered product has low mechanical strength. The binder may also include alcohols which increase the gel strength of the agar. Polyethylene glycol, a water soluble polymer alters the viscosity of the binder system and improves the fluidity of the mixture of the injection raw material at the injection

moulding step and improves the separation of the binder and metallic powder during subsequent debinding operations. Further binder additives such as formic acid, stearic acid and erucic acid are also referenced as a lubricant at the injection moulding stage in the process.

US Patent 6262150 B1, Behi, Duyckinck and Faelli (2001), describes a binder system which allegedly reduces undesirable cracks and distortion following the sintering process. The invention provides a process for forming moulded articles comprising at least one metallic powder, a gel forming polysaccharide binder and a sugar. The invention also describes the use of polyethylene glycol as an additive to enhance the wettability of the powder and binder mix.

US Patent Application Publication 2001/0049412 A1, Seyama, Shimizu and Iijima (2001), describes a binder comprised of 2 different resin types. The first resin is soluble in a predetermined solvent, a second resin is insoluble in the predetermined solvent of the first resin. The purpose of this invention is to minimise internal component defects and also to improve the processing time associated with binder removal.

A binder meeting the above criteria (Polyethylene glycol) was used as the water soluble resin and polymethyl methacrylate (PMMA) used as the water insoluble second resin.

The metallic powder particles are coated with the second water insoluble resin and subsequently kneaded to bind the encapsulated particles together with the first water soluble resin.

The detail of this patent can be clarified through the following example. An iron cobalt powder having an approximate powder particle size of 20μm can be mixed with binder to form a product having 40% binder by weight. The metallic powder particles and the PMMA are kneaded at 180ºC for one hour then cooled to 100ºC. The PEG is then added to the mixture. The combined mixture is then kneaded for one further hour and allowed to cool to room temperature to provide a raw material for injection moulding . Following injection moulding the PEG was removed by immersion in water for approximately 3 hours. The PEG removal was calculated by weight loss. In the example quoted in the patent almost 100% of the PEG was eluted following a 3 hour immersion cycle.

The moulded test pieces were found to exhibit good handling properties after the calculated 100% of PEG had been removed.

US Patent Application Publication 2005/0196312 A1, Nyberg, Weil and Simmons (2005), captures an enhanced binder composition for minimising the Carbon and Oxygen pick up by less than or equal to 0.2wt%. This patent is specific to the processing of highly reactive elements such as titanium and titanium alloys.

2.2.3 MIM Patent Search – Mixing

Table 9: Mixing Patents

No	Granted Date	Publication Number	Patent Office	Company	Sub Category
1	**11/05/1982**	**4329175**	**US Patent**	**Rolls-Royce Limited**	**M - Method**
5	02/05/1989	4826645	US Patent	Rolls-Royce Limited	M - Method
7	14/05/1991	5015289	US Patent	King Invest Co Ltd, Hiroshima	M - Composition
8	14/05/1991	5015294	US Patent	GTE Products Corporation	M - Composition
9	**12/11/1991**	**5064463**	**US Patent**	**Ciomek Michael**	**M - Composition**
11	16/09/1992	EP050396A2	European Patent App	Fujitsu Ltd	M - Method
26	24/06/1997	5641920	US Patent	Thermat Precision Technology	M - Composition
29	12/01/1999	5860055	US Patent	BASF	M - Method
34	30/11/1999	5993507	US Patent	Remington Arms	M - Composition
38	27/06/2000	6080808	US Patent	BASF	M - Composition
39	03/10/2000	6126873	US Patent	Allied Signal Inc	M - Method
42	22/05/2001	6234660/B1	US Patent	Gebrueder Loedige	M - Method
43	17/07/2001	6261336/B1	US Patent	Rutgers / Honeywell International Inc	M - Others
44	**17/07/2001**	**6261496/B1**	**US Patent**	**Allied Signal Inc**	**M - Method**
55	03/12/2002	6488887/B1	US Patent	Denso Corporation	M - Method
62	15/01/2004	0009089/A1	US Patent App	Ex One Co	M - Method
73	11/05/2006	0099103/A1	US Patent App	BASF AG	M - Composition
84	**02/10/2008**	**0237403/A1**	**US Patent App**	**General Electric**	**M - Method**

2.2.3 MIM Patent Search – Mixing (continued)

Table 9: Mixing Patents (continued)

No	Granted Date	Publication Number	Patent Office	Company	Sub Category
89	21/05/2009	0129961/A1	US Patent App	Viper Technologies LLC DBA Thortex Inc	M - Method
101	31/05/2012	DE 10 2010 061 960 A1	Deutsches Patent	Rolls-Royce Deutschland Ltd	M - Method
102	19/09/2012	EP 2 292 806 B1	European Patent App	Uexküll & Stolberg	M - Others
107	27/08/2013	CA 2806365	Canadian Intellectual Property Office	Pratt & Witney Canada Corp, CA	M - Method
109	22/07/2014	8784037 B2	United States Patent	Pratt & Witney Canada Corp, CA	M - Others
110	22/07/2014	8784044 B2	United States Patent	Pratt & Witney Canada Corp, CA	M - Others

A variety of methods are available to ensure the homogeneity of the feedstock. Planetary mixers are commonly used, however extruders can also be used for final feedstock preparation.

US Patent 4329175, Turner (1982), describes a method of manufacturing gas turbine rotor blade type components and bladed assemblies by the consolidation of moulded metallic powders by hot isostatic pressing. The shape of the component is obtained by powder filling moulds which are subsequently filled with an inert gas prior to being placed in an autoclave at approx 1200ºC and subjected to a gradually increasing pressure of between 12,000 to 14,000 psi for several hours. The component mould is filled by powdered metallic alloy. Vibratory assistance ensures that the powder fills the mould cavity prior to exposure to elevated temperatures. A variety of metallic powders having differing properties can be introduced to the mould in order to provide the finished component with tailored mechanical properties.

US Patent 5064463, Ciomek (1991), relates to a metal injection moulding feedstock comprised of a least one reactive element from a group consisting of aluminium,

magnesium and titanium. The objective of this patent is to capture a metal injection moulding feedstock having a reactive metal constituent which has good flow properties during the injection moulding process and can be used with conventional injection moulding equipment. The key element of this patent is that reactive metal powders which have historically been difficult to process, due to the tendency to form tenacious oxide films during processing, can be utilised without inherent adverse effects.

US Patent 6261496 B1, Duyckinck *et al* (2001), describes a novel process for preparing injection moulding feedstock in a continuous manner. This method of manufacture of feedstock is suitable for high volume manufacturing processes in which the metallic or ceramic powders in conjunction with a binder are fed into the barrel of a twin screw extruder for mixing and ultimately pelletising the extruded strands. The twin screw extruder ensures consistent pellet weight, it is widely accepted that the quality of the green state and final sintered product is largely dependent on the uniformity of the precursor moulding feedstock.

US Patent Application Publication 0237403 A1, Kelly *et al* (2008), describes a method of producing bimetallic high temperature components for gas turbine applications. The application cited relates to the manufacture of bimetallic gas turbine blades. The method of manufacture involves extruding 2 different alloy types separately into the mould followed by heating the combined alloy mixtures prior to sintering. This method challenges the current method of manufacture of bimetallic components which have traditionally been manufactured using joining processes such as electron beam welding, inertia welding and brazing processes. High temperature alloys such as RENE 77, RENE 80, RENE 142 and RENE N4 and N5 nickel base alloys are combined with a second alloy. The second alloy is required to have superior high temperature oxidation resistance to the first alloy and is utilised at the blade tip. The alloy selected for this application is normally a rhodium based alloy comprised of rhodium, platinum and palladium. The combined preform is sintered at a temperature below the solidus of the metallic powders yet high enough to cause the metallic powder particles to fuse together and consolidate. When the sinter cycle is complete the resulting turbine blade is allowed to cool. Further consolidation of the structure may be achieved by hot isostatic pressing. This achieves an almost 100% density.

2.2.4 MIM Patent Search – Injection

Table 10: Injection Patents

No	Granted Date	Publication Number	Patent Office	Company	Sub Category
4	08/11/1988	4783297	US Patent	NGK Insulators Ltd	I - Process
30	26/10/1999	5972269	US Patent	Taurus International Manufacturing Inc	I - Others
35	07/12/1999	5997603	US Patent	Shimizu Shokuhin Kaisha Ltd / Apex Co Ltd	I - Tools
37	02/05/2000	6056915	US Patent	Allied Signal Inc	I - Tools
49	11/12/2001	6328918/B1	US Patent	Honeywell International Inc	I - Tools
53	15/08/2002	0109260/A1	US Patent App	Jean Marc Boechat	I - Tools
56	**03/04/2003**	**0063993/A1**	**US Patent App**	**Delphi Technologies Inc**	**I - Others**
60	**24/07/2003**	**0138339/A1**	**US Patent App**	**Emerson Climate Technologies Inc**	**I - Tools**
63	05/05/2004	GB2394724A	UK Patent App	Alliance SA	I - Others
71	26/01/2006	0018780/A1	United States Patent App	Precision Castparts Corp	I - Others
72	02/02/2006	0024190/A1	US Patent App	General Electric	I - Others
77	**10/05/2007**	**0102572/A1**	**US Patent App**	**MTU Aero Engines GMBH**	**I - Process**
79	17/05/2007	0107216/A1	US Patent App	General Electric	I - Coating
81	**29/11/2007**	**0274854/A1**	**US Patent App**	**General Electric**	**I-Others**

2.2.4 MIM Patent Search – Injection (continued)

Table 10: Injection Patents (continued)

No	Granted Date	Publication Number	Patent Office	Company	Sub Category
83	21/08/2008	0199557/A1	US Patent App	Husky Injection Molding Systems	Tools
85	11/09/2008	0217817/A1	US Patent App	Cool Options Inc	I-Others
86	11/02/2009	0041607/A1	US Patent App	MTU Aero Engines GMBH	I-Others
87	16/04/2009	0096138/A1	US Patent App	MTU Aero Engines GMBH	I-Others
88	30/04/2009	0107646/A1	US Patent App	Husky Injection Molding Systems	Tools
91	**20/08/2009**	**0208360/A1**	**US Patent App**	**Boeing Co**	**I - Others**
93	04/02/2010	0028163/A1	US Patent App	Siemens	I - Others
94	**25/03/2010**	**0074740/A1**	**US Patent App**	**MTU Aero Engines GMBH**	**I - Others**
95	06/05/2010	0111745/A1	US Patent App	David J Urevich	I - Others
98	**16/02/2012**	**0039738/A1**	**US Patent App**	**Snecma**	**I - Process**
111	10/11/2014	RU 2532783 C 2	Russian Federation for Intellectual Property	Snecma (FR)	I - Others

The metal injection moulding process shares the same processing equipment as the traditional polymer injection moulding process. Advances in the injection moulding process are detailed below.

US Patent Application Publication 2003/0063993 A1, Reiter *et al* (2003), describes an injection moulding method in which composite components can be manufactured by the injection of dissimilar material types. Two or more material types are individually mixed with a binder system to form feedstocks. The feedstocks are melted and concurrently or sequentially injected into the mould and allowed to solidify. This particular invention provides composite injection moulded parts for applications such as permanent magnets.

US Patent Application Publication 2003/0138339 A1, Scancarello (2003), describes Metal Injection Moulding as an alternative method to traditional casting methods for the manufacture of compressor scroll type components. This method is novel in its approach to tackling the manufacture of components having a complex geometry in that the component is divided into component parts which are subsequently recombined using an appropriate joining process such as brazing.

US Patent Application Publication 2007/0102572 A1, Bohdal (2007), reveals a method of manufacture for the production of gas turbine vane assembly type components. One vane segment is manufactured by injection moulding several vane components. This patent recognises that there are several methods currently being utilised for the manufacture of such components from titanium and nickel base alloys such as forging and investment casting. Electro Chemical Machining is also utilised to a lesser extent. Cost reduction is the driver for manufacturing vane assemblies by the Metal Injection Moulding process from MTU Aero Engines GMBH. This disclosure provides 3 possible manufacturing methods for the manufacture of compressor vane segments. The preferred method of manufacture is to injection mould the vanes individually and then join together prior to a debinding process to form a moulded body for the vane segment. The second alternative method is a further refinement and comprises the moulded bodies of the vane undergoing a separate debinding process. The component parts are then joined together to form a vane segment. The third proposed alternative method of manufacture relies on a novel approach to injection moulding in which the joining together of the individual

vanes takes place during the injection moulding cycle via injection in the tool. Manufacturing the vane segment by this method requires the entire component to be subjected as a single unit to a uniform debinding process and subsequently sintered.

US Patent Application Publication 2007/0274854 A1, Kelly and Parks (2007), describes a method of producing metallic composite components for use in gas turbine applications. This disclosure could be used to manufacture compressor or turbine aerofoil type components from alloys such as Titanium 6/4, Udimet 720, 718 alloy and iron based alloys such as A286. The method of manufacture would involve the creation of a foam metal preform which is subsequently filled by the Metal Injection Moulding process with the alloy type specific to the relevant component application.

US Patent Application Publication 2009/0208360 A1, Wilkinson (2009), describes a binderless Metal Injection Moulding process in which the powdered alloy is assisted during the moulding process by the use of an ultrasonic transducer which is placed in contact with the mould die.

US Patent Application Publication 2012/0074740 A1, Sikorski *et al* (2009), describes the manufacture of a guide vane of a turbo engine, particularly a gas turbine engine. The disclosure recognises metal injection moulding as an interesting alternative to forging or casting for the manufacture of such components and offers a novel guide vane ring and a typical manufacturing method. The preferred embodiment of the invention would be a carrier ring of the guide vane manufactured from a forged nickel base alloy such as 718 alloy. The guide vanes would be manufactured from a more thermally stable alloy such as Udimet 720. The vanes would be produced by the Metal Injection Moulding process. The injection method of producing the vanes would involve the creation of multiple guide vanes simultaneously by a continuous moulding method.

US Patent Application Publication 2012/0039738 A1, Benard, Mengeling and Mottin (2012), describes the manufacture of a bladed disc, more commonly known as a stator guide vane assembly. The bladed sections of the assembly are manufactured separately from the platform. An intermediate powder compound is utilised in order to bond the vanes to the platform. Further sintering consolidates and strengthens the vane assembly.

2.2.5 MIM Patent Search – Debinding

Table 11: Debinding Patents

No	Granted Date	Publication Number	Patent Office	Company	Sub Category
2	28/04/1987	4661315	US Patent	Fine Particle Technology Corp	D - Aqueous
21	29/08/1995	5445788	US Patent	National Research Council of Canada	D - Others
22	02/07/1996	5531958	US Patent	BASF Corporation	D - Temperature
24	18/03/1997	5611978	US Patent	BASF Aktiengesellschaft	D - Acid
25	06/05/1997	5627258	US Patent	Komatsu Seisakusho KK	D - Aqueous
27	09/09/1997	5665289	US Patent	Chang I Chung	D - Temperature
28	24/11/1998	5840785	US Patent	Megamet Industries	D -Others
31	**02/11/1999**	**5977230**	**US Patent**	**Planet Polymer**	**D - Temperature**
33	23/11/1999	5989493	US Patent	Allied Signal Inc	D - Others
65	29/07/2004	0146424/A1	US Patent App	Forschungszent	D - Others
67	**03/03/2005**	**0046062/A1**	**US Patent App**	**Honeywell International Inc**	**D - Aqueous**
75	**09/11/2006**	**0251536/A1**	**US Patent App**	**General Electric**	**D - Others**
82	**20/12/2007**	**0292556/A1**	**US Patent App**	**Luptatech S A**	**D - Others**

Debinding is the term used in the metal injection moulding process to describe the removal of the binder from a ‘green’ body. The debinding step of the metal injection moulding process transforms the green preform into what is often referred to as the ‘brown’ preform. This is one of the most critical stages in the production of metal injection moulded components and has a direct effect on the dimensional stability and homogeneity of the finished component. Binder selection and chemistry for

particular alloy types is well established. Recent binder related advances relate to the further enhancement of established processes in order to meet economic, legislative or commercial requirements.

US Patent 5977230, Yang and Petcavick (1999), relates to a binder system which claims to be non-hazardous, safe, harmless and fully degradable. The binder system is comprised of a predetermined amount of polypropylene or polyethylene in order to provide the desired amount of strength to the brown part and polyvinyl alcohol (PVOH) to enhance the injection moulding properties. A typical injection moulding formulation created in accordance with the invention would contain 38 to 67 parts by weight of PVOH and approximately 8 to 32 parts by weight of PP or PE. The remaining 25 to 32 parts by weight are reserved for processing aids.

The processing aids typically contain from 3 to 19 parts by weight of water, 9 to 19 parts by weight of plasticiser, 3 to 6 parts by weight release agent and optionally 3 to 5 parts by weight debinding aid.

The PVOH used during the invention is a partially hydrolysed water soluble species of the alcohol available from Dupont under brand name Evanol. Stearic acid is used as a debinding aid. Glycerine is used as a suitable plasticiser.

Following injection moulding the green state preforms are immersed in water at ambient temperature to dissolve the PVOH out of the green preform thus turning it to the brown preform consisting of powdered metal and an amount of PP or PE sufficient to provide a stable structure and allow for handling. The residual polymer is vaporised during the subsequent sintering cycle.

US Patent Application Publication 2005/0046062 A1, Stevenson *et al* (2005), describes a method for recycling water based powder injection moulding compounds applicable to scrap material. This invention requires regranulation equipment and a rehydration process. This invention is specific to material scrap prior to the thermal processing operation.

US Patent Application Publication 2006/0251536 A1, Kelly (2006), relates to the use of microwave energy to remove the residual binder from the preform and sinter the powders particles. The microwave sintering operation replaces the traditional furnace sintering method of production and is followed by hot isostatic pressing.

This invention is a significant step change in the method of manufacture of metal injection moulded components. Prior art methods for sintering MIM preforms require controlled furnace heat treatment at elevated temperatures in order to sinter the metallic powder particles together. This method of thermal processing requires long heat treatment cycles and can often result in internal voids being created due to the surface of the component reaching temperature prior to the core. This phenomenon can result in variable sintering rates between the surface and the core of the component.

In this particular patent the author describes a method of manufacturing aerofoil type components from a variety of aerospace alloys such as 718 alloy or Udimet 720 as well as the iron based alloy A286. The particle size of the alloy should be less than 100µm.

The patent is applicable to rotating turbine blades, stationary turbine vanes and turbine shrouds. Components manufactured to this particular method would follow the following manufacturing sequence illustrated in Figure 6 below.

Mix powder & binder
Melt binder
Form mixture into preform
Remove preform from forming apparatus
Leach binder from preform
Microwave sintering
Hot isostatic pressing
Final Processing

Figure 6: Metal Injection Moulding - Operation Sequence

This operational sequence and processing technique enable the manufacture of high quantities of net shaped components. During the microwave sintering operation the component may be heated by a mixture of direct and reflected microwave energy. The rate of heating is dependent on the wattage of the microwave source and also the component size. A microwave frequency of 2.4 GHz is known to couple with and heat metallic parts without passing through solid metals.

US Patent Application Publication 2007/0292556 A1, Machado *et al* (2007), describes a method for plasma assisted thermal debinding of powder injection moulded parts. In the conventional metal injection moulding process the debinding step has traditionally been conducted by solvent and thermal processing. This

disclosure offers a significant step change in the way that components are manufactured. Traditionally after injection moulding, debinding must be performed carefully in order that the component integrity is not undermined. Another disadvantage with the conventional process is that the component processing furnaces often have organic residues deposited onto the furnace internals and vacuum pumping system.

Plasma assisted thermal debinding enables the debinding cycle to be incorporated into the sintering cycle using the same processing equipment. This process significantly enhances the processing time of components.

The plasma assisted debinding process avoids the formation of organic residues in the furnace and vacuum pumping systems when compared to the traditional thermal debinding process.

2.2.6 MIM Patent Search – Sintering

Table 12: Sintering Patents

No	Granted Date	Publication Number	Patent Office	Company	Sub Category
3	23/08/1988	4765950	US Patent	Risi Industries	S - Others
32	**16/11/1999**	**5985208**	**US Patent**	**Allied Signal Inc**	**S - Atmosphere**
46	23/10/2001	6306196/B1	US Patent	Hitachi Metals Ltd	S - Temperature
47	27/11/2001	6322746/B1	US Patent	Honeywell International Inc	S - Temperature
50	26/02/2002	6350407/B1	US Patent	Injex Corporation	S - Others
52	06/08/2002	6428595/B1	US Patent	Injex Corporation	S - Temperature
54	14/11/2002	0168282/A1	US Patent App	Honeywell International Inc	S - Temperature
57	**22/04/2003**	**6551551/B1**	**US Patent**	**Caterpillar Inc**	**S - Others**
68	26/05/2005	0112016/A1	US Patent App	Japanese / Taisei Kogyo Co Ltd	S - Others
74	27/07/2006	0162494/A1	US Patent App	Japanese / Mitsubishi Steel MFG Co Ltd	S - Temperature
76	04/01/2007	0003426/A1	US Patent App	Honeywell International Inc	S - Others
78	17/05/2007	0110608/A1	US Patent App	Ex One Co	S - Atmosphere
80	**30/08/2007**	**0202000/A1**	**US Patent App**	**MTU Aero Engines GMBH**	**S - Others**
90	**06/08/2009**	**0196761/A1**	**US Patent App**	**Siemens**	**S - Others**
104	17/10/2012	EP 2 511 031 A1	European Patent App	Höganäs (SE)	S - Others
105	20/06/2013	DE 10 2011 089 260 A1	Deutsches Patent	Rolls-Royce Deutschland Ltd	S - Others

2.2.6 MIM Patent Search – Sintering (continued)

Table 12: Sintering Patents (continued)

No	Granted Date	Publication Number	Patent Office	Company	Sub Category
113	12/05/2015	9028744 B2	United States Patent	Pratt & Witney Canada Corp, CA	S - Others
114	25/06/2015	WO 2015/ 091366 A1	WIPO	Hoganas AB (PUBL), SE	S - Others

Sintering is the joining process utilised to bond the powder particles together and create a structurally sound component. Control of the key process variables of temperature and time is important as is the surface condition of the powdered alloy.

US Patent 5985208, Zedalis, Sherman and LaSalle (1999), describes a debinding and sintering method for the production of net shaped components using 17-4PH stainless steel by metal injection moulding. In this case the debinding and sintering cycles may be combined to achieve a more economically viable process for both the consumer and aerospace industries. The invention is unique in that it claims to produce mechanical properties comparable to cast and wrought 17-4 PH components for aerospace and other structural components. The patent cites a jet engine diffuser vane as a possible application of the process. The components are manufactured by the net shape metal injection moulding process using an aqueous feedstock binder. An agar based aqueous binder has been identified as applicable to the manufacture of stainless steel components using MIM. Debinding in an air atmosphere is the most significant factor in minimising carbon pick up. Air debinding was also found to be a factor in maximising the sintered density of the component. The final sintering operation is conducted using a hydrogen atmosphere to reduce any residual oxides formed during the debinding operation.

US Patent 651151 B1, Gegal and Ott (2003), provides a method for joining powder metallurgy components. The method incorporates a bonding agent which is comprised of a binder and particulate powder material. During the sintering cycle the surfaces to be joined are consolidated and the joint is formed by solid state diffusion of fine particles.

US Patent Application Publication 2007/0202000 A1, Andrees *et al* (2007), describes a method of manufacturing gas turbine components. The disclosure recognises the difficulties encountered by adopting the metal injection moulding process for components having variable sectional thicknesses. In order to overcome these problems the team of inventors devised a method of joining several injection moulded components during the sintering operation. Mechanical interlocking (form fitting surface contact) and pressure are used to supplement the traditional surface diffusion bonding methods.

This manufacturing method is used for the production of blades and blade segments made from nickel base alloys or titanium alloys.

Following sintering, if required, the components may be subjected to a further finishing process or alternatively the assembly may be in a suitable condition for installation.

US Patent Application Publication 2009/0196761 A1, James (2009), describes an alternative method of joining metal injection moulded components which incorporate a series of channels which are subsequently filled with a powder and binder mixture in a region common to the component parts of the assembly. The strength of the joint is supplemented by mechanical interlocking.

2.2.7 Patent Review Summary

Analysis of the metal injection moulding time line indicates that the process continues to evolve, fuelled by innovations in the key processing steps as well as the manufacture of the powdered raw materials.

Commercially available gas atomised nickel based superalloy powders such as 713 alloy, 718 alloy and Udimet 720 provide a suitable platform for powder metallurgy research.

The Metal Injection Moulding process delivers a stable and consistent method of manufacture and has driven the application of the process to compete in the manufacture of components which have traditionally been produced using established manufacturing techniques such as casting or precision die forging.

Successful advances in the binder chemistry and debinding methods have enhanced the environmental credentials of the metal injection moulding process which is considered to have minimal environmental impact .

The availability of a net shape three dimensional forming process, which can compete with traditional manufacturing methods, has led scientists and engineers to explore the possibilities of metal injection moulding as a credible manufacturing method for applications within the compressor of the modern gas turbine engine.

Market leaders of gas turbine technology such as Rolls Royce, General Electric and MTU Aero Engines are actively researching the merits of the metal injection moulding process in order to exploit the commercial benefits of the process and realise a commercial advantage.

The potential applications for the process lie in the families of compressor components whose current method of manufacture involves labour intensive operations, a large proportion of thermo-mechanical processing steps or a significant amount of waste raw material being produced per part. To this end the manufacture of compressor blades, vanes and vane assemblies is the main focus for the application of the process.

Figure 7 below illustrates the rise in process interest, while Figure 8 illustrates the key industry participants.

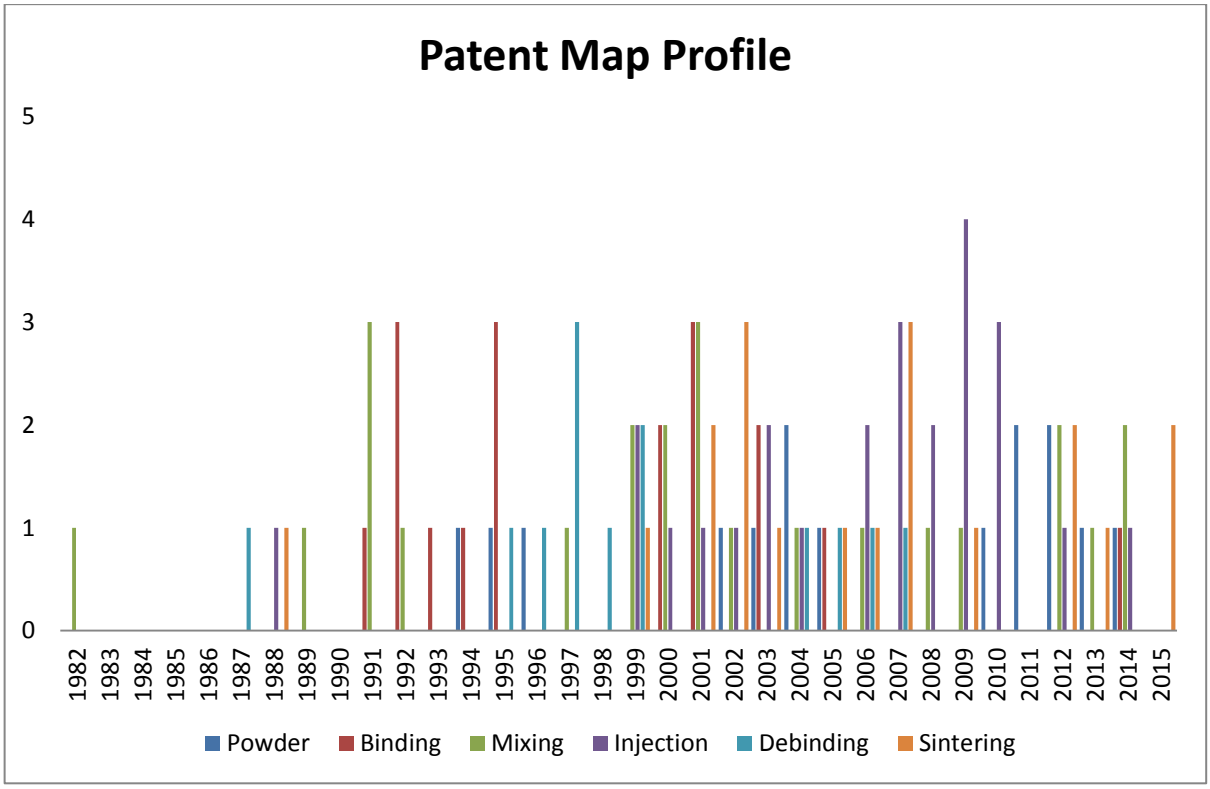

	Powder	Binding	Mixing	Injection	Debinding	Sintering
Totals	15	18	24	25	13	19

Figure 7: Patent Timeline

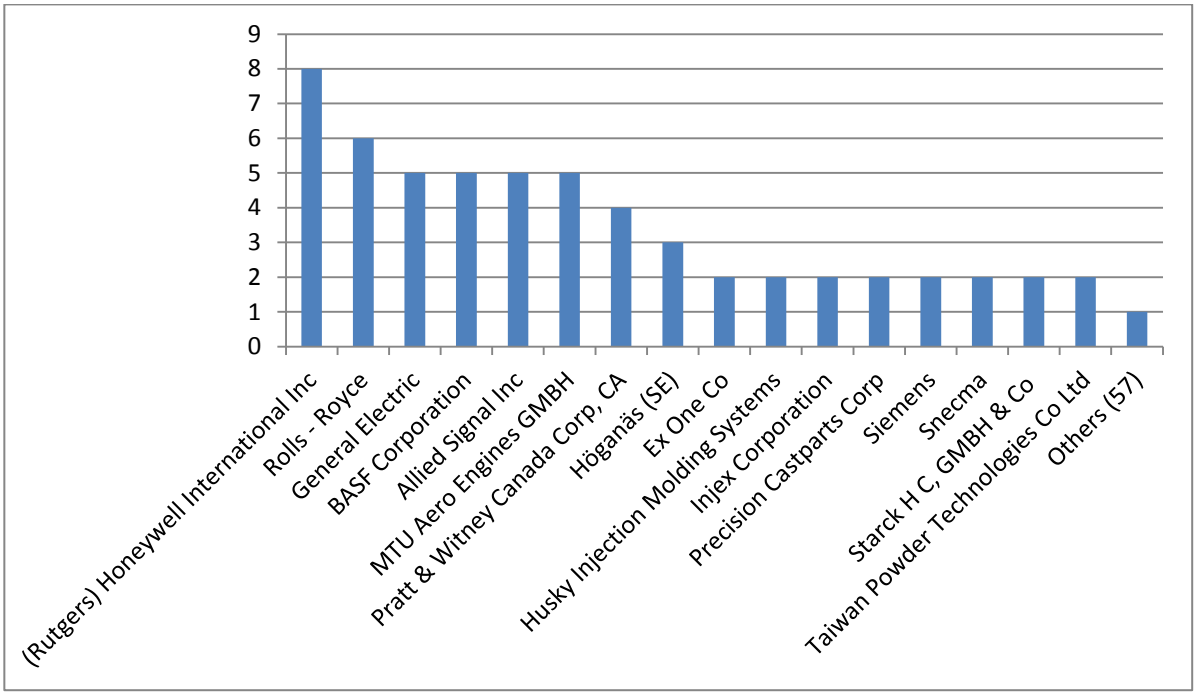

Figure 8: Main Industry Players

CHAPTER 3

FEEDSTOCK AND TEST PIECE PREPARATION

3. Feedstock and Test Piece Preparation

3.1 MIM Feedstock

The injection moulding feedstock used to manufacture the 718 alloy products specific to this research was developed in situ and based upon prior injection moulding knowledge with alloy types of a similar powder particle size distribution and binder system. Tables 13 to 15 capture the key powder characteristics. One factor which influenced the selection of the argon gas atomised 718 alloy powder was the cost of the raw material. Commercially available powders are specified by the powder particle size and distribution. The smaller the powder size the higher the cost of the alloy due to increased manufacturing costs. The powder particle size selected for injection moulding trials presenting a particle size less than 16μm (90%-16μm), with a distribution as detailed below. The 718 alloy powder complied with the chemical compositions detailed below. The product was commercially available without additional customer specific requirements.

In order to transform the powdered 718 alloy into a form which can be readily injection moulded, blending with further materials is necessary. The blended materials form what is commonly referred to as injection moulding feedstock.

Control of the composition and properties of the metal injection moulding feedstock are recognised as critical aspects of the process. The feedstock composition used for injection moulding both trial components and test bars was manufactured from the following constituents.

- Argon atomised powdered 718 Alloy (90% -16μm)
- Polymethyl methacrylate (PMMA)
- Stearic Acid (SA)
- Polyethylene glycol (PEG).

The role of the Polyethylene glycol is to provide adequate green strength to the moulding prior to the debinding and sintering operations. Polymethyl methacrylate (PMMA) provides inter particle powder cohesion during the debinding and sintering operations. The stearic acid provides good mould release properties ensuring the moulding is not damaged following completion of the forming cycle. Stearic acid provides mould lubrication.

Table 13: 718 Alloy Powder Chemical Analysis

Powder specification 90%-16 µm*			
Element	Minimum	Actual	Maximum
Nickel	50.0	52.4%	55.0
Chromium	17.0	18.9%	21.0
Niobium	4.7	5.0%	5.5
Molybdenum	2.8	3.1%	3.3
Silver	0	2ppm	5
Titanium	0.7	0.98%	1.15
Aluminium	0.3	0.43%	0.70
Silicon	0.000	0.22%	0.35
Manganese	0.000	0.16%	0.35
Carbon	0.020	0.050%	0.080
Copper	0.000	0.023%	0.200
Cobalt	0.000	0.017%	1.000
Phosphorus	0.000	0.010%	0.015
Sulphur	0.000	0.003%	0.008
Boron	0.000	0.001%	0.006
Iron	Remainder		

Table 14: 718 Alloy Particle Size and Cost

Specification	Size (µm)	Weight (kg)	Price (GBP/kg)
90%-16 µm *	-16	200.00	94.68
95%-12 µm	-12	200.00	122.98
90%-10 µm	-10	200.00	188.94

Table 15: 718 Alloy Particle Size Distribution

Specification	D0.1	D0.5	D0.9
90%-16 µm *	3.5-4.5	8.0-9.0	15.0-16.0
95%-12 µm	2.5-3.5	5.5-6.5	9.5-11.0
90%-10 µm	2.0-3.0	4.5-5.5	9.0-10.0

Prior to the formulation of the feedstock the 718 alloy powder was analysed in detail. This is an important part of the raw material characterisation. A series of trials were initiated to substantiate the maximum powder particle size and also to gain an appreciation of the powder particle distribution throughout the powder lot.

The trials were conducted using specialised industry standard powder classification equipment. A Malvern Mastersizer Hydro 2000G was used for the analysis.

The Malvern Mastersizer utilises laser diffractometry techniques to determine the powder characteristics. The key components are captured in Figure 9. Laser diffraction is considered to be the preferred method for spherical particle characterisation in the size range of 0,10μm to 3.0mm. The operation of the laser classifier is detailed in Figure 9 below.

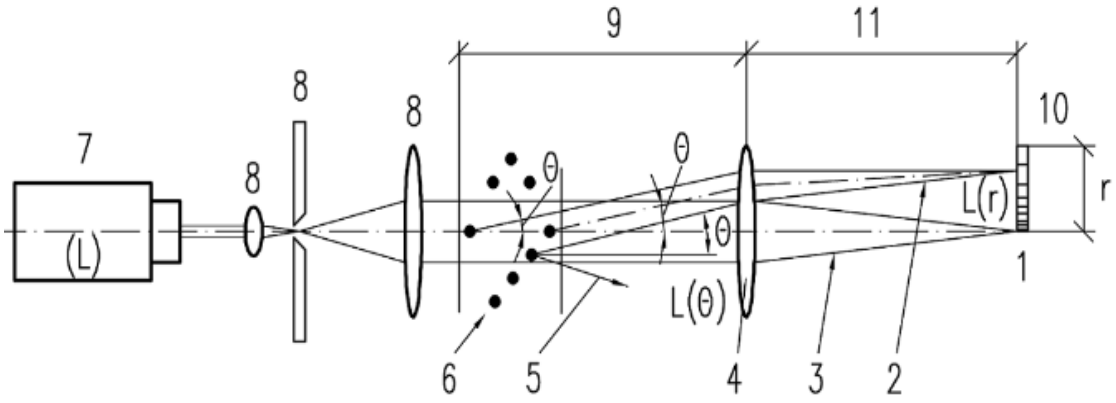

1 Obscuration detector
2 Scattered beam
3 Direct beam
4 Fourier lens
5 Scattered light not collected by lens
6 Particle ensemble
7 Light source laser
8 Beam processing unit
9 Working distance of lens
10 Multi element detector
11 Focal distance of lens

Figure 9: Typical Laser Diffraction Instrument Schematic Diagram

The principles and controls associated with particulate material analysis are captured in ISO 13320-1:1999. The laser diffraction system is based upon the principle that the powder particles will scatter the monochromatic light in various directions. The light source is normally provided by a low power He/Ne laser. The beam processing unit expands the monochromatic light. The amount of dispersed light is a function of the powder particle size. Large particles scatter light at small angles and vice versa ($\theta \sim 35/d$). The light scattered from large particles is more intense than the light from the smaller particles. The measurement instrumentation assumes that the powder particle size is spherical in nature. The diffracted light of the particles creates a radial symmetrical interference pattern, which represents a measure of the particle size distribution. The laser diffraction system cannot differentiate between large particles and agglomerations of small particles, however if powder agglomeration is suspected conventional optical microscopy can be used for further investigation. The powdered sample is suspended in a suitable medium. The suitability of the medium is based upon several considerations such as refractive index, inertness, corrosiveness and hazardous effects. In terms of powder sample

concentration in the dispersant, it is important to operate within the recognised parameters in order to avoid multiple light scattering. When the sample is introduced to the light beam, a number of scans take place. Each detector calculates an average signal which is stored on the computer. The calculation method depends on the difference between the dispersed light sample and a bland test run. This measurement provides an indication of the total amount of scattered light.

Powder Particle Size Distribution

In order to capture the key characteristics of the 718 alloy powder, nine powder samples were analysed using the Malvern Mastersizer 2000. The purpose of the analysis was to corroborate the powder particle size and the particle size distribution within the powder lot. Prior to sampling, appropriate care was taken to ensure that the powder samples selected were representative of the powder lot.

The experiment was repeated several times to ensure good repeatability and accuracy of test results. Due to the nature of the test, no specific equipment calibration was performed.

Malvern Classifier settings
Particle RI 1.980
Dispersant RI 1.330
Sample range 0.020-2000.000μm
Span 10-90%

The output from the powder trials is captured in Figures 10 to 18 and illustrates the consistency of the powder samples. A particle size summary is documented in Figure 19. A summary of all nine trials and corresponding statistical analysis is captured in Tables 16 and 17.

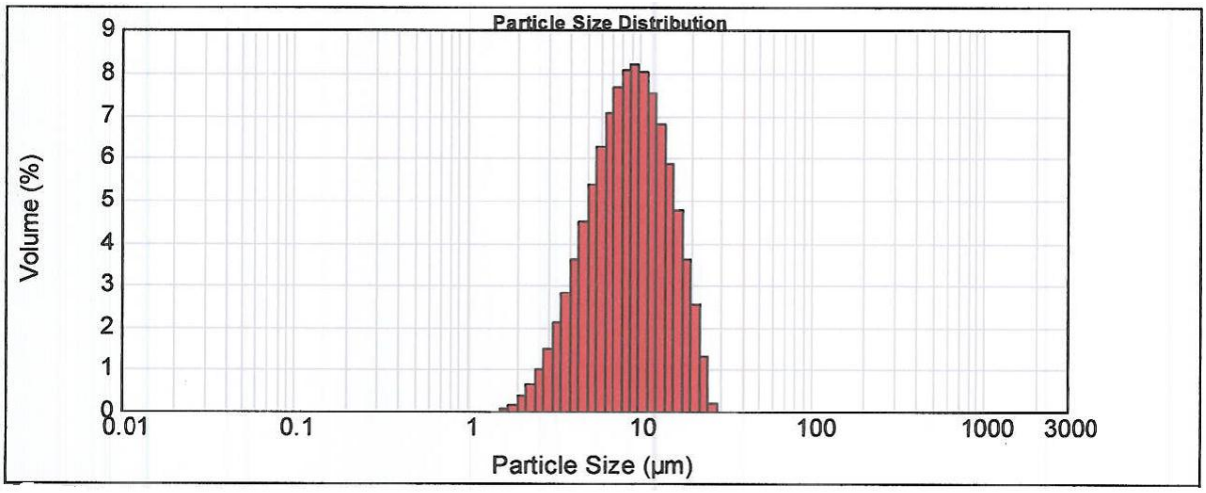

Figure 10: Distribution Analysis 1

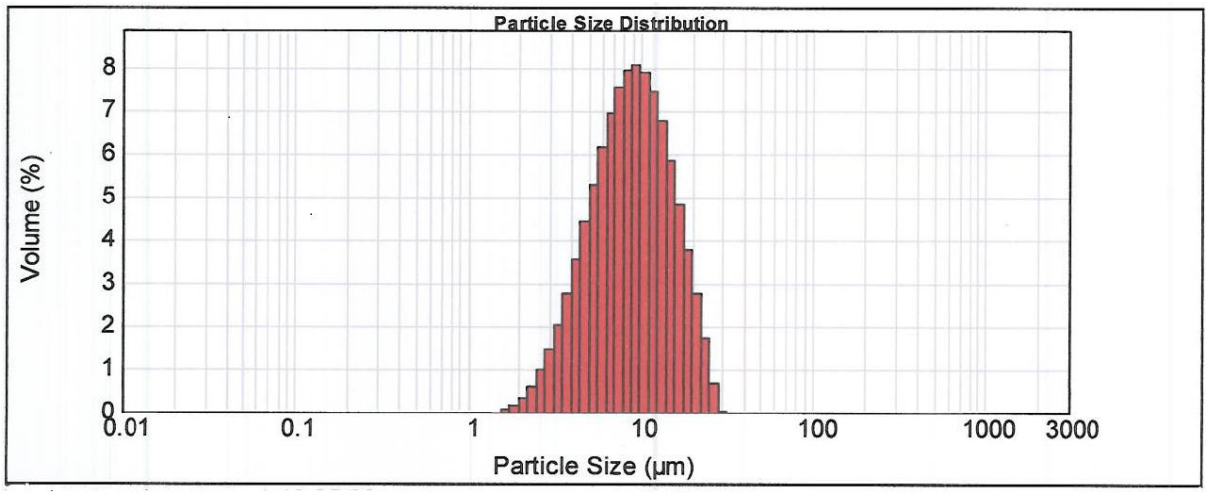

Figure 11: Distribution Analysis 2

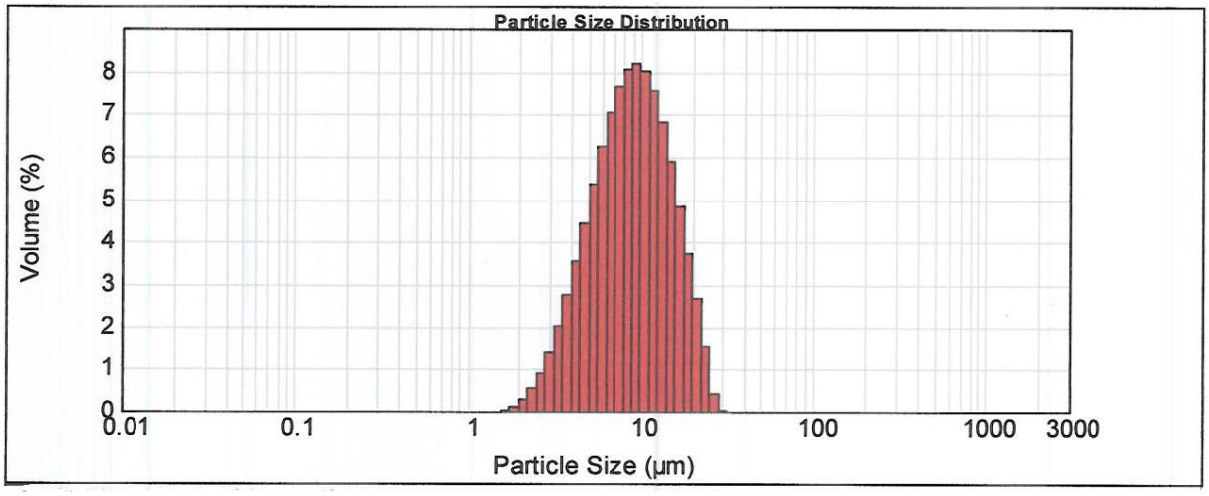

Figure 12: Distribution Analysis 3

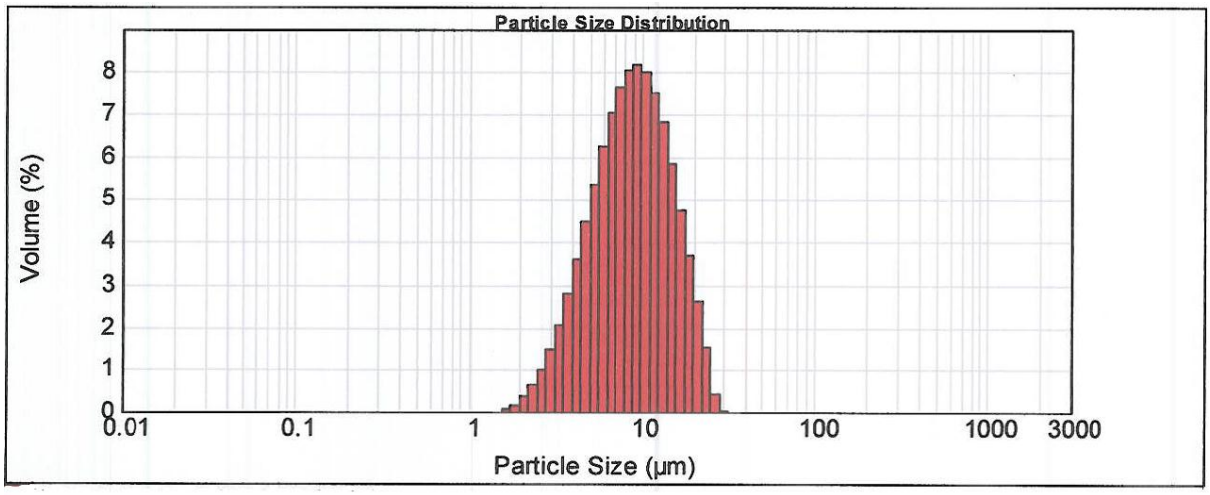

Figure 13: Distribution Analysis 4

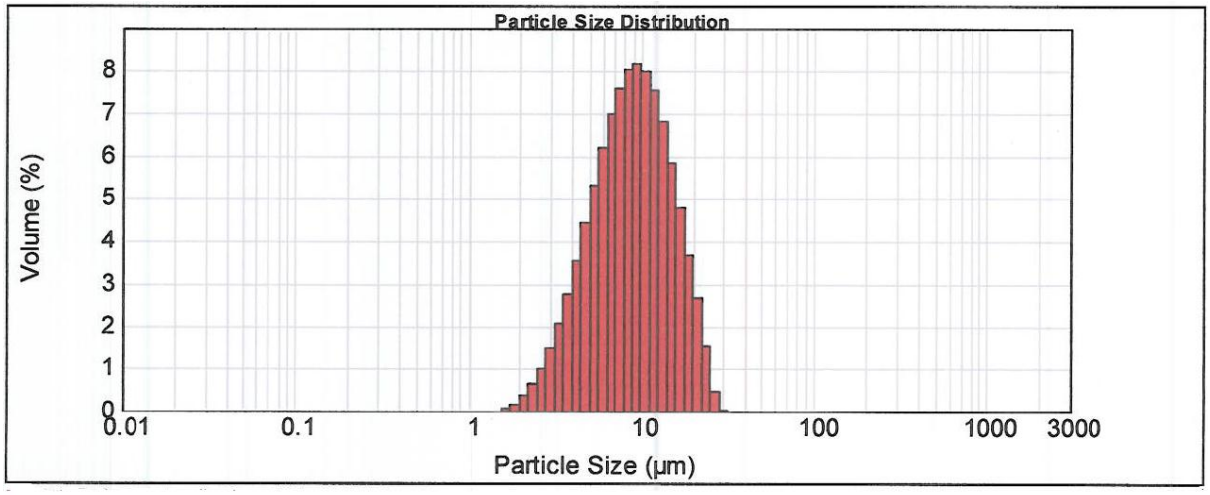

Figure 14: Distribution Analysis 5

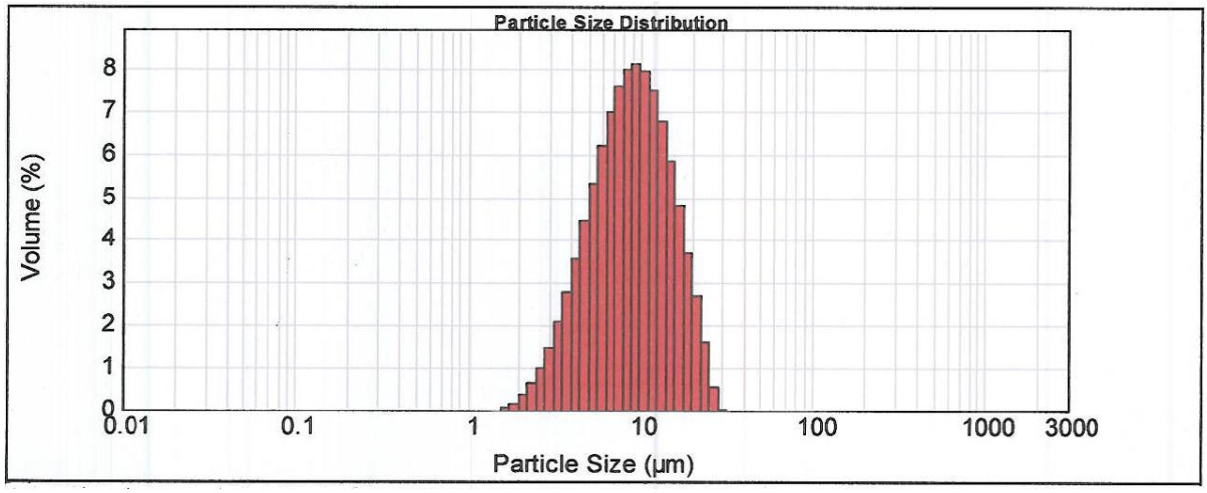

Figure 15: Distribution Analysis 6

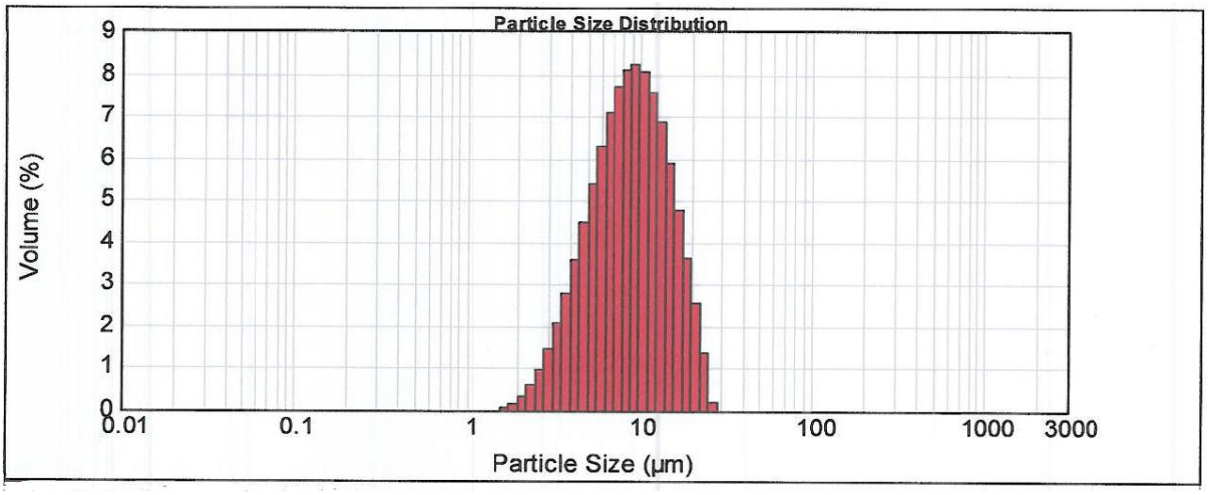

Figure 16: Distribution Analysis 7

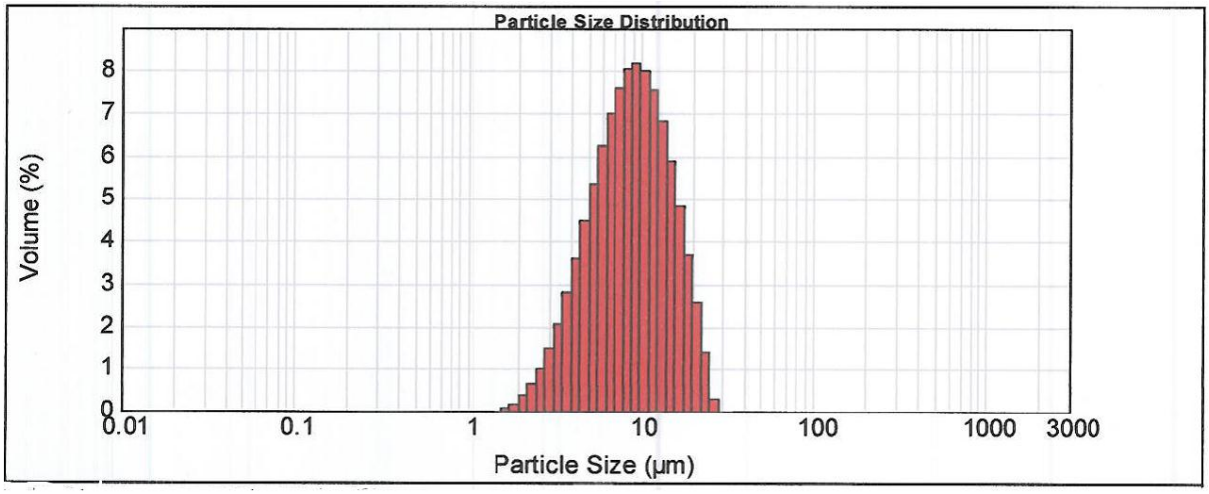

Figure 17: Distribution Analysis 8

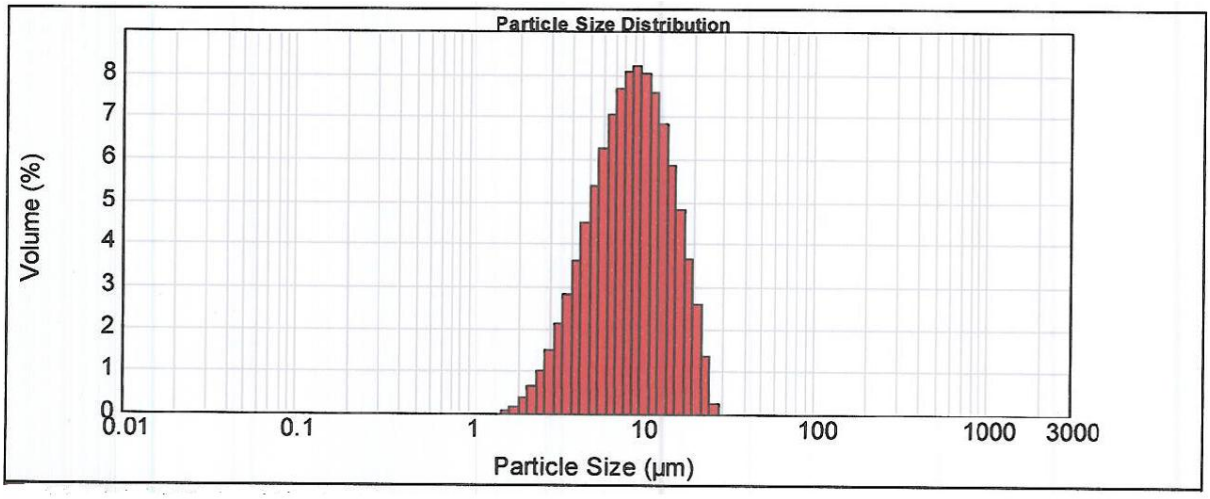

Figure 18: Distribution Analysis 9

Table 16: Distribution Analysis Results

Sample Number	D(10) µm	D(50) µm	D(90) µm
1	4.176	8.789	16.785
2	4.225	8.916	17.348
3	4.265	8.889	17.090
4	4.204	8.837	17.018
5	4.204	8.862	17.057
6	4.205	8.872	17.182
7	4.212	8.813	16.815
8	4.193	8.834	16.924
9	4.177	8.807	16.848

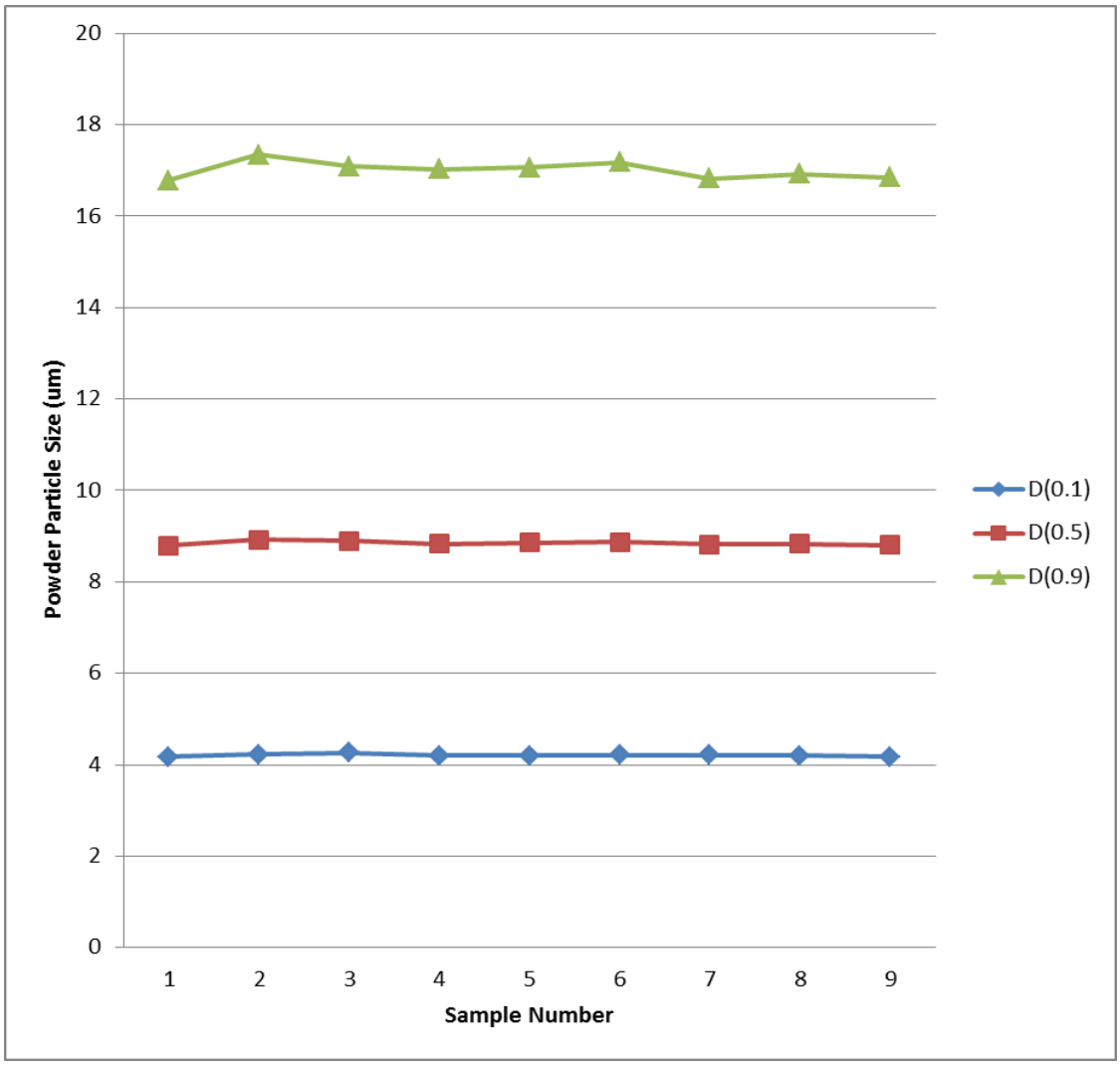

Figure 19: Particle Size Summary

Table 17: Particle Size Distribution - Data Analysis

Powder Sample	D(10) µm	D(50) µm	D(90) µm
Arithmetic Mean (*A*)	4.207	8.847	17.007
Range	0.089	0.127	0.563
Variance (σ^2)	0.0006	0.0015	0.0305
Standard deviation (σ)	0.025	0.039	0.175

Four measures of the powder were selected to describe the variation around each of the distribution levels. The measures were selected in order to establish a base line of the powder characteristics.

Arithmetic Mean (A)

The arithmetic mean was calculated for each of the three powder distribution levels. The mean is the average of the individual numerical values for each of the distributions. This provides an indication of the central tendency. This value estimates the centre of a set of numbers and is shown in Figure 20 below.

$$A = \frac{1}{n} \sum_{i=1}^{n} (x_i)$$

Figure 20: Arithmetic Mean Equation

Using the above formula, n is the total number of values and x_i ($x2$, $x1$, ... xn) are the individual numbers in the data set.

Range

The range is a measure of dispersion of the recorded values. This measure provides an indication of how much the values in the measured sample are likely to differ from their mean.

Range = maximum (x_i) – minimum (x_i)

The range is easily calculated by subtracting the lowest from the highest value.

Variance (σ^2)

The variance is one of the measures of dispersion, that is a measure of by how much the values in the data set are likely to differ from the mean of the values. It is the average of the squares of the deviations from the mean. Squaring the deviations ensures that negative and positive deviations do not cancel each other out. The variance was calculated for the entire population at each distribution level. The variance is one of the measures of dispersion. This is a measure of how much the values in the sample set are likely to differ from the mean of the values. The variance is the average of the squares of the deviations from the mean as Figure 21. Using the formula below N is the population size and μ is the population mean.

$$\sigma^2 = \frac{1}{N}\sum_{i=1}^{N}(x_i - \mu)^2$$

Figure 21: Variance Equation

Standard Deviation (σ)

Standard deviation is the square root of the variance, and is captured in Figure 22 below. It is another measure of dispersion and is a measure of by how much the values in the data set are likely to differ from the mean. This measure corroborated the findings of the variance analysis.

$$\sigma = \sqrt{\frac{1}{N}\sum_{i=1}^{N}(x_i - \mu)^2}$$

Figure 22: Standard Deviation Equation

In the illustration above N is the population size and μ is the population mean.

The Malvern Classifier results provided a good repeatable measure of the powder particle size distribution within the powder lot. From the further data analysis carried out using 4 statistical measures, we are able to say that D10 powders demonstrate a more reduced level of powder particle size distribution than D90 powders. This phenomena is likely to be as a result of the manufacturing tolerances being applied during the powder manufacturing process. At this stage in the research it is

considered to be more important to recognise and document the characteristics of the powder so that future trials will provide accurate repeatable data. The ability of the powder to flow uniformly during the injection moulding process and also to provide strength to the moulding during debinding and sintering trials are critical characteristics of the powder particle size distribution.

3.2 Formulation of Feedstock Binder

The binder is made up of three main constituents, the chemical formulae and state are illustrated by Figures 23 to 26.

Synthetic Acrylic Emulsions

Polymethyl methacrylate is considered to be one of the most widely used commercially available acrylic polymers, due partly to the relative ease in which the polymer can be manufactured. The polymer is used extensively for optical applications as an alternative to glass, due to the transparency of the product and is readily available under many commercial trade names.

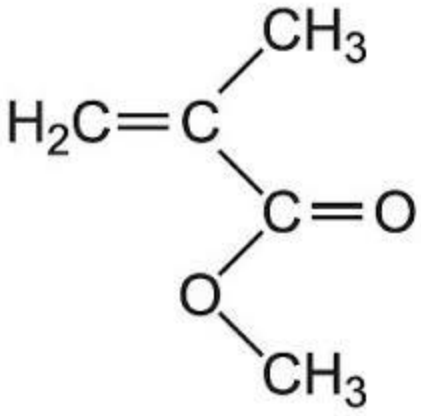

Figure 23: Polymethyl Methacrylate Formula

The polymers are generally not branched, with the exception of the methyl and methacrylate side groups. The main difference between uncompounded commercial grades is the molecular weight of the polymer. Cast polymethyl methacrylate has a relatively high average molecular weight of around 10^6.

The glass transition temperature may be around 104ºC, however the length of the molecular chains and entanglements inhibit material flow below the decomposition temperature. For injection moulding and extrusion applications significantly lower molecular weight materials are used.

Commercially available material is considered to be more syndiotactic than atactic. The glass transition temperature (Tg) is generally recognised as being higher than polyethylene. The tacticity of the polymer has an influence on the glass transition temperature due to the influence of intermolecular dipole forces on the polar groups.

As a constituent of the 718 alloy feedstock, the polymer melt viscosity is another factor which requires consideration. Since the polymer melt viscosity is sensitive to fluctuations in temperature, accurate control and monitoring equipment is necessary.

Polyethylene Glycol

Polyethylene glycol is a polyether compound widely used in industrial and pharmaceutical applications. The manufacture of polyethylene glycol is achieved by the polymerisation of ethylene oxide. The molecular weight of the product is a significant factor, as it can exist in both liquid and waxy solid conditions.

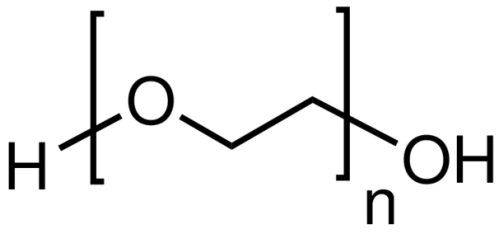

Figure 24: Polyethylene Glycol Formula

Polyethylene glycol is incorporated in the feedstock formulation in order to act as a wetting agent for the individual feedstock constituents. The wetting and binding properties of polyethylene glycol are well established through extensive utilisation in the ceramics industry. The melting point of the product utilised in the feedstock formulation is approximately 70ºC. This corresponded to molecular weight of approximately 284.48g/mol.

Stearic Acid

Stearic Acid is a saturated fatty acid which is widely available commercially. The inclusion of small amounts of stearic acid to the formulation of the feedstock was to enhance the mould release of the components / test bars following the moulding operation.

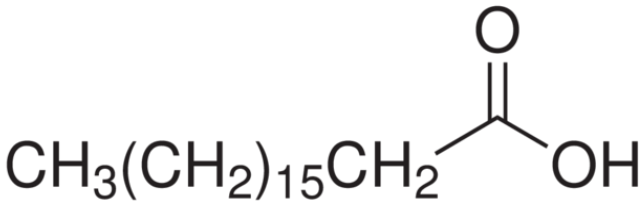

Figure 25: Stearic Acid Formula

Polymethyl methacrylate Polyethylene glycol Stearic acid

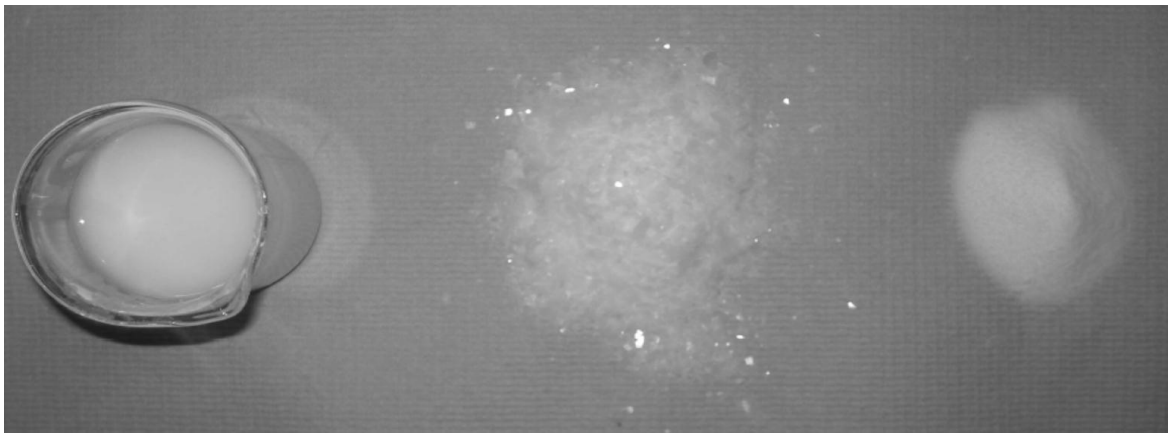

Figure 26: Binder Constituents

Feedstock Manufacture

The manufacture of the injection moulding feedstock is a critical preparatory part of the manufacturing process. The powdered 718 alloy is initially mixed manually with the polyethylene glycol and stearic acid additives. The dry mix is then decanted into clean centrifuge tins. The mix is then gently rotated to break up and disperse the polyethylene glycol flakes and disperse the stearic acid granules. Care is required to avoid over heating as a result of frictional forces between the walls of the container and the dry feedstock materials. The key processing steps are captured in Figures 27 to 31 below.

Figure 27: Initial Feedstock Compounding

Once the additives are thoroughly mixed the rotational speed of the centrifugal mixer is increased in order to melt the polyethylene glycol particles. The temperature of the mix reaches approximately 60ºC forming a homogeneous paste. At this stage the last remaining additive, the polymethyl methacrylate is then added and mixed thoroughly.

Figure 28: Fully Compounded Feedstock

When the mixing process is complete the dough is removed from the centrifuge, spread thinly and allowed to dry for a period of 24 to 36 hours at approximately 40ºC.

Figure 29: Feedstock Drying

Once dried the feedstock is then broken up and ground down into large granules which are approximately 15mm in length. In order to further homogenise the feedstock mix an extrusion operation is conducted.

Figure 30: Feedstock Granules

The feedstock extrusion process involves heating the dried granules to 120ºC - 130ºC and under a pressure of 6 bar extruding the molten mix. Heating is effected by the use of 2 collars on the reservoir. The outlet from the reservoir is a 4mm nozzle. The feedstock is then cut into 5-10mm strands and allowed to cool.

This process is then repeated several times to ensure that the product is well mixed. Once cooled the feedstock is stored in a clean dry container.

Figure 31: Feedstock Strands

To assess the quality of the injection moulding properties of the feedstock several random samples, which were considered to be representative of the batch, were processed using a capillary rheometer. The rheological properties of injection moulding feedstock are considered to be one of the most important process variables. The capillary rheometer is essentially a highly engineered ram extruder from which accurate processing data such as the time and pressure are collected.

The feedstock manufacturing process is detailed in Table 18.

Op	Process step	Description & Equipment	Method
1	**Feedstock mixing**	The purpose of this operation is to ensure thorough mixing of the feedstock ingredients. Mixing was conducted using a dual axis centrifugal mixer. Hauschild DAC 3000	Powdered 718 Alloy - 2306g Polyethylene glycol - 113.2g Polymethyl methacrylate - 51.2g Stearic Acid - 2.75g Powdered 718 alloy is manually mixed with the polyethylene glycol flakes and stearic acid granules. The mixture is then centrifugally mixed. 800 rpm for a duration of 2 minutes 800 rpm for a duration of 2 minutes 800 rpm for a duration of 2 minutes PMMA added 1000 rpm for a duration of 2 minutes 1200 rpm for a duration of 2 minutes 1200 rpm for a duration of 2 minutes The feedstock was then inspected for homogeneity
2	**Feedstock drying**	The purpose of this operation is to remove the excess moisture from the polymethyl methacrylate emulsion. A thermostatically controlled air circulating oven.	The thoroughly compounded feedstock was then rolled to thin sections in order to increase the surface area for drying. The rolled mixture was dried at 40ºC for 36 hours.
3	**Feedstock fragmentation**	Manual process in which the dried feedstock mixture is roughly broken up into approximately 20mm square sections. Manual process	The dried feedstock was divided where previously marked.
4	**Feedstock extrusion**	Manual or automatic process in which the dried feedstock is extruded to optimise homogeneity and remove any entrapped trapped air. Manual	Orifice size - 4mm Temperature - 110-125ºC Pressure - 6bar (comp air from mains) No of cycles - 3 cycles per batch Cut pellet length - approximately 10mm
5	**Feedstock rheology**	Malvern RH2100 Rheometer	Laminar flow in the region 3000-10000 s-1 Assigned acceptance limits at 140 or 150ºC
6	**Feedstock complete**	Feedstock storage The feedstock was provisionally lifed at 6 weeks.	Pelletised feedstock was stored in an air tight container to prevent the ingress of moisture or other contaminants.

Table 18: Feedstock Method of Manufacture Summary

3.3 Manufacture of Metal Injection Moulded Test Pieces and Components

The manufacture of suitable injection moulded test pieces and components was achieved using and a combination of processing equipment. A standard Arburg 320C polymer injection moulding machine was utilised to manufacture both the injection moulded test pieces and the trial components. Following injection moulding, water leaching was performed to remove the polyethylene glycol from the moulded products.

Water Leaching Design of Experiments

The purpose of this trial was to assess the effectiveness of the water leaching process for the removal of the polyethylene glycol from the mouldings. Ideally 100% removal would be desirable to prevent volatilisation during the furnace consolidation stage of the process.

Eight trial test pieces (20mm in length x 15mm diameter) were weighed and placed in a Clifton NE2-8D water bath. Test pieces 1 and 2 were removed after 24 hrs, test pieces 3 and 4 were removed after 48 hrs and test pieces 5 and 6 were removed after 72 hrs. The bath temperature was then increased to 60ºC for a further 6 hrs (78 hours in total), after which samples 7 and 8 were removed. Prior to re-weighing, the test pieces were oven dried at 40ºC for 12 hrs and allowed to cool to ambient temperature. Test results detailed in Table 19 below.

Table 19: Water Leaching Test Results

Test piece number	Leaching (hrs)	Temperature (ºC)	Weight before (g)	Weight after (g)	Weight Difference (g)	Removal (%)
1	24	40	20.58	19.80	0.78	3.79
2	24	40	20.70	19.90	0.80	3.86
3	48	40	20.66	19.76	0.90	4.36
4	48	40	20.66	19.76	0.90	4.36
5	72	40	20.68	19.76	0.92	4.45
6	72	40	20.66	19.74	0.92	4.45
7	78	60	20.60	19.66	0.94	4.56
8	78	60	20.70	19.74	0.96	4.64

The starting temperature of 40ºC was chosen based upon prior binder leaching experience from a dissimilar alloy of similar powder particle size. It is widely accepted that removing the polyethylene glycol too quickly can result in sample distortion. Conversely inefficient removal can lead to gaseous turbulence during the sintering operation. The parameters used for binder removal, following injection

moulding, require to be chosen carefully in order to achieve a processing compromise which minimises the potential to undermine the structural integrity of the moulding.

By increasing the time that the samples were present in the water bath, it was found that the binder removal rates improved. Test piece exposure to 60ºC water temperatures for an additional 6 hours resulted in a further increase in the removal rates. Several conclusions and limitations were drawn from this experiment. Knowing the total sample weight in the 'green state', it is possible to estimate the percentage of polyethylene glycol which has been removed from the test pieces. While test pieces 7 and 8 achieved the best removal rates, none of the test pieces reached 100% polyethylene glycol removal.

Whilst the water bath was equipped with a thermostatic control and water circulation facilities, there are still factors within the experiment which could give rise to further variations in the weight loss analysis calculations. In this experiment 8 test pieces of known mass were placed in the water bath. A greater mass or alternative sample geometry may affect the circulation of the deionised water resulting in variable removal rates.

The deionised water used to leach the polyethylene glycol from the test pieces was continuously circulated within the water bath. The effects of the gradually increasing polyethylene glycol content of the distilled water on the leaching rate are not known.

Where the moulded test piece has variable sectional thicknesses, the binder removal assumptions require to be based on the largest sections.

Sintering

Sample sintering was conducted in a graphite free (molybdenum lined) vacuum furnace. Figure 32 below illustrates the key furnace controls.

Furnace hot zone dimensions (mm)	
Zone width	300
Zone width	320
Zone height	670

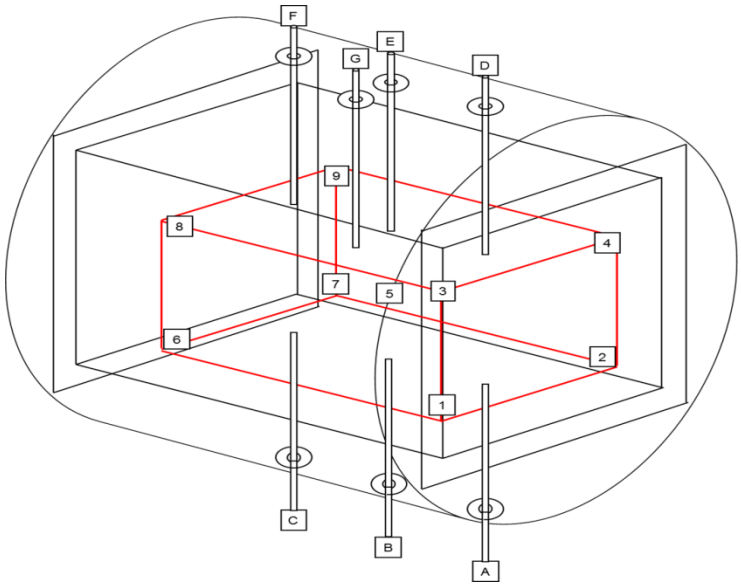

Thermocouple Position (fixed)	
A	Slave
B	Master
C	Slave
D	Slave
E	Slave
F	Slave
G	Over temperature

Thermocouple Position (survey)	
1	Front bottom left
2	Front bottom right
3	Front top left
4	Front top right
5	Centre
6	Back bottom left
7	Back bottom right
8	Back top left
9	Back top right

Figure 32: Vacuum Furnace Diagram

Furnace Pyrometry

Prior to performing the sintering trials, a work zone within the furnace was established. The temperature uniformity (Table 20) within the work zone was verified independently by a 9 position thermocouple survey. Type N thermocouples were used or the survey. The maximum variation around the furnace set point of 1265ºC was found to be within the +/-10ºC tolerance as illustrated in Figure 33 below.

Table 20: Temperature Uniformity (Minimum and Maximum Results)

	T/C 1	T/C 2	T/C 3	T/C 4	T/C 5	T/C 6	T/C 7	T/C 8	T/C 9
Max Temp	1263.7	1265.3	1266.5	**1267.9**	1262.3	1265.1	1265.2	1264.3	1264.7
Min Temp	1263.2	1264.8	1265.8	1267.2	**1261.6**	1264.5	1264.5	1263.7	1264.2

From the table above it can be seen that the maximum variation around the set point is +2.9ºC, while the minimum was found to be -3.4ºC.

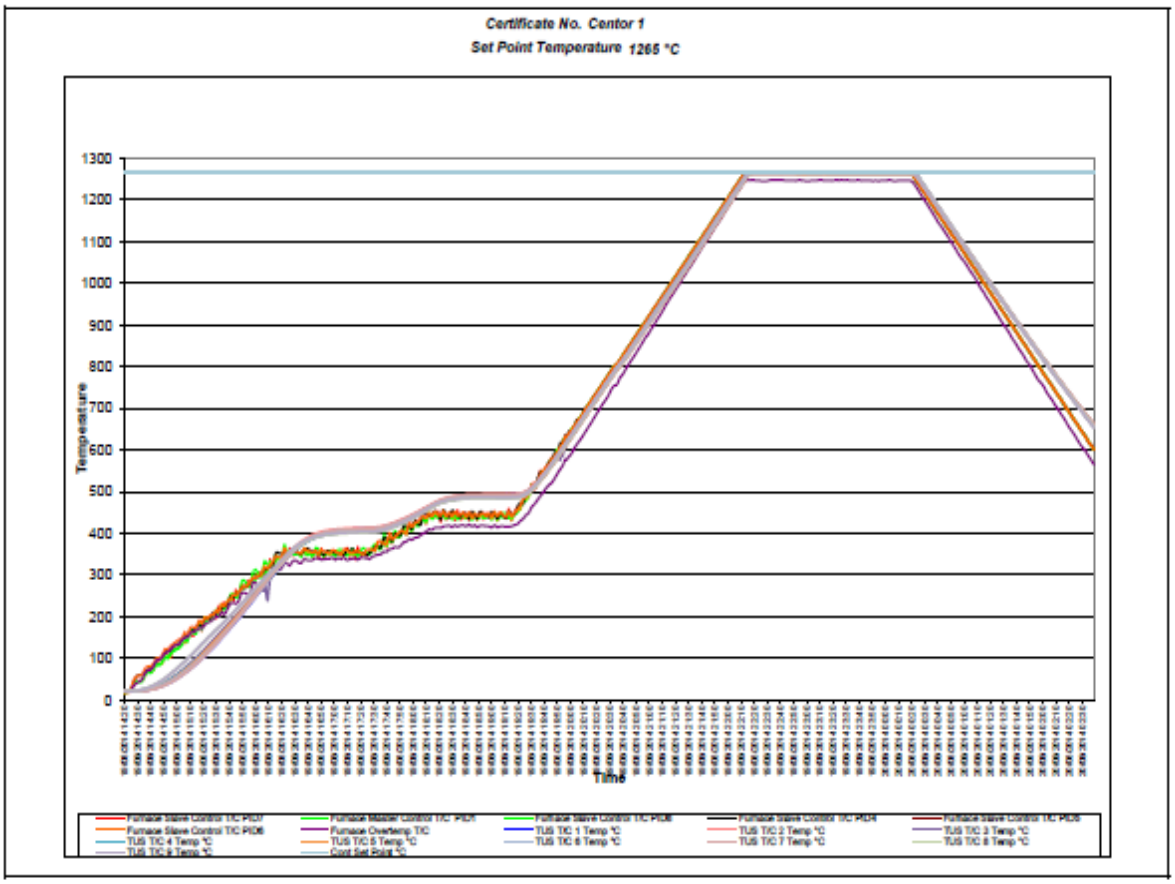

Figure 33: Temperature Uniformity (Minimum and Maximum Results)

Vacuum Furnace Characteristics

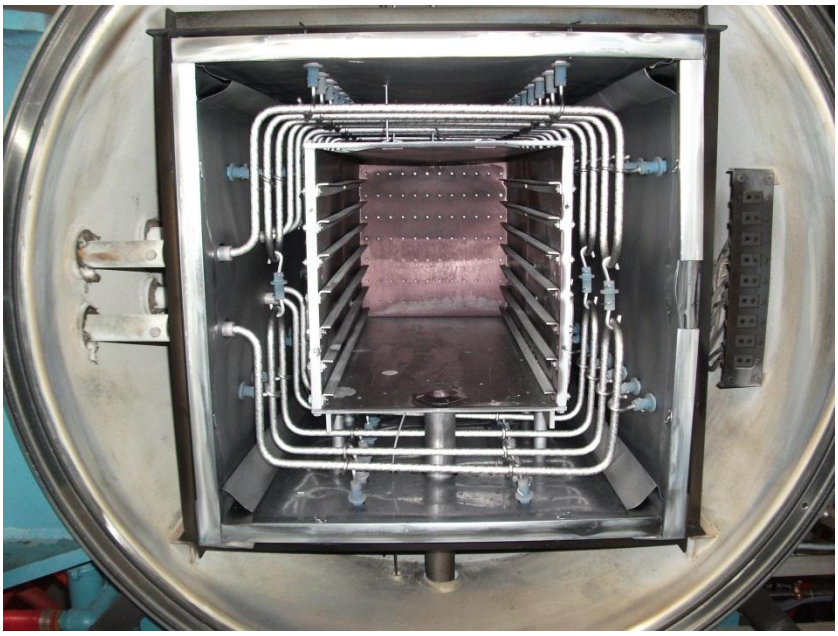

Figure 34: Furnace Work Zone

Figure 35: Furnace Loading

For metal injection moulded products, densification and microstructural integrity are achieved by sintering and subsequent heat treatment operations. Figure 34 and Figure 35 illustrate the all metal nature of the furnace lining.

For this research, both operations were conducted in a high specification vacuum furnace. The furnace was comprised of a graphite free heating chamber and utilised molybdenum furniture. No load thermocouples were available to accompany the injection moulded components, however the temperature uniformity survey results were considered to be sufficient to demonstrate a stable and accurate work zone. To minimise contamination, the injection moulded components were placed on aluminium oxide supports which had previously been subjected to a high temperature decontamination cycle to remove any residual moisture or contaminants from the surface. For all the sintering trials the gap between the trial components was between 20mm and 50mm. This was considered to be sufficient to allow uniform radiant heating of the charge components.

A furnace heat treatment cycle consists of three main segments. The ramp up rate, the dwell time and cooling rate are the key process variables. In the vacuum furnace the temperature ramp up rate can be between 1ºC per minute to approximately 20ºC per minute. The dwell time is the time at the specified set point which is considered to commence when the last recording thermocouple reaches the set point minus the lower section of the set point tolerance. The temperature tolerance assigned to the furnace sintering and heat treatment cycle was +/-10ºC. Both the temperature ramp up rate and the cooling rate are influenced strongly by the thermal mass of the components and supporting fixtures within the furnace.

The furnace cooling rate has less significance than the ramp up rate for metal injection moulding sintering operations. The ramp up rate is significant because the components still contain a significant amount of acrylic polymer. Removal of the acrylic polymer requires a steady controlled heating cycle in order to prevent uncontrolled volatilisation.

Furnace Sintering Parameters

The sintering temperature set point parameters adopted for the 718 alloy components and test pieces were established from published literature. However a design of experiments was conducted in to substantiate the furnace heating cycle used for this research.

Details of the sintering cycle are illustrated in Table 21 below.

Table 21: Sintering Summary

Furnace Function	Temperature (ºC)	Rate / Time (ºC/min)
Ramp up 1	Ambient to 350ºC	3ºC / min
Hold	350ºC	60mins
Ramp up 2	350ºC to 440ºC	2ºC / min
Hold	440ºC	60mins
Ramp up 3	440ºC to 800ºC	5ºC / min
Hold	800ºC	60mins
Ramp up 4	800ºC to 1270ºC	5ºC / min
Hold	1270ºC	120mins

Experimental trials found that high furnace ramp up rates (20ºC per minute) were unacceptable as this resulted in fractures occurring between the largest and smallest sectional thicknesses of the mouldings, most likely to be caused by stress as a result of variable expansion rates between the adjoining regions. Test pieces processed at high ramp up rates also exhibited gross internal porosity and macro cracking within the structure due to the rapid expulsion of the binder.

A cautious approach of adopting a ramp up rate of 3ºC per minute to 350ºC followed by 2ºC per minute to a set point of 440ºC was found to be sufficient to enable good temperature uniformity to be achieved and a controlled release of the residual binder.

Following removal of the binder, the ramp up rate was increased to 5ºC per minute to reach a set point of 1270ºC for 120 minutes. The final sintering temperature and the time at temperature were found to have a pronounced effect on the 718 alloy microstructure.

Sintering trials were conducted at between 1250ºC and 1290ºC for between 60 and 180 minutes. Short duration, lower temperature sintering cycles revealed the presence of incompletely sintered powder particles within the microstructure. The isolated powder particle boundaries were still clearly visible in certain regions of the

microstructure. These test pieces presented fine equally distributed micro porosity throughout the sections evaluated.

Sintering conducted at 1270ºC produced the most desirable results. These test pieces were found to contain the lowest levels of porosity.

Sintering trials conducted at temperatures of 1290ºC resulted in greater dimensional instability at relatively short (one hour at temperature) sintering. The test pieces sintered at 1290ºC presented a glazed appearance. This appearance is most likely to have been caused by the onset of melting of the lower melting point alloy constituents.

Several observations were made which were applicable to all the component samples which were evaluated.

- Thinner component sections (<2mm) which were typically the aerofoil sections of the component tended to be more uniform in terms of the distribution of micro porosity.
- There was a visible increase in the amount of grain boundary precipitation throughout all component sections that were microscopically examined.
- Large sections (>4mm) were prone to random agglomerations of linked porosity.
- Isolated unreacted particles could be seen in the microstructure. The particles appeared to have a continuous surface boundary layer and did not appear to have bonded with adjacent powder particles.

All the sintered samples were evaluated in the fully heat treated condition. Figures 36 to 38 illustrate the etched microstructures.

A detailed processing sequence is illustrated in Table 22 below.

Furnace Sintering Parameters

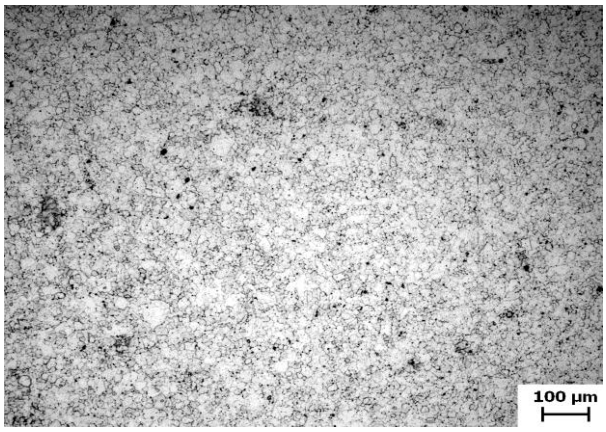

Figure 36: Sintering Temperature 1250ºC

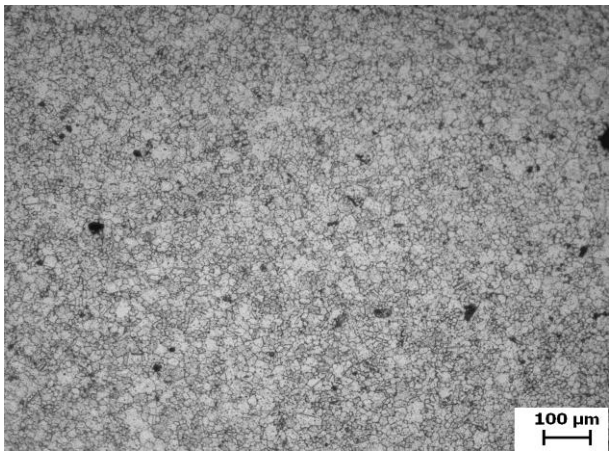

Figure 37: Sintering Temperature 1270ºC

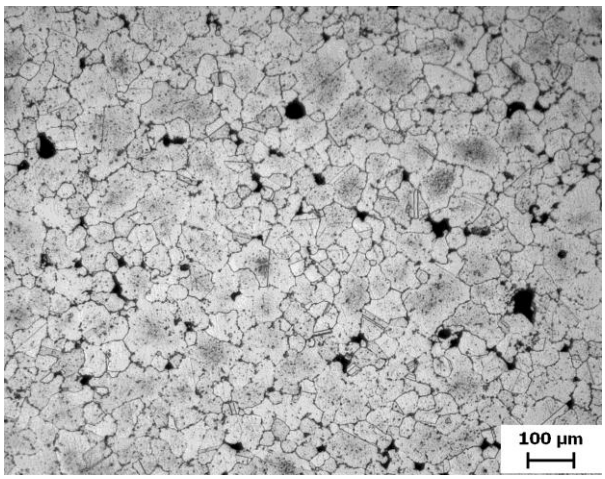

Figure 38: Sintering Temperature 1290ºC

Table 22: Thermal Debinding, Sintering and Heat Treatment Summary

Op	Process	Description & Equipment	Method
1	Injection Mould	3 dimensional forming of component geometry and test bars Arburg 320C	Nozzle temperature 150ºC Pressure & flow rate - component / test bar specific settings were determined by short shot & moulding trials. For both the component and the test bar mouldings, single injection points were used. Moulding dies were manufactured independently by an external supplier with prior injection moulding die manufacturing capability.
2	Water leach	Removal of polyethylene glycol from mouldings in the 'green state' Clifton water bath	Both trial components and test bars were immersed in a deionised water bath. The immersion temperature was initially 40ºC rising to 60ºC in order to leach the polyethylene glycol from the mouldings.
3	Oven Dry	Removal of residual moisture prior to thermal processing' Air circulating oven	Both components and test bars were placed on stainless steel trays with adequate spacing to ensure adequate hot air circulation.
4	Debind & Sinter	Thermal debinding to remove polymethyl methactylate and consolidate 718 alloy Vacuum furnace	This is possibly the most critical part of the processing cycle. The key process variables associated with this operation are the ramp up rates and soak time. During the debinding phase a slow ramp rate in desirable to ensure a controlled release of the polymethyl methacrylate. Prior to and following the release of the binder it is essential to ensure that the moulding achieves temperature at a uniform rate, this is achieved by introducing several dwells in the processing cycle. When approaching the final set point it is imperative not to overshoot. This can be managed by reducing the ramp rate of introducing a further dwell 10ºC below the set point.
5	Solution Treat	Vacuum furnace	Ramp to 970ºC, at 10ºC per minute, hold for 15 minutes. Ramp to 980º at 5ºC per minute, hold for one hour. Argon gas fan quench to room temperature.
6	Age	Vacuum furnace	Ramp to 710ºC, at 10ºC per minute, hold for 15 minutes. Ramp to 720ºC at 5ºC per minute, hold for 8 hours. Furnace cool to 620ºC. Hold at 620ºC for a total ageing cycle of 18 hours minimum.

3.4 Manufacture of Wrought Forged Components

The conventional method of manufacture for wrought forgings is complex and relies upon the redistribution of the 718 alloy through sequential thermo-mechanical processing operations. The starting point for the manufacture of such items is a cylindrical billet of high purity vacuum melted 718 alloy. The billet dimensions are approximately 40mm in length by 19mm diameter and weigh approximately 190g. Four separate forging operations are required in order to achieve the fully finished component geometry weighing approximately 130g. Forging operations are performed at temperatures ranging from 1010ºC to 1100ºC. Pre heating is normally conducted in an atmosphere of 96% nitrogen and 4% hydrogen in order to minimise surface oxidation in a rotary hearth furnace. Each forging operation requires a significant amount of material preparation at each forging stage in order to minimise the likelihood of deleterious oxides becoming part of the finished product. The material preparation consists of mechanically removing surface oxides by abrasive blasting the raw material with aluminium oxide grit. This process coupled with sequential chemical etching and inspection operations are an integral part of the process for manufacturing compressor blades from wrought 718 alloy.

Traditional forging methods are labour intensive requiring the furnace operative to manually load the rotary hearth and also remove components from the hearth to the forging press. Forging key process variables are recognised as billet or component temperature, furnace to press transfer time and press strain rate. The thickness of ceramic forging lubricant applied to the component and also the uniformity of the die lubricant can also have an influence on the process. While the key process variables associated with forging operations are well understood, they present a challenge when the forging process in not automated due to inherent variations such as furnace to press delays, variable application of lubricants, press wear and other human factors. These inherent variations have a combined effect on the product being manufactured and result in dimensional variations throughout the manufacture of production quantities of components. Table 23 details the process.

Table 23: Wrought Forging Method of Manufacture Summary

Op	Process	Description & Equipment	Method
1	Lubricate	Application of forging lubricant	Spay mist coating
2	Extrude billet	Manual split die extrusion press	Transfer from furnace to press. 1100ºC
3	Descale	Automated all over application of abrasive	Archimedes screw to deliver all over application
4	Chemical etch	Semi automated process, component immersion	Programmable sequence of operations
5	Polish (external)	Polish key component dimensions	Proprietary polishing process
6	Surface treatment	Semi automated surface enhancement process	Programmable barrelling operation.
7	Specific polish	Manual polishing operation.	Removal of specific surface discontinuities
8	Chemical etch	Semi automated process, component immersion	Verification of removal of surface discontinuities
9	Descale	Automated all over application of abrasive	Archimedes screw to deliver all over application
10	Lubricate	Application of forging lubricant	Spray mist coating
11	Pre-stamp - 1	Manual split die forging press	Transfer from furnace to press. 1080ºC
12	Pre-stamp - 2	Manual split die forging press	Transfer from furnace to press. 1080ºC
13	Descale	Automated all over application of abrasive	Archimedes screw to deliver all over application
14	Chemical etch	Semi automated process, component immersion	Verification of removal of surface discontinuities
15	Descale	Automated all over application of abrasive	Archimedes screw to deliver all over application
16	Lubricate	Application of forging lubricant	Spay mist coating
17	Final stamping	Manual split die forging press	Transfer from furnace to press. 1080ºC
18	Descale	Automated all over application of abrasive	Archimedes screw to deliver all over application
19	Heat Treat - Solution	Automated vacuum furnace	980ºC for one hour
20	Heat Treat - Age	Automated vacuum furnace	720ºC, 620ºC 18hours minimum
21	Test - Hardness	Manual Brinell hardness test	Percentage hardness batch overcheck
22	Dimensional inspect	Semi automatic process focused on KPV's	Measurements from datum points
23	Chemical mill	Semi automated process, component immersion	Metal removal to standardise dimensions
24	Dimensional inspect	Semi automatic process focused on KPV's	Measurements from datum points
25	Binocular examination	Manual inspection process using x8 binocular	Surface evaluation process
26	Visual examination	Manual inspection technique x2 binocular	All over visual inspection technique
27	Polish	Manual operation to remove surface	Removal of specific surface discontinuities

Table 23: Wrought Forging Method of Manufacture Summary (continued)

Op	Process	Description & Equipment	Method
28	Fit	Manual process to correct aerofoil alignment	Apply predetermined force for correction
29	Visual	Manual inspection technique x2 binocular	All over visual inspection technique
30	Check	Aerofoil specific inspection of KPV's	Part specific inspection tooling
31	Check	Aerofoil specific inspection of KPV's	Part specific inspection tooling
32	Penetrant inspect	Fully automated process, manual inspection	Immersion technique to detect surface defects
33	Material check	Raw material positive verification	XRF
34	Final	Manual review of all completed operations	Manufacturing router completeness check

Method of manufacture summary

The image below, Figure 39 shows a typical injection moulded 718 alloy test bar.

Figure 39: MIM Billet x 1 approx

The image below, Figure 40 illustrates both the established wrought component and the injection moulded equivalent both manufactured from 718 alloy.

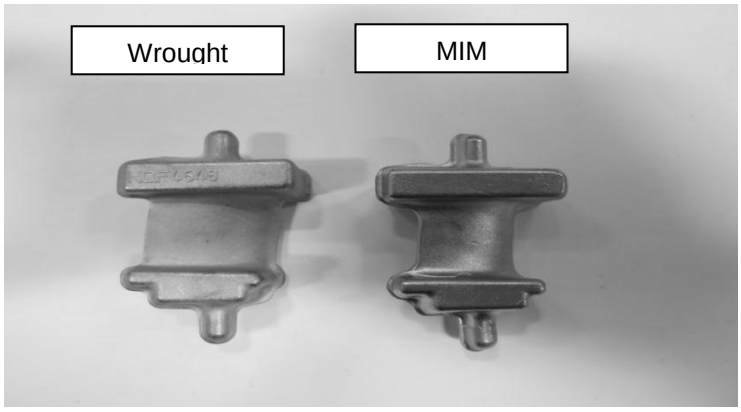

Figure 40: Wrought and Injection Moulded Components x 0.5 approx

In comparing the manufacturing methods for both the wrought and the injection moulded components the most obvious difference is the amount of processing operations required to complete the manufacture of the wrought component. The desired geometry of the wrought component isn't achieved until Op 17 (final stamp). This operation is the 4th thermo-mechanical processing operation to be performed on the component.

By contrast the injection moulded equivalent component is manufactured in a single moulding operation identified from the method of manufacture as Op 1 (Injection mould).

From the wrought method of manufacture it can be seen that Op 22 through to Op 33 are devoted to verifying conformity, performing the necessary corrections and re-inspecting the product for both dimensional attributes in addition to assuring the metallurgical integrity of the product. These operations are necessary to correct process variations arising from the key forging input variables. For economical or practical reasons these variations cannot be controlled to a sufficiently high level to minimise the part to part variation found in the manufacture of production quantities of components.

From the initial research questions it can be seen that if the material properties of the injection moulded 718 alloy are equivalent to the wrought 718 alloy properties there will be a significant opportunity to challenge the current manufacturing costs and lead times. An injection moulded component could be introduced into the conventional manufacturing method at Op 12 (Pre-stamp-2) or as a direct replacement for Op 17 (Final stamp).

By comparing and contrasting the manufacturing routes for both wrought and injection moulded components the vision and the commercial drivers for this research become apparent. Depending on the mechanical test results there is also the future potential to manufacture net shaped components.

The part to part variation and dimensional stability of the metal injection moulding as applied to production quantities of components is outside the scope of this research.

CHAPTER 4

TESTING STRATEGY

4. Testing Strategy

The 718 alloy characterisation and testing which was performed to compare and contrast the material structures and properties from both wrought and injection moulded variants has been grouped by the type of test which was performed. This grouping logic chosen enables the test results to be compared in a comprehensive manner, and the numerical test output data to be captured and compared with other test data of a similar nature.

The initial testing strategy was based upon comparing and contrasting the mechanical properties from both wrought and injection moulded 718 alloy, however as the research testing strategy progressed and in response to variable test results, it was found necessary to introduce sophisticated non-destructive testing methods to verify the homogeneity of the injection moulded test pieces. X-ray computed tomography was selected in order to accurately verify the homogeneity of the test pieces and to enable non homogeneous sections to be disregarded. The elevated temperature 718 alloy test results obtained for injection moulded test pieces which were subsequently thermo-mechanically processed to achieve 20%, 40% and 60% reductions were subjected to X-ray computed tomography analysis prior to mechanical testing.

Both Vickers and Brinell hardness testing assessments were performed on the test pieces in order to assess localised and bulk properties of the fully heat treated 718 alloy. While hardness testing is not normally recognised as an assessment criteria for precipitation strengthened alloys, these tests were initiated in order to provide an overall indication of the consistency of the test piece being assessed.

A testing matrix has been created in order to capture clearly which type of test was performed and the type of test piece which was used from which the test data was generated.

Table 24 provides an overview of the testing strategy.

The test matrix below summarises the testing strategy.

Table 24: Testing Matrix

Test Type	Wrought 718 alloy test bar (a)	MIM 718 alloy test bar (b)	MIM 718 alloy test bar 20% (c)	MIM 718 alloy test bar 40% (c)	MIM 718 alloy test bar 60% (c)	Wrought 718 alloy component (d)	MIM 718 alloy component (e)
1	x	x	x	x	x	-	-
2	x	x	x	x	x	-	-
3	x	x	x	x	x	-	-
4	x	x	x	x	x	x	x
5	x	x	x	x	x	x	x
6	-	x	x	x	x	-	-
7	x	x	x	x	x	-	-
8	x	x	x	x	x	-	-
9	-	-	-	-	-	x	x

(a) Fully heat treated wrought 718 alloy bar.
(b) Fully heat treated metal injection moulded 718 alloy bar.
(c) Sample (b) reduced by thermo-mechanical processing operations to achieve approx. 20%, 40% and 60% reductions.
(d) Fully heat treated wrought 718 alloy component.
(e) Fully heat treated metal injection moulded 718 alloy component.

Test Type

1 Elevated Temperature Tensile Testing

2 Test Piece Density Measurement

3 Scanning Electron Microscopy

4 Test Piece Preparation

5 Reflected Light Microscopy

6 X-ray Computed Tomography

7 Brinell Hardness

8 Vickers Hardness

9 Small Punch Testing

4.1 Elevated Temperature Tensile Testing

Elevated temperature tensile testing is one method of assessing the mechanical properties of alloys which perform in service at elevated temperatures. 718 alloy is an alloy which has been designed to withstand prolonged exposure to elevated temperatures in the compressor of the modern gas turbine engine. For the purpose of this research the elevated temperature testing was performed at 650ºC. This test temperature is in accordance with published technical data for this alloy type.

Tensile testing is a uniaxial testing procedure from which an assessment can be made of several key material attributes. This research focuses on 4 outputs from the test and compares the test results from the metal injection moulded process test pieces with baseline data for 718 alloy. The baseline data was obtained by testing several wrought test pieces from differing production casts.

The load extension curve below illustrated by Figure 41shows the typical outputs from a tensile test. As can be seen the load applied to the test specimen and the corresponding extension are captured graphically.

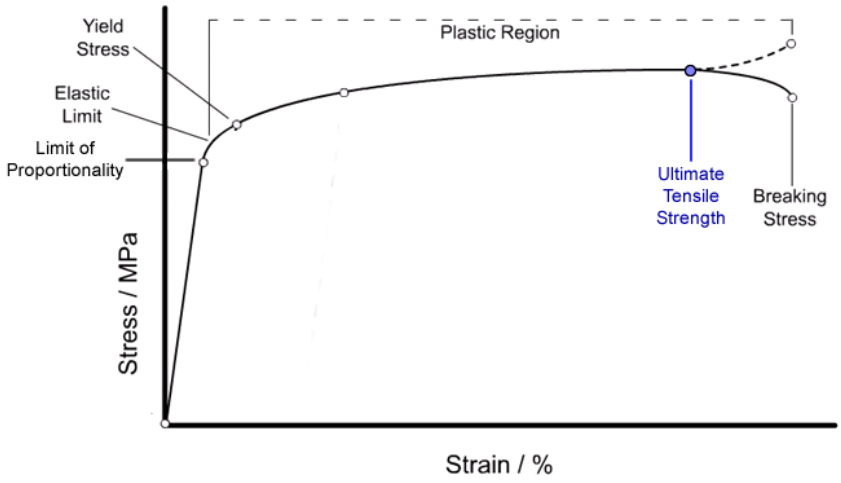

Figure 41: Typical Tensile Graph

The 4 key process outputs from this test which were used for comparison purposes are listed below

- Ultimate Tensile Strength (MPa)
- 0.2% Proof Stress (MPa)
- Elongation (%)
- Reduction in Area (%).

The Ultimate Tensile Strength (UTS) is the load at which failure occurs divided by the original cross sectional area. This measure is calculated by taking the maximum force divided by the original cross sectional area of the test piece

The Proof Stress (PS) is recognised as the point at which a non proportional extension is equal to a specified percentage of the extensometer gauge length. For highly alloyed materials such as 718 alloy, the yield point is not clearly defined, and in order to standardise the measurement a 0.2% Proof Stress is reported.

718 alloy derives it's strength at elevated temperatures through several recognised mechanisms. Fine grain sizes improve tensile strength by providing a greater resistance to the movement of dislocations.

The recognised precipitation strengthening mechanisms associated with 718 alloy include

- Gamma prime, Ni_3Al which is an intermetallic compound capable of dissolving titanium and aluminium.
- Gamma double prime, Ni_3Nb forms a coherent precipitate providing increased resistance to the movement of dislocations. Delta phase, while having the same Ni_3Nb composition, forms an incoherent precipitate which does not offer improved strength when present in large quantities.

Carbides formed at the grain boundaries are recognised as providing increased resistance to grain boundary sliding in wrought 718 alloys.

Figure 42 below illustrates the changes that occur to the test piece following testing and also the key regions of the test piece from which the comparative test data is derived. Diagram (a) relates to the elongation of the test piece, while (b) is associated with the reduction of area. Both values give an indication of the specimen ductility.

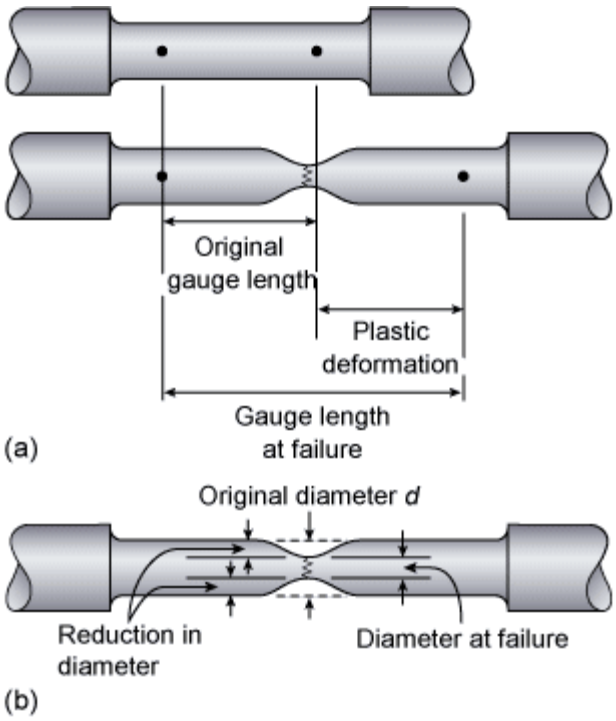

Figure 42: Tensile Test Piece Description

The elongation % (El) and reduction in area % (RoA) of the failed test piece provides key information about the ductility of the material.

The percentage elongation of the test piece during testing provides an indication of both elastic and plastic deformation and also the modulus of the material.

The percentage reduction in area after fracture is a measure of the reduction in parallel length diameter at the actual fracture point of the test piece.

Experimental Procedure

The test equipment used to conduct the elevated temperature tensile testing was a Zwick Z100 tensile tester. Equipment detailed in Figure 43.

Figure 43: Tensile Tester

The test temperature selected for the conduct of the test was 650ºC. The temperature and strain rate employed for the test was identical for both wrought and metal injection moulded test pieces. The manufacture of test pieces was conducted to a controlled procedure in order to minimise the likelihood of inducing surface discontinuities or surface layer effects. Two different test piece geometries were used for the elevated temperature tensile testing trials. A standard test piece having a gauge length of 25mm and a smaller test piece having a gauge length of 16.5mm. Both test pieces were proportional. The smaller test piece allowed test data to be obtained from metal injection moulded test bars which had been subsequently reduced in diameter by thermo-mechanical processing.

The elevated temperature test pieces from the wrought and injection moulded 718 alloy test pieces were manufactured with 25mm extensometer gauge lengths. The elevated temperature test pieces from the 20%, 40% and 60% reductions were smaller and presented 16.5mm lengths.

Elevated Temperature Test Specimens

The images below capture the types of test piece used to generate data from the elevated temperature tensile test. Specimen images in Figure 44 and 45 below.

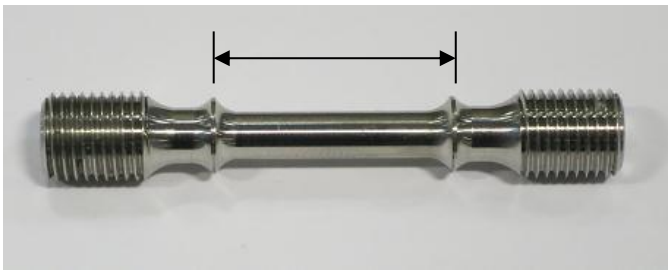

Figure 44: 25mm Gauge Length - Standard Specimen

Figure 45: 16.5mm Gauge Length - Small Specimen

Test Sample Identification

Table 25 below is an illustration of the quantity of test pieces, the type of test pieces and also the manufacturing route employed to produce the test pieces.

Table 25: Test Piece Identification

Description	Sample size	Sample Type
Wrought Tensile	10	Standard Specimen
Injection Moulded Tensile	10	Standard Specimen
Injection Moulded 20% reduction	2	Small Specimen
Injection Moulded 40% reduction	2	Small Specimen
Injection Moulded 60% reduction	2	Small Specimen

The finished machined test pieces were located in the elevated temperature extensometry with three type N thermocouples attached to the parallel gauge length of the test piece. The fixturing is illustrated in Figure 46 below.

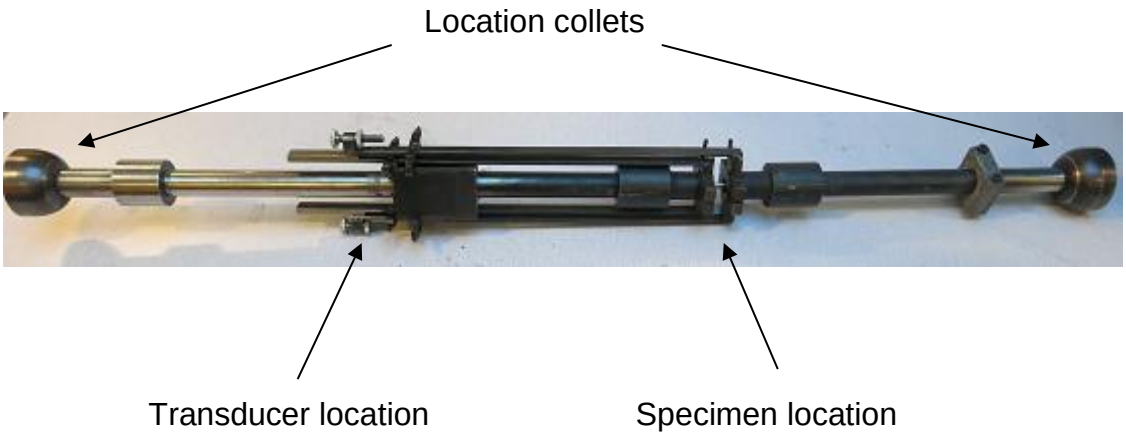

Figure 46: Tensile Test Piece Fixturing

The extensometer assembly was then inserted into the furnace chamber at ambient temperature. The furnace used to provide the elevated temperature requirements was a three zone electrically heated resistance element furnace. Each of the three furnace zones were controlled independently from the type N thermocouples attached to the parallel length of the test piece with high temperature bindings.

The loading bars were then attached to the machine location collets. The test was performed under uniaxial conditions. Upon reaching the 650ºC +/-3ºC temperature set point, the test piece was allowed to soak for a further 30 minutes prior to testing. The initial strain rate used was 0.002mm/minute. This strain rate was used to beyond the 0.2% proof stress after which the strain rate to specimen failure was increased to 2.0mm/minute.

This procedure was followed for all the test pieces that were processed. Three of the test results were calculated automatically following failure while the remaining reduction in area value was calculated upon removal of the failed test piece.

Tables 26 to 30 detail the test results for both wrought and MIM test pieces.

Table 26: Test Piece Results (Wrought)

Test result number	Ultimate tensile strength (MPa)	Proof Stress 0.2% (MPa)	Specimen Elongation (%)	Specimen Reduction (%)
1	1200	1000	22.6	63.6
2	1200	1030	23.1	66.5
3	1230	1040	18.1	44.5
4	1200	984	18.7	58.7
5	1190	1050	20.4	41.8
6	1210	1030	15.7	31.8
7	1180	1080	18.8	42.9
8	1120	956	12.5	21.0
9	1160	977	18.4	33.2
10	1150	971	26.4	49.3

Table 27: Test Piece Results (MIM)

Test result number	Ultimate tensile strength (MPa)	Proof Stress 0.2% (MPa)	Specimen Elongation (%)	Specimen Reduction (%)
1	815	806	4.4	3.6
2	813	806	4.1	3.6
3	836	833	4.1	3.2
4	983	904	4.0	4.0
5	536	536	4.7	3.0
6	860	859	4.2	1.8
7	864	859	4.3	1.3
8	729	728	4.3	0.6
9	696	696	4.0	1.2
10	870	872	4.3	0.8

Table 28: Test Piece Results (MIM 20% Reduction)

Test result number	Ultimate tensile strength (MPa)	Proof Stress 0.2% (MPa)	Specimen Elongation (%)	Specimen Reduction (%)
1	993	993	7.5	4.2
2	991	989	5.6	1.3

Table 29: Test Piece Results (MIM 40% Reduction)

Test result number	Ultimate tensile strength (MPa)	Proof Stress 0.2% (MPa)	Specimen Elongation (%)	Specimen Reduction (%)
1	1130	1020	4.9	8.8
2	1070	996	4.6	7.2

Table 30: Test Piece Results (MIM 60% Reduction)

Test result number	Ultimate tensile strength (MPa)	Proof Stress 0.2% (MPa)	Specimen Elongation (%)	Specimen Reduction (%)
1	1150	1010	11.9	10.4
2	1050	1000	9.2	6.2

Statistical Evaluation Techniques

Due to the use of two different mechanical test piece types and the corresponding difference in sample sizes, two separate methods were used for the analysis of the mechanical test results.

Test results derived using the standard elevated temperature test pieces were assessed using the following statistical techniques.

- Individual Value Plot. (Figures 47 and 51)
- Data Normality Plot with Probability Graph. (Figures 48,49,52 and 53)
- 95% Mean Confidence Interval Plot. (Figures 50 and 54)

This analysis method was used to assess the Ultimate Tensile Strength and test piece Elongation values.

For comparison purposes the test data derived from the small mechanical test pieces were assessed using the following technique.

- Individual Value Plot. (Figures 55,56,58 and 58)

This method was used to assess grouped test data (derived from both the standard and the small test specimens). The test data was used to create the individual value plot where the test results from both the standard and the small proportional test pieces could be assessed.

The analysis combines the mechanical properties from both the standard and the small elevated temperature test piece. The mechanical properties included in the Individual Value Plot are the Ultimate Tensile Strength, 0.2% Proof Stress, Specimen Elongation and the specimen Reduction in Area.

In order to provide objective criteria for sentencing the elevated temperature test results the following gas turbine industry specific criteria was used. Ref Table 31.

Table 31: Industry Standard - Elevated Temperature (650ºC) Tensile Properties

UTS (MPa)	0.2% PS (MPa)	Elongation (%)	Reduction in area (%)
1000 minimum	860 minimum	10 minimum	18 minimum
Elevated temperature (650ºC) tensile properties			

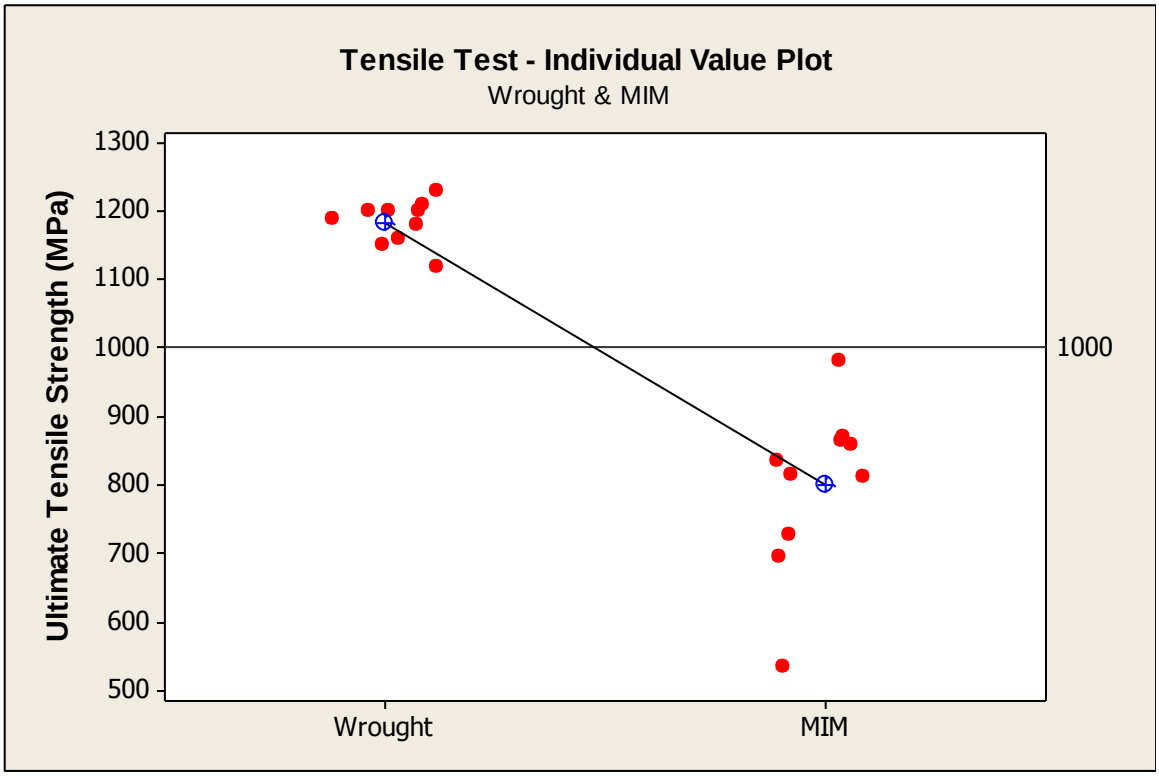

Figure 47: Individual Value Plot

The test piece means from each of the two groups of trials are summarised in Table 32 below.

Table 32: Test Piece Mean Results - Ultimate Tensile Strength (Wrought and MIM)

718 alloy test condition	Mean Ultimate Tensile Strength (MPa)
Wrought	1184
MIM	800.2

The test piece minimum / maximum values and ranges are summarised in Table 33 below.

Table 33: Test Piece Value and Ranges (Minimum and Maximum) - Ultimate Tensile Strength (Wrought and MIM)

718 alloy test condition	Minimum Ultimate Tensile Strength (MPa)	Maximum Ultimate Tensile Strength (MPa)	Range Ultimate Tensile Strength (MPa)
Wrought	1120	1230	110
MIM	536	983	447

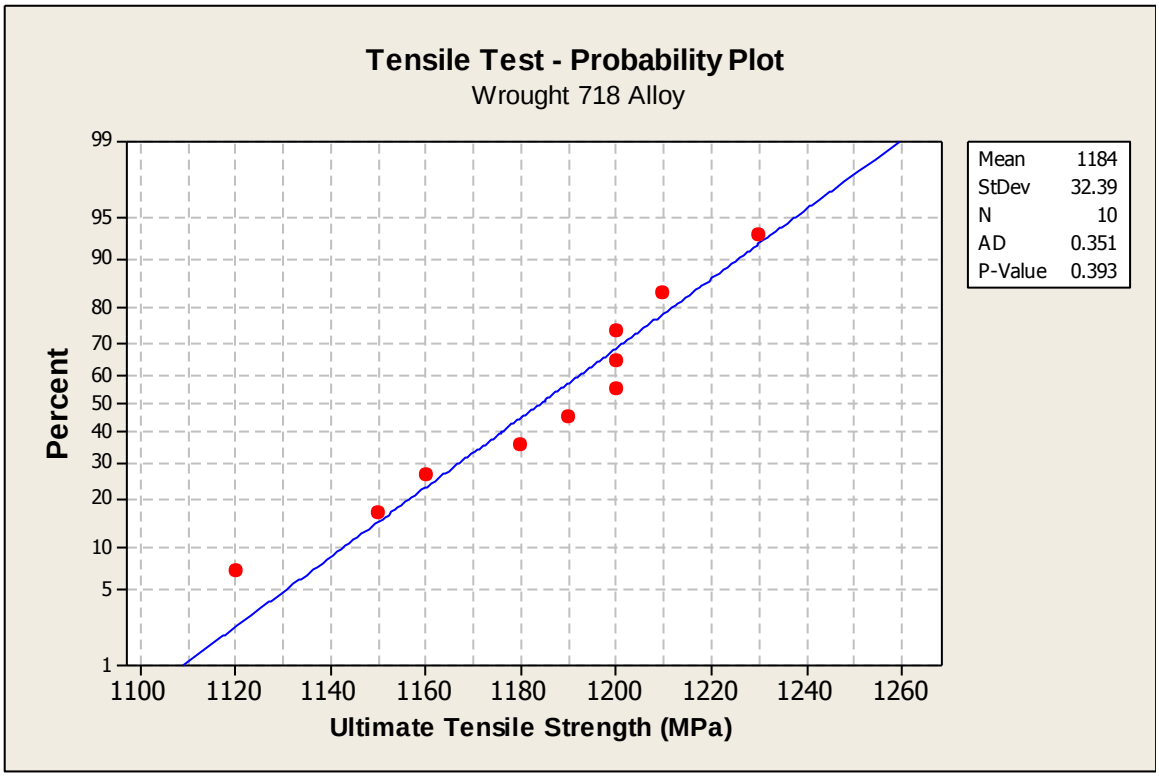

Figure 48: Normality Test with Probability Plot (Wrought 718 Alloy)

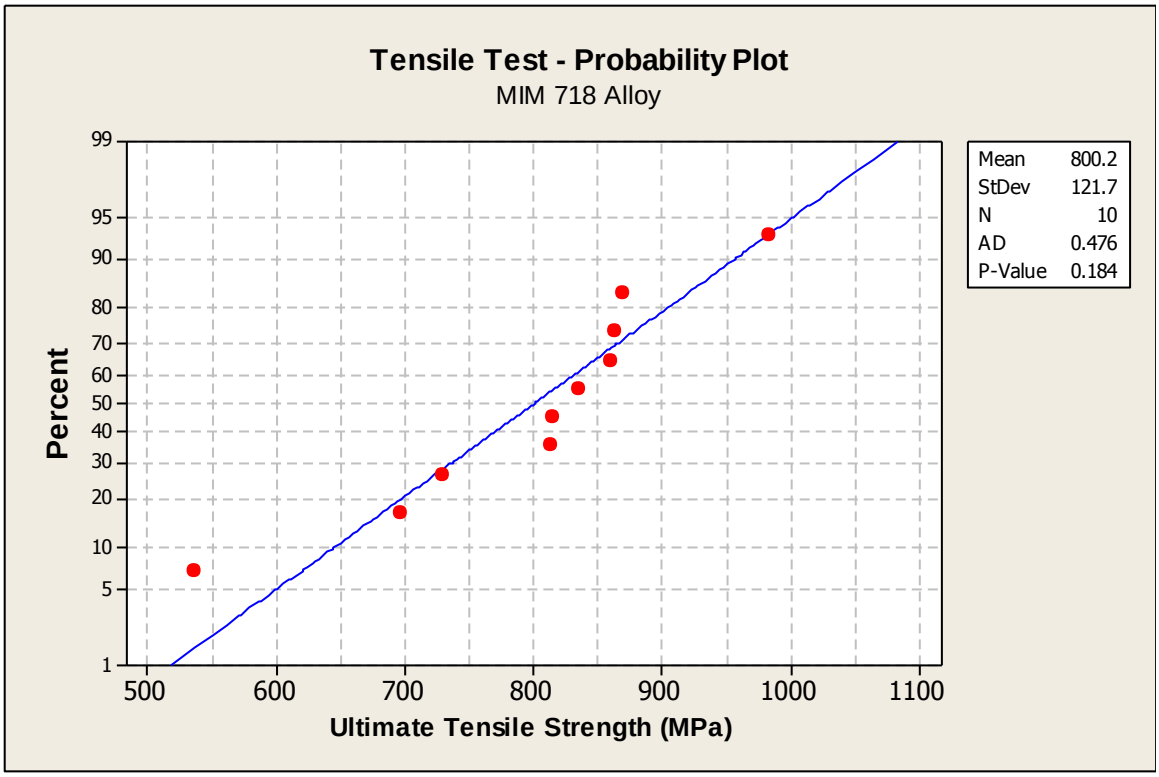

Figure 49: Normality Test with Probability Plot (MIM 718 Alloy)

The Normality Test with Probability Plot was conducted in order to assess the characteristics of the distribution of the test data from each of the two groups of Ultimate Tensile Strength results.

From the graphs which were constructed for both the wrought and the injection moulded test results the normality of the test data can be assessed both visually and objectively.

Both sets of test data were found to meet the Anderson-Darling Normality criteria. The test results for wrought and MIM were p-value 0.393 and p-value 0.184 respectively.

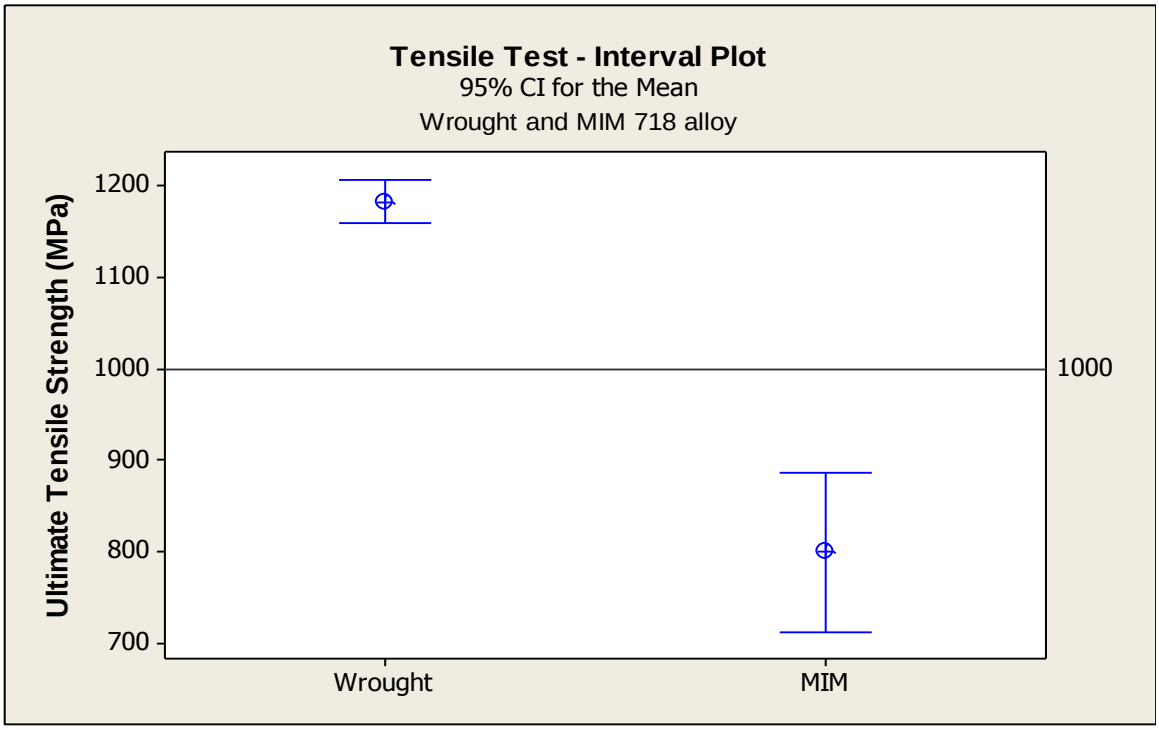

Figure 50: 95% Mean Confidence Interval (CI) Plot (Wrought and MIM 718 Alloy)

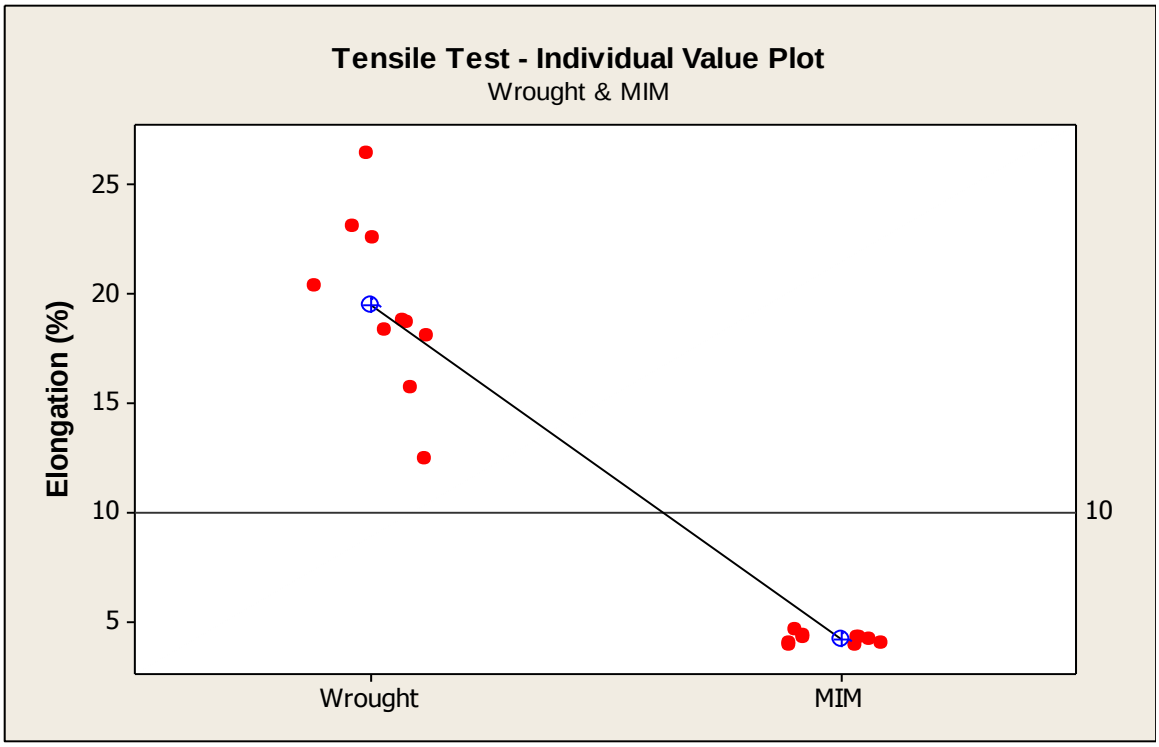

Figure 51: Individual Value Plot (Wrought and MIM)

The test piece means from each of the two groups of trials are summarised in Table 34 below.

Table 34: Test Piece Mean Results - Elongation (Wrought and MIM)

718 alloy test condition	Sample Mean Elongation (%)
Wrought	19.47
MIM	4.24

The test piece minimum / maximum values and ranges are summarised in Table 35 below.

Table 35: Test Piece Values and Ranges (Minimum and Maximum) - Elongation (Wrought and MIM)

718 alloy test condition	Minimum Elongation (%)	Maximum Elongation (%)	Range Elongation (%)
Wrought	12.5	26.4	13.9
MIM	4.0	4.7	0.7

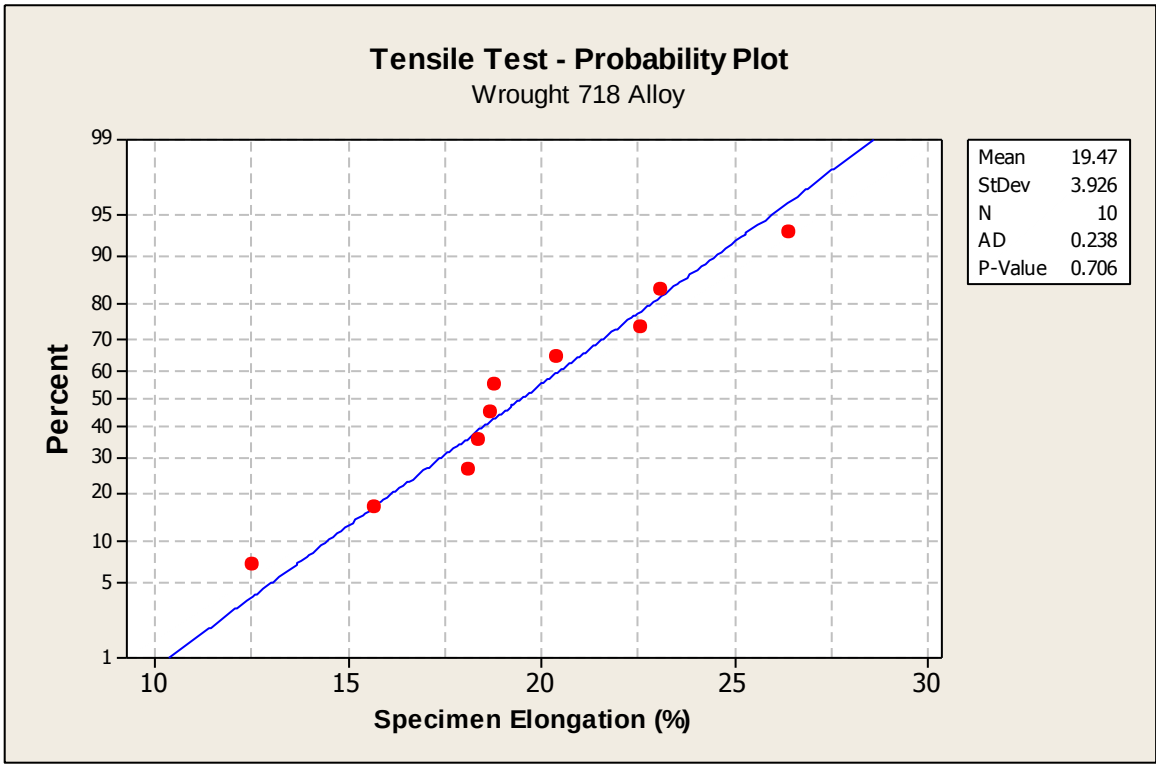

Figure 52: Normality Test with Probability Plot (Wrought 718 Alloy)

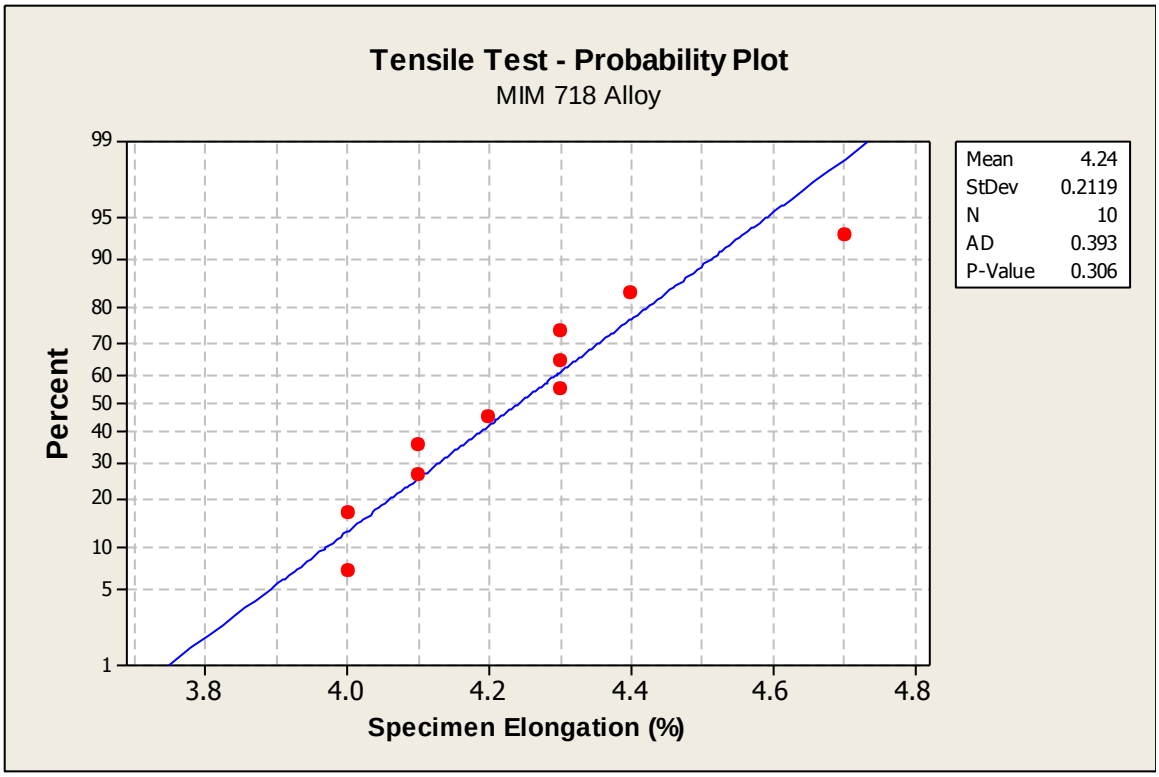

Figure 53: Normality Test with Probability Plot (MIM 718 Alloy)

The Normality Test with Probability Plot was conducted in order to assess the characteristics of the distribution of the test data from each of the two groups of Ultimate Tensile Strength results.

From the graphs which were constructed for both the wrought and the injection moulded test results the normality of the test data can be assessed both visually and objectively.

Both sets of test data were found to meet the Anderson-Darling Normality criteria. The test results for wrought and MIM were p-value 0.706 and p-value 0.306 respectively.

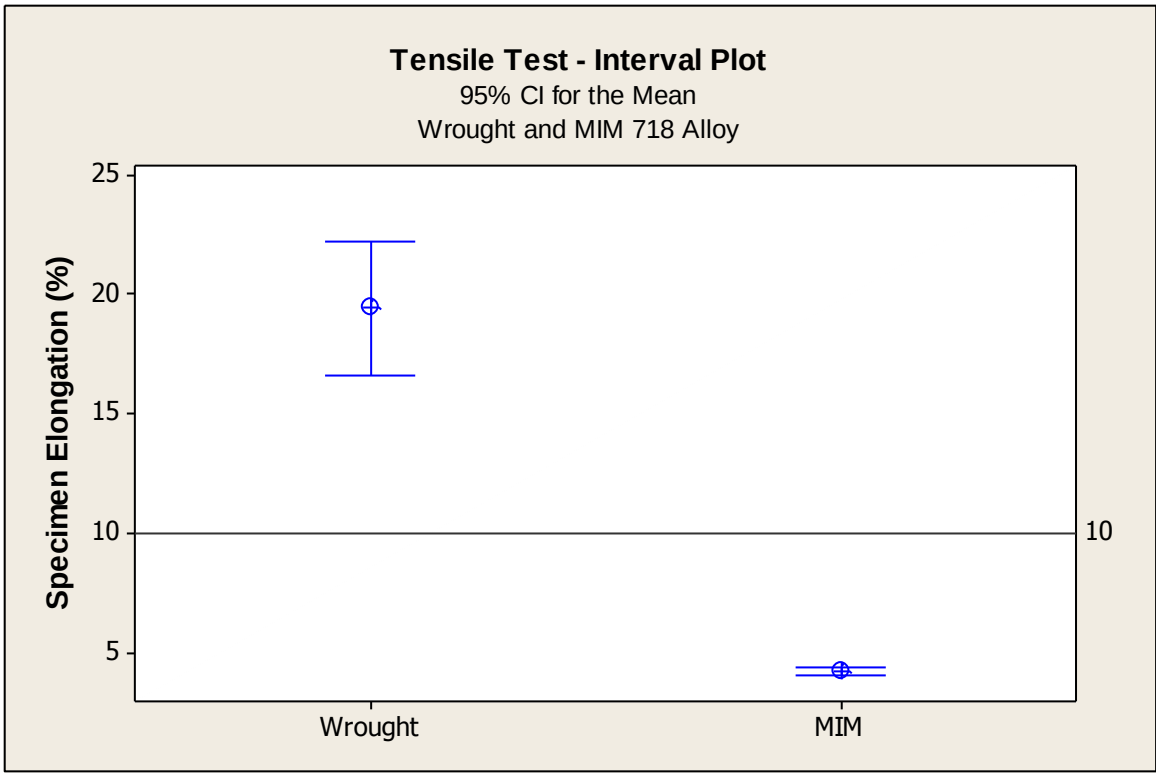

Figure 54: 95% Mean Confidence Interval (CI) Plot (Wrought and MIM 718 Alloy)

Discussion

The data for the Ultimate Tensile Strength and Elongation % derived from the uniaxial elevated temperature tensile test illustrates several key differences between the groups of test results.

By comparing the test piece means it can be seen that the Ultimate Tensile Strength data indicates that the injection moulded 718 alloy presents a reduction in mechanical properties of greater than 30%. The injection moulded test results also present a wide range of values ranging from 536 MPa to 983 MPa. These results are indicative of an inconsistent material structure. By comparing the test piece means it can be seen that the Elongation % data indicates that the injection moulded 718 alloy presents a reduction in ductility of greater than 75%. These test results were obtained from a standardised testing regime where the test piece type and testing methods were identical.

Further elevated temperature tensile testing was performed based upon the more homogeneous sections of the injection moulded test pieces. In order to improve upon the relatively poor injection moulded test results the test pieces were subjected

to progressive increases in thermo-mechanical processing by reducing the bar diameter by approximately 20%, 40% and 60%.

Prior to performing the thermo-mechanical processing operations the homogeneity of the test pieces was confirmed by computed tomography prior to machining further test pieces. Due to the limited availability of injection moulded test pieces 'smaller' proportional tensile test pieces were used.

The data derived from the smaller test pieces was then plotted in conjunction with the standard test piece data for comparison purposes. No further statistical analysis was performed due to the differing sample sizes.

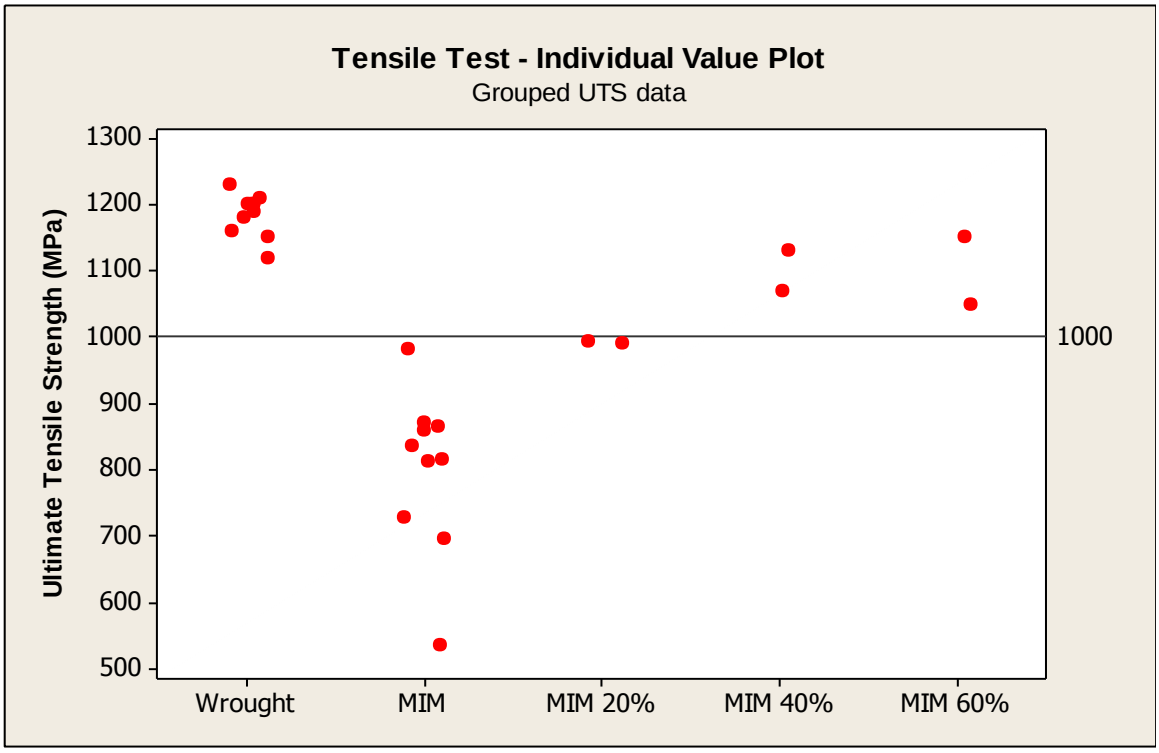

Figure 55: Individual Value Plot - Grouped UTS Data

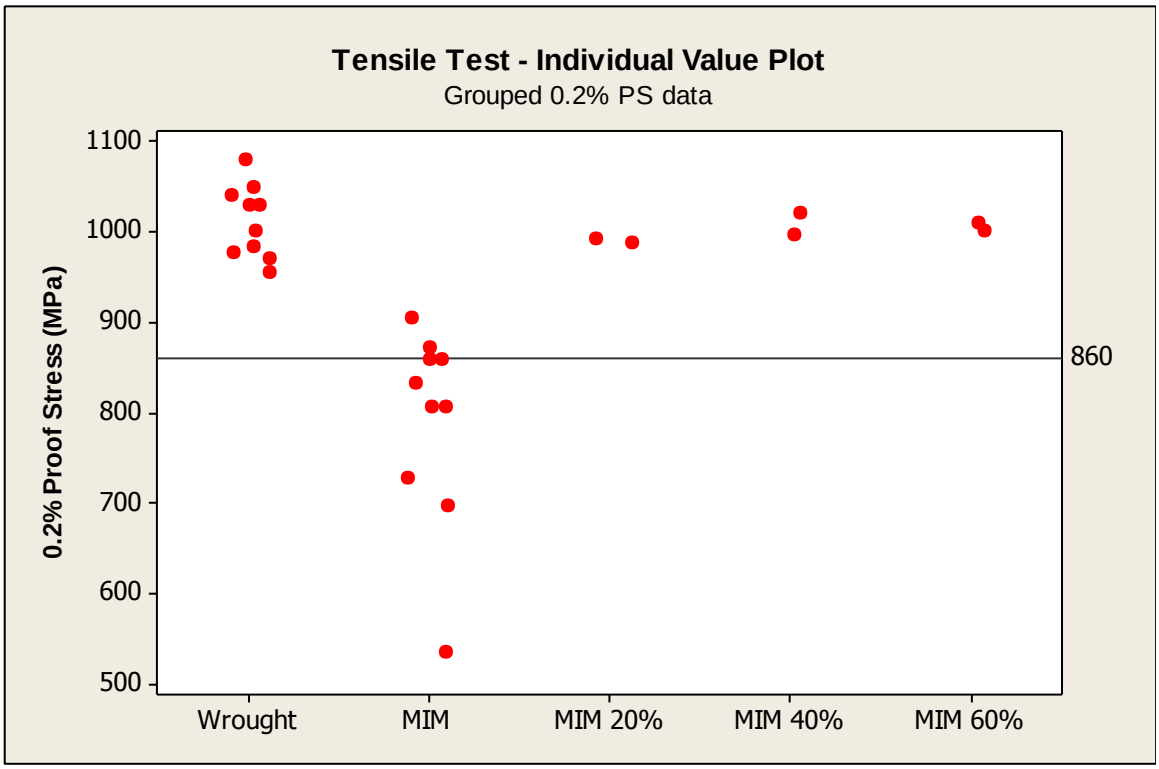

Figure 56: Individual Value Plot - Grouped 0.2% PS Data

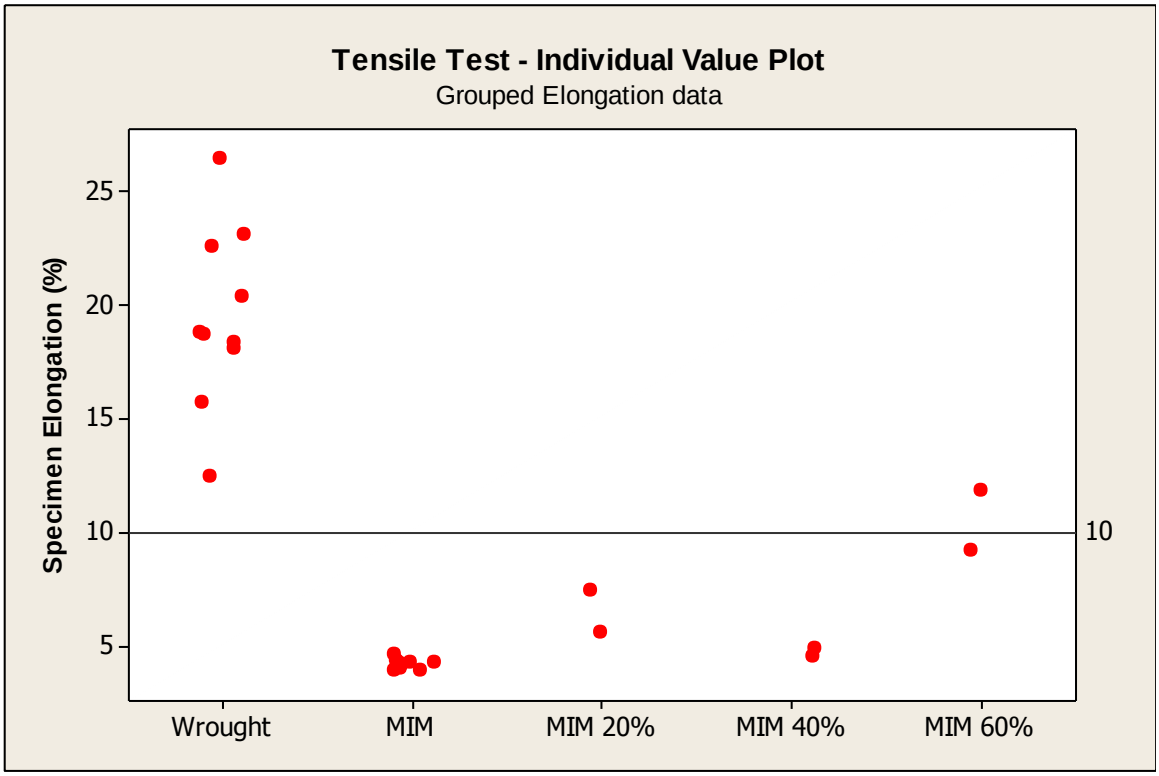

Figure 57: Individual Value Plot - Grouped Elongation Data

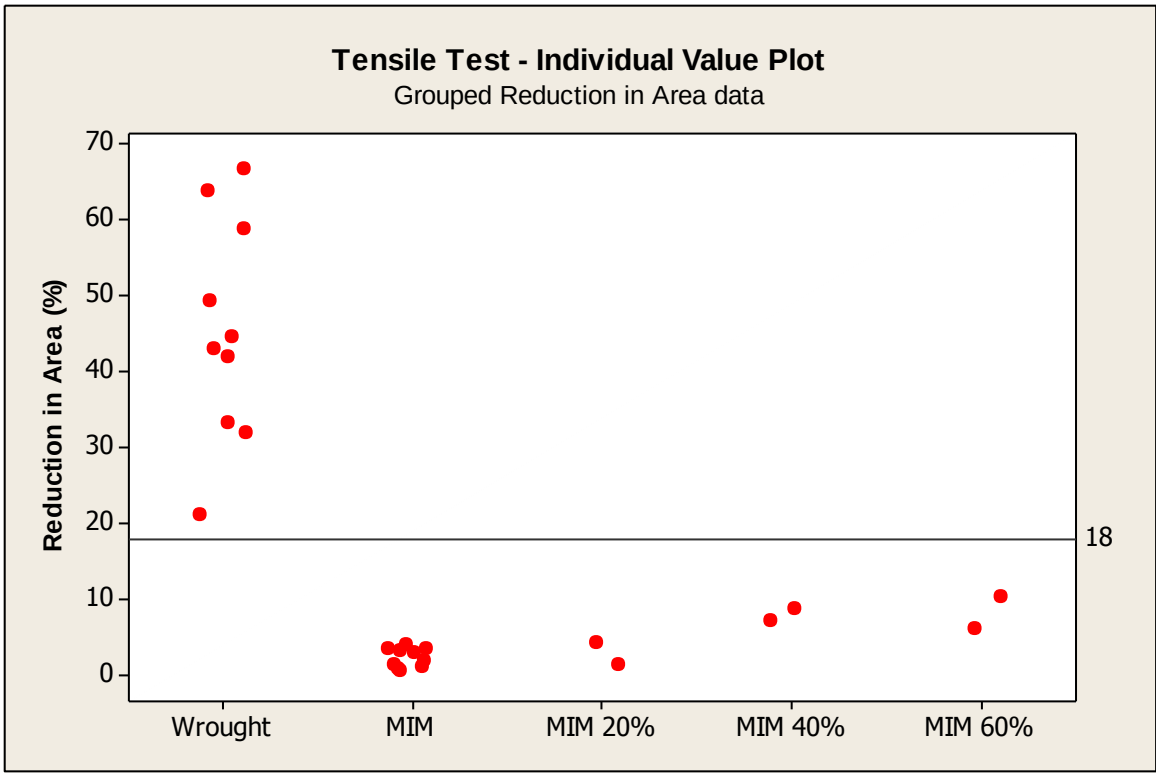

Figure 58: Individual Value Plot - Grouped Reduction in Area Data

Discussion

The Individual Value Plot of the grouped test data indicates that by selecting more homogeneous sections from the injection moulded test piece and introducing progressive amounts of thermo-mechanical processing the Ultimate Tensile Strength and 0.2% Proof Stress data can be improved upon.

This trend was also detected when examining the test data for the Reduction in Area and % Elongation, however as can be seen the ductility of the test pieces was still considerably less than the values obtained from the baseline wrought test pieces and also below the acceptance criteria for the test results.

Microstructural examination of the 'as moulded' 718 test pieces and also of the 20%, 40% and 60% reductions indicated that there was no gross porosity present in at the fracture faces of the small test pieces, however small amounts of randomly distributed porosity varying in size up to 15µm were present.

The presence of porosity in the microstructure is considered to be the cause of the reduced test piece ductility.

4.2 Test Piece Density Measurement

Test piece density measurements were performed in order to assess the density of the metal injection moulded test pieces. The experiments were conducted at ambient temperature and compared to a wrought 718 alloy billet. The density measurement technique was based upon the Archimedes Principle in which the test pieces were weighted both in air and in deionised water. Ref. Figure 59 below.

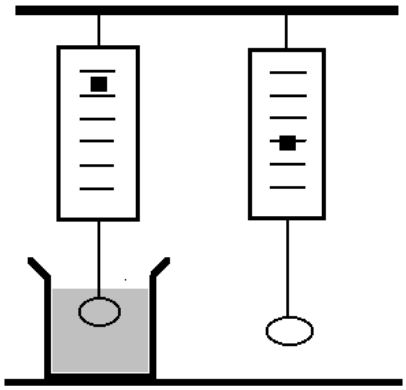

Figure 59: Archimedes' Principle

Experimental Procedure

All the test pieces to be tested were aqueous cleaned, water washed and oven dried at 40ºC to ensure the surface was free from debris. For the purpose of the experiment the density of the deionised water was assumed to be 1.0g/cm^3.

Figure 60: Oertling NA 114 Balance

The test pieces were firstly weighted in air using the Oertling NA 114 balance illustrated in Figure 60 above. The weight of the individual test pieces was recorded. The process was then repeated in deionised water using the Oertling NA 264

balance. The test piece was suspended in a wire mesh cradle and immersed fully in the deionised water. The weight of the individual test pieces was recorded. In order to calculate the sample density the following equation was followed. Ref Tables 37 to 43.

Sample density (g/cm^3) = Weight (g) of sample in air (a) x Density of Water (g/cm^3) ÷ Weight (g) of sample in air - Weight (g) of sample in water (b)

Test Piece Matrix

The test piece matrix below provides an overview of the type and quantity of density measurement samples which were performed. Ref Table 36.

Table 36: Density Measurement Sample Matrix

Trial	Material	Sample history	Sample quantity
1	Wrought	Billet	4
2	MIM	Billet	4
3	MIM	Failed elevated tensile test pieces	4*
4	MIM 20%	Failed elevated tensile test pieces	4*
5	MIM 40%	Failed elevated tensile test pieces	4*
6	MIM 60%	Failed elevated tensile test pieces	4*

*Two broken tensile test pieces provided 4 samples for density measurement purposes.

Table 37: Density Measurement - Trial 1 Results

Wrought (billet)	Weight in air (g)	Weight in water (g)	Difference (g)	Density (g/cm^3)
1	13.69	12.03	1.66	8.25
2	13.71	12.04	1.67	8.21
3	13.26	11.66	1.60	8.29
4	17.05	14.99	2.07	8.24
Average				**8.25**

The average density of the wrought billet specimens equates to $8.25 g/cm^3$. The test results were reasonably consistent as would be expected from the wrought 718 alloy billet.

Table 38: Density Measurement - Trial 2 Results

MIM (billet)	Weight in air (g)	Weight in water (g)	Difference (g)	Density (g/cm^3)
1	13.07	11.47	1.60	8.17
2	14.03	12.55	1.76	7.97
3	14.25	12.49	1.75	8.14
4	14.80	12.98	1.82	8.13
Average				**8.10**

The average density of the injection moulded test pieces from the MIM billet also proved to be reasonably consistent. As expected the density of the injection moulded test pieces was found to be less than the wrought 718 alloy billet. From the comparison between wrought and MIM billets it can be concluded that the density of the MIM billet is approximately 98.5% of the wrought 718 alloy datum.

This methodology was then repeated using the residual test pieces from the elevated temperature tensile test trials.

Table 39: Density Measurement - Trial 3 Results

MIM (tensile)	Weight in air (g)	Weight in water (g)	Difference (g)	Density (g/cm^3)
1	0.91	0.80	0.11	8.27
1a	1.37	1.20	0.17	8.06
Ave				**8.17**
2	1.12	0.98	0.14	8.00
2a	1.18	1.04	0.14	8.43
Ave				**8.22**

The test results were derived from the tested elevated temperature MIM tensile test pieces. A difference in specimen density can be detected between the 2 sections of the tested specimen and also between the average of individual test pieces. Test result 2a indicates a greater sample density than the baseline wrought sample.

Table 40: Density Measurement - Trial 4 Results

MIM 20% (tensile)	Weight in air (g)	Weight in water (g)	Difference (g)	Density (g/cm^3)
1	0.74	0.65	0.09	8.22
1a	1.57	1.38	0.19	8.26
Ave				**8.24**
2	0.66	0.58	0.09	7.33
2a	1.57	1.37	0.20	7.85
Ave				**7.59**

The test results were derived from the tested elevated temperature MIM 20% tensile test pieces. Test result 1a indicates a greater sample density than the baseline wrought sample. This increase is reflected in the overall sample average density of $8.30g/cm^3$.

Table 41: Density Measurement - Trial 5 Results

MIM 40% (tensile)	Weight in air (g)	Weight in water (g)	Difference (g)	Density (g/cm³)
1	0.96	0.84	0.12	8.00
1a	1.36	1.19	0.17	8.00
Ave				**8.00**
2	0.87	0.76	0.11	7.91
2a	1.44	1.27	0.17	8.47
Ave				**8.19**

The test results were derived from the tested elevated temperature MIM 40% tensile test pieces. Test result 2a indicates a greater sample density than the baseline wrought sample. The consequence of this is an average sample density is 8.30g/cm³.

Table 42: Density Measurement - Trial 6 Results

MIM 60% (tensile)	Weight in air (g)	Weight in water (g)	Difference (g)	Density (g/cm³)
1	0.79	0.69	0.10	7.90
1a	1.52	1.34	0.18	8.44
Ave				**8.17**
2	0.87	0.77	0.10	8.70
2a	1.43	1.25	0.20	7.15
Ave				**7.93**

The test results were derived from the tested elevated temperature MIM 60% tensile test pieces. Test result 1a indicates a greater sample density than the baseline wrought sample.

Discussion

The sample density results achieved from Trials 1 and 2 appear consistent in terms of the individual test results and the overall comparison between average test results. The resulting data is in accordance with published literature and is generally accepted that the density of injection moulded 718 alloy provides results approaching those which can be achieved from wrought 718 alloy.

Table 43: Density Measurement Trials Summary

Trial Summary	Material	Averaged trial Density g/cm³
Trial 1	Wrought billet	8.25
Trial 2	MIM billet	8.10
Trial 3	MIM tensile	8.20
Trial 4	MIM 20% tensile	7.92
Trial 5	MIM 40% tensile	8.10
Trial 6	MIM 60% tensile	8.05

The results from Trials 3 to 6 are inconsistent in terms of the variation or scatter in the individual test result values. In addition there are occasional individual results which are greater than the density obtained from the baseline wrought billet data.

Further evaluation of the trial test pieces is deemed necessary in order to fully understand the underlying cause of what are considered to be spurious test results. This evaluation is captured in the Scanning Electron Microscopy section of this thesis.

4.3 Scanning Electron Microscopy (SEM)

The Scanning Electron Microscopy (SEM) was chosen for the evaluation of both wrought and injection moulded test pieces. This capability compliments the reflected light microscopy techniques and offers additional more searching sample analysis. The capabilities of the SEM which were key to the selection of this type of analysis equipment were the improved depth of focus at higher magnifications and also the ability to collect and analyse information from the test piece surface to assist with the chemical characterisation. The basic operation of the SEM is illustrated in Figure 61 below.

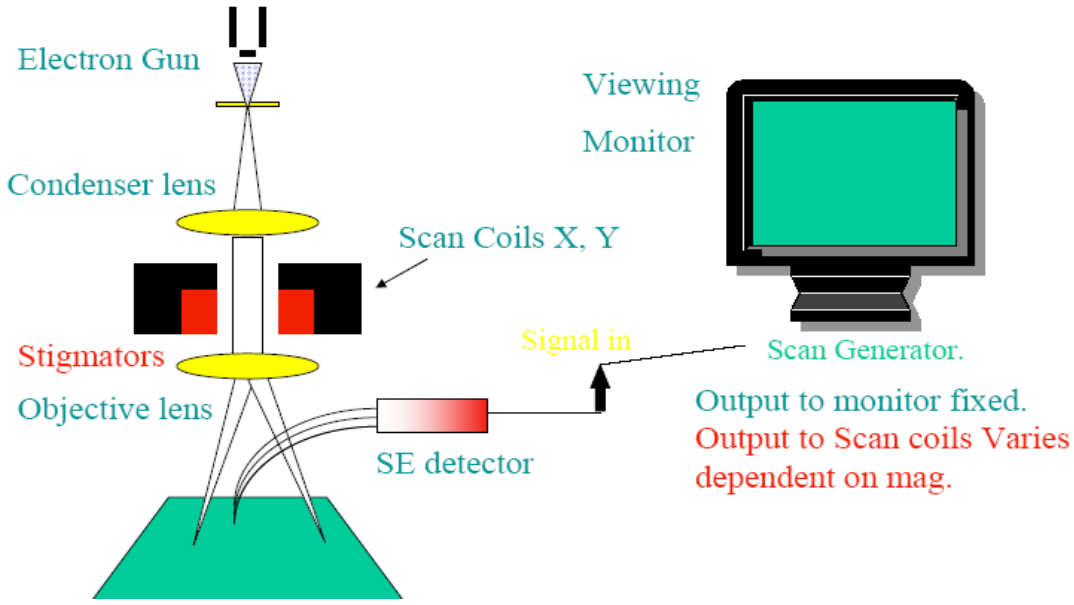

Figure 61: SEM Operation

In the scanning mode, areas ranging from approximately 1 cm to 5 microns in width can be imaged. Magnification up to x 500,000 is possible which greatly exceeds the capability of conventional reflected light microscopy. The electron gun generates a stream of electrons which are accelerated under vacuum conditions to the positive anode. In order to focus the stream of electrons accurately onto the target electromagnetic coils are used. The electrons collide with the surface of the object under examination, are deflected and subsequently collected by the detector. The image resolution is much superior to reflected light microscopes due to the shorter wavelength of the electron stream. The resulting image is then greatly magnified for viewing purposes.

Energy Dispersive X-Ray Analysis (EDAX)

Chemical characterisation of the specimen is achieved by the interaction of a focused beam of electrons with the surface of the test piece. This characterisation technique relies on the relationship between the unique atomic structure of the element under examination corresponding to an exclusive X-ray emission peak.

Interaction with the stream of electrons results in ground state electrons being ejected from their nucleii. An electron from an outer higher energy shell then claims the vacancy and in doing so releases X-ray energy which equates to the difference between the shells. The quantity and energy of the X-rays emitted from the specimen are then captured and measured by the energy dispersive spectrometer. A collimator ensures that only X-rays from the area being excited by the electron beam are collected of analysis. As the energy of the X-rays are characteristic of the difference in energy between the two shells, and of the atomic structure of the element from which they were emitted, this allows the elemental composition of the specimen to be measured.

In order to obtain this characteristic X-ray from the specimen, a beam of high energy electron particles is focused on the area of interest. This beam must possess a minimum amount of energy necessary to dislodge a particular electron from a particular shell. The energy and wavelength of an X-ray are related by the following equation. Ref. Figure 62 below.

$$\lambda\ (\text{nm}) = 1.2398 / E\ (\text{keV})$$

Figure 62: Energy and Wavelength Equation

From this equation it can be seen that as the voltage increases the wavelength decreases resulting in more energetic X-rays. Electrons in shells closer to the nucleus of the atom require a greater amount of energy.

The characteristic X-rays are identified in accordance with the shell in which the initial vacancy occurs and the shell from which an electron drops to fill that vacancy. From Figure 63 below, if the initial vacancy occurs in the K shell and the vacancy filling electron drops from the adjacent (L) shell, a Kα X-ray is emitted. If the electron drops from the M shell (two shells away), the emitted X-ray is a Kβ X-ray.

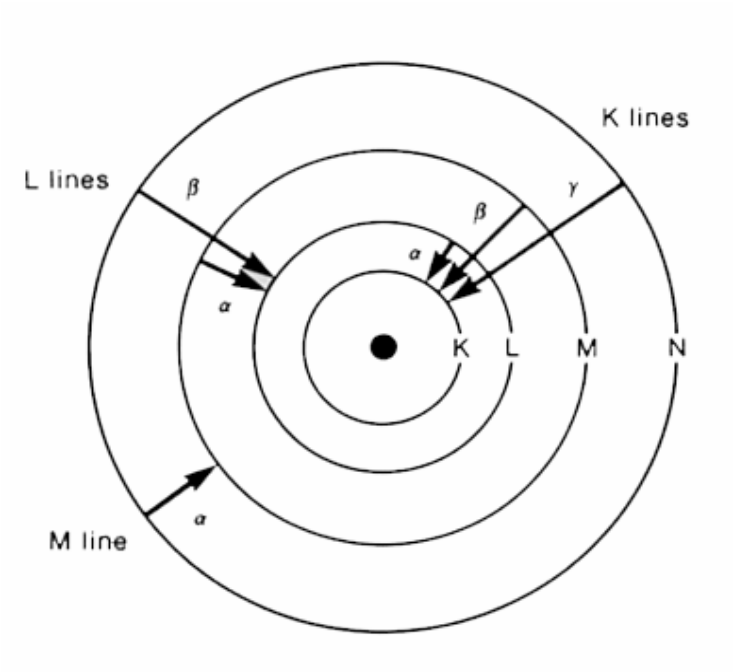

Figure 63: Characteristic X-ray Diagram

Moseley's Law is the basis for elemental analysis with EDAX. If the energy of a given K, L or M line is measured, then the atomic number of the element producing that line can be determined. The K, L and M series X-rays increase in energy with increasing atomic number. Ref. Figure 64 below.

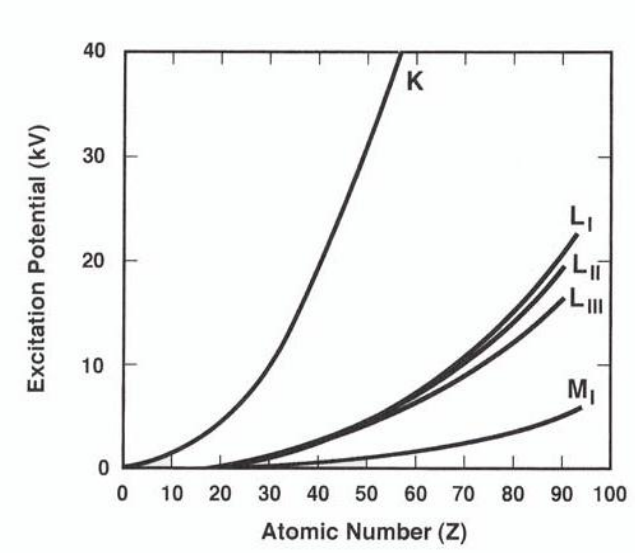

Figure 64: Characteristic Radiation Energy

The energy of the characteristic radiation within a given series of lines varies monotonically with atomic number. Figure 65 below captures the key relationships.

$$E = C_1 (Z - C_2)^2$$

E = energy of the emission line for a given X-ray series (e.g. Kα)

Z = atomic number of the emitter

C_1 and C_2 are constants

Figure 65: Moseley's Law Equation

During a typical EDAX analysis scan various elemental peaks can be seen and this is in accordance with Moseley's Law. Lighter elements will emit X-rays of the K series, intermediate elements will emit X-rays from the L series or K and L series. Heavy elements will emit X-rays from the M series or L and M series.

SEM-EDAX Output

The distribution of the different chemical elements from which the sample under examination is comprised can be captured and documented.

The desired outputs can be either qualitative or quantitative or indeed both measures can be used. Qualitative analysis involves the identification of the elements present.

Major Elements >10 wt%
Minor Elements >1-10 wt%
Trace Elements < 1 wt%

Quantitative assessments are an indication of how much if the element is present in At% or wt%.

Experimental Procedure

The Hitachi S4800 scanning electron microscope with EDAX analysis capability was used for both low magnification comparative assessments of both wrought and MIM 718 alloy samples. Two sample types were chosen for assessment, samples which were in the polished and chemically etched condition and samples which presented fractured surfaces. The fractured samples that were used were from the elevated temperature tensile test. Ref. Figure 66 below.

Figure 66: Mounted Tensile Fixture

SEM sample preparation for the fractured tensile surfaces required the failed section to be located on round platen. Conductive media was used for both fracture surface and micro assessments. Table 44 illustrates the SEM analysis matrix. Table 45 illustrates the EDAX analysis matrix.

Table 44: SEM Analysis Sample Matrix

SEM Analysis Sample Type	Number of Images	Sample Magnification	Sample Magnification
'Small' wrought tensile fracture surface	1	x 25	-
'Standard' MIM tensile fracture surface	1	x 25	-
Etched wrought micro	1	x 500	-
Etched MIM micro	1	x 500	-
'Small' wrought tensile fracture	1	x 1000	-
'Standard' MIM tensile fracture	1	x 1000	-
'Small' MIM tensile fracture surface 20%	2	x 300	x 1500
'Small' MIM tensile fracture surface 40%	2	x 300	x 1500
'Small' MIM tensile fracture surface 60%	2	x 300	x 1500
Misc – 'Small' MIM tensile fracture surface 40%	1	x 40	-
Misc – 'Standard' MIM-poor particle cohesion	1	x 200	-
Misc – 'Standard' MIM-poor particle cohesion	1	x 1000	-

The scanning electron microscope images for the wrought samples are captured by Figures 67,69 and 71.

A more comprehensive range of MIM sample images are detailed in Figures 68,70 and 72.

Figures 73 to 78 represent the microstructures in thermo-mechanically processed test pieces.

In order to illustrate the variation in MIM sample integrity Figures 79 to 81 have been included.

Table 45: EDAX Analysis Sample Matrix

EDAX Analysis Sample Type	Number of Images	Qualitative Analysis	Quantitative Analysis	Quantitative Analysis
Etched wrought micro	1	Spectrum	At%	Wt%
Etched MIM micro	1	Spectrum	At%	Wt%
Etched MIM micro	1	Spectrum	At%	Wt%
Etched MIM micro	1	Spectrum	At%	Wt%
Etched MIM micro	1	Spectrum	At%	Wt%

Figures 82 and 83 illustrate the contrasting wrought and MIM 718 alloy microstructures. The corresponding chemical composition of Figures 84 and 85 appear to be similar.

Figures 86 to 91illustrate the localised variation in chemical composition of the major elements.

SEM Results

Figure 67: Wrought 718 Alloy x 25

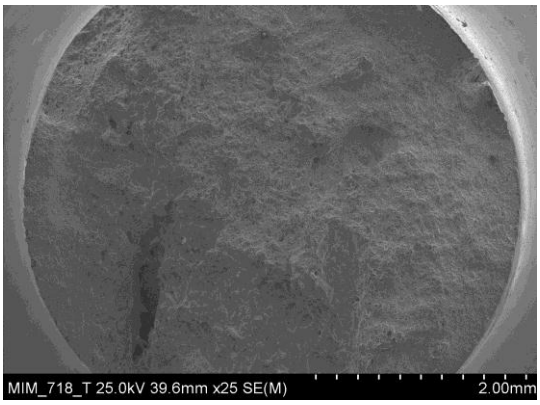

Figure 68: MIM 718 Alloy x 25

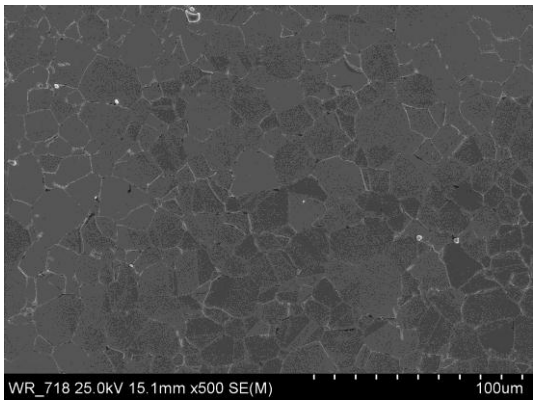

Figure 69: Wrought 718 Alloy x 500

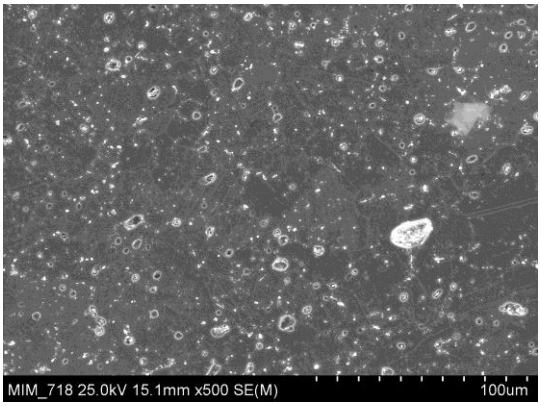

Figure 70: MIM 718 Alloy x 500

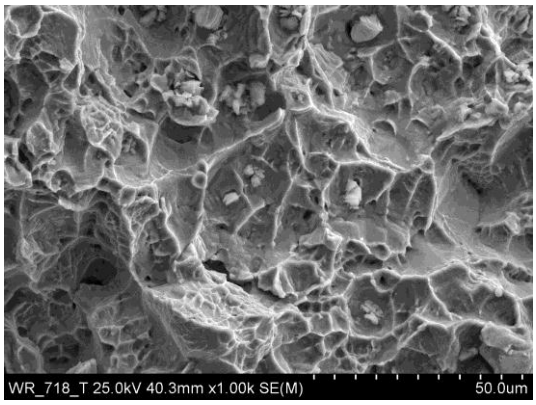

Figure 71: Wrought 718 Alloy x 1000

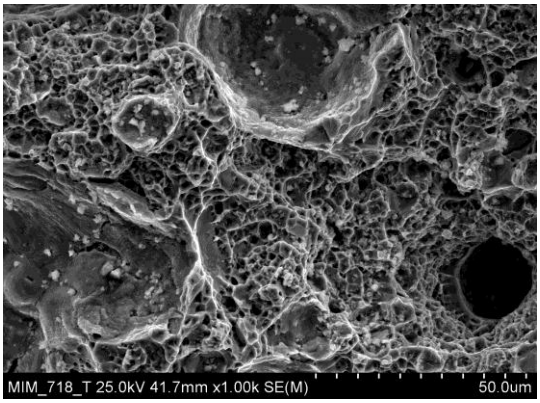

Figure 72: MIM 718 Alloy x 1000

Discussion

The low magnification images (x 25) of the fracture faces from a ‘small’ wrought elevated temperature tensile specimen and a standard injection moulded test piece are typically ductile fractures, however this ductility is not reflected in the overall tensile test results of the injection moulded sample.

As can be seen from the injection moulded test piece fracture face, a large void is present within the structure. Close to the void location can be seen smaller structural abnormalities.

The images of both the wrought and the injection moulded microstructures (x 500) in the chemically etched condition illustrate two contrasting microstructures. The wrought microstructure is essentially polycrystalline in appearance, while the injection moulded microstructure presents a mixture of fine porosity and an unusually high quantity of unidentified finely dispersed precipitates throughout the structure.

The higher magnification images (x 1000) of both wrought and injection moulded 718 alloy are equally contrasting. The scanning electron microscope images of the wrought fracture faces illustrate a high degree of structural uniformity with evidence of a uniform distribution of precipitates throughout the area under observation. The ridged surface is evidence of sample ductility during the plastic deformation stages of the elevated temperature test.

The scanning electron microscope image of the injection moulded fracture face reveals several interesting features which are not part of the failure analysis expected for 718 alloy. Three features were noted to be of particular interest as they did not appear in the fracture surface of the wrought specimen.

- Small circular void possibly corresponding to the size of a powder particle was noted.
- Smooth circular surface also corresponding to the size of a powder particle and which did not form part of the surrounding ductile fracture landscape.
- Relatively large smooth plane containing small linked precipitates.

All three of the fracture face structural abnormalities are thought to be a consequence of inadequate interparticle cohesion. The cause of the variable occurrence of these features is not known however it may be as a result of fine oxide

layers present on certain powder particles which may prevent homogeneous sintering occurring.

SEM Results - MIM 718 Alloy (20%, 40% and 60% forged reduction)

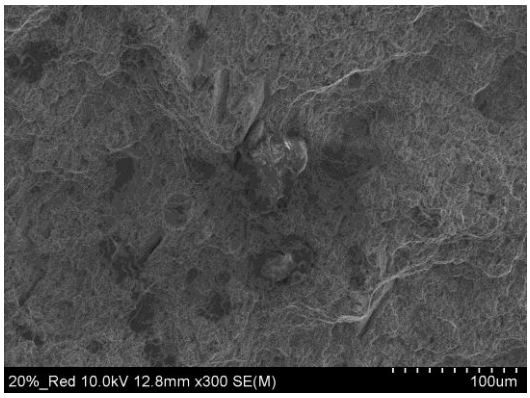

Figure 73: 20% x 300

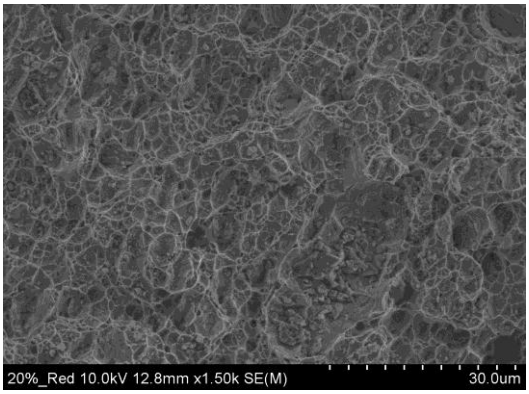

Figure 74: 20% x 1500

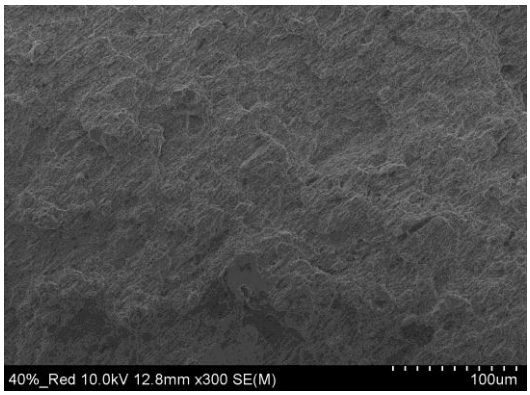

Figure 75: 40% x 300

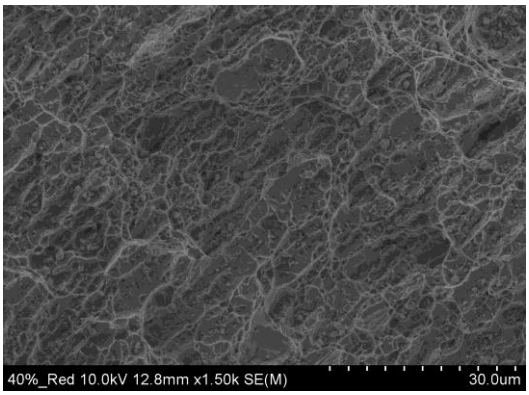

Figure 76: 40% x 1500

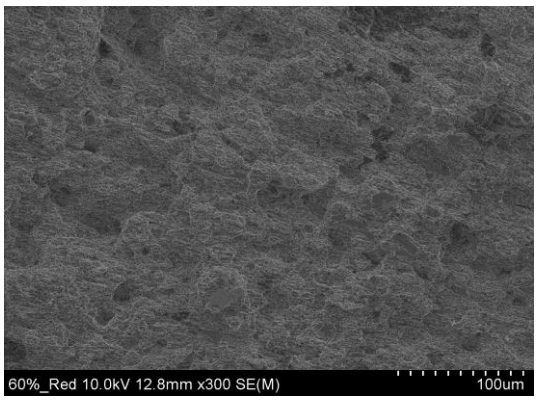

Figure 77: 60% x 300

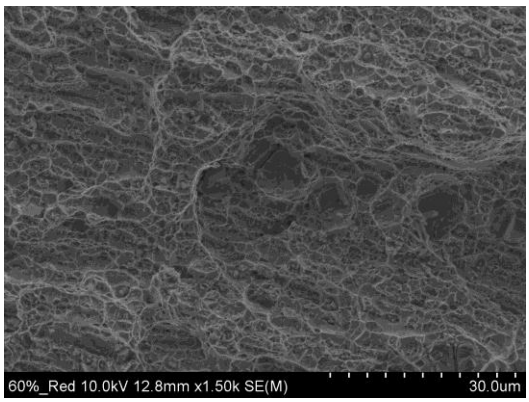

Figure 78: 60% x 1500

SEM Results (continued)

Supplementary MIM 718 Alloy Structures

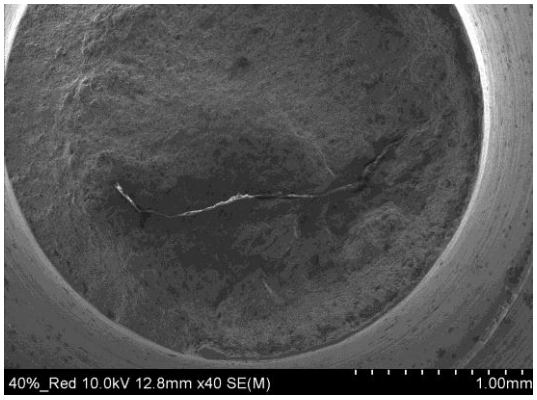

Figure 79: 40% x 40

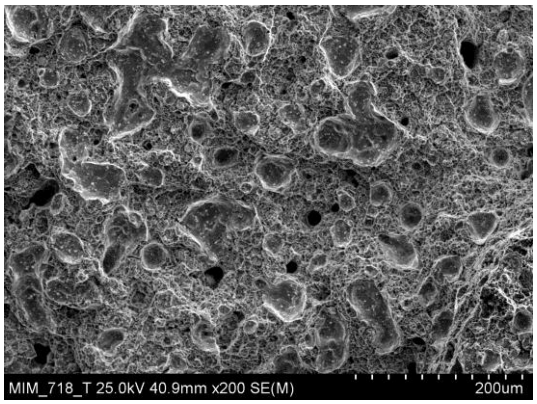

Figure 80: x 200

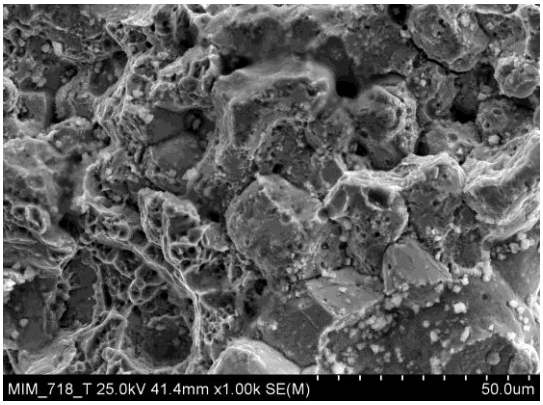

Figure 81: x 1000

Discussion

The scanning electron microscope images of the 20%, 40% and 60% thermo-mechanically processed injection moulded 718 alloy test pieces were generally found to be consistent in terms of the overall ductile nature of the fracture surfaces. As can be seen, small pores are evident in all the samples that were examined however there was no evidence of large voids as was expected since the small tensile samples were taken from sections of the test bar following CT analysis and mapping of the obvious discontinuities. The higher magnification images illustrated by figures 74, 76 and 78 depict the directional microstructural effects which have been produced by progressively increasing amounts thermo-mechanical processing.

Included in the 'Supplementary Microstructures' section there are three images of the fracture surfaces from three different elevated temperature tensile test pieces. During low magnification examination of the fractured surfaces, the sample representing 40% reduction presented evidence of foreign material entrapment. Figure 79 illustrates the presence of the relatively large amount of foreign material within the test piece. This feature was not detected during the rigorous CT analysis which was performed on the test bars prior to manufacturing the small tensile test specimens, presumable due to a similarity in density to the parent 718 alloy. It is not known at which stage in the manufacturing sequence the object became entrapped and therefore it is possible that the material could have been present in the original powder lot, or any of the binder constituents.

Figures 80 and 81 illustrate the variation in test piece failure modes that were noted during the examination of the tested elevated temperature injection moulded test pieces. Figure 80 presents a fracture face which is ductile in nature. Figure 81 however presents a contrasting fracture surface. The fracture surface of this sample is indicative of an intercrystalline brittle failure mode.

The reason why some particles do bond successfully yet others do not, is not fully understood however it could be related to the surface condition or the size of the original powder particles.

EDAX Analysis Results

The sample preparation procedure is detailed in section 5.4

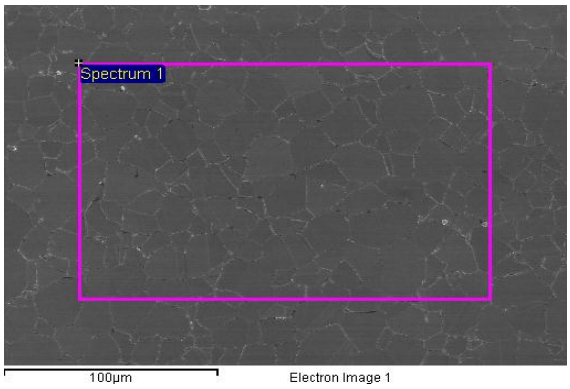

Element	Weight%
Al K	0.86
Ti K	0.97
Cr K	19.32
Fe K	18.59
Ni K	51.53
Nb L	5.17
Mo L	3.57
Totals	100.00

Figure 82: Electron Image (Wrought 718 Alloy)

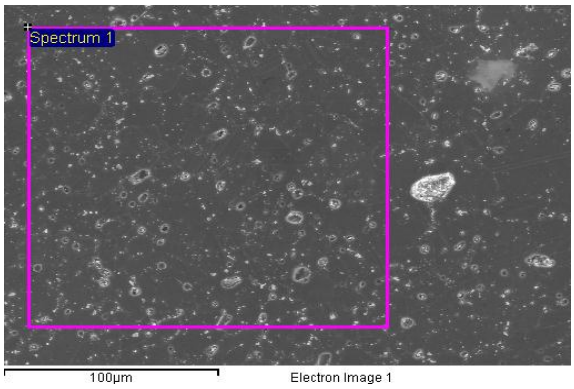

Element	Weight%
Al K	0.55
Ti K	1.13
Cr K	19.88
Fe K	19.23
Ni K	50.09
Nb L	5.65
Mo L	3.48
Totals	100.00

Figure 83: Electron Image (MIM 718 Alloy)

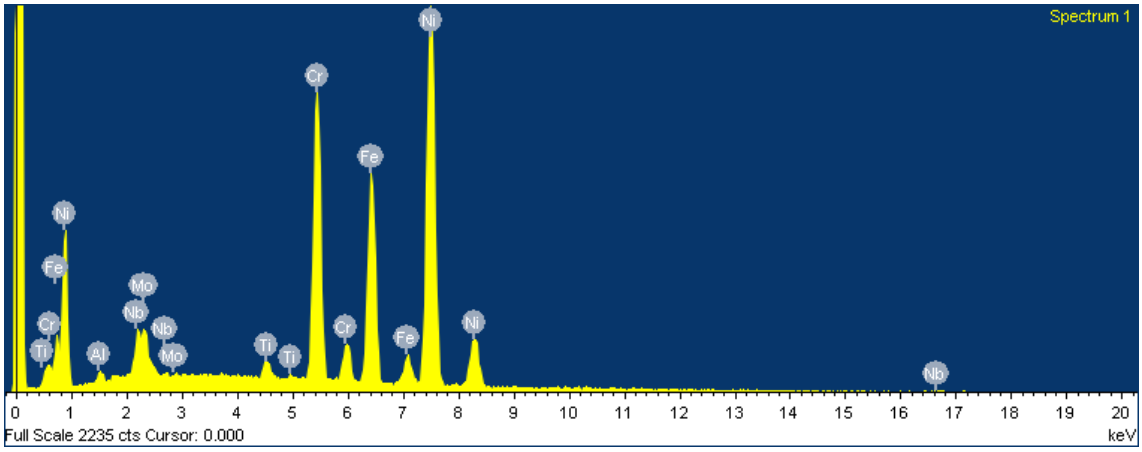

Figure 84: Spectrum Image (Wrought 718 Alloy)

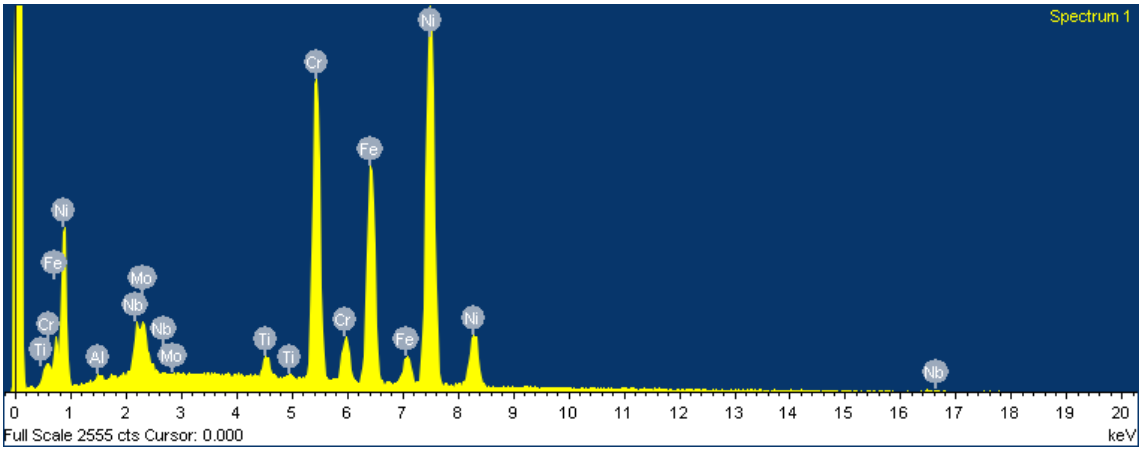

Figure 85: Spectrum Image (MIM 718 Alloy)

As can be seen from the low magnification spectra, both wrought and MIM 718 alloy spectra appear similar. This analysis was conducted without reference to traceable standards and is purely comparative.

The weight % of the major elements present in both spectra would correspond with both national and international standards for 718 alloy.

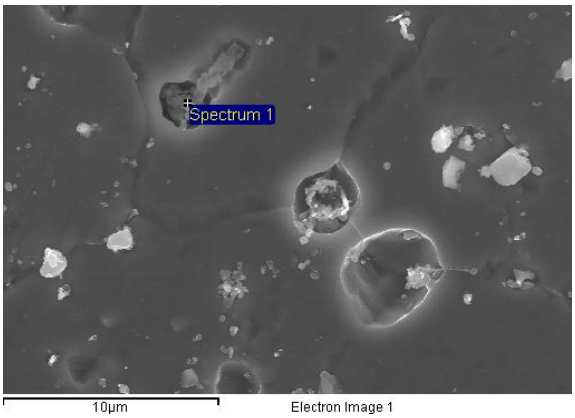

Element	Weight%
C K	0.00
O K	26.05
Al K	16.04
Ti K	6.12
Cr K	10.54
Fe K	9.26
Ni K	22.79
Nb L	9.19
Totals	100.00

Figure 86: Electron Image (MIM 718 Alloy)

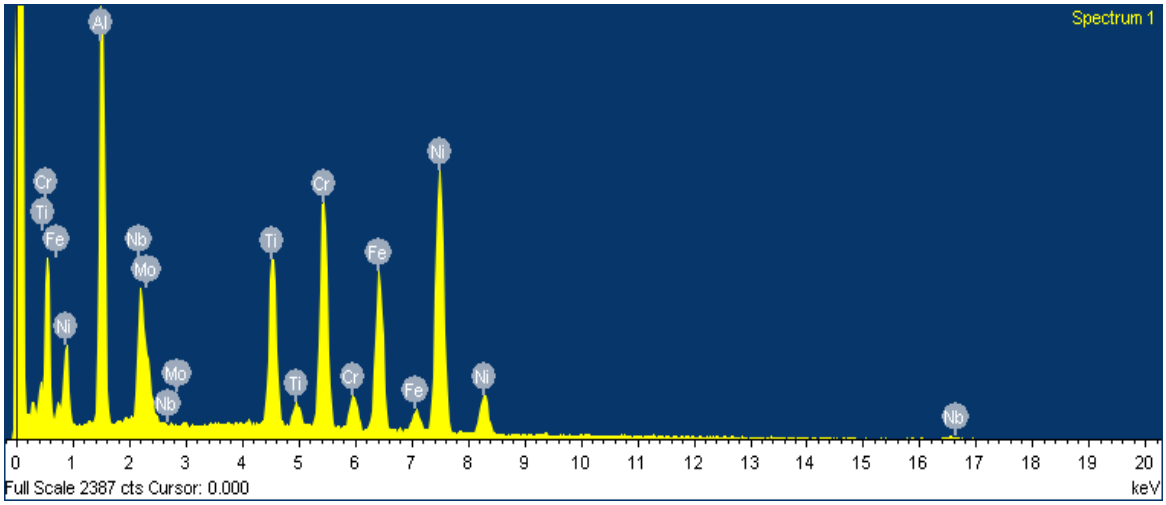

Figure 87: Spectrum Image (MIM 718 Alloy)

As can be seen from the spectrum analysis results the chemical composition of the precipitate can be described as containing the following elements:

Major Elements - Oxygen, Chromium and Nickel

Minor Elements - Iron, Niobium and Titanium.

EDAX Analysis Results

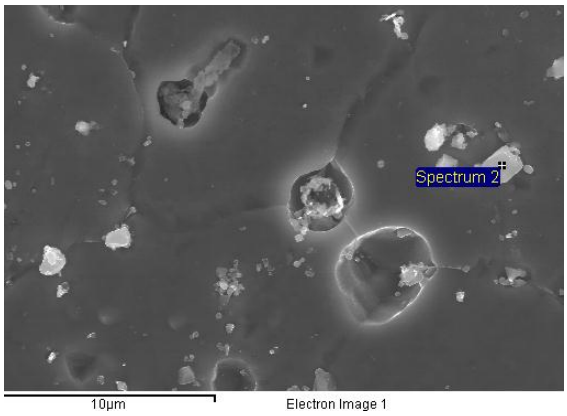

Element	Weight%
Al K	1.02
Ti K	7.33
Cr K	6.53
Fe K	5.58
Ni K	12.30
Nb L	67.24
Totals	100.00

Figure 88: Electron Image (MIM 718 Alloy)

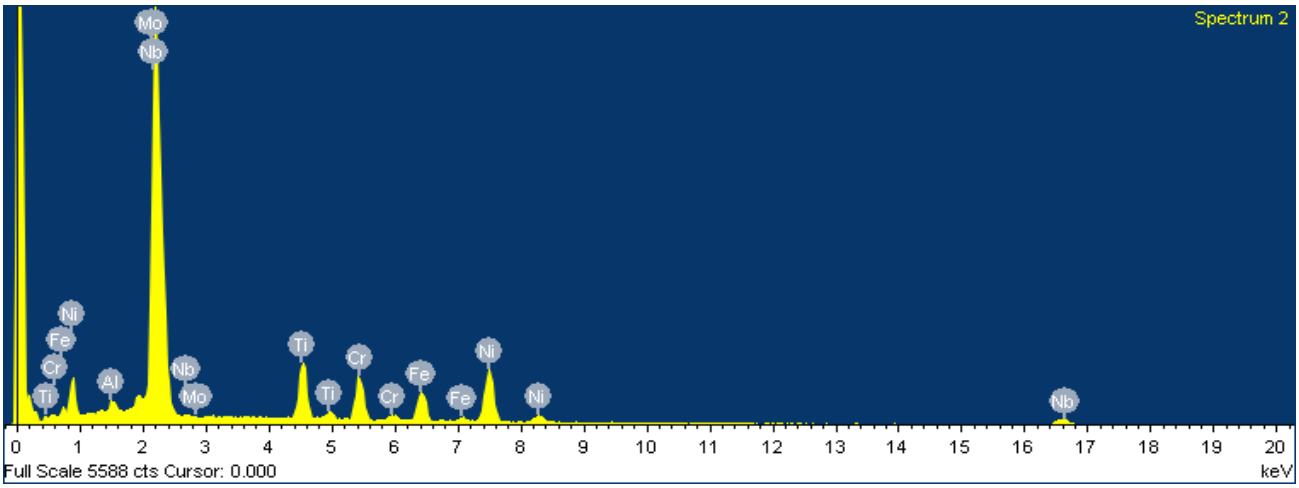

Figure 89: Spectrum Image (MIM 718 Alloy)

As can be seen from the spectrum analysis results the chemical composition of the precipitate can be described as containing the following elements:

Major Elements - Niobium and Nickel

Minor Elements - Titanium, Chromium, Iron and Aluminium.

EDAX Analysis Results

Figure 90: EDAX - Electron Image (MIM 718 Alloy)

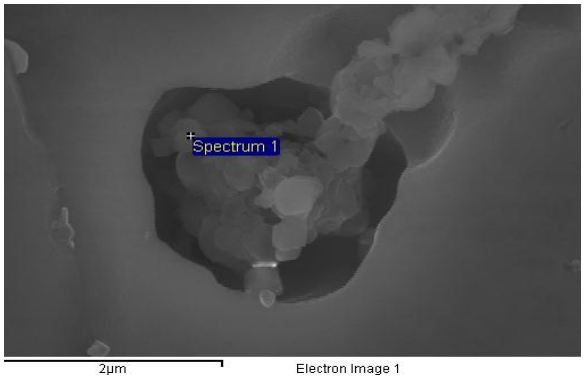

Element	Weight%
C K	0.00
N K	0.00
O K	8.60
Al K	7.53
Ti K	7.43
Cr K	16.48
Fe K	14.55
Ni K	36.58
Nb L	8.83
Totals	100.00

Figure 91: Spectrum Image (MIM 718 Alloy)

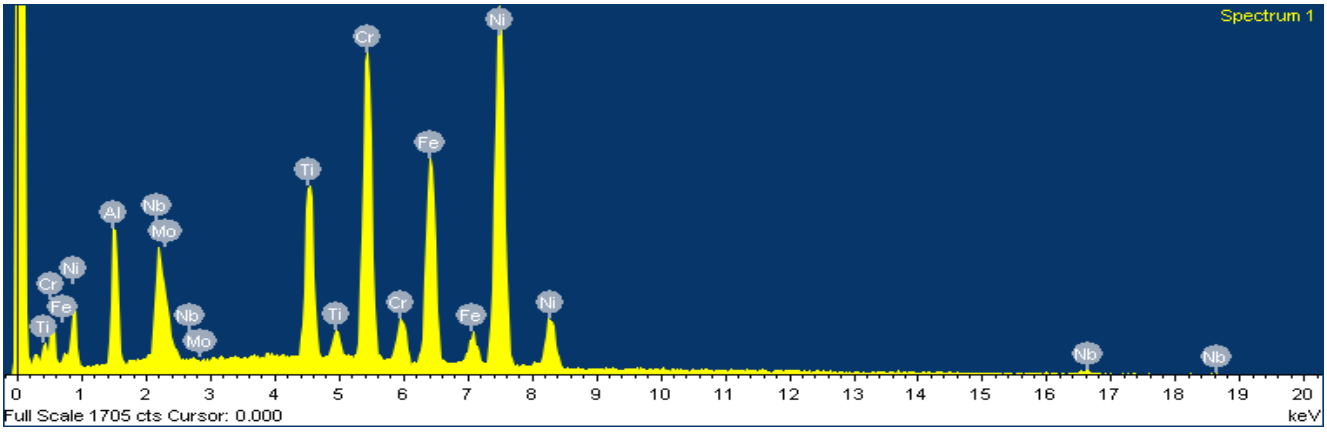

As can be seen from the spectrum analysis results the chemical composition of the precipitate can be described as containing the following elements:

Major Elements - Nickel, Iron and Chromium

Minor Elements - Niobium, Oxygen, Aluminium and Titanium.

Discussion

The microstructure of wrought 718 alloy in the fully heat treated condition would normally contain a discrete mixture of both carbides and delta phase (Ni_3Nb) distributed throughout a polycrystalline grain structure.

The spectral images of the precipitates present in the injection moulded 718 alloy can be seen to differ considerably from the wrought sample which was analysed for comparison purposes.

The quantity of precipitates present in the injection moulded sample is much greater than that wrought 718 alloy sample. The morphology of the precipitates present in the injection moulded samples also differs considerably from the discrete nature of the wrought precipitates. The chain or bridged nature of the injection moulded precipitates is a salient feature of the SEM analysis.

During the manufacture of wrought 718 alloy several thermo-mechanical processing sequences are employed in order to break up and homogenise the alloy. Due to the size and agglomeration of particles present in the injection moulded variants the omission of these operation could account for their presence

Wrought 718 alloy is melted and processed under vacuum conditions however the powdered 718 alloy used for the generation of feedstock was melted under argon. This difference in processing is reflected in the analysis results listed in Table 46 below.

Table 46: Elemental Analysis (Carbon, Nitrogen and Oxygen)

718 Alloy Condition	Carbon Wt%	Nitrogen Wt%	Oxygen Wt%
Wrought slug	0.027	0.005	<0.001
Finished forging	0.027	0.005	<0.001
718 alloy powder	0.050	0.065	0.054
Injection moulded component	0.065	0.068	0.052

While the values of carbon nitrogen and oxygen appear to be stable for the wrought manufacturing route it can be see that there is an increase in these elements in the 718 alloy powder.

4.4 Test Piece Preparation

The importance of consistent preparation methods and techniques during both the early and final processing stages of the test piece preparation are key to providing repeatable test results. The following preparation equipment and methods were utilised prior to microscopic examinations and hardness testing.

Rough Sectioning Techniques

A selection of preparation equipment was used in order to section both test pieces and trial components. In all instances the section adjacent to the required piece was mechanically clamped so no additional force was exerted on the test piece. Sectioning was achieved by using silicon carbide abrasive wheels which were fed manually through the work piece. Throughout the sectioning process the work piece was flooded with coolant to avoid overheating. Ref. Figure 92 and 93 below.

Figure 92: Struers Discotom 5

Figure 93: Struers Labotom 3

Test Piece Mounting

Both wrought and injection moulded 718 alloy test pieces were mounted in a thermosetting polymer resin. The mounting press utilised for mounting the cut test pieces was a programmable unit incorporating a fully automatic electro hydraulic press for consistency of processing. This was considered an adequate mounting method to support to the test piece for both micro hardness testing and also for general optical microscopy. Ref. Figure 94 below.

Figure 94: Beuhler SimpliMet 3000 Mounting Press

Test Piece Polishing

The test piece polishing regime utilised for both the wrought and the injection moulded test pieces is documented below. Each stage of the polishing technique was followed by a water wash to remove residual polishing debris and abrasive grit.

Figure 95: Struers Rotopol-31 Sample Polisher

The polishing machine chosen for this operation was fully programmable which ensured that the specimen loads and polishing times were repeatable. Ref figure 95 above.

Test Piece Polishing Sequence

The polishing sequence documented in Table 47 below was utilised for both wrought and MIM samples.

Table 47: Test Piece Polishing Sequence (Wrought and MIM)

		Media Type	Force	Wheel Speed	Head Rotation	Lubricant Type	Time (s)
Grinding	Stage 1	80 SiC grit	150 N	300 rpm	either	water	120
	Stage 2	120 SiC grit	150 N	300 rpm	either	water	120
	Stage 3	180 SiC grit	150 N	300 rpm	either	water	120
	Stage 4	220 SiC grit	150 N	300 rpm	either	water	120
	Stage 5	320 SiC grit	150 N	300 rpm	either	water	120
	Stage 6	500 SiC grit	150 N	300 rpm	either	water	60
	Stage 7	800 SiC grit	150 N	300 rpm	either	water	60
	Stage 8	1000 SiC grit	150 N	300 rpm	either	water	60
	Stage 9	1200 SiC grit	150 N	300 rpm	either	water	30
	Stage 10	2500 SiC grit	150 N	300 rpm	either	water	30
Polishing	Stage 1	OP-Chem polish cloth	150 N	150 rpm	either	OPS	120
	Stage 2		150 N	150 rpm	either	water	60-120

Test Piece Etching

The chemical composition of the 718 alloy metallurgical etch is detailed in Table 48 below.

Table 48: Test Piece Etching (Wrought and MIM)

Constituent	Quantity (ml)
Hydrochloric acid	80
Hydrofluoric acid	4
Distilled water	100
Hydrogen peroxide activator	16

Test pieces prepared for chemical etching were immersed in the metallurgical etch. The etching time was deemed to commence from the visible onset of gas evolving from the surface of the test piece.

Once chemical etching was complete the test pieces were removed from the beaker of etchant, water washed and dried.

4.5 Reflected Light Microscopy

Reflected light microscopy was selected to analyse both the wrought baseline 718 alloy test pieces and the injection moulded variants. This equipment was selected in order to obtain a low magnification overview of the test pieces integrity in both the ‘as polished’ and ‘chemically etched’ surface conditions.

In the reflected light microscope the light source used to illuminate the sample passes through a condenser lens and is then reflected by a glass reflector down into the objective. Once focused on the sample, the light is then reflected back from the sample surface and back into the objective. The reflected light travels at a different angle allowing it to pass back through the glass reflector. The light then travels until it reaches the eyepieces or oculars where the surface image is visible. Sample magnification is achieved through the objective lenses combined with the ocular lenses. Ref Figure 96 below.

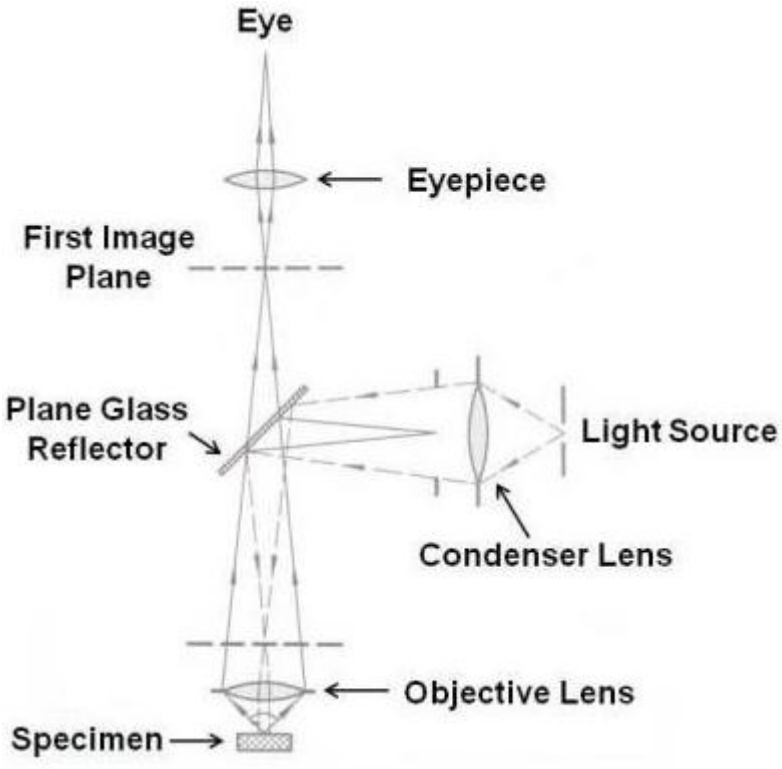

Figure 96: Reflected Light Microscopy Schematic Diagram

Experimental Procedure

The test pieces which were analysed using an inverted reflected light microscope. The test pieces were prepared using conventional specimen preparation techniques. Representative sample sections were removed from the wider sample area, mounted in bakelite and polished using an established 718 alloy preparation technique. Ref. Figure 97 below. Table 49 illustrates the analysis matrix.

Figure 97: Zeiss Axio - Inverted Microscope

Table 49: Reflected Light Microscopy Sample Matrix

Reflected light microscopy Sample type	Number of Images	Sample Magnification
Wrought - as polished	1	x200
Wrought - chemically etched	1	x200
MIM - as polished	1	x200
MIM - chemically etched	1	x200
MIM 20% as polished	1	x200
MIM 20% chemically etched	1	x200
MIM 40% as polished	1	x200
MIM 40% chemically etched	1	x200
MIM 60% as polished	1	x200
MIM 60% chemically etched	1	x200
Misc 20%	1	x200
Misc 40%	1	x200
Misc 60%	1	x200
Misc - sample strain band	1	x200

Figures 98 to 108 detail the microscopic examination of wrought and MIM sections.

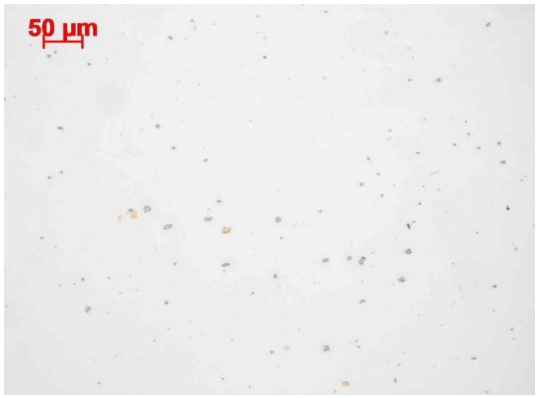

Figure 98: Wrought 718 Alloy x 200

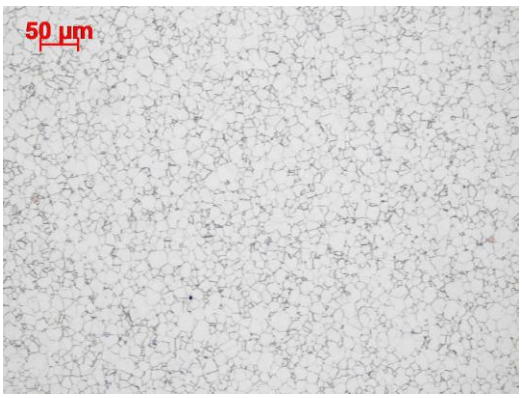

Figure 99: Wrought 718 Alloy x 200

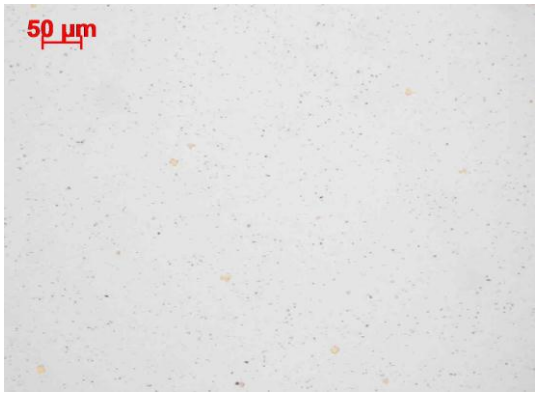

Figure 100: MIM 718 Alloy x 200

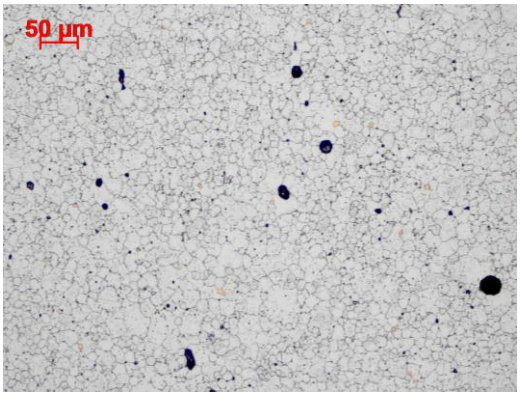

Figure 101: MIM 718 Alloy x 200

Discussion

The images above represent wrought and injection moulded 718 alloy in both the ‘as polished’ and ‘chemically etched’ conditions.

From the wrought images in the ‘as polished’ condition, precipitates of delta phase and carbides can be seen. In the ‘chemically etched’ condition the microstructure of the wrought 718 alloy sample is typically homogeneous presenting an average grain size finer than ASTM 8.

By contrast the injection moulded 718 alloy image does not reveal as much delta phase or carbides in the microstructure. A range of pores and voids can be seen in the etched condition.

Thermo-mechanically Processed MIM 718 Alloy Samples

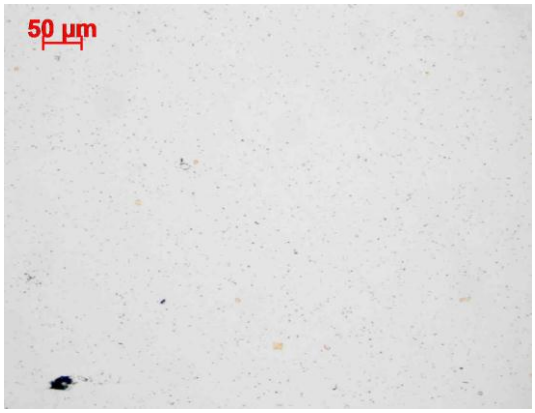

Figure 102: 20% x 200

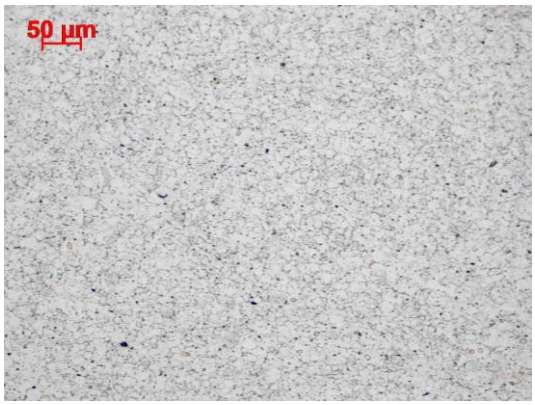

Figure 103: 20% x 200

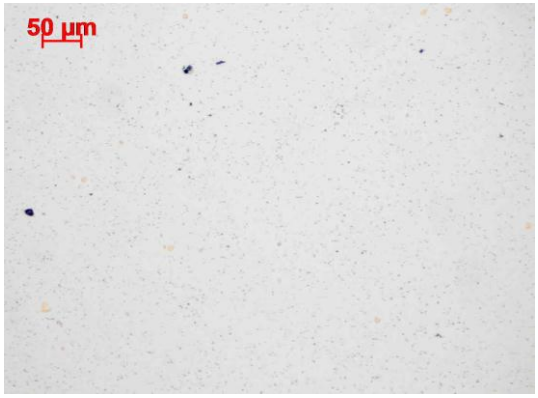

Figure 104: 40% x 200

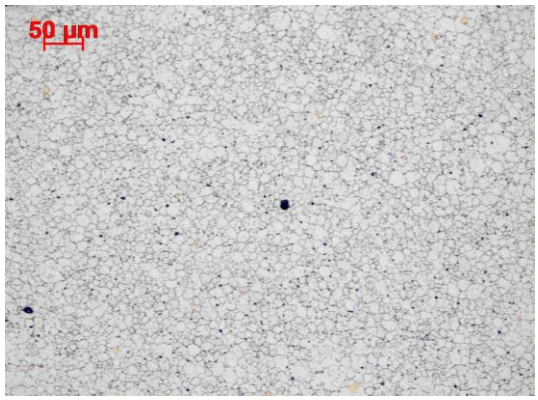

Figure 105: 40% x 200

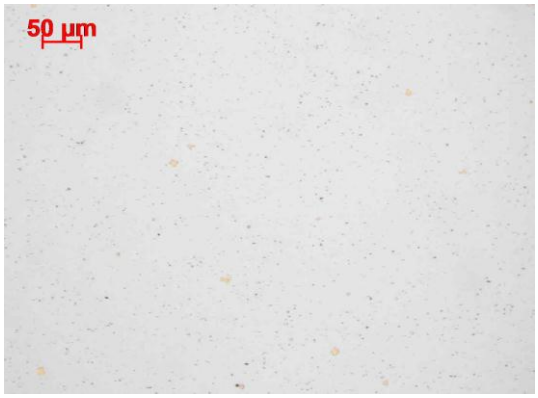

Figure 106: 60% x 200

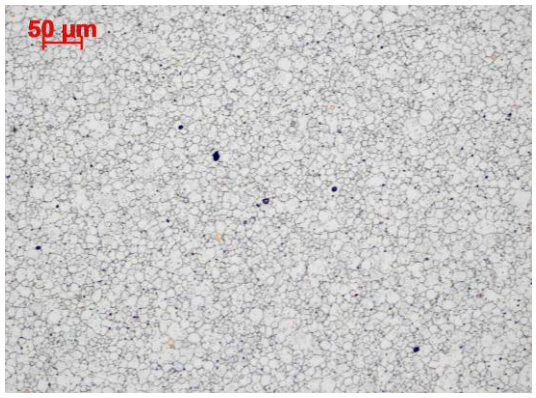

Figure 107: 60% x 200

Strain Band

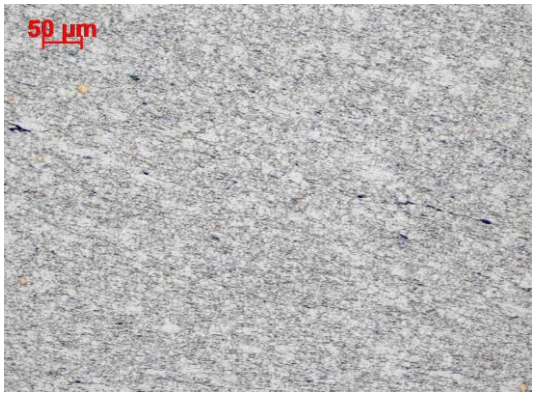

Figure 108: Alloy 60% x 200

Discussion

The thermo-mechanically processed test pieces were samples which had been removed from the injection moulded 718 alloy test bar following X-ray Computed Tomography. By carefully selecting specific regions in the test bar for analysis it can be seen that the amount and size of the porosity has been greatly reduced, however it is still present and randomly distributed throughout the test piece microstructures from the 20%, 40% and 60% samples.

A distinguishing feature that was noted was the presence of thermo-mechanical 'strain bands' across the test samples representing 40% and 60% reductions. These features were most prevalent in the 60% test piece reduction. The strain bands provided a directional effect to the microstructure and elongated some of the larger pores as seen above.

4.6 X-ray Computed Tomography (CT)

Several established technologies exist for the detection of sub surface material discontinuities. Magnetic particle inspection techniques are credited with finding both surface and near surface discontinuities, while Ultrasonic inspection techniques and ionising radiation offer a more searching assessment to a greater depth.

Conventional X-ray inspection techniques have evolved considerably as a result of computer and microprocessor advances over the last three decades. Early industrial uses of X-ray inspection procedures were predominantly focused on joining applications where the joint failure could have catastrophic consequences. These inspection techniques were used to assess the integrity of the welded structures associated with the manufacture of pressure vessels and gas pipeline installations.

X-ray computed tomography is a process whereby the x-ray images are computer processed in order to provide an output which is in the format of a tomographic image or slice of the area under observation. Figure 109 below shows the key componentry of an industrial X-ray CT scanner.

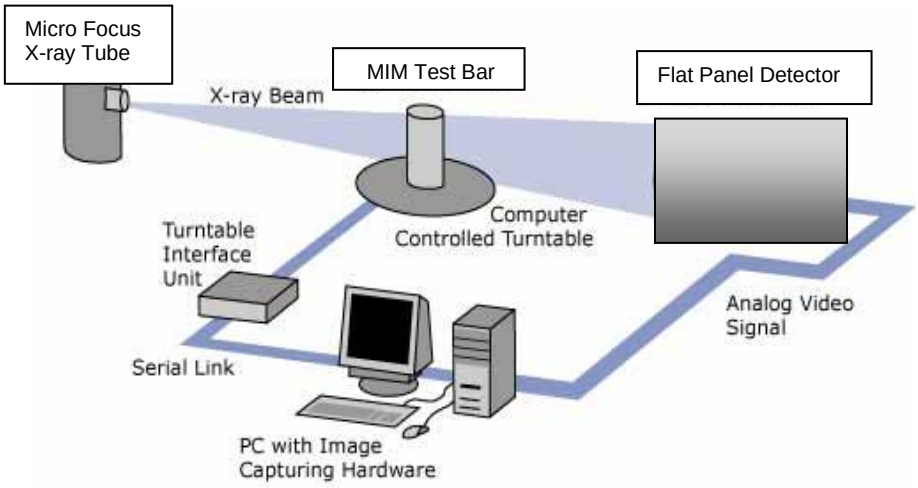

Figure 109: X-ray Computed Tomography (CT) Schematic Diagram

The MIM test bar is rotated while being exposed to penetrating electromagnetic radiation. The imaging system collects many (up to 3500) 2D radiographs that are converted to sinograph images and these are used to create a 3D volume image file. The continuous image collection and processing, results in data being collected from different component angles, which further enhances the final image.

The resulting 3D image can then be manipulated in order to produce ‘slices’ from different planes in order to obtain a more comprehensive view of the test component under evaluation. Each CT slice is comprised of voxels. Voxels are volumetric pixels which represent the smallest distinguishable cube shaped part of a 3D image.

Experimental Procedure

Ten fully heat treated injection moulded 718 alloy test bars were selected for X-ray CT analysis. The test bars were approximately 70mm in length by 13mm diameter. The equipment utilised to perform the X-ray CT analysis was a Nikon x-tek laboratory scanner. Ref Figure 110 below. The Nikon analysis equipment was specifically designed for the assessment of new and post repair turbine blades although the lab system is used for many other inspections including material analysis.

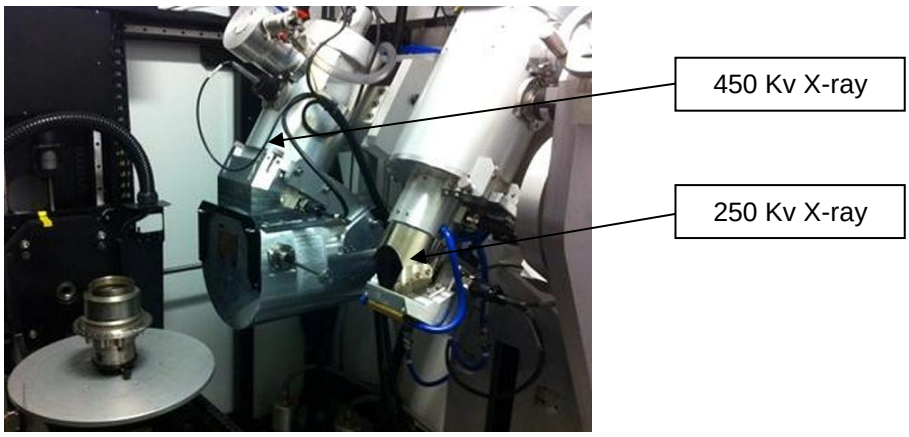

Figure 110: Nikon x-tek Laboratory Scanner

Each of the test bars had been produced using a single injection moulding point. For identification and orientation purposes each test bar was identified with the letter ‘I’ to indicate the injection moulding point.

Key processing parameters are listed below

X-ray - 430Kv

X-ray - 600uA

Voxel size X - 0.040mm

Voxel size Y - 0.040mm

Voxel size Z - 0.040mm

Computed Tomography Images

The images below were created by analysing the X-ray CT scan images. Ten bars were analysed, the diagram below illustrates the position of the 'slices' through the bar. The images are at x 2 approx. magnification. Ref. Figures 111 and 112 below.

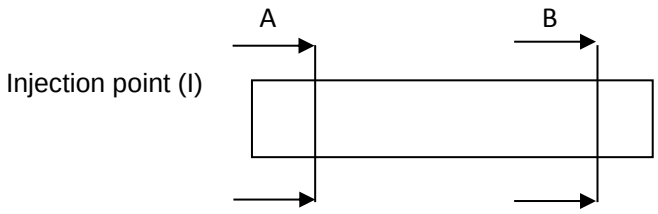

Figure 111: Billet Sectioning Diagram

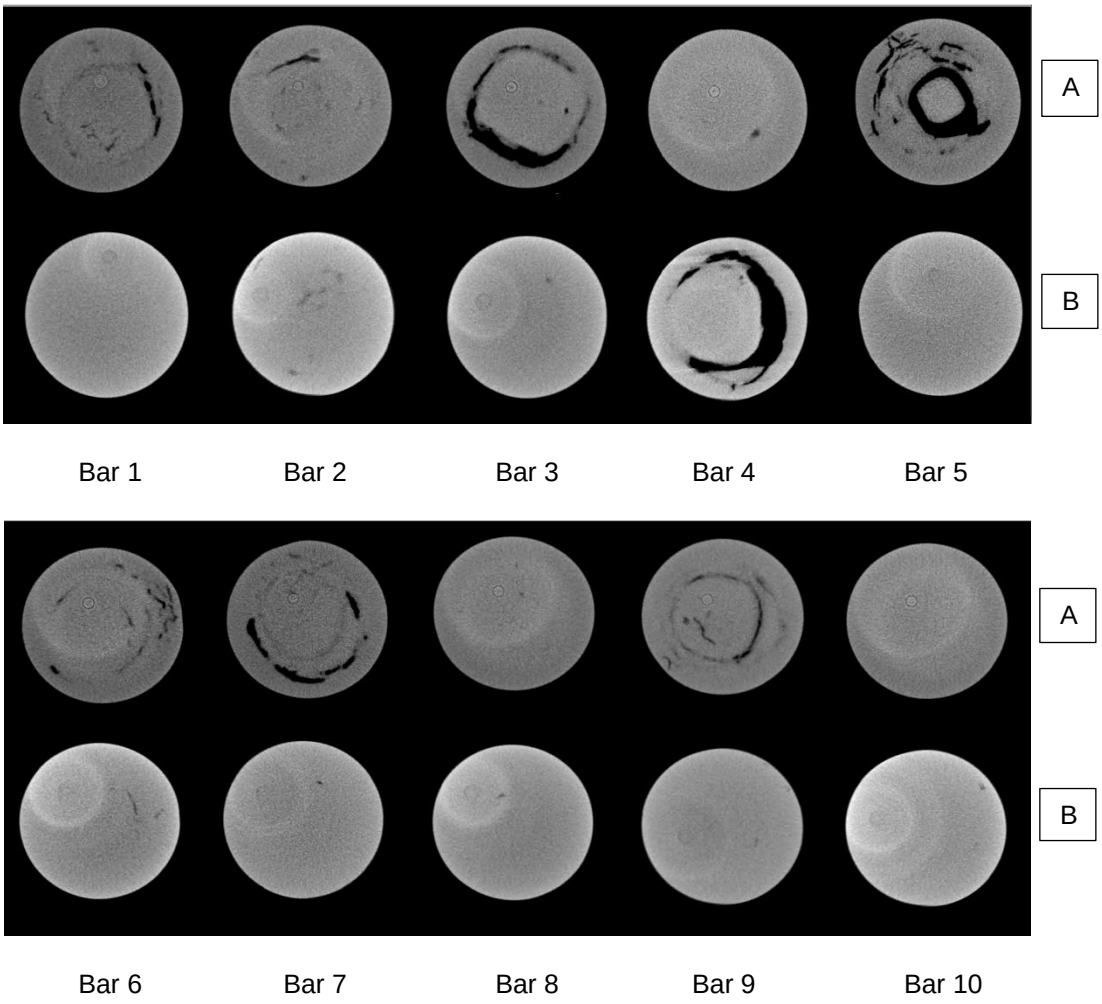

Figure 112: Billet CT Scans

Discussion

The CT images captured above are reconstructed ‘slices’ through the injection moulded and fully heat treated 718 alloy test bars.

Observations from the full CT images are captured below

Bar 1 - sub surface discontinuities, circumferential voids, small isolated pores.

Bar 2 - sub surface discontinuities, networks of small micro cracks, isolated pores.

Bar 3 - sub surface discontinuities, circumferential voids.

Bar 4 - sub surface discontinuities, circumferential voids, isolated pores.

Bar 5 - sub surface discontinuities, circumferential voids, chain porosity.

Bar 6 - sub surface discontinuities, circumferential voids.

Bar 7 - sub surface discontinuities, circumferential voids, chain porosity.

Bar 8 - sub surface discontinuities, small isolated pores.

Bar 9 - sub surface discontinuities, circumferential voids.

Bar 10 - sub surface discontinuities, small isolated pores.

The structural homogeneity of all ten injection moulded 718 alloy test bars was found to be variable. While similar features such as circumferential voids and chain porosity were noted during the examination of each of the individual bar CT scans, none of the injection moulded test bar CT scans could be considered to be identical.

One observation common to all ten test bars that were examined was that the structural variations were all found to be sub surface in bar location. None of the voids or cracks appeared to outcrop onto the surface of the bars. Visually inspecting the test bars immediately following heat treatment revealed no indication of the sub surface variations which were present in each of the test bars. Whilst this discussion focuses on the structural variations within each of the test bars it should also be noted that there were regions within each of the test bars where no sub surface discontinuities were detected.

There are several possible reasons for the variation in structural integrity of the injection moulded test bars, all hypothesis relate to the controls associated with the key processing input variables.

4.7 Brinell Hardness Testing

Hardness testing is not usually chosen for the purpose of characterising the material properties of 718 alloy, however in order to gain an appreciation of the macro hardness properties of both wrought and injection moulded test pieces Brinell hardness testing was adopted. The principle surrounding the test involves pressing a hardened steel ball (tungsten carbide) into the surface of a prepared test piece for a pre-determined time, normally between 12 and 15 seconds. Upon removal of the test load the diameter of the resulting impression is then measured accurately. Figure 113 below illustrates the measurement principle.

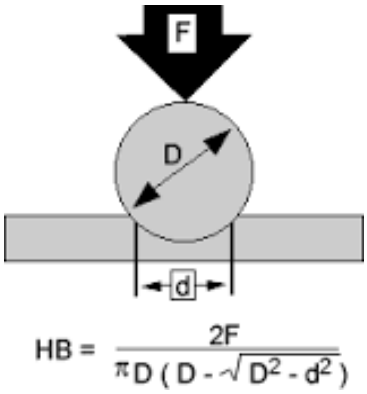

Figure 113: Brinell Hardness Test Schematic Diagram

The illustration above captures both the operation of the test and also the relationship between the force or load being employed, the diameter of the indenter and also the diameter of the resulting specimen indentation.

In order to obtain both comprehensive and corroborative test data, Brinell hardness testing was performed over a range of metal injection moulded pieces which were extracted from injection moulded billets. These test piece results were then compared to the test results derived from five different casts of wrought 718 alloy test pieces. Both wrought baseline samples and the injection moulded 718 alloy test pieces were in the fully heat treated condition. The injection moulded test pieces had not been subjected to further thermo-mechanical processing, and were in the ‘as moulded’ and fully heat treated condition.

Experimental Test Procedure

The test equipment used to conduct the Brinell hardness testing survey was a Struers Duramin 500 hardness tester. Ref. Figure 114 below.

Figure 114: Brinell Hardness Tester

The samples to be tested were prepared by sectioning the billet and polishing both faces of the sample parallel. The sample face to be presented to the indenter was further polished using progressively finer grades of silicon carbide grit and finished using 0,4µm colloidal silica suspension. All the samples tested were in the 'as polished' condition. Prior to performing the hardness survey, the accuracy of the hardness testing apparatus was verified independently using a certified test block. Both wrought and injection moulded test pieces were located on the platen directly below the indenter. The test load selected for the trials was 187.5kg, the indenter used was a 2.5mm tungsten carbide ball. The load was applied automatically for a period of 12 seconds. On completion of the test the indentation diameter on the test piece was measured automatically.

The test results for both the wrought and MIM 718 alloy are detailed in Table 50 below.

Table 50: Brinell Hardness - Test Results (Wrought and MIM)

Wrought 718 alloy - HBW		MIM 718 alloy - HBW	
431	420	395	365
431	423	398	418
438	430	394	426
445	431	405	417
448	432	395	416
445	435	390	413
449	438	392	405
448	429	401	413
448	438	396	414
448	436	316	414

Statistical Evaluation Techniques

The test data obtained from the Brinell hardness survey of both the wrought datum samples and the metal injection moulded samples analysed using Minitab™ statistical software. Three specific analysis techniques were selected to present and analyse the test data.

- Individual Value Plot. (Figure 115)
- Data Normality Plot with Probability Graph. (Figures 116 and 117)

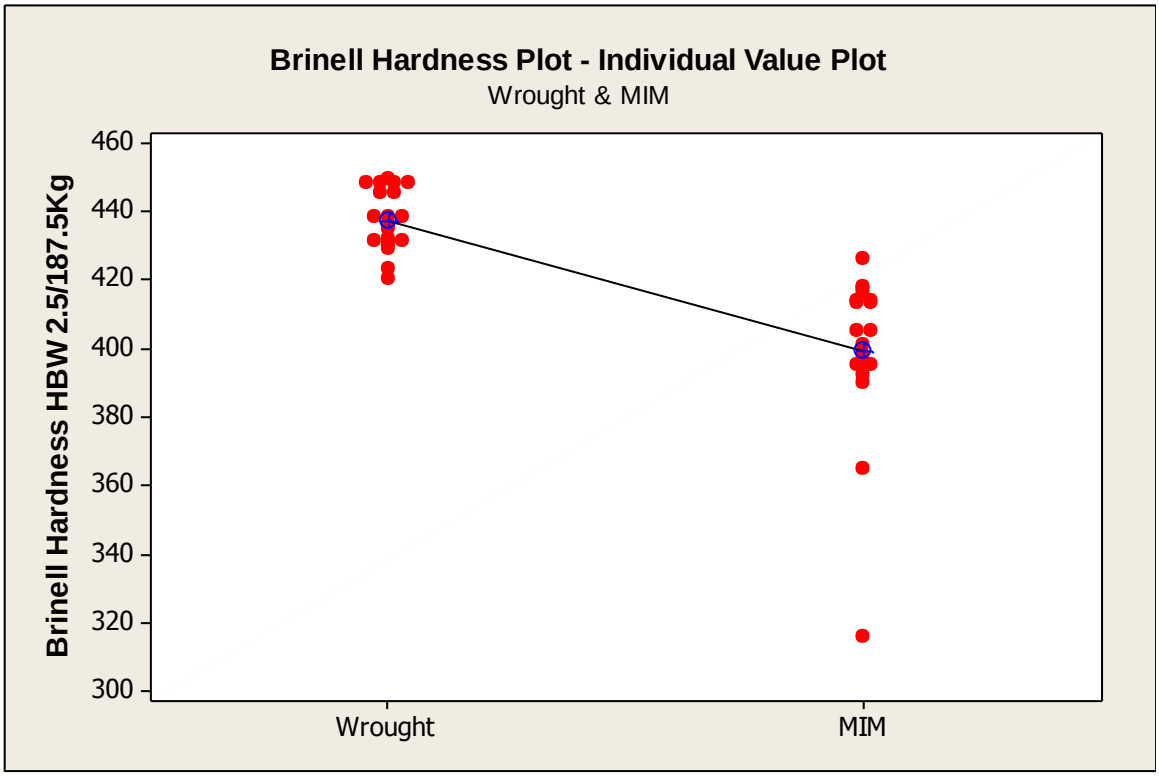

Figure 115: Individual Value Plot (Wrought and MIM)

The Individual Value Plot provides an illustration of the dispersion of the test result data from each of the hardness tests that were conducted. By plotting the data results side by side it can immediately be seen that there is a marked contrast in hardness between the wrought 718 alloy datum test pieces and the injection moulded 718 alloy test pieces. The sample mean has been identified for each group of test piece test results. The mean connect line has been added to emphasise the downward trend between the wrought and the metal injection moulded test pieces.

The test piece means from each of the two groups of trials are summarised in Table 51 below.

Table 51: Test Piece Mean Results (Wrought and MIM)

718 alloy test condition	Sample Mean (HBW)
Wrought	437.15
MIM	399.15

The test sample minimum / maximum values and ranges are summarised in Table 52 below.

Table 52: Test Piece Values and Ranges - Minimum and Maximum (Wrought and MIM)

718 alloy test condition	Minimum (HBW)	Maximum (HBW)	Range (HBW)
Wrought	420	449	29
MIM	316	426	110

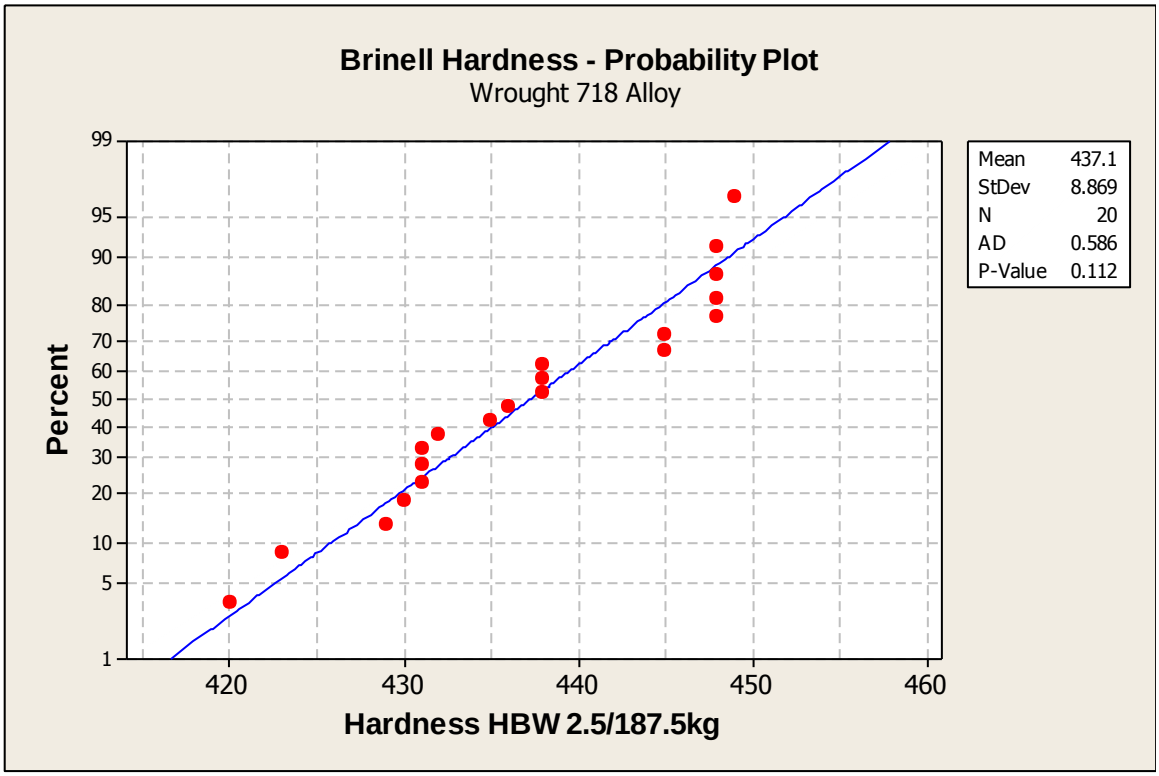

Figure 116: Normality Test with Probability Plot (Wrought 718 Alloy)

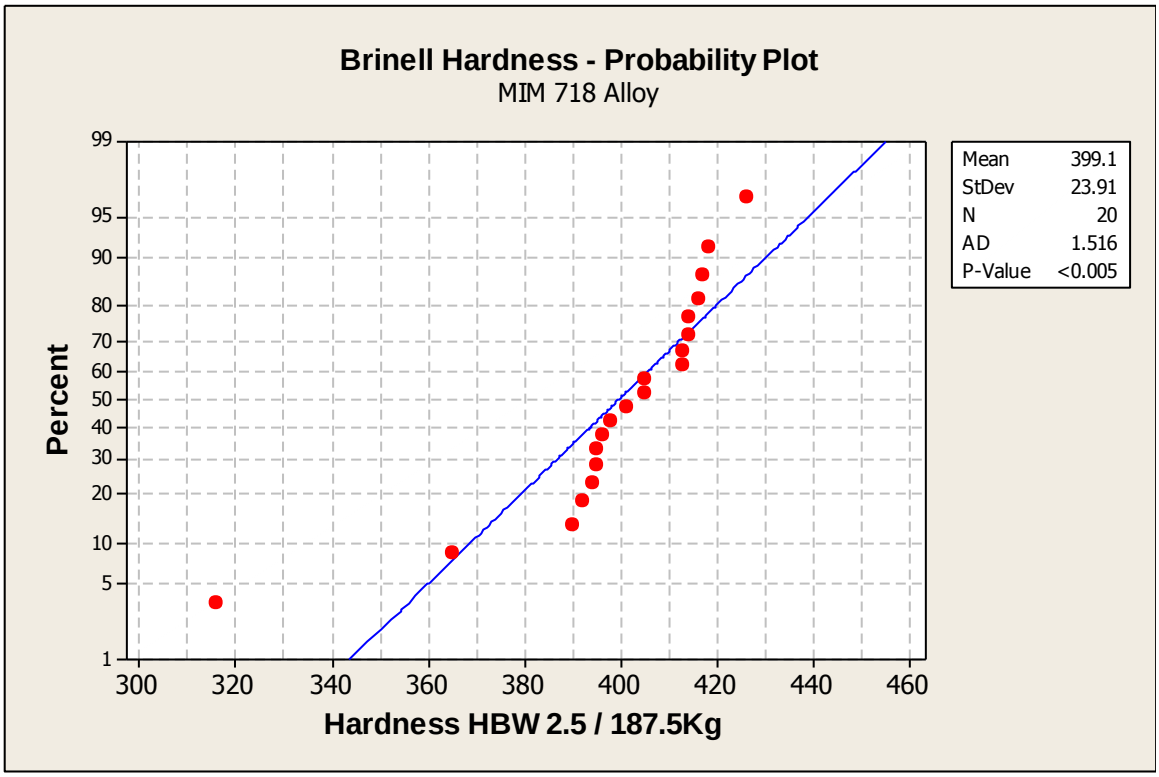

Figure 117: Normality Test with Probability Plot (MIM 718 Alloy)

The Normality Test with Probability Plot was conducted in order to assess the characteristics of the distribution of the test data from each of the two groups of hardness test results.

From the graphs which were constructed for both the wrought and the injection moulded test results the normality of the test data can be assessed both visually and objectively.

Visually the closer the test results are to following the blue line the more uniformly the data is distributed. Using this criteria it can be seen that the test data derived from the five separate casts of wrought 718 alloy are more normally distributed than the corresponding metal injection moulded test results.

By using the Anderson Darling Normality Test criteria it can be seen that the p-value for the wrought data is 0.112. By contrast the p-value for the injection moulded 718 alloy test data is <0.005. Since the Anderson Darling p-value is very low (<0.005), we can be reasonably confident that the test data from the metal injection moulded 718 alloy test pieces is not normally distributed.

Discussion

Due to the distribution of test data derived from the injection moulded 718 alloy test pieces no further statistical analysis was performed.

The test data derived from the wrought 718 alloy specimens represented 5 different material casts of wrought 718 alloy. Each of the five wrought test pieces had been heat treated separately. The injection moulded 718 alloy test pieces were taken from four different test bars which were heat treated together as a single batch. While the scatter in test results from the wrought 718 alloy samples is relatively small given the variation in test inputs, the scatter in test results from the injection moulded samples is much greater.

By comparing the test piece means it can be seen that there is a deficit of approximately 8.7% in the injection moulded hardness results, however the key finding from this experiment is the scatter in test results which is indicative of non homogeneous injection moulded 718 alloy.

4.8 Vickers Hardness Testing

The Vickers microhardness test is an established technique for determining the hardness of metallic materials. The wide range of indenter forces which can be applied make this test particularly suitable for the assessment of relatively small test pieces. In order to minimise test impression measurement errors the microhardness test was performed using a force of 1Kg. The indenter used throughout the test piece hardness assessment was a certified 136º pyramidal indenter (Figure 118).

Microhardness testing is conducted by pressing a diamond indenter into the surface of a sample for a fixed time under a predetermined load. The resulting impression is measured across the diagonals of the square indentation (D) and averaged in order to obtain a result which is recorded as Vickers Hardness (HV). Interpretation of the output from the Vickers Hardness test is straight forward, the harder the material, the higher the reported Vickers Hardness result. The diagram below illustrates the angular dimensions of the diamond indenter and the resulting specimen impression.

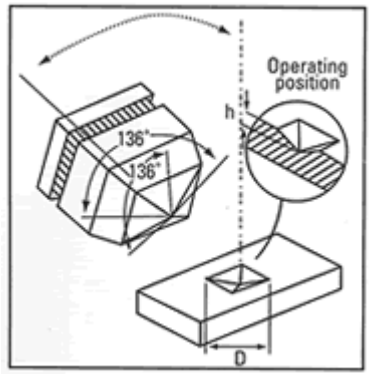

Figure 118: Vickers Hardness Test Schematic Diagram

In order to obtain both comprehensive and corroborative test data, the Vickers microhardness test was performed over a range of metal injection moulded specimen types. The injection moulded test pieces which were subjected to the Vickers microhardness survey ranged from basic metal injection moulded (MIM) samples to MIM samples which had received subsequent thermo-mechanical processing. These samples were identified as MIM 20%, MIM 40% and MIM 60%. The test results from the four MIM variants were then compared to a wrought 718 alloy datum. All the microhardness test pieces were tested in the fully heat treated condition.

Whilst the hardness of 718 alloy in the fully heat treated condition is not recognised as a fundamental material property, the microhardness survey was conducted primarily to assess the homogeneity of the individual metal injection moulded test samples.

Experimental Test Procedure

The test equipment used to conduct the microhardness testing survey was a Future-Tech Corp™ FM700 hardness tester (Figure 119).

Figure 119: Microhardness Tester

The samples to be tested were prepared using the same sample polishing technique detailed previously. All samples tested were in the 'as polished' condition. Prior to performing the hardness survey, the accuracy of the hardness testing apparatus was verified independently using a certified test block. The optical measuring monocular eyepiece was also checked for measurement errors. Both wrought and injection moulded test pieces were located in a vice below the indenter. The test pieces were checked and corrected for acceptable alignment prior to the commencement of each test. Each test piece was firmly held to prevent movement during the test. Positioning of the test pieces and selection of the impression area was achieved using the X-Y table adjustment. The Future-Tech™ FM700 hardness tester incorporates an automatic turret rotation feature and is comprised of two objective lenses offering x10 and x50 magnification. A x10 eyepiece was used for the measurement of the diamond indentations. The test load selected for the trials was 1Kg. The test load was applied using a pre-set timer. The time that the

diamond indenter was in contact with the test piece surface was 12 seconds. The diamond impression was measured using a stage micrometer. Measurement of the diamond indenter impressions was conducted manually. The diagonals of the impression were measured individually and averaged automatically. The averaged reading was then converted and displayed as Vickers Hardness. If the difference in diagonal length was found to be greater than 5% the test result would have been disregarded. No false readings were recorded during the hardness testing survey and no test readings were disregarded.

The table below captures the microhardness test results from all five 718 alloy test piece variants. Ten microhardness tests were performed on each of the samples. The test was performed uniformly across the available test piece surface in order to obtain representative test data.

The microhardness test results are detailed in Table 53 below.

Table 53: Test Results (Wrought and MIM)

Test result number	Wrought Hardness (HV 1.0)	MIM Hardness (HV 1.0)	MIM 20% Hardness (HV 1.0)	MIM 40% Hardness (HV 1.0)	MIM 60% Hardness (HV 1.0)
1	441.0	419.7	433.6	461.1	454.7
2	449.5	436.8	445.9	451.4	462.9
3	445.8	439.9	447.7	459.5	463.8
4	456.3	400.0	430.1	458.0	478.3
5	457.2	397.9	447.1	462.3	467.4
6	444.0	415.5	457.2	455.3	474.0
7	453.4	428.6	444.6	455.4	467.2
8	458.6	426.9	430.5	458.6	460.0
9	441.3	431.6	445.7	463.4	455.8
10	455.8	437.6	436.0	454.7	467.0

Statistical Evaluation Techniques

The test data obtained from the hardness survey of both the wrought datum sample and the metal injection moulded variants was analysed using Minitab™ statistical software. Three specific analysis techniques were selected to present and analyse the test data.

- Individual Value Plot (Figure 120).
- Data Normality Plot with Probability Graph (Figures 121 to 126).
- 95% Mean Confidence Interval Plot (Figure 127).

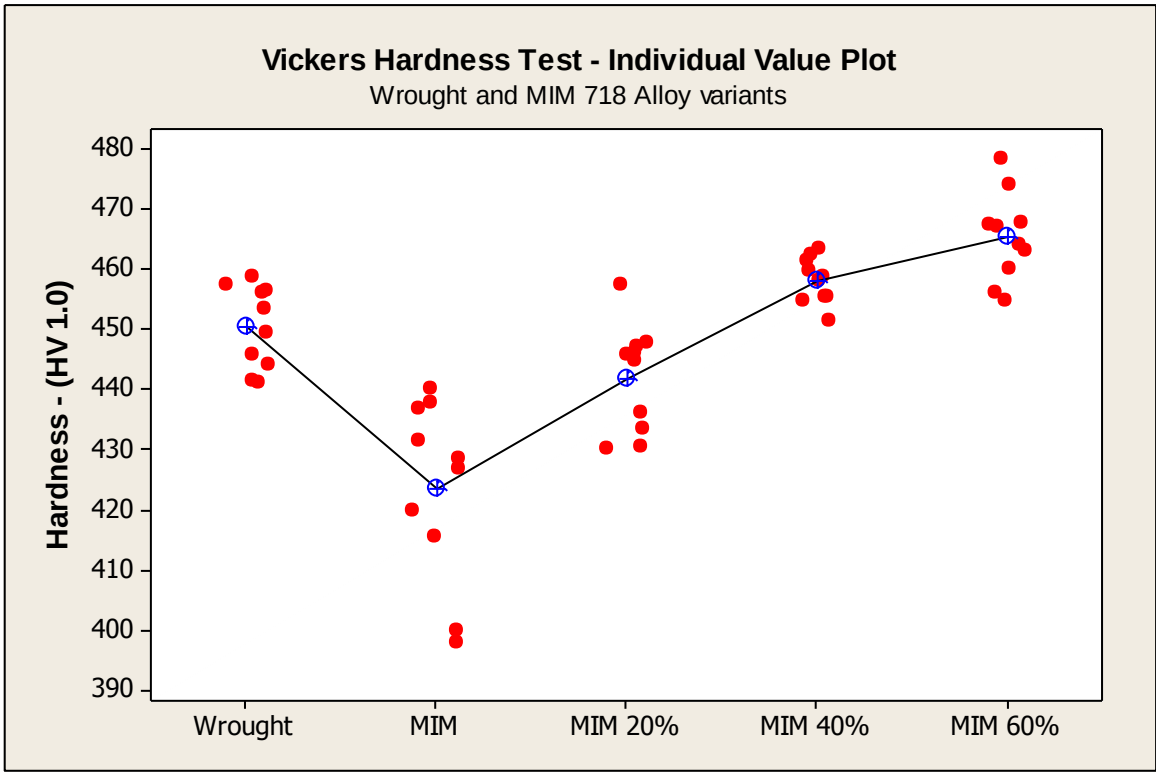

Figure 120: Individual Value Plot (Wrought and MIM 718 Alloy Variants)

The Individual Value Plot provides an illustration of the dispersion of the test result data from each of the five trials that were conducted. By plotting the data results side by side it can immediately be seen that there is a marked contrast in hardness between the wrought 718 alloy datum specimen and unprocessed MIM group of hardness test results. It can also be seen that the unprocessed MIM test piece exhibits the greatest scatter in hardness test results when compared to both the wrought datum test results and also the thermo-mechanically processed MIM 20%, MIM 40% and MIM 60% variants.

The sample mean has been identified for each group of sample test results. The mean connect line has been added to emphasis the trend. The application of progressively increasing amounts of thermo-mechanical processing on the metal injection moulded test pieces can be seen to result in progressive increases in hardness. The mean specimen hardness of the MIM 40% and MIM 60% specimen reductions can be seen to exceed the mean hardness of the wrought datum specimen. The gradient of the mean connect line suggests the hardness of the injection moulded test pieces could possibly be increased further with a level of thermo-mechanical processing in excess of 60%.

The test piece means from each of the five groups of trials are summarised in Table 54 below.

Table 54: Test Piece Mean Results (Wrought and MIM)

718 alloy test condition	Sample Mean (HV1.0)
Wrought	450.3
MIM	423.5
MIM 20% Reduction	441.8
MIM 40% Reduction	458.0
MIM 60% Reduction	465.1

The test sample minimum / maximum values and range are shown in Table 55.

Table 55: Test Piece Values and Ranges - Mimimum and Maximum (Wrought and MIM)

718 alloy test condition	Minimum (HV1.0)	Maximum (HV1.0)	Range (HV1.0)
Wrought	441.0	458.6	17.6
MIM	397.9	439.9	42.0
MIM 20% Reduction	431.0	457.2	26.2
MIM 40% Reduction	451.4	463.4	12.0
MIM 60% Reduction	454.7	478.3	23.6

The Normality Test with Probability Plot was conducted in order to assess the characteristics of the distribution of the test data from each of the five groups of hardness test results. The test results illustrated are derived from the hardness test data from the baseline wrought test pieces.

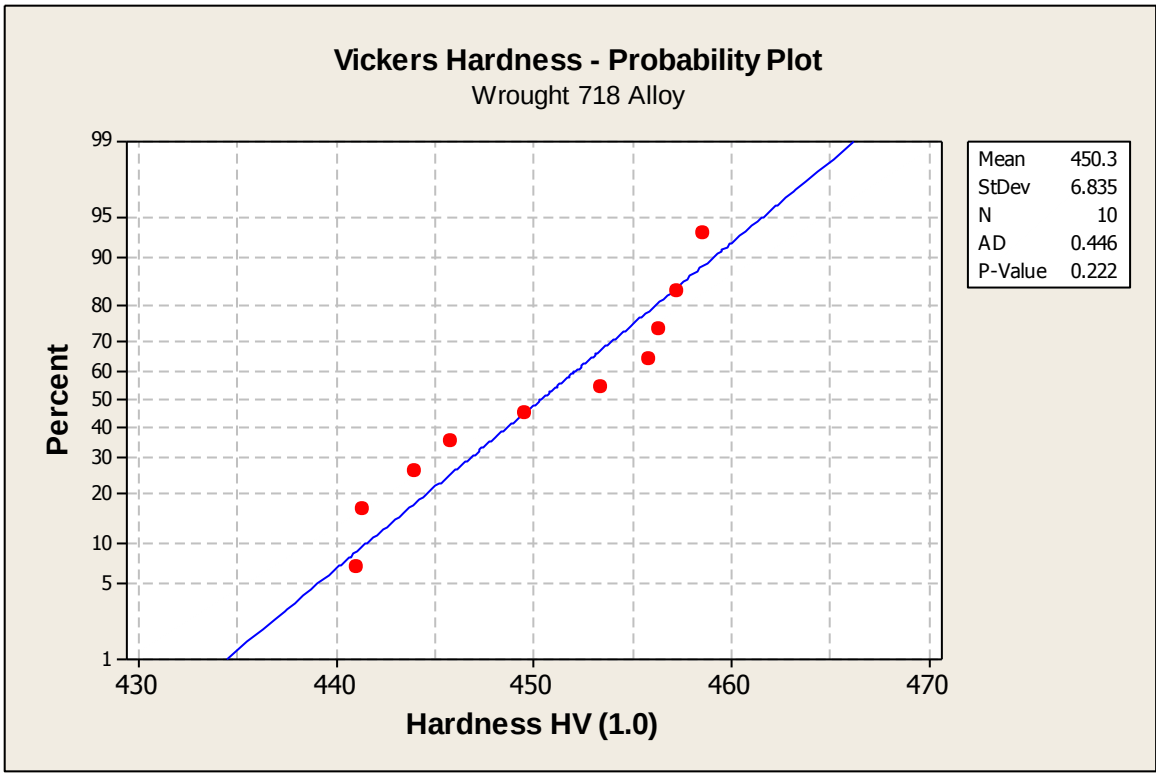

Figure 121: Probability Plot (Wrought 718 Alloy)

Determining whether the test data follows a Normal distribution is significant if further statistical analysis is to be performed. In order to confirm numerically the normality or non normality of the test data the Anderson-Darling (AD) Normality Test was performed using Minitab ™ statistical software. The Anderson-Darling test for normality was developed in order to detect all departures from the normal distribution.

$$AD = -n - \frac{1}{n}\sum_{i=1}^{n}(2i-1)[\ln F(X_i) + \ln(1 - F(X_{n-i+1}))]$$

Figure 122: Anderson-Darling Equation

Using Minitab statistical software, the test rejects the hypothesis of normality when the p-value is less than or equal to 0.05.

Failing the normality test allows you to state with 95% confidence the data does not fit the normal distribution. Passing the normality test only allows you to state no significant departure from normality was found. Ref. Tables 56 to 59.

Based upon the Anderson-Darling criteria the following statistical assumptions have been made.

Table 56: Anderson-Darling Test Piece Mean Results (Wrought)

	Sample size	Mean (HV1.0)	Standard deviation (HV1.0)	AD	p-value	Normality
Wrought	10	450.3	6.835	0.446	0.222	Normal distribution

The probability plot which accompanies the numerical evaluation of the data is a simple visual aid to assessing the Normality of a sample distribution. If your data is perfectly normal, then the data points on the probability plot will form a straight line. The reference line forms an estimate of the cumulative distribution function for the population from which the data are drawn.

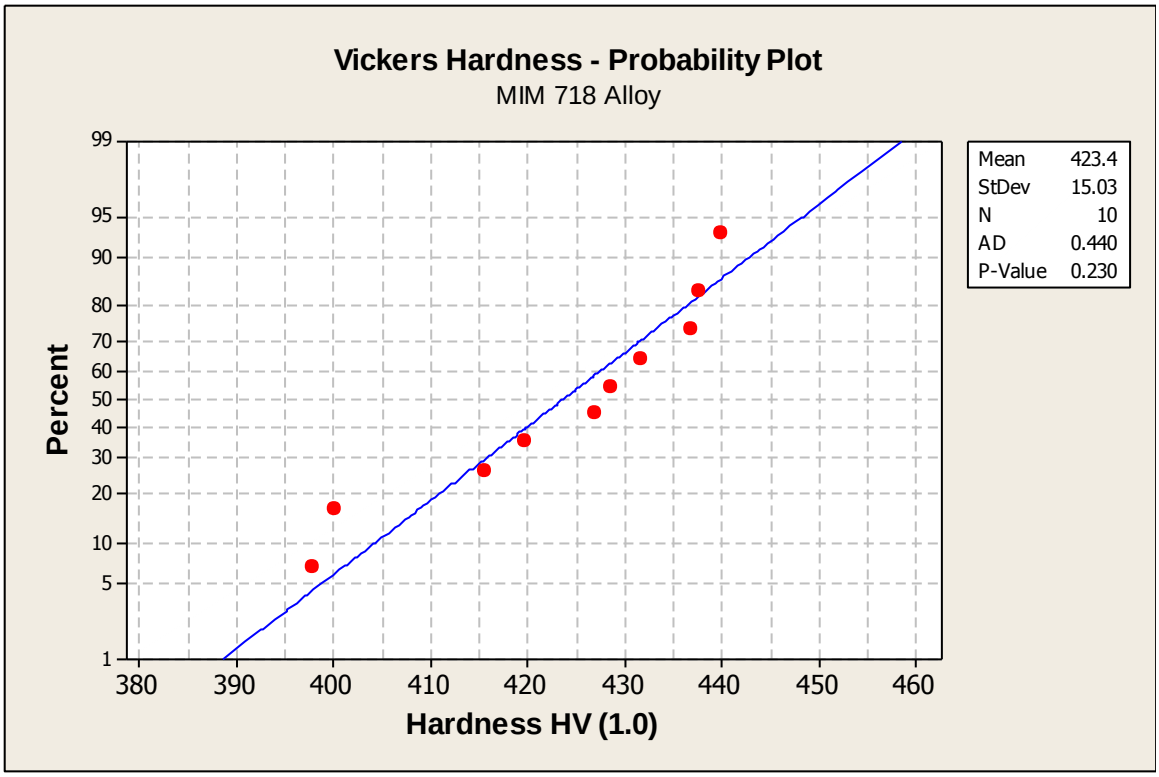

Figure 123: Probability Plot (MIM 718 Alloy)

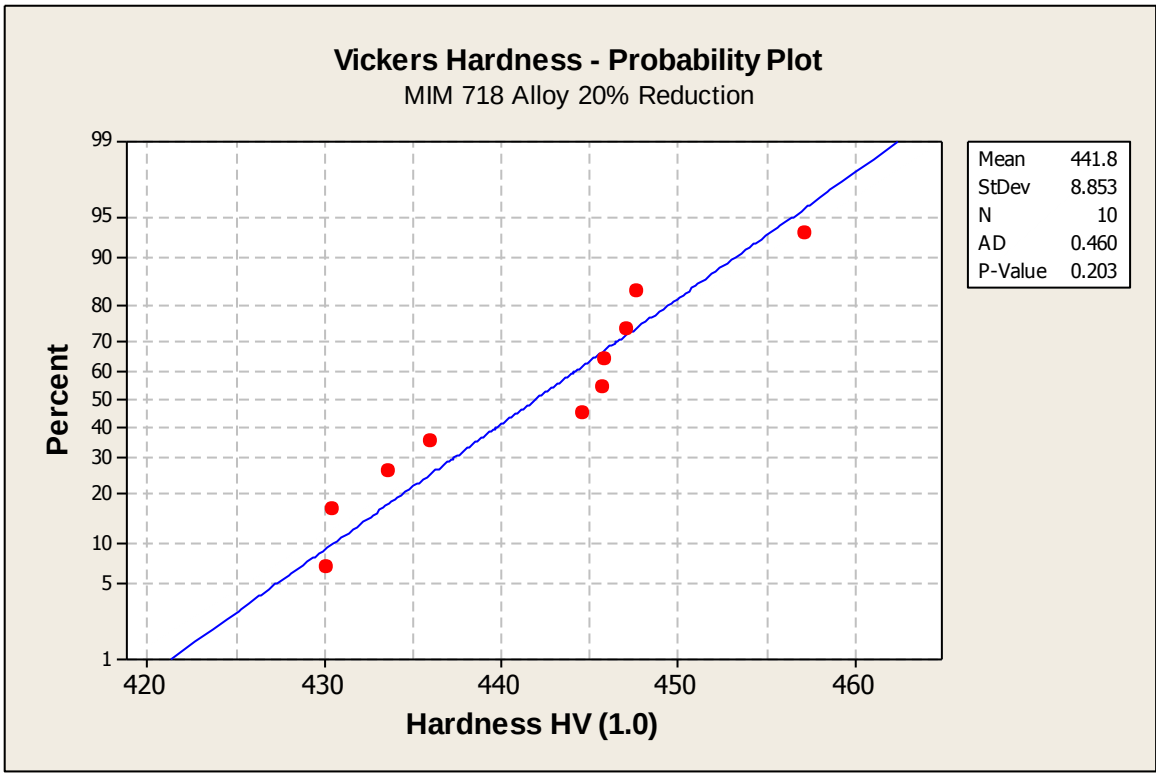

Figure 124: Probability Plot (MIM 718 Alloy 20% Reduction)

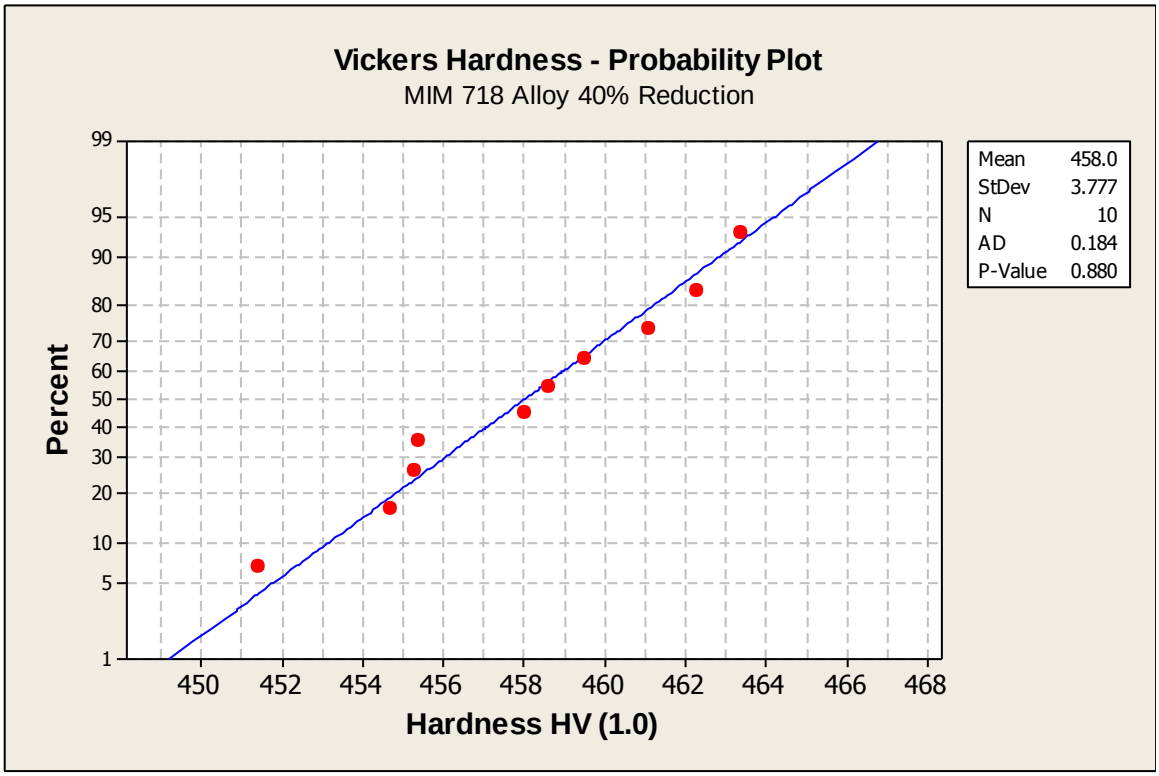

Figure 125: Probability Plot (MIM 718 Alloy 40% Reduction)

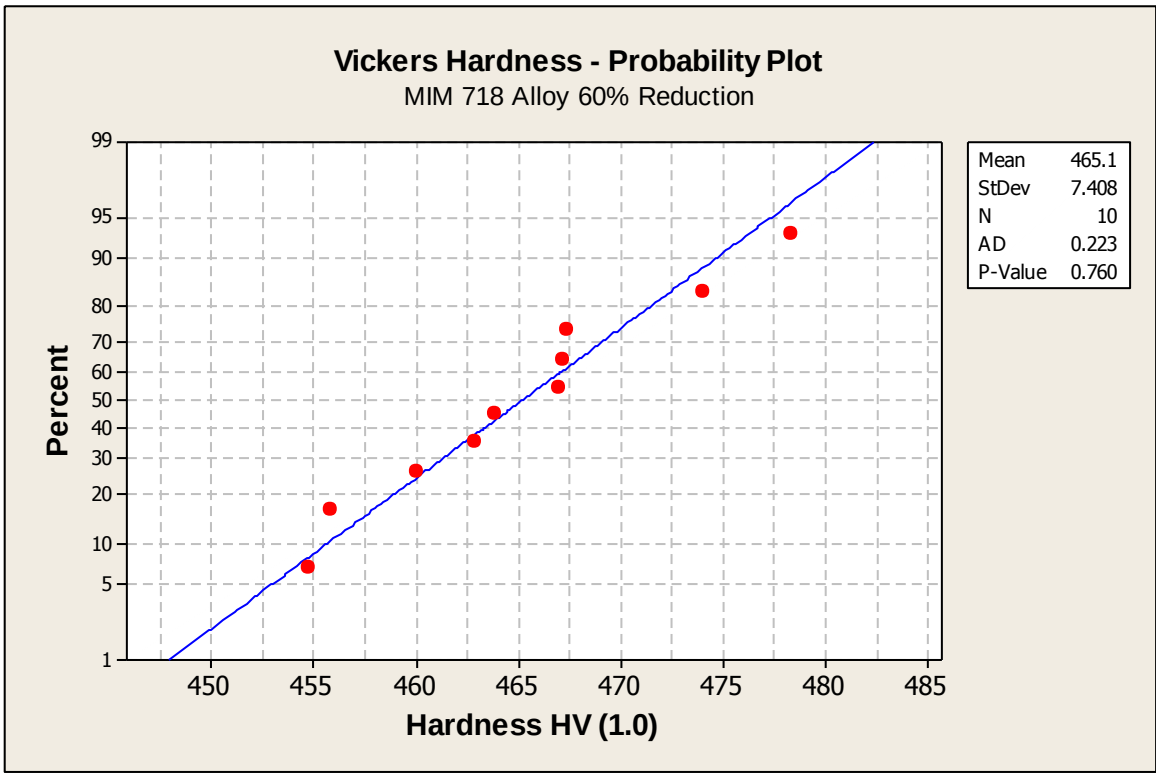

Figure 126: Probability Plot (MIM 718 Alloy 60% Reduction)

Table 57: Normality Test with Probability Plot Summary

	Sample size	Mean (HV1.0)	Standard deviation (HV1.0)	AD	p-value	Normality
Wrought	10	450.3	6.835	0.446	0.222	Normal distribution
MIM	10	423.4	15.03	0.440	0.230	Normal distribution
MIM 20%	10	441.8	8.853	0.460	0.203	Normal distribution
MIM 40%	10	458.0	3.777	0.184	0.880	Normal distribution
MIM 60%	10	465.1	7.408	0.223	0.760	Normal distribution

Using the Anderson-Darling Normality test it can be seen that the p-value is greater than 0.05 for all the 718 alloy specimens that were hardness tested. From this we can assume that the data collected for the wrought and MIM test samples is normally distributed.

The 95% Confidence Interval (CI) plot provides a range within which the true process statistic is likely to be with a given level of confidence. The limits applied are dependent on the size of the sample. A higher confidence level would result in a greater confidence interval.

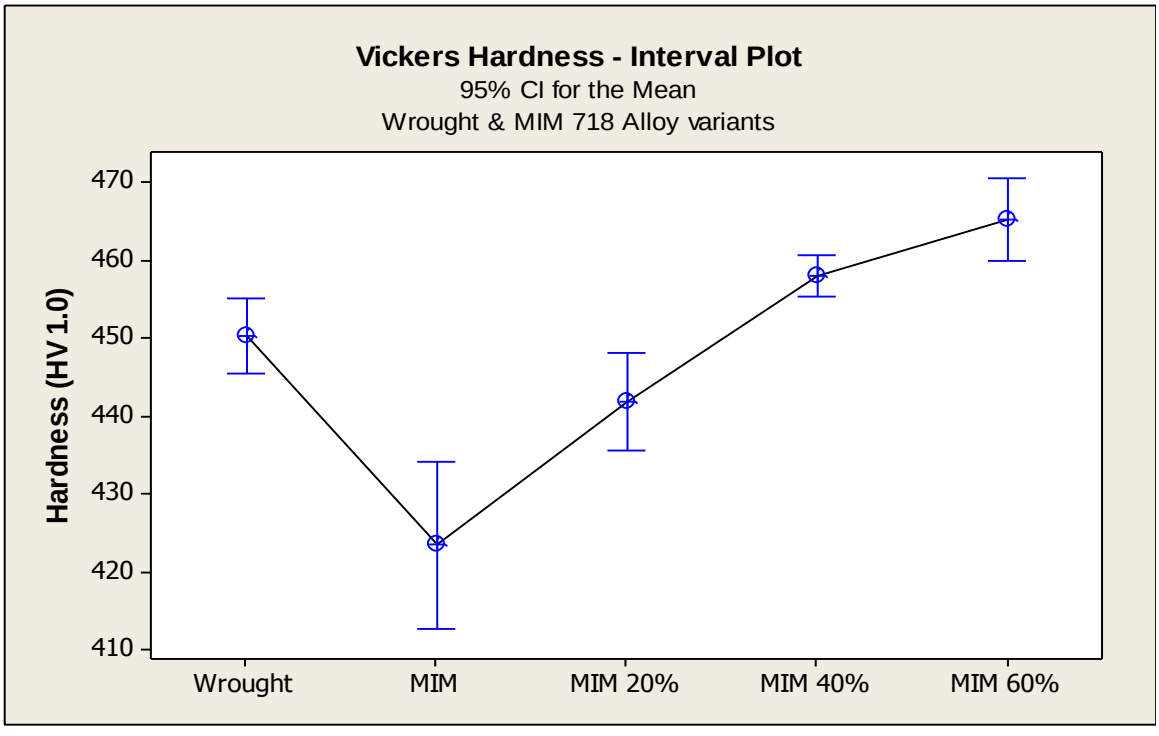

Figure 127: Interval Plot - 95% Mean Confidence Interval (CI) Plot (Wrought and MIM 718 Alloy Variants)

Table 58: 95% Mean Confidence Interval (CI) Plot

718 alloy test condition	95% CI Sample Mean (HV1.0)
Wrought	450.3
MIM	423.4
MIM 20% Reduction	441.8
MIM 40% Reduction	458.0
MIM 60% Reduction	465.1

Table 59: 95% Confidence Interval and Range

718 alloy test condition	95% Mean CI Minimum (HV1.0)	95% Mean CI Maximum (HV1.0)	95% CI Range (HV1.0)
Wrought	445.4	455.2	9.8
MIM	412.7	434.2	21.5
MIM 20% Reduction	435.5	448.2	12.7
MIM 40% Reduction	455.3	460.7	5.4
MIM 60% Reduction	459.8	470.4	10.6

Vickers Hardness Testing Summary

By using minitab™ statistical software the test data derived from the Vickers microhardness survey can be arranged to enable certain conclusions to be made. The conclusions which can be made from this test are detailed below. The wrought 718 alloy datum sample was included in the hardness test as a datum from which the injection moulded test pieces could be assessed.

By applying 95% confidence intervals to both the wrought 718 alloy and the unprocessed MIM data it can be seen that the groups of test results are quite separate. The most noticeable feature about the unprocessed MIM test results is the range or dispersion of the hardness test data. The variable test results suggest that the unprocessed MIM test specimen is inherently non homogeneous in nature.

During the microhardness survey, small amounts of microporosity were noted on the polished specimen surface. Isolated macro pores, pores greater than 0.5mm were noted at the periphery of the test piece. Care was taken during the hardness testing survey to avoid such regions and focus on what appeared to be homogeneous sections.

Progressive dimensional reductions of the MIM samples by 20%, 40% and 60% resulted in a pronounced improvement in hardness test results. The dispersion of test results derived from these test pieces was greatly reduced in comparison with the unprocessed MIM test piece and the upper band of the MIM 20% confidence interval can be seen to breach the lower confidence interval associated with the wrought 718 alloy test data results.

The improvement in the metal injection moulded test piece hardness test results continued with subsequent increases in thermo-mechanical processing, however by examining the test results from the MIM 60% test piece it can be seen that the results are significantly higher than those obtained from the baseline wrought 718 alloy datum results.

The test data suggests that while lower amounts (MIM 20%) of thermo-mechanical processing is effective in normalising the effects of sub surface microporosity, greater processing reductions could result in the onset of strain hardening. This phenomena was further explored during the microscopic evaluation of the samples.

4.9 Small Punch Testing

Small Punch Testing is a process whose origins can be traced to the power generation and petrochemical industries. In harsh operating environments advanced materials can be in use at elevated temperatures for prolonged periods of time. In such operating conditions there are many degradation processes which can have an effect on the metallurgical structure and the corresponding mechanical properties of the alloy systems being employed.

The ability to derive real test data from actual operating components or from a running process, has always been desirable in order to substantiate the design criteria and ensure safe and reliable processes. In such studies, a small volume of material is typically extracted from in-service components for fracture mechanics or remnant creep life assessments

Small Punch Testing is a mechanical test in which a load is applied to one side of a standardised disc shaped test piece. Both Small Punch Tensile and Small Punch Creep tests allow meaningful mechanical property data to be obtained from otherwise restrictive material volumes.

During Small Punch Tensile testing, small disc shaped test pieces are subjected to progressive loading conditions until rupture occurs. Small Punch Creep testing involves similar principles to conventional creep testing, however the test piece is again a small disc shaped specimen. During Small Punch Creep testing the test piece is subjected to high temperature creep style static loading conditions.

Small Punch Tensile testing techniques have more recently been adopted for the characterisation of novel aerospace materials, including additive layer and net shape manufacturing processes such as metal injection moulding.

Comparative Small Punch Testing was selected for this research project in order to obtain meaningful comparative test data from both wrought and injection moulded 718 alloy component sections which would not be readily accessible for assessment using conventional testing methods.

The illustration below shows the uniaxial nature of the test and also illustrates the orientation of the test piece relative to the punch. This type of test set up is common to both Small Punch Tensile and Small Punch Creep applications. Ref. Figures 128 and 129.

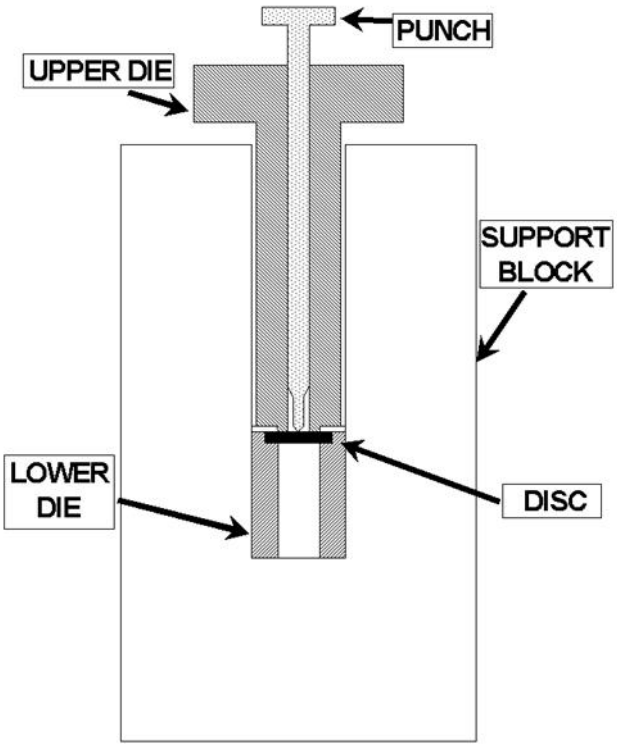

Figure 128: Small Punch Test Schematic Diagram

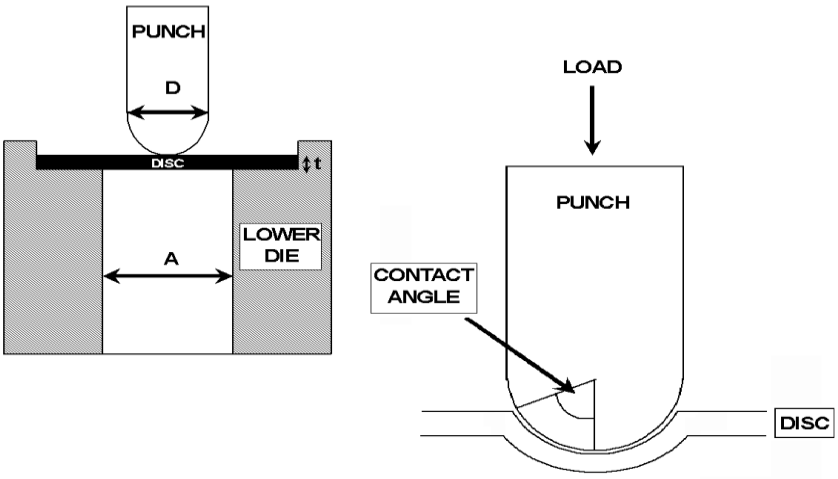

Figure 129: Punch, Disc and Die Orientation Schematic Diagram

Three variations of the Small Punch Test have been selected for this research. These are listed below.

- Small Punch Tensile (Room Temperature)
- Small Punch Tensile (Elevated Temperature 630ºC)
- Small Punch Creep (Elevated Temperature 630ºC)

4.9.1 Test Piece Preparation

For the purpose of the Small Punch Tensile and Small Punch Creep experiments three fully heat treated 718 alloy forged components were compared to three fully heat treated 718 alloy injection moulded components. The component geometry is illustrated below in Figure 130. For identification purposes the regions from which the test pieces were selected have been identified as ‘shroud’ and ‘root’. Due to the complex geometry of the abridging aerofoil section no test samples were taken from this region.

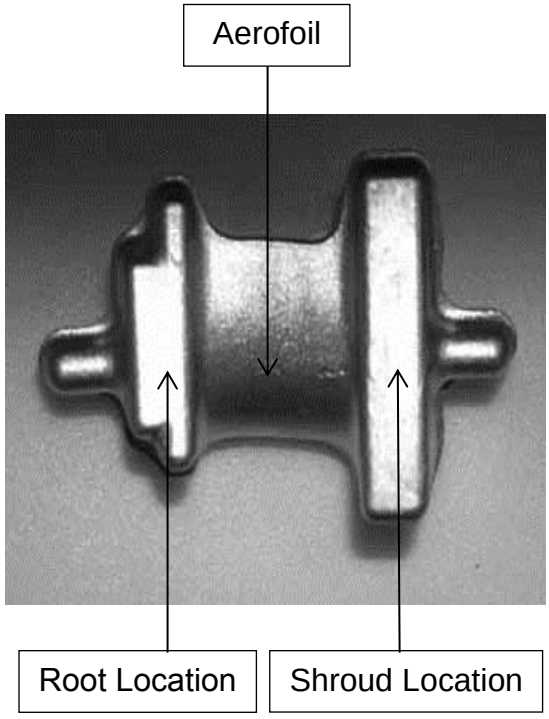

Figure 130: MIM Test Component

In order to produce the Small Punch Test samples, cylindrical blanks of test material were wire electro discharge machined from both the shroud and root locations. The sample diameter was 9.5mm. Ref. Figure 131.

The cylindrical sample blanks were subsequently precision cut to approx 0,7mm thickness using a precision alumina sectioning wheel. Coolant was used during the sectioning process to ensure that no overheating took place. The cut test pieces were subsequently visually inspected for evidence of overheating.

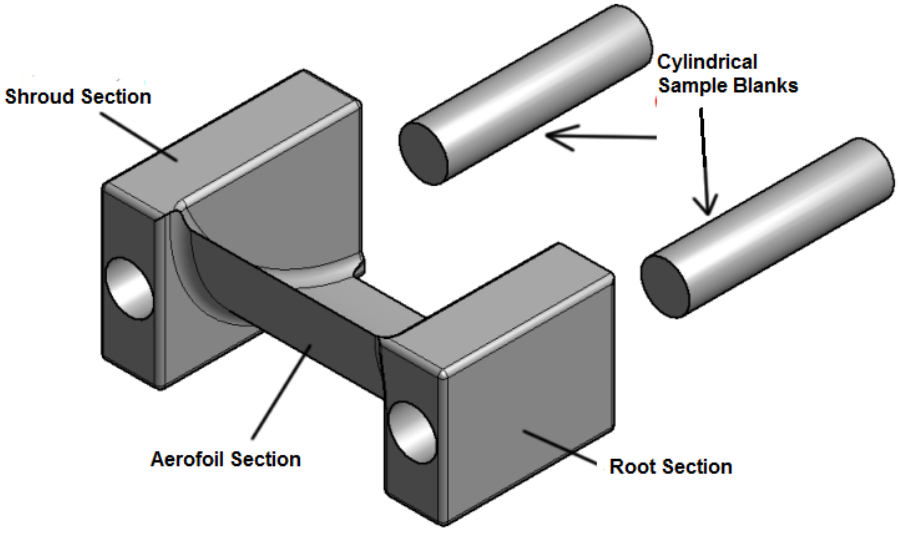

Figure 131: Test Piece Sectioning Diagram

The disc samples (Ref. Figure 132) were then progressively polished in accordance with EU CoP guidelines. The final thickness of the test samples was 0.5mm ± 5µm. Dimensional verification was conducted at several points to check for compliance to the drawing intent. Test discs were manufactured from both wrought components and the development MIM components to an identical procedure in order to reduce the likelihood of erroneous test results due to variable test specimen quality. Test discs were manufactured from both the root and shroud regions in order to assess the consistency of the injection moulding process at the extremes of the component geometry.

These test discs were used for all three types of Small Punch Testing (Small Punch Tensile Room Temperature, Small Punch Tensile Elevated Temperature and Small Punch Creep).

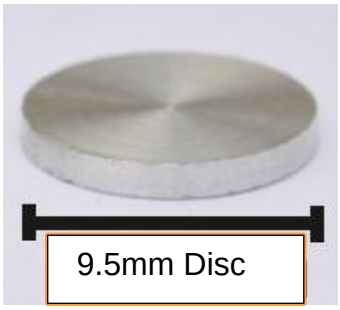

Figure 132: Test Piece Disc

4.9.2 Small Punch Tensile (Room Temperature)

For room temperature tests, a typical tool steel was used for the manufacture of both the indenter and the die materials. The steel used was Silver Steel (BS1407) which had been hardened and tempered to achieve a hardness of 60+ HRC.

Lower Punch Die Diameter = 6.4mm
Punch Head Diameter = 4mm
Clearance = 1.4mm
Punch Head Rate = 1.2mm/min = 0.02mm/s
Disc Thickness 0,5mm

Small Punch Tensile Testing Apparatus - Room Temperature

The testing apparatus detailed in Figure 133 below illustrates the position of the extensometry and location collets. The test disc is held securely between location dies.

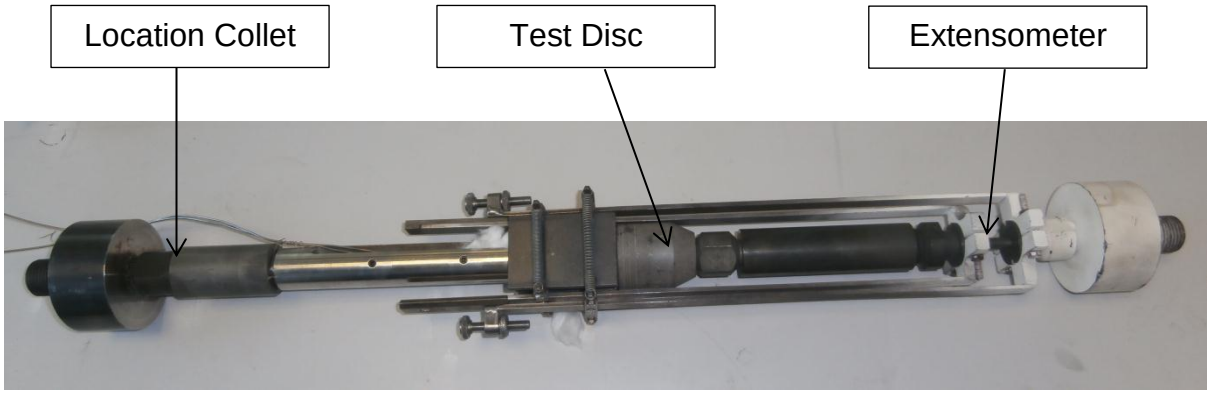

Figure 133: SPT Testing Apparatus

Small Punch Tensile (Room Temperature) - Test Matrix

Table 60 below details the quantity of samples taken from both wrought and injection moulded components.

Table 60: Room Temperature Sample Matrix

Small Punch Test Type	Test Temperature	Number of Samples	Sample Source (as detailed)
Small Punch Tensile Wrought	Room Temperature	18	Component
Small Punch Tensile MIM	Room Temperature	18	Component

Room Temperature Test Results

Tables 61 and 62 document the test results derived from the Small Punch Tensile room temperature testing trials. The test pieces were extracted from component specimens and are identified by Wrought (W), Sample (A) and Root or Shroud (R or S).

Table 61: Room Temperature Test Results (Wrought 718 Alloy)

Wrought Sample A	Small Punch Tensile	Ultimate Load kN
W A S a	Room Temperature	4.64
W A S b	Room Temperature	5.23
W A S c	Room Temperature	n/a
W A R a	Room Temperature	5.36
W A R b	Room Temperature	5.69
W A R c	Room Temperature	5.43
Wrought Sample B	**Small Punch Tensile**	**Ultimate Load kN**
W B S a	Room Temperature	4.21
W B S b	Room Temperature	4.48
W B S c	Room Temperature	n/a
W B R a	Room Temperature	5.00
W B R b	Room Temperature	4.75
W B R c	Room Temperature	5.11
Wrought Sample C	**Small Punch Tensile**	**Ultimate Load kN**
W C S a	Room Temperature	4.31
W C S b	Room Temperature	5.16
W C S c	Room Temperature	n/a
W C R a	Room Temperature	5.19
W C R b	Room Temperature	5.19
W C R c	Room Temperature	3.98

Table 62: Room Temperature Test Results (MIM 718 Alloy)

MIM Sample A	Small Punch Tensile	Ultimate Load kN
M A S a	Room Temperature	1.36
M A S b	Room Temperature	1.53
M A S c	Room Temperature	1.26
M A R a	Room Temperature	1.29
M A R b	Room Temperature	1.01
M A R c	Room Temperature	1.17
MIM Sample B	**Small Punch Tensile**	**Ultimate Load kN**
M B S a	Room Temperature	1.48
M B S b	Room Temperature	1.34
M B S c	Room Temperature	1.76
M B R a	Room Temperature	2.00
M B R b	Room Temperature	2.12
M B R c	Room Temperature	1.54
MIM Sample H	**Small Punch Tensile**	**Ultimate Load kN**
M H S a	Room Temperature	2.17
M H S b	Room Temperature	2.24
M H S c	Room Temperature	1.86
M H R a	Room Temperature	1.84
M H R b	Room Temperature	1.94
M H R c	Room Temperature	1.87

Figures 134 to 137 below capture the statistical analysis of the test data.

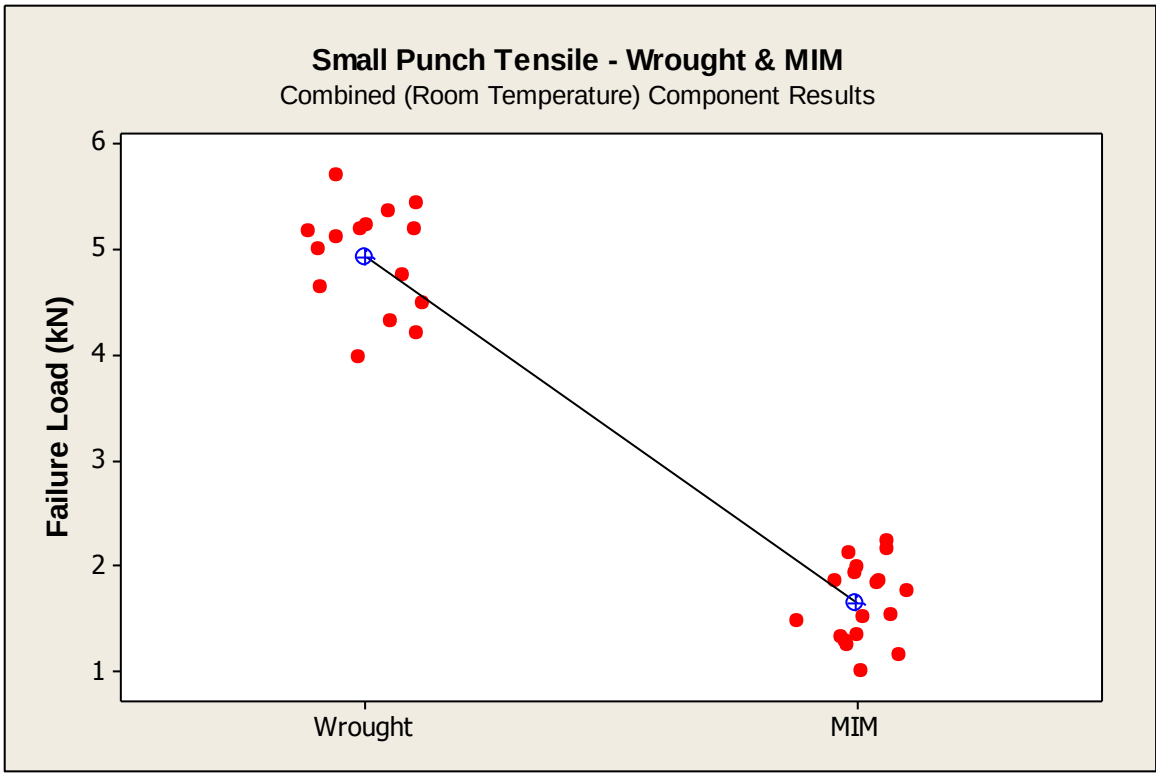

Figure 134: Individual Value Plot - Room Temperature (Wrought and MIM)

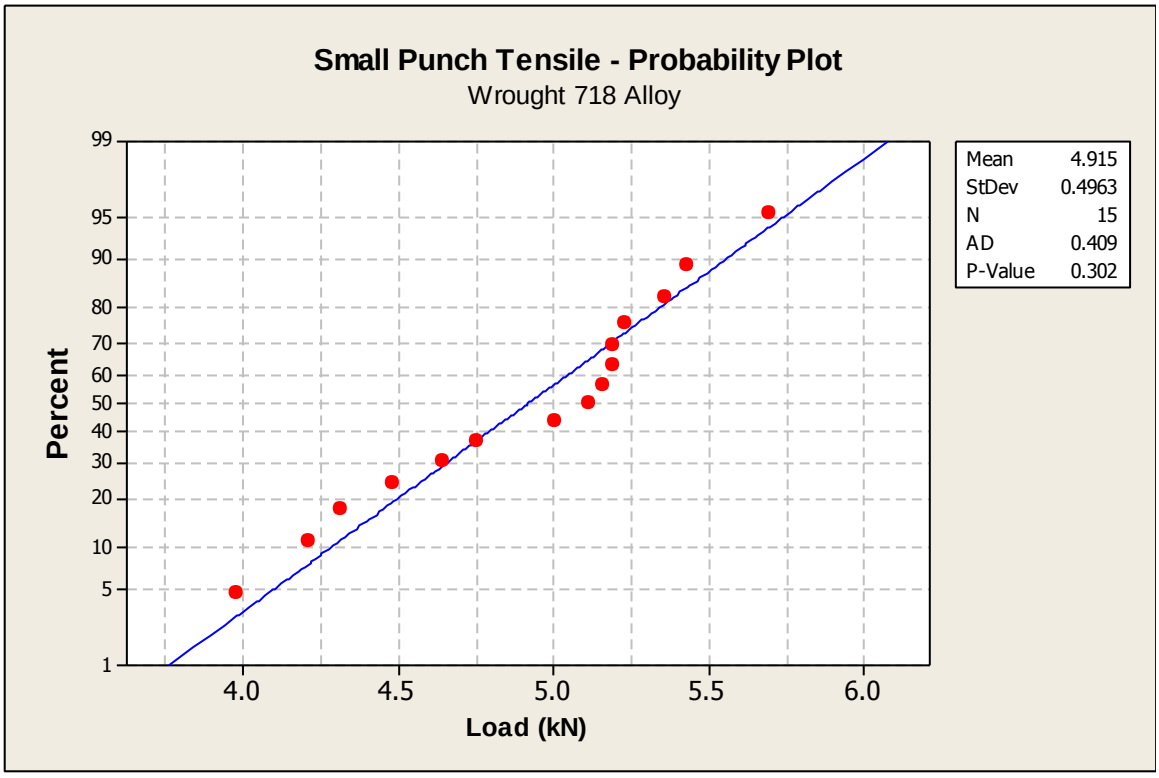

Figure 135: Normality Test with Probability Plot - Room Temperature (Wrought 718 Alloy)

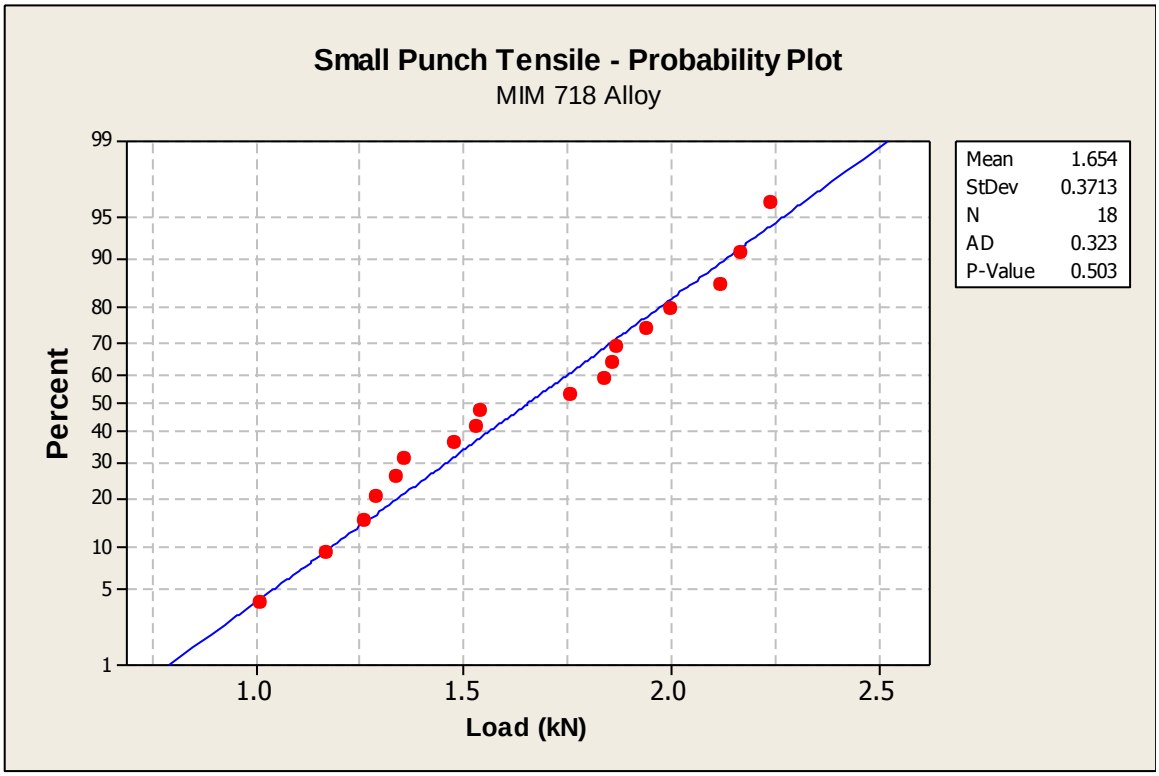

Figure 136: Normality Test with Probability Plot - Room Temperature (MIM 718 Alloy)

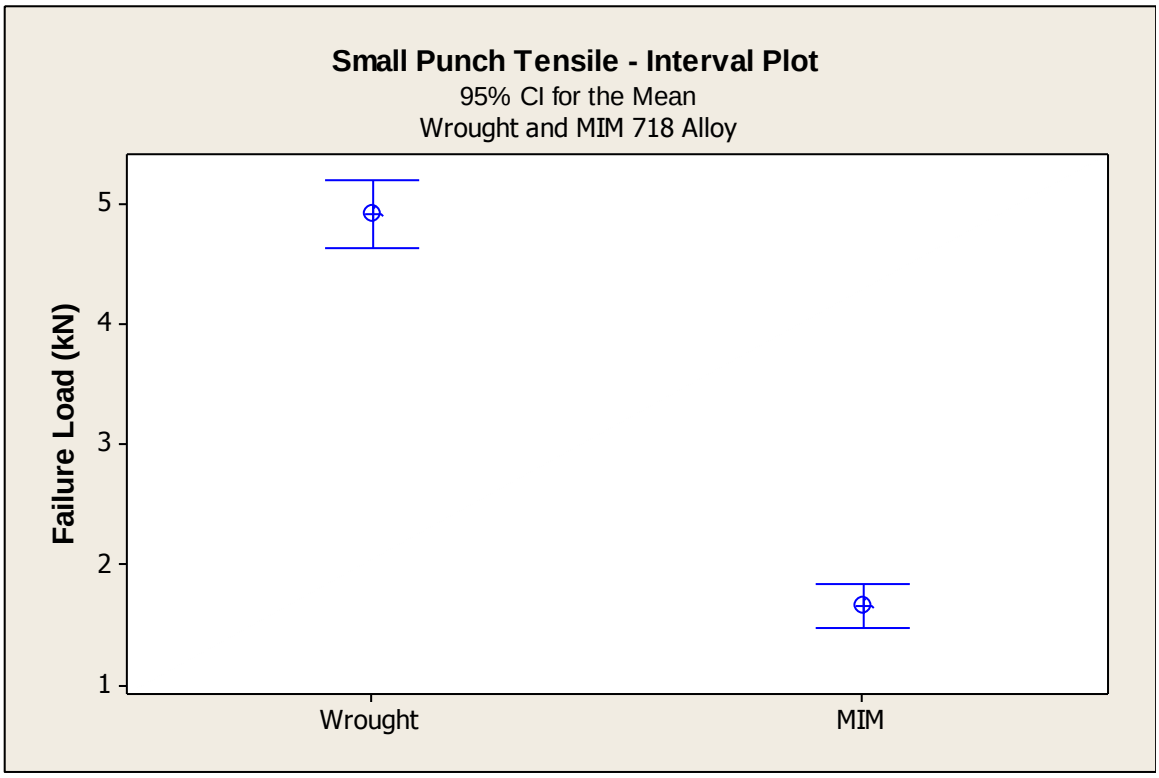

Figure 137: 95% Mean Confidence Interval (CI) Plot (Wrought and MIM 718 Alloy)

Discussion

The test results obtained from the Small Punch Tensile (Room Temperature) trials revealed a significant difference in material properties between the injection moulded 718 alloy test pieces and the established 718 alloy datum samples.

The maximum and minimum values obtained from the datum wrought 718 alloy samples were found to be 5.69kN and 3.98kN respectively. A range of 1.71kN
By contrast the test results obtained from the injection moulded samples were from 2.24kN to 1.01kN, a range of 1.23kN.

By comparing the mean test result from each of the sample groups it can be seen that the mean wrought test result is 4.92kN, while the mean MIM test result is 2.24kN
By comparing the mean values from each of the groups of samples analysed the property deficit from the MIM samples equated to approximately 54.47%.

Statistical analysis of the data provided from both the wrought and the MIM test samples revealed both groups of test results conformed to a normal distribution. The p value derived from the Anderson-Darling equation for the datum samples was 0.302. The p value obtained from the Anderson Darling equation for the MIM samples was 0.503.

By calculating the 95% Mean Confidence Interval for both groups of test data the following conclusions can be made.

Wrought 718 Alloy - Mean 4.92kN, Interval 4.64kN to 5.19kN.
MIM 718 Alloy - Mean 1.65kN, Interval 1.47kN to 1.84kN.

As can be seen from both the Individual Value Plot of both Wrought 718 alloy and MIM 718 alloy and also the 95% Confidence Interval Plot, both groups of test results are quite distinct with no overlapping of test data across sample groups.

4.9.3 Small Punch Tensile (Elevated Temperature 630ºC)

For the elevated temperature testing, Nimonic 90 dies and punches were used.

Lower Punch Die Diameter = 6.4mm

Punch Head Diameter = 4mm

Clearance = 1.4mm

Punch Head Rate = 1.2mm/min = 0.02mm/s

Disc Thickness 0,5mm

Soak Time 30 mins

Small Punch Testing Apparatus (ET)

The apparatus used for the elevated temperature Small Punch Testing was specifically developed for the purpose of this research in order minimise the likelihood of test punch degradation during the trial. Ref. Figure 138 below.

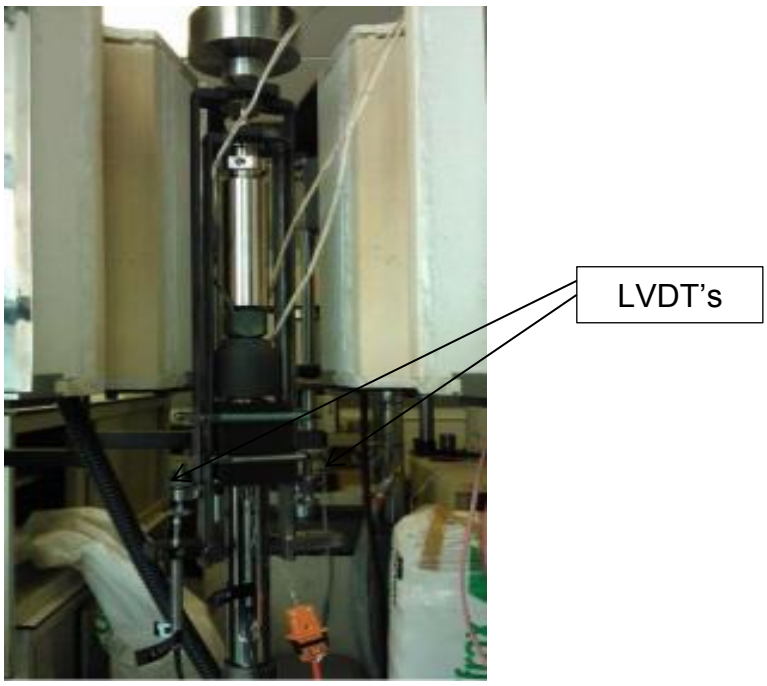

Figure 138: Split Furnace Image

Small Punch Tensile (Elevated Temperature 630°C) – Test Matrix

Table 63 below details the quantity of samples taken from both wrought and injection moulded components.

Table 63: Elevated Temperature (630ºC) Sample Matrix (Wrought and MIM)

Small Punch Test Type	Test Temperature (ºC)	Number of Samples	Sample Source (as detailed)
Small Punch Tensile Wrought	630	2	Component
Small Punch Tensile MIM	630	2	Component

Elevated Temperature (630°C) – Test Results

The following tables (64 and 65) document the test results derived from the Small Punch Tensile elevated temperature testing trials. The test pieces were extracted from component specimens and are identified by Wrought (W), Sample (A) and Root or Shroud (R or S).

Table 64: Elevated Temperature Test Results (Wrought 718 Alloy)

Wrought Sample A	Small Punch Tensile (630ºC)	Ultimate Load kN
W A S	Elevated Temperature	3.25
W A R	Elevated Temperature	2.90

Table 65: Elevated Temperature Test Results (MIM 718 Alloy)

MIM Sample A	Small Punch Tensile (630ºC)	Ultimate Load kN
M A S	Elevated Temperature	0.83
M A R	Elevated Temperature	0.70

Figure 139 below illustrates the difference in test results.

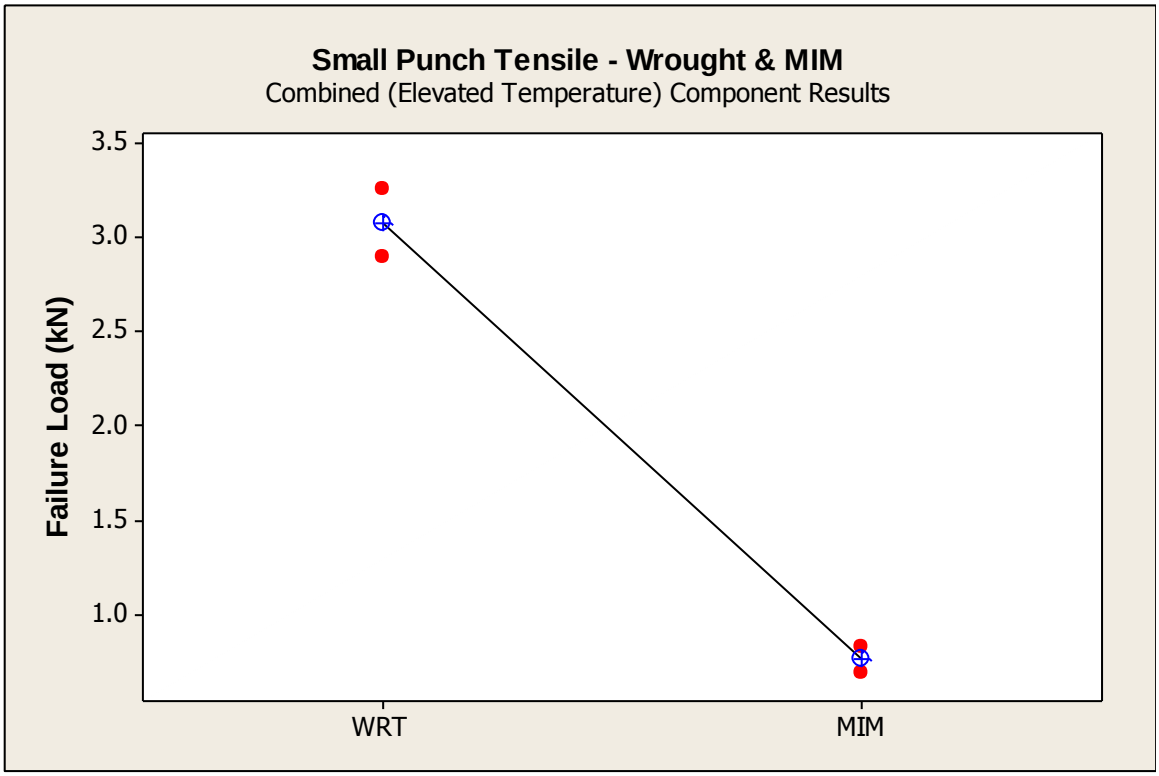

Figure 139: Individual Value Plot (Wrought and MIM 718 Alloy)

Discussion

The test results obtained from the Small Punch Tensile (Elevated Temperature) trials revealed a significant difference in material properties between the injection moulded 718 alloy test pieces and the established 718 alloy datum samples.

Due to the limited amount of test data a full statistical analysis of the test results could not be performed, however from the test data that was obtained from the Small Punch Tensile (Elevated Temperature) test the following conclusions can be made.

The maximum and minimum values obtained from the datum wrought 718 alloy samples were found to be 3.25kN and 2.90kN respectively. A range of 0.35kN
By contrast the test results obtained from the injection moulded samples were from 0.83kN to 0.70kN. A range of 0.13kN.

By comparing the mean test result from each of the sample groups it can be seen that the mean wrought test result is 3.075kN, while the mean MIM test result is 0.765kN. This equates to a deficit of approximately 75.12%.

4.9.4 Small Punch Creep

Creep testing is widely used to characterise the properties of alloys operating at elevated temperature. The phenomenon of creep is characterised by plastic deformation occurring at loadings which would normally be considered to be below the yield point of the alloy. This occurrence is time dependent. Ref. Figure 140.

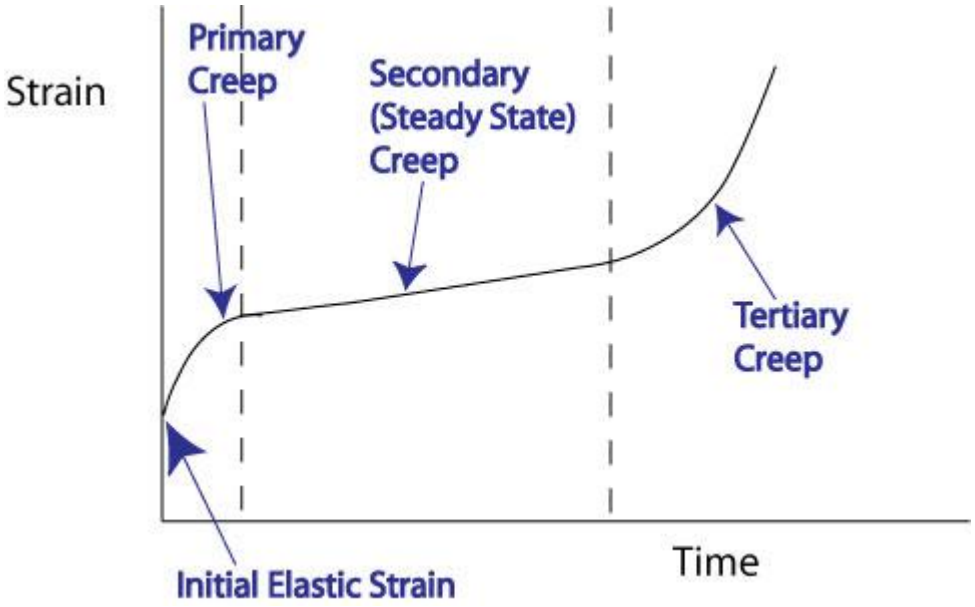

Figure 140: Typical Creep Curve

The mechanisms responsible for creep deformation are generally recognised to be governed by diffusion and dislocation principles. In practice both mechanisms may actively contribute to creep deformation taking place in the test piece or component and are known as Diffusion Creep and Dislocation Creep.

Diffusion Creep can be as a result of diffusion taking place at the grain boundary interfaces (Coble Creep) or within the actual grains themselves *(*Nabarro-Herring Creep). Creep mechanisms which takes place at the grain boundaries can be influenced by the grain size of the alloy.

Dislocation Creep is centered upon the generation and movement of dislocations through the material. Factors which influence dislocation creep may be the presence of precipitates or grain boundary area of the alloy.

Small Punch Creep Testing Apparatus

An illustration of the Small Punch Creep testing equipment used is captured below in Figure 141 below.

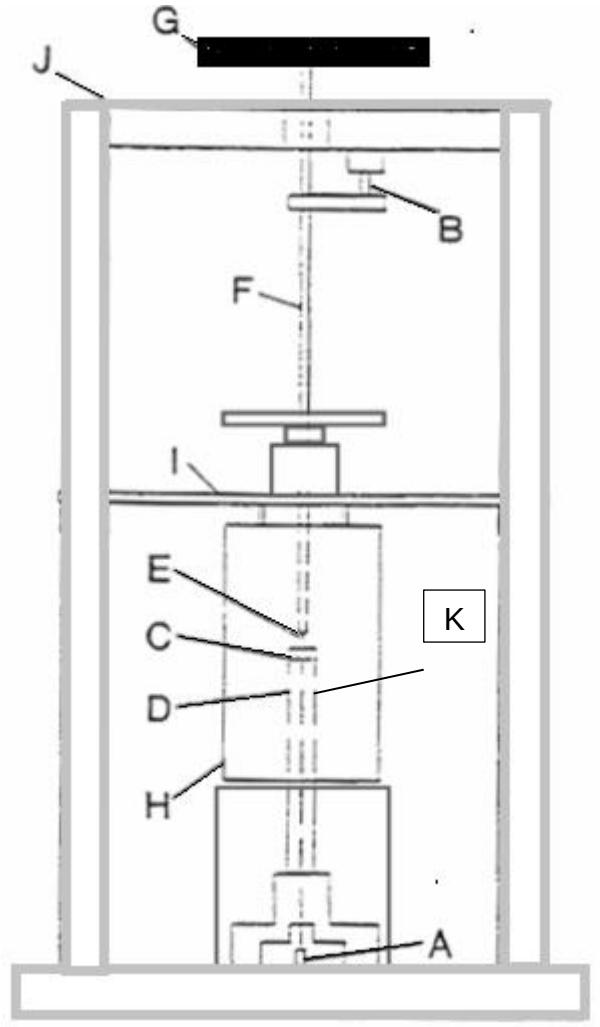

A	Lower transducer
B	Upper transducer
C	Disc location
D	Lower die
E	Hemispherical punch
F	Push rod
G	Load pan
H	Furnace
I	Cross beam
J	Frame
K	Type N thermocouple

Figure 141: Small Punch Creep Schematic Diagram

The test disc is located in the centre of the creep testing apparatus (identified as C above) and located securely in the lower die. The hemispherical punch rests on the upper surface of the disc shaped test piece.

A type N thermocouple is placed in contact with the test disc, and the upper and lower transducers are put in place. The test piece is then raised to the test temperature 630ºC and the test load applied.

The output from a Small Punch Creep test is measured in test piece displacement as a result of deformation under constant load versus time.

For the small punch creep testing CMSX-4 punch material was used with a Nimonic 90 die.

Lower Punch Die Diameter = 4mm

Punch Head = 2mm

Clearance = 1 mm

Disc Thickness 0,5mm

The test matrix is shown in Table 66, with the wrought and MIM results presented in Tables 67 and 68.

Table 66: Small Punch Creep Sample Matrix

Small Punch Test Type	Test Temperature (ºC)	Number of Samples	Sample Source (as detailed)
Small Punch Creep Wrought	630	3	Component
Small Punch Creep MIM	630	3	Component

Table 67: Small Punch Creep Test Results (Wrought 718 Alloy)

Sample	Load (N)	Temperature (ºC)	Final Displacement (mm)	Rupture Time (hours)
Wrought	700	630	1.847	292.6
Wrought	850	630	0.860	8.256
Wrought	900	630	0.865	7.610

Table 68: Small Punch Creep Test Results (MIM 718 Alloy)

Sample	Load (N)	Temperature (ºC)	Final Displacement (mm)	Rupture Time (hours)
MIM	600	630	0.614	14.34
MIM	700	630	0.576	0.652
MIM	900	630	0.629	0.267

Figures 142 and 143 provide a general overview of the creep test results. Figures 144 and 145 specifically focus on 700N and 900N trials.

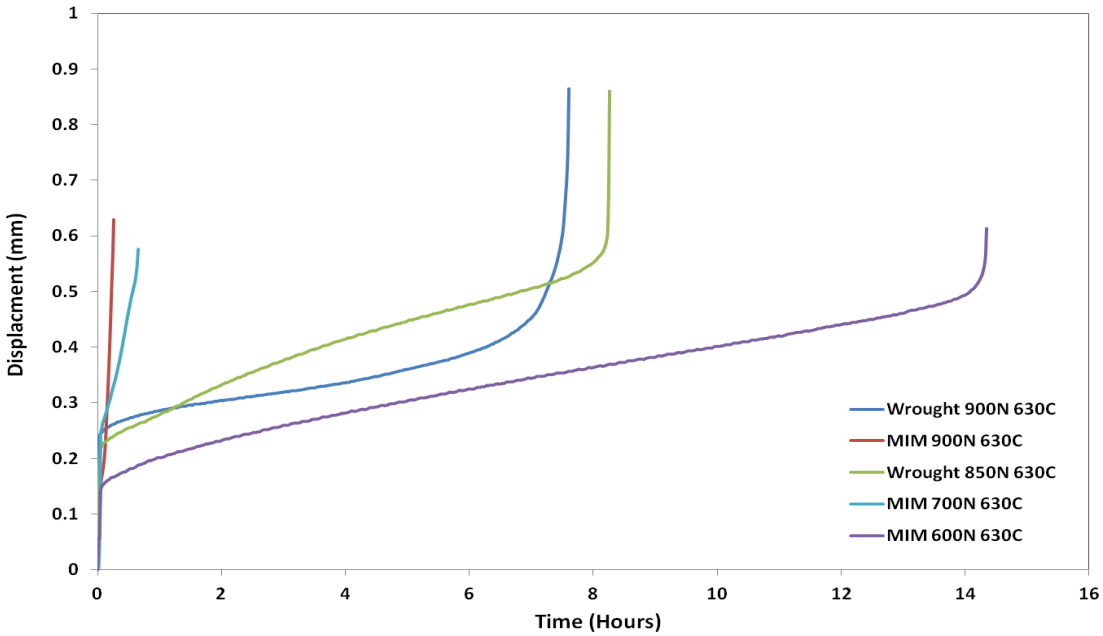

Figure 142: Small Punch Creep Test Results (Wrought and MIM)

Test results presented in Figure 142 above.

	MIM 600N, 630ºC
Wrought 850N, 630ºC	MIM 700N, 630ºC
Wrought 900N, 630ºC	MIM 900N, 630ºC

Comprehensive results are shown in Figure 143 below.

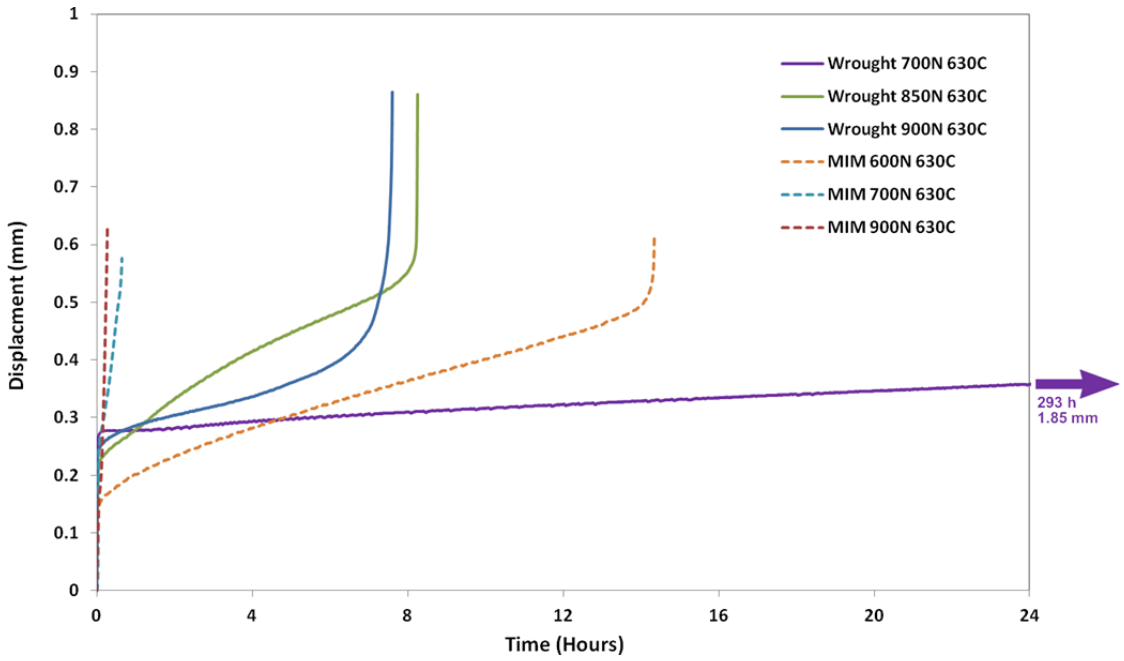

Figure 143: Combined Small Punch Creep Test Results (Wrought and MIM)

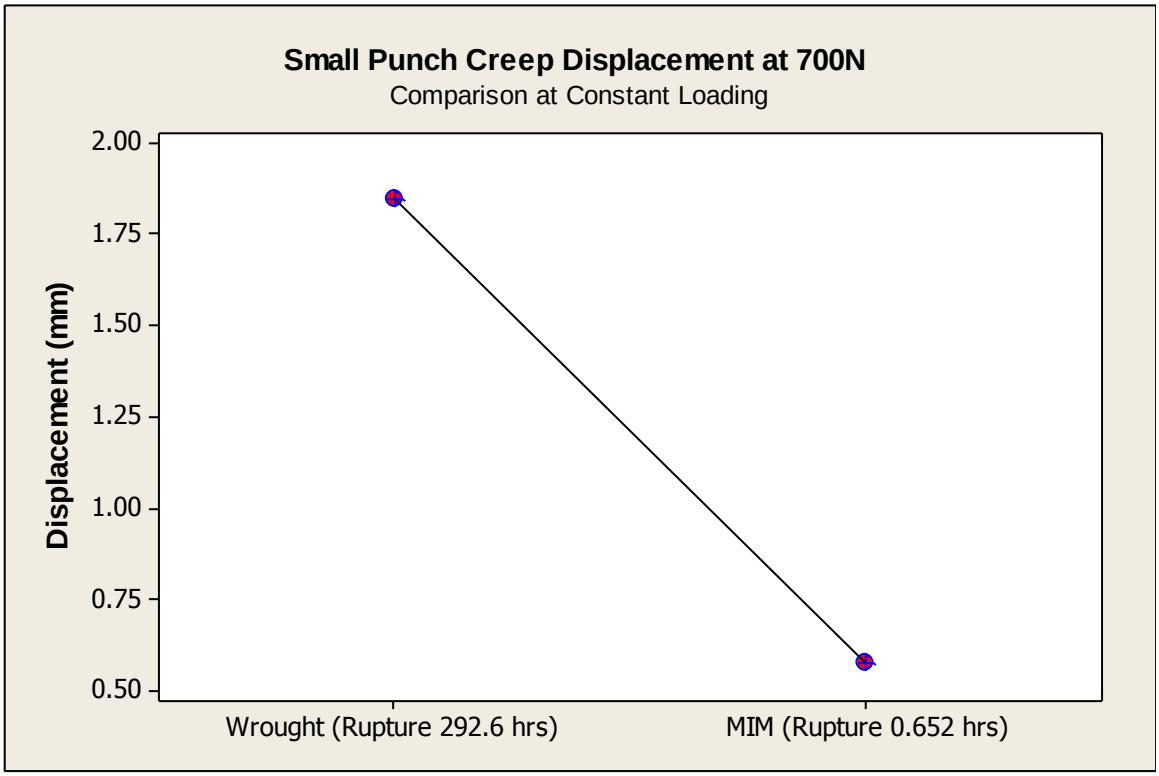

Figure 144: Individual Value Plot - Creep Displacement at 700N (630°C)

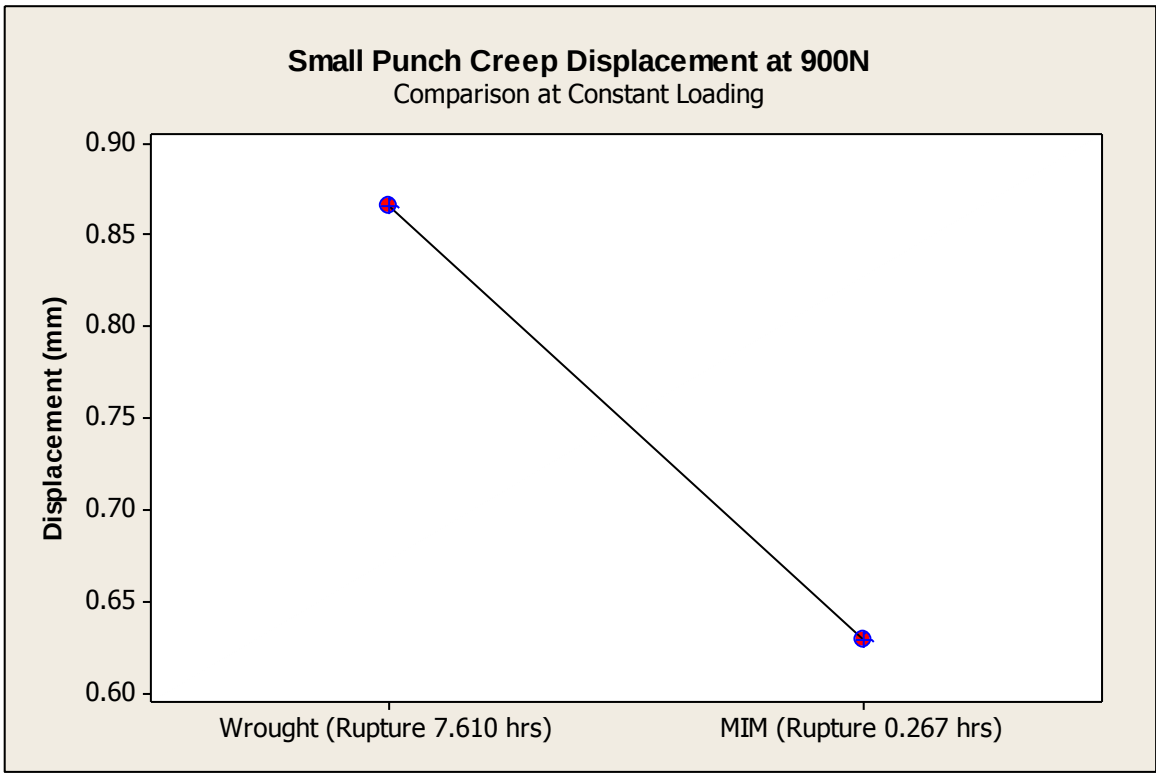

Figure 145: Individual Value Plot - Creep Displacement at 900N (630°C)

Discussion

For discussion purposes two comparative Small Punch Creep tests have been analysed in detail.

- 700N at 630°C.
- 900N at 930°C.

The Creep Test results associated with each of the above trials are directly comparable due to the loading on the test disc and the temperature at which the test was conducted.

At 700N loading the injection moulded test piece presented a deficit in the time to rupture of 99.78% when compared to the wrought 718 alloy specimen also tested with a load of 700N at 630°C.

At 900N loading the injection moulded test piece presented a deficit in the time to rupture of 96.49% when compared to the wrought 718 alloy specimen also tested with a load of 900N at 630°C.

By comparing the final displacement for each of the test types listed above the following attitional features were noted. At a test load of 700N the final displacement of the wrought disc was 1.847mm, by contrast the MIM test disc displacement at rupture was 0.576mm. The test results indicate a 68.81% decrease in the MIM test disc displacement at rupture compared to the wrought 718 alloy datum.

At a test load of 900N the final displacement af the wrought disc was 0.865mm, by contrast the MIM test disc displacement at rupture was 0.629mm. The test results indicate a 27.28% decrease in the MIM test disc displacement at rupture compared to the wrought 718 alloy datum.

The differences that were noted in the final displacement values between the wrought 718 alloy datum samples and the Injection moulded 718 alloy samples has been attribited to differences in the ductility of the samples being tested.

4.9.5 Test Disc Fractography

The tested disc samples from the Small Punch suite of trials were collected and analysed following the completion of each of the testing trials. Test discs from each of the following test types were assessed at magnifications up to x 20 in order to assess the failure modes of the test pieces.

- Small Punch Tensile (Room Temperature).
- Small Punch Tensile (Elevated Temperature).
- Small Punch Creep (630°C).

The samples were assessed as individual groups and also relative to other testing methods. Both sides (concave and convex) of the discs were assessed, however particular attention was focused on the failure region associated with the position of the hemispherical punch.

Since the Small Punch suite of testing trials was specific to Wrought 718 alloy component types and Injection moulded 718 alloy component types, representative images were taken of the disc samples from both the Root and Shroud sections of the trial components.

All the small punch testing trials were performed on disc shaped test pieces which were subsequently removed from components which were in the fully heat treated 718 alloy condition.

The test disc images were photographed at x 2.5 magnification and represent the convex fracture surface of the tested disc.

While the dimensions of the test disc were constant throughout each of the three types of Small Punch test, the dimensions of the punch used for the Small Punch Tensile (Room Temperature and Elevated Temperature) was 4mm. While the punch used for the Small Punch Creep trials was 2mm.

Figures 145 to 165 provide a visual comparison of the fracture surfaces of the Small Punch suite of testing trials.

Test Disc Fractography - Room Temperature - Wrought 718 Alloy

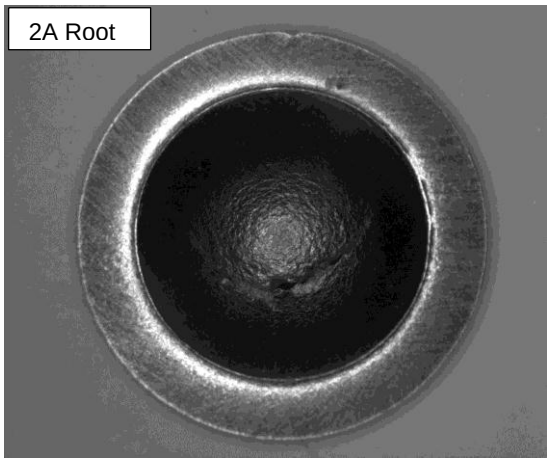

Figure 146

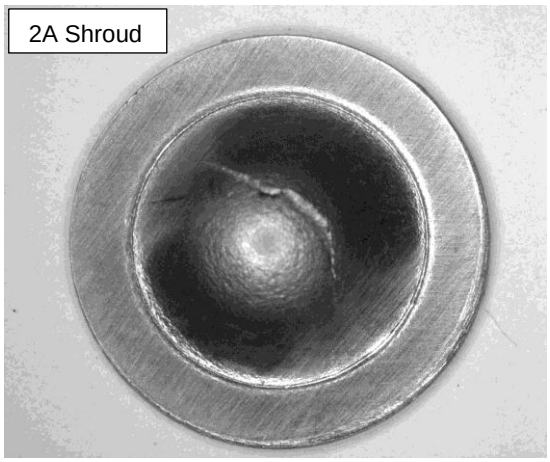

Figure 147

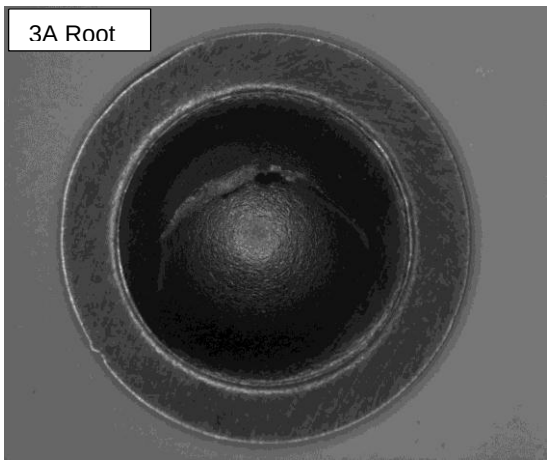

Figure 148

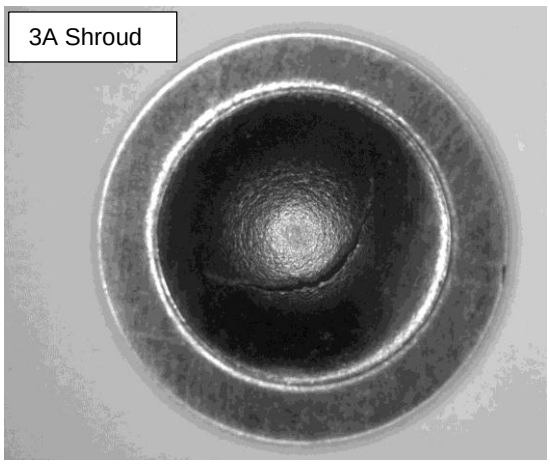

Figure 149

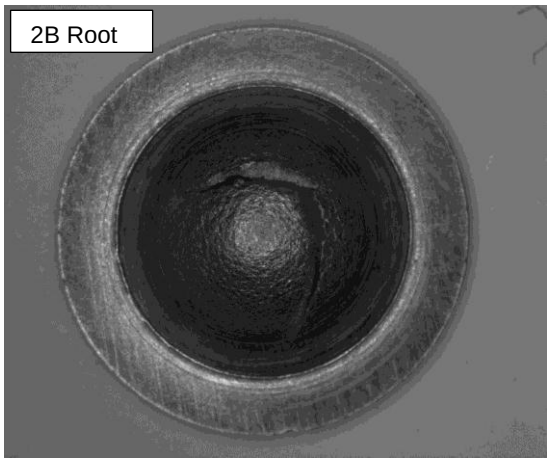

Figure 150

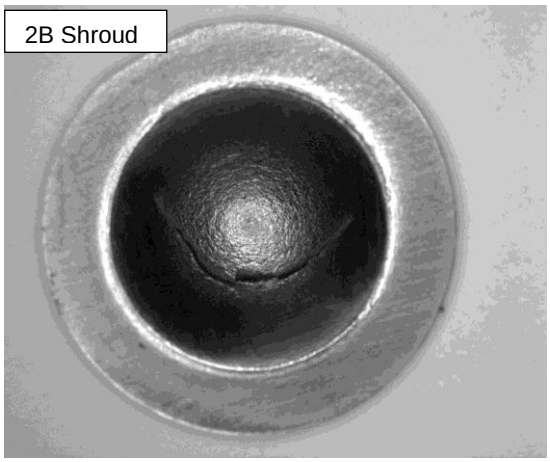

Figure 151

Test Disc Fractography - Room Temperature - MIM 718 Alloy

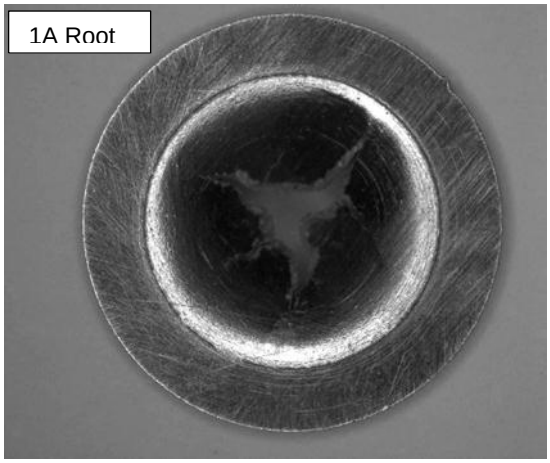

Figure 152

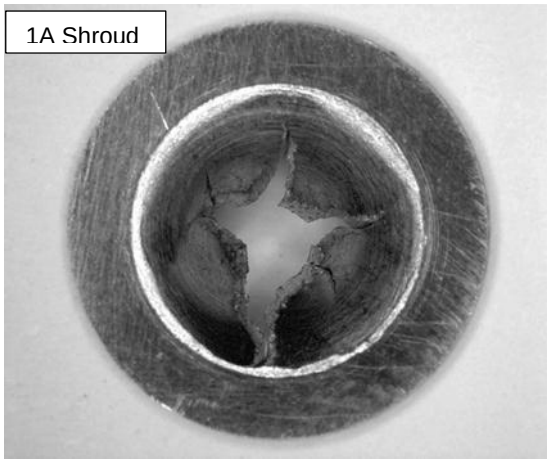

Figure 153

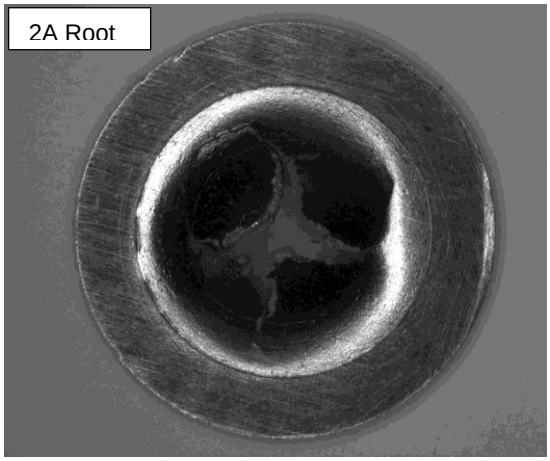

Figure 154

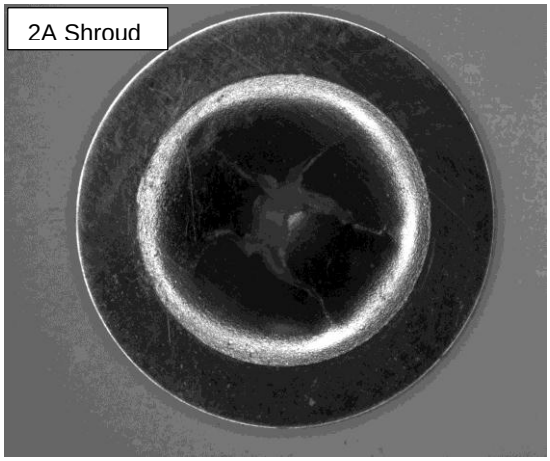

Figure 155

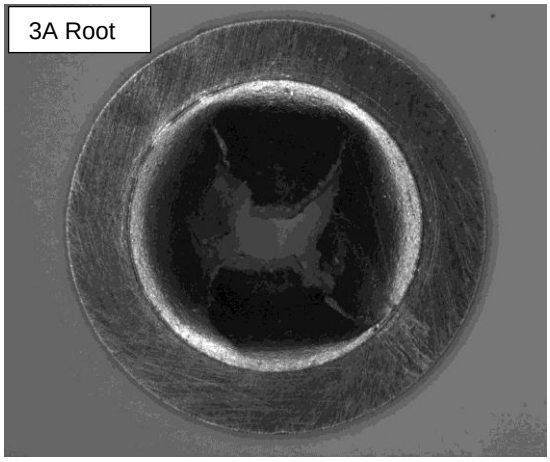

Figure 156

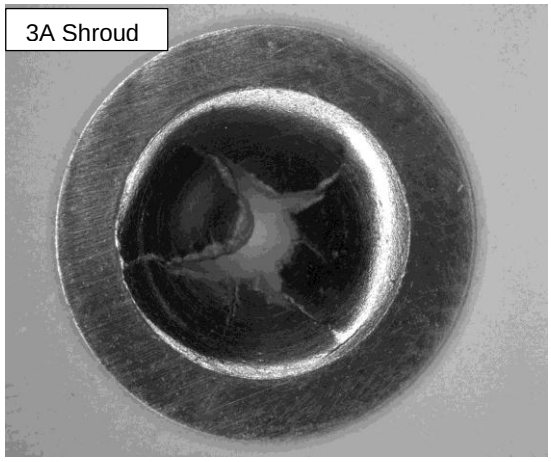

Figure 157

Test Disc Fractography - Elevated Temperature (630°C) - Wrought 718 Alloy

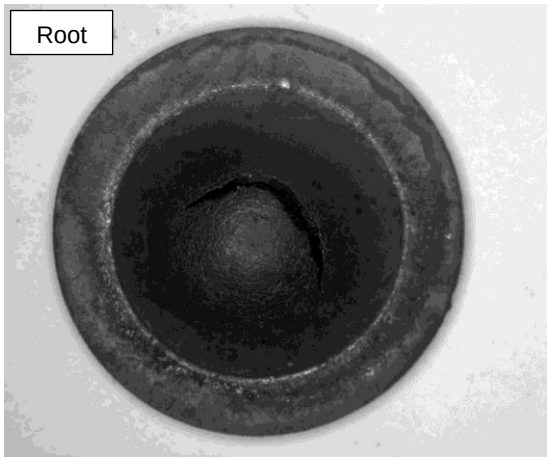

Figure 158

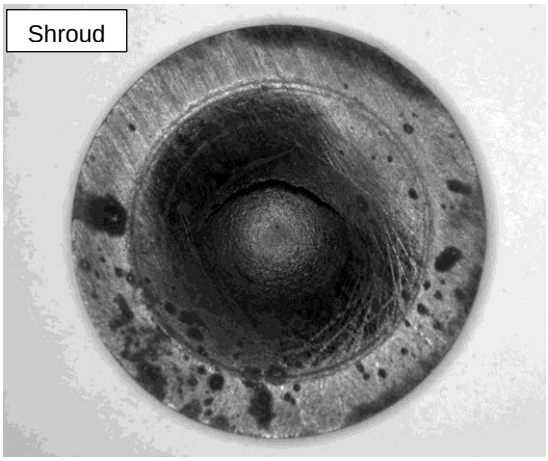

Figure 159

Test Disc Fractography - Elevated Temperature (630°C) - MIM 718 Alloy

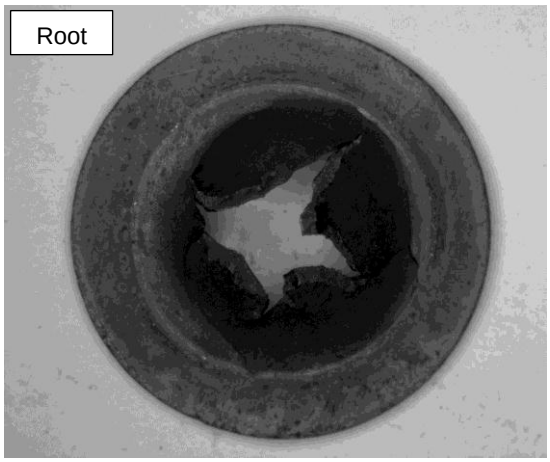

Figure 160

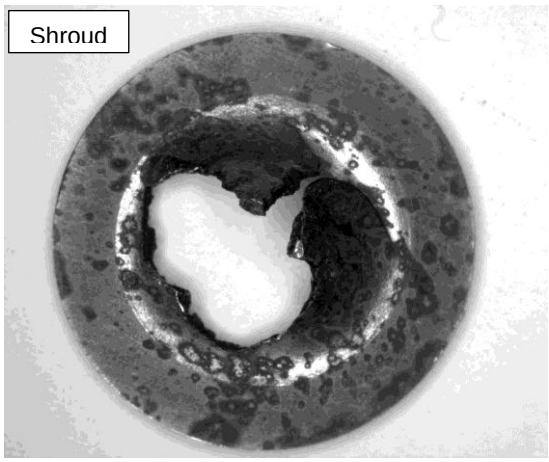

Figure 161

Test Disc Fractography - Small Punch Creep (630ºC) - Wrought 718 Alloy

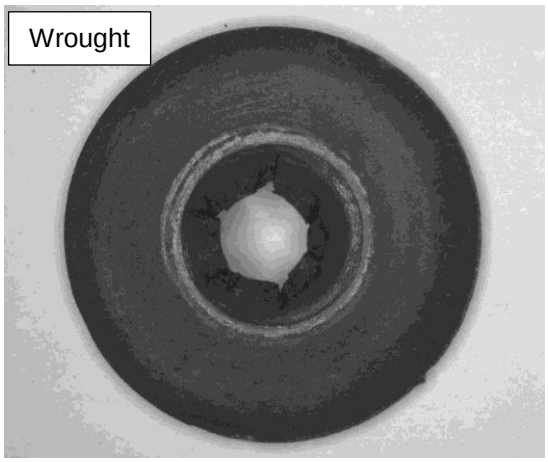

Figure 162: 700N

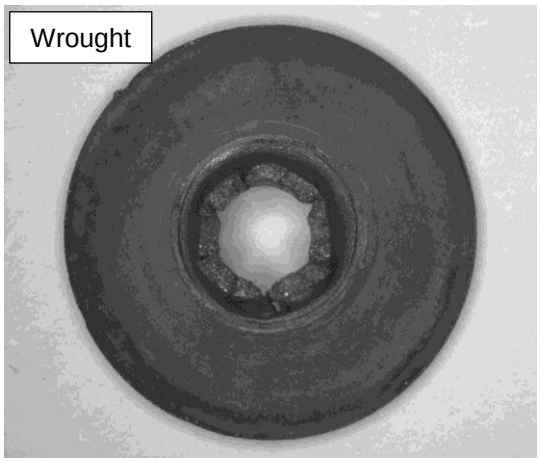

Figure 163: 900N

Test Disc Fractography - Small Punch Creep (630ºC) - MIM 718 Alloy

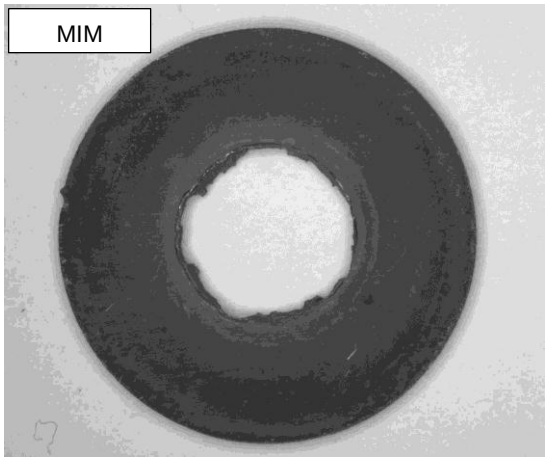

Figure 164: 700N

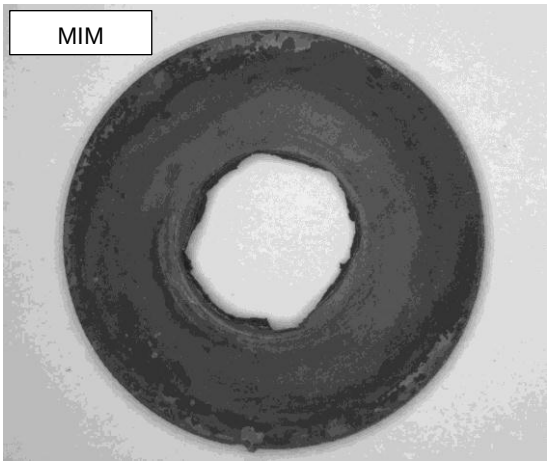

Figure 165: 900N

Test Disc Fractography Discussion

Evaluation of the fracture surfaces and the raised hemispherical regions of the tested disc samples revealed the following.

Small Punch Tensile (Room Temperature)

Wrought 718 alloy specimens from both the Root and the Shroud regions presented typically ductile fracture modes of failure. The test discs were raised as a result of the applied force during testing and indicative of good specimen ductility. The discs appeared similar with regard to the position and the orientation of the failed surface. The path which the fracture surface followed was found to be continuous with no evidence of secondary failure initiation sites and without loss of material.

The MIM 718 alloy specimens from the Root and the Shroud regions presented less ductile fracture modes than the wrought 718 samples. While the samples were found to be consistent in terms of appearance between Root and Shroud regions there was a clear difference in appearance when compared to the wrought 718 alloy samples. Multiple crack failure initiation sites were present resulting in a multi-faceted failure surface. The Injection moulded test discs appeared to present much less ductility than the wrought datum samples with clear evidence of material release.

Small Punch Tensile (Elevated Temperature)

Evaluation of the failed test disc samples from both the MIM 718 alloy discs and the wrought 718 alloy samples revealed similar characteristics to those obtained from the room temperature disc evaluations.

Small Punch Creep (630°C)

Both the Wrought 718 alloy samples from the Root and the Shroud regions of the component were found to be visually similar. The raised surface on the test disc suggested that the material still exhibited a certain amount of ductility at the 630°C testing temperature. The test discs from the Root and Shroud regions of the injection moulded test component also looked similar however failure had occurred with minimal evidence of ductility and was of a fragmented nature.

4.9.6 Test Disc Microscopy

The tested disc samples from the Small Punch suite of trials were collected and analysed following the completion of each of the testing trials. Microsections were taken through representative discs, mounted in clear acrylic resin and polished to reveal the fracture surface.

The microsections from each of the following test types were assessed at magnifications up to x 500 in order to locate the failure initiation points and to assess the mode of failure.

Microsections from the following test groups were analysed

- Small Punch Tensile (Room Temperature)
- Small Punch Tensile (Elevated Temperature)
- Small Punch Creep (630°C)

For the purpose of the assessment, reflected light microscopy was used. No light filters were used. The polished specimens were viewed in both the as polished condition and following chemical etching to reveal the microstructure.

The microscopic evaluation consisted of assessing the tested samples against the wrought 718 alloy datum. For each trial that was conducted, datum wrought 718 alloy samples were also prepared and tested to an identical procedure as the injection moulded 718 alloy variants.

The test samples were assessed initially at low magnification (x 50) to obtain an overall assessment of the metallurgical structure in addition to the structure at the point of failure.

Comparative images of both wrought and injection moulded 718 alloy test discs were taken for evaluation purposes.

Figures 166 to 171 capture the microscopic examinations of the fractures test pieces.

Test Disc Microscopy - Room Temperature - Wrought and MIM 718 Alloy

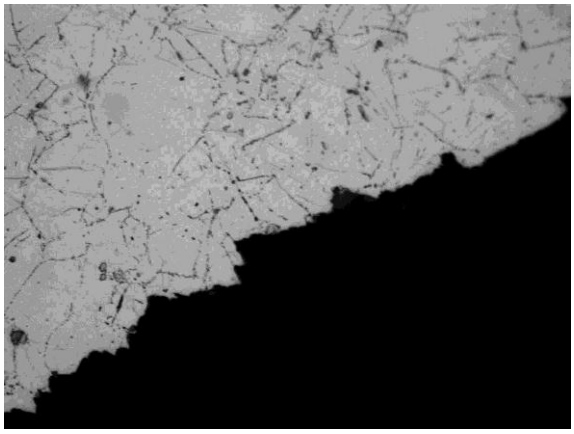

Figure 166: Wrought x 500

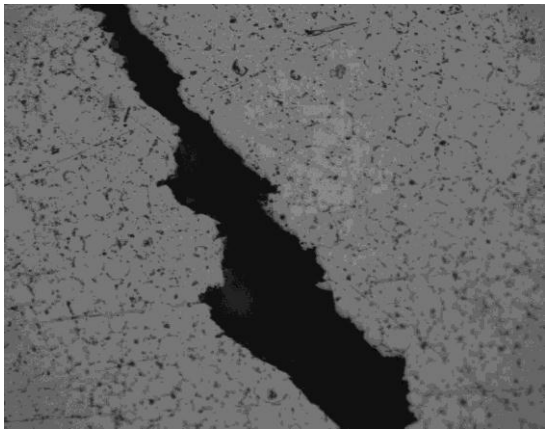

Figure 167: MIM x 500

Test Disc Microscopy - Elevated Temperature - Wrought and MIM 718 Alloy

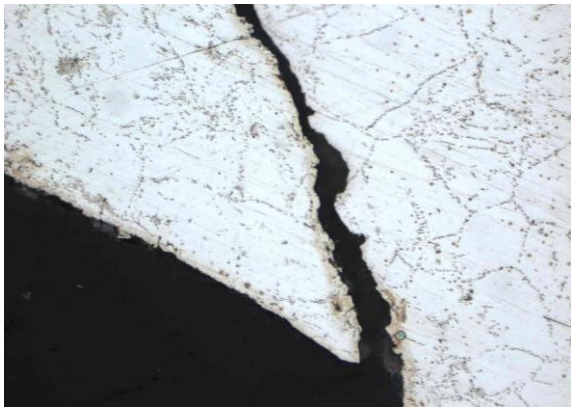

Figure 168: Wrought x 500

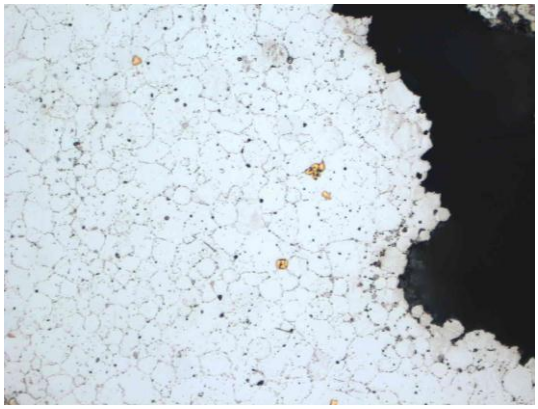

Figure 169: MIM x 500

Test Disc Microscopy - Small Punch Creep (630ºC) - Wrought and MIM 718 Alloy

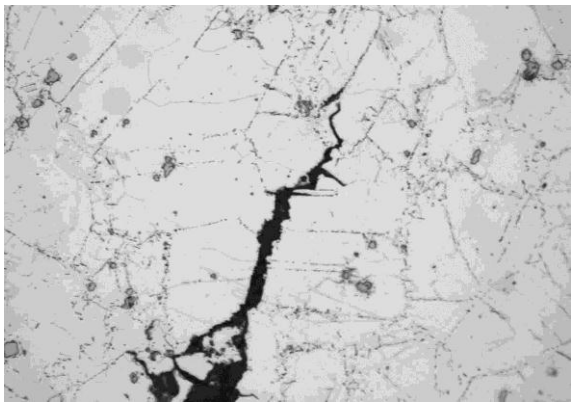

Figure 170: 900N - Wrought x 500

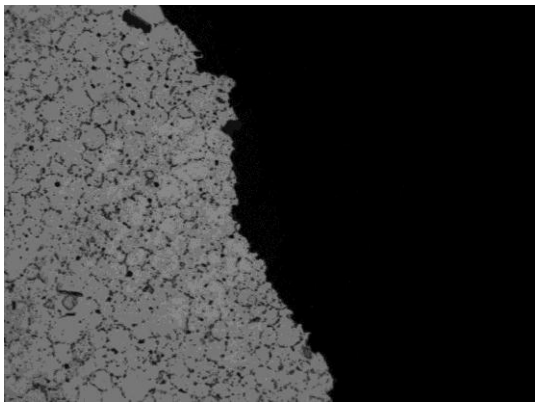

Figure 171: 900N - MIM x 500

Test Disc Microscopy Discussion

Microscopic evaluation of the general microstructure and fracture surfaces of representative Small Punch disc samples revealed the following:

Small Punch Tensile (Room Temperature)

The wrought 718 alloy datum sample presented an intragranular mode of failure. Following initiation the crack propagation and direction was almost linear in nature through the section which was evaluated. This is indicative of high grain boundary alloy strength. Several failure modes were detected upon examination of the injection moulded 718 sample. The microstructure of the MIM samples were found to contain randomly distributed voids which were up to 15um in diameter. The much reduced strength of the MIM material may be attributed to the presence of these pores. Normal micro void formation during room temperature and elevated temperature testing could be superseded by the porosity already inherent in the microstructure resulting in a more rapid failure mode with less specimen ductility.

Small Punch Tensile (Elevated Temperature)

The microstructures of the elevated temperature test discs for both wrought and MIM 718 alloy variants were found to be similar in structure and features to those obtained from the room temperature evaluation.

Small Punch Creep (630°C)

The failure mode and crack propagation of the wrought 718 alloy specimen was found to be intragranular. By comparison the injection moulded 718 alloy variant appeared to fail by an intergranular/interparticle failure mode. The crack can be seen to propagate through the boundaries of adjacent powder particles in the injection moulded sample. The initiation points for the cracks were found to be isolated pores and microstructural irregularities at the powder particle boundaries. Analysis of the creep curves suggests that no tertiary creep occurs, possibly because the existing pores in the microstructure provides a suitable failure initiation point.

CHAPTER 5

GENERAL DISCUSSION

5. General Discussion

Metal injection moulding of Gas Turbine Compressor Components has identified several challenges both in the application of the process but also in the necessary processing standards that would be required in order to meet the needs of the aerospace industry.

While polymer injection moulding is a well-established and understood process, metal injection moulding requires a much broader cross functional awareness of the behaviour of both polymeric materials and metallic materials.

In the research that has been completed the rigorous back to back characterisation and testing of both wrought and injection moulded 718 alloy variants demonstrated a significant deficit in material properties from the injection moulded 718 alloy.

The inability of the injection moulded 718 alloy to meet the same testing specification as the conventional wrought alloy using identical testing pieces and testing parameters has been attributed to two key processing areas.

- The manufacture of the powdered 718 alloy.
- The processing of MIM 718 alloy.

Conventional wrought 718 alloy is an aerospace grade gas turbine superalloy which has been specifically designed to operate at elevated temperatures offering superior strength and corrosion properties. In order to achieve the required material properties, the alloy chemistry and impurity levels are closely controlled. By contrast the powdered 718 alloy used in this research had not followed the same rigorous melting route, being melted under an argon atmosphere as opposed to the conventional VIM / VAR melting route used to manufacture aerospace grade wrought 718 alloy such as wrought products manufactured to AMS5662.

This could be the reason that critical elements such as the Carbon, Nitrogen and Oxygen were found to be greater in the powdered alloy than those from the wrought alloy. High concentrations of these elements are associated with deficits in alloy ductility.

Upon Reflection on this research, the largest single improvement which could be offered for the application of the metal injection moulding process for the

manufacture of gas turbine compressor components would be the adoption of a full supply chain Process Failure Mode and Effect Analysis. This process should be inclusive of both the manufacturers of the powdered 718 alloy and supported by technical experts from the aerospace industry having expertise in both metallic materials, plastics materials and the application of aerospace standards.

Manufacture of the Powdered Alloy

Conventionally manufactured 718 alloy undergoes a substantial amount of thermo-mechanical processing combined with homogenising and recrystallisation heat treatments in order to achieve a commercially attractive product which is microstructurally homogeneous. The thermo-mechanical processing operations are key to breaking up networks of carbide particles and other strengthening precipitates found in the microstructure. This is an essential part of the manufacturing process as it ensures that the end product is metallurgically uniform due to a fine dispersion of strengthening particles, uniform grain size and freedom from chemical segregation. The chemical elements and processing techniques associated with the manufacture of wrought 718 alloy have been developed to maintain the elevated temperature mechanical properties and corrosion resistance of the alloy.

Due to the nature of the manufacturing process, the powdered 718 alloy particles used for the injection moulded test pieces had not been through a homogenisation process. The test results obtained from the scanning electron microscope and EDAX analysis found that both the morphology and distribution of the alloy precipitates differed from the wrought baseline samples.

Metallurgical evaluation of the fractured tensile test pieces using the scanning electron microscope revealed evidence of powder particles being plucked out of the surrounding sintered powder matrix. This feature is considered to be caused by poor inter particle cohesion due to the inability of certain powder particles to form a sufficiently strong diffusion bond with the surrounding matrix. This phenomenon is most likely to be a direct result of localised low powder packing density due to non homogeneous feedstock or as a result of powder particle surface contamination resulting in a barrier being created at the surface of the powder which restricts diffusion and subsequent bonding taking place.

Conventionally manufactured wrought 718 alloy conforms to exceptionally high cleanliness standards due to the nature of the melting process from which the alloy is manufactured. As would be expected none of the wrought 718 test pieces which were microstructurally examined exhibited any evidence of undesirable features such as inclusions, oxide stringers or chemical segregation effects. The probability of 718 alloy contamination in powdered alloys is much higher than that of the wrought equivalent.

For aerospace grade wrought 718 alloy, the method of manufacture is closely controlled, documented and considered to be sealed in terms of process changes. The wrought product is traceable from the original melt route through to the individual casts. This level of cast traceability is maintained throughout the manufacturing sequence to the finished machined 'in service' gas turbine component.

With insufficient technical processing controls, the likelihood of powdered alloy contamination will be high. There are numerous potential sources of alloy contamination ranging from the quality of the original ingot from which the powdered alloy is formed through to the injection moulding binder constituents, processing apparatus and furnace fixturing. The identification of foreign material in the fracture face of an injection moulded test piece was a significant finding. It is not known at which stage in the manufacturing process the material entered the injection moulded 718 alloy constituents however its presence does however provide an indication of the vulnerability of powdered alloy to contamination.

In order to minimise the likelihood of powder contamination dedicated 718 alloy processing equipment should be used. In addition there should be a documented cleaning and maintenance plan in place to further minimise the likelihood of metallic and non metallic alloy contamination.

Only certified wrought aerospace grade 718 alloy ingot material should be used and melted under vacuum conditions for conversion to powdered alloy. Revert material excluded from the melting process.

Multiple sieve classifications in order to minimise the likelihood of foreign material entrapment could also be adopted. Whilst the adoption of a smaller powder sieve

classification size would help to reduce the size of foreign particles, it is generally accepted that not all powder impurities are spherical in nature and small elongated impurities may pass through to the final 718 alloy powder lot.

Binocular inspection techniques applied to multiple samples of each powder lot could be used to verify the shape and cleanliness of the powdered alloy.

Once manufactured and verified for conformance the powdered alloy could be stored in suitable containers in a temperature and humidity controlled environment to minimise the likelihood of contamination by both airborne particles and also due to corrosion.

Manufacture of the Injection Moulding Feedstock

The 718 alloy feedstock used in this research project was manufactured under laboratory conditions as opposed to being purchased from a dedicated supplier. This decision was made based upon prior experience using a specific binder formulation which could be removed relatively easily from injection moulded test pieces of similar powder size without the need to purchase additional industrial processing equipment.

The preparation of the 718 alloy metal injection moulding feedstock could be improved by performing the key mixing operation in a clean room environment, with appropriate controls being applied to the containerisation of powdered 718 alloy and documented procedures for the storage and shelf life of consumable mixing products and finished feedstock.

For example the Polymethyl methacrylate used during this research was an emulsion polymer. The condition of supply of the product was a colloidal liquid with serialised traceability. The product was found to be comprised of a solid polymer particle dispersed in water and surfactants. Further investigation revealed the polymer to be a free radical addition polymer of molecular weight >100,000 to 1,000,000. The particle size of the polymer was within the range of 100 to 300 nanometers. It is widely accepted that increases to the particle size results in decreased solution viscosity, while decreases to the particle size would result in increased solution viscosity. The free monomer in the product was limited to 0.1% maximum. The solids content of the product was found to be approximately 40% by

weight, controlled by the product supplier to within +/-1%. This data was obtained by the product supplier as a result of solids determination trials at 110ºC for one hour. The acidity of the product was found to be pH 6.5-7.5, essentially neutral by nature. The minimum film formation temperature was 105ºC. As received, the product was a pourable low viscosity liquid, of approximately 250-500 millipascal seconds.

For a product such as this, which is an integral part of the feedstock preparation, there could be receipt inspection checks to verify key product attributes such as the solids content or the pH. Since the product has a high water content it would be worthwhile establishing the shelf life of the product as based upon moisture loss over time.

A similar methodical approach to all the injection moulded binder constituents would be worthwhile to standardise in incoming product condition of supply and also to maintain traceability of the individual binder constituents.

Feedstock preparation could be performed in an atmosphere controlled clean room environment, to prevent exposure of the feedstock and feedstock constituents to humidity, ambient air and also airborne particles of contaminant materials. The shelf life of the mixed feedstock could also be determined monitored before use.

The defects which were identified using the X-ray CT scan identified features which were most probably caused at the injection moulding stage of the process. The variable positions of both consistent and inconsistent regions of the injection moulded test pieces indicates either an intermittent equipment proceeding fault or a failure to recognise and maintain the process input parameters.

Comparative mechanical test results derived from both the small punch tensile and the small punch creep testing trials proved to be useful both in terms of the corroboration of test results but additionally small punch creep testing provided data in a relatively short time from which conclusions could be made on the creep strength of the wrought and injection moulded variants.

Injection Moulding

Injection moulding is a well-established high volume manufacturing process for polymeric materials. The operation and repeatability of the process is a function of the key process input variables. The parameters selected to manufacture test pieces of green state 718 alloy test pieces should be traceable to a substantiated moulding method. Test pieces and components should not pass beyond this part of the manufacturing process until thorough process controls have determined that the product is free from gross internal defects. One method of achieving this could be through batch sampling in the green state by examining the quality of the injection mouldings after the initial component, followed by 1 in 20 to ensure that the continuity of the batch is maintained. The equipment used to perform the injection moulding operation must have the ability to retain and recall the key processing variables within a reasonable pre-determined accuracy. The stages of the injection moulding cycle utilised during the manufacture of production batches of components should be reviewed and assessed against the parameters which were used to substantiate the original process. The injection moulding key process variables should be documented and stored electronically or in an appropriate recall system. The method of manufacture should be frozen upon the completion of all substantiation trials.

In order to avoid material contamination there should be an equipment cleaning regime in place. A dedicated injection moulding capability would be the ideal to avoid cross contamination with other alloy types.

Sintering Controls

With all vacuum heat treatment and processing applications, cleanliness of the vacuum furnace is a high priority. The furnace chamber and fixturing should be cleared of any visible debris dust particles prior to usage. The fixturing used to support the components should be standardised and experiments undertaken to understand whether or not the component supports used during the sintering operation react with the test pieces being sintered. Dedicated equipment is necessary in order to minimise contamination from alternative fixturing and minimise the likelihood of foreign material volatilising during the sintering cycle. The working zone of the furnace should be clearly defined in terms of the expected temperature uniformity at key positions within the working volume of the furnace, to ensure that all

test pieces placed within the furnace receive the appropriate heat treatment cycle. When establishing the heat treatment cycle there must be a clear instruction on how the time at temperature is measured. This could be derived from the time taken for the last furnace control thermocouple to reach the agreed set point minus the lower section of the temperature tolerance or more accurately from the positioning of load thermocouples within the working area of the furnace. To avoid contamination the load thermocouple could be placed within a ceramic sheath in close proximity to the components being sintered.

Due to the nature of the sintering process volatilisation of binder constituents will take place within the vacuum furnace chamber. In order to ensure that the volatilisation of binder products does not compromise the thermocouple readings, an independent survey of the accuracy of the thermocouple operation should be conducted at regular intervals to ensure against temperature drift.

The furnace gasses employed during the sintering and gas fan quenching operations should be measured for moisture content. A dew point meter is considered to be essential with the monitoring results forming part of the documented processing record.

Following successful binder removal and sintering trials, all the key sintering furnace processing variables require to be captured and documented and traceable to a satisfactory metallurgical substantiation report. The following points should be noted with an appropriate tolerance for a particular sintering and heat treatment cycle.

- Furnace basket and component fixturing requirements.
- The maximum number of components or test pieces per furnace load.
- The position or orientation of the components or test pieces in the furnace basket.
- The position of the load thermocouple.
- The furnace ramp up rates and corresponding vacuum levels.
- Calibration status of key process monitoring gauges.

If the debinding and sintering processes are performed in a vacuum furnace it would further enhance the cleanliness of the process if a high temperature bake out or

gettering run was performed using titanium components to absorb residual gaseous elements prior to the onset of the furnace program.

Following the completion of debinding, sintering and heat treatment furnace cycles, the furnace record needs to be checked against the processing parameters. If a discrepancy is noted the batch being processed requires to be quarantined until an investigation of the product quality and if necessary rectification heat treatment can be performed.

The quality of the sintered and heat treated product requires to be verified on completion of the heat treatment process. The validation may involve binocular inspection of the surface of all the components, metallurgical evaluation or a suitable form of non-destructive testing. Where sample inspection is employed, such as hardness testing, there should be sufficient historical data to justify the chosen reduced sample inspection.

Where non-destructive testing techniques are employed to verify the integrity of the final product, the appropriate aerospace controls require to be instigated. During this research thesis the use of aerospace level investigation techniques and capabilities such as X-ray computed tomography proved decisively the integrity of the test specimens being inspected and enabled the origins of the 718 alloy defects to be traced to the injection moulding and debinding/sintering operations.

The consequences of using NDT processes and techniques which are not recognised and controlled by aerospace governing standards could result in the inability to detect the presence and location of sub surface material defects.

Testing Standards

During the initial literature review it was noted that there were several different test piece geometries from which mechanical test data was being obtained and reported. Not all of the data was produced by conventional aerospace testing methods.

This research was focused on conducting comparative back to back trials using argon gas atomised 718 alloy to order to achieve equivalent mechanical properties to conventionally manufactured test pieces and components manufactured from wrought 718 alloy.

Whilst the quantity of test result data is limited, the data that has been produced suggests that the chosen manufacturing method incorporating the powdered 718 alloy is not capable of producing a product of equivalent mechanical properties to the wrought 718 alloy datum.

One of the most influential papers published in the last 3 years was found to be *Metal Injection Moulding of Alloy 718 for Aerospace Applications,* Ott and Peretti (2012). In this research the metal injection moulded test pieces were subsequently hot isostatically pressed in order to obtain finished specimen densities which approached the density of wrought 718 alloy.

Despite this positive achievement the authors did however find it necessary to launch a further technical standard specifically tailored to components and test pieces manufactured using injection moulded 718 alloy. The elevated temperature mechanical properties detailed in the additional 718 alloy material specification (AMS5917) are below the mechanical properties that would be expected from wrought 718 alloy material (AMS5662) and other industry 718 alloy material specifications followed by aerospace manufacturers.

Table 69: Comparison of Industry Tensile Testing Standards

Standard/ Test temp	Ultimate tensile strength (MPa – Min)	Proof Stress 0.2% (MPa - Min)	Specimen Elongation (% - Min)	Specimen Reduction (% - Min)
Industry (wrought) 650°C	1000	860	10	18
AMS5662 (wrought) 649°C	1000	862	12	15
AMS5917 (MIM+HIP) 649°C	931	827	6	6

The industry standard wrought 718 alloy test results are stated for testing conducted at 650ºC. Both AMS5662 and AMS5917 standards are for testing conducted at 649ºC. From Table 69 above it can be seen that there is a reduction in mechanical properties from both the wrought standards to the MIM + HIP standard.

CHAPTER 6

RESEARCH CONCLUSIONS

6. Research Conclusions

The aim of this research was to determine the suitability of utilising the Metal Injection Moulding Process for the manufacture of gas turbine compressor components from 718 alloy. As a consequence of this study the following conclusions have been made.

- The material quality of the powdered 718 alloy and the process control methods associated with the injection moulding capability were not found to be sufficiently robust to minimise both material and processing variations.
- The test data obtained from the MIM 718 alloy elevated temperature (650ºC) tensile test results indicated a deficit in mechanical properties. The test results failed to meet the minimum industry standards in terms of Ultimate Tensile Strength, 0.2% Proof Stress, % Elongation and % Reduction in Area. Subsequent thermo-mechanical processing operations were found to improve the alloy strength however a deficit in material ductility was still present.
- Small Punch Test data corroborated the findings of the elevated temperature (650ºC) tensile test results and additionally highlighted the Creep property deficit during 700N and 900N load conditions.
- Metallurgical analysis of both the wrought and the MIM 718 alloy variants revealed contrasting structures. The MIM 718 alloy was found to be non homogeneous with evidence of random amounts of porosity, foreign material contamination and networks of metal oxides present.
- From the literature review, the methods employed to declare the properties of injection moulded 718 alloy are varied. The testing methods, test piece geometries and test piece surface condition were found to vary significantly without evidence of correlation to conventional aerospace testing methods.

On this occasion it can be concluded that the Metal Injection Moulding process has not proved to be a viable alternative to conventional manufacturing methods for the manufacture of gas turbine compressor components from 718 alloy.

6.1 Contribution to Knowledge

The metal injection moulding process has had limited exposure in the Aerospace Industry. As a result of this research the following contributions have been made to the foundations already being developed by Ott and Peretti (2012) in order to exploit the potential benefits of utilising the metal injection moulding process for the manufacture of gas turbine components.

The properties of metal injection moulded 718 alloy can be improved by subsequent thermo-mechanical processing operations. However the presence of random microstructural voids is a limiting factor which prevents the powered alloy reaching the full potential of the wrought 718 alloy equivalent.

Metal injection moulding component suppliers are required to adopt the intent of aerospace technical quality controls and procedures throughout the manufacturing process in order to minimise product variation and to be able to demonstrate process stability by statistical methods. This research found that feedstock quality and injection moulding repeatability were key process input variables which require technically robust controls.

There is also a need for the standardisation and reporting of test data derived from metal injection moulded test pieces which is intended to be used by the aerospace industry. Clear material test result corroboration with recognised aerospace testing standards is required in order to substantiate testing methods and procedures.

Small Punch testing of both wrought and injection moulded 718 alloy variants proved to be a cost effective and technically decisive method of distinguishing between the wrought and injection moulded 718 alloy properties. This testing method enabled the removal and testing of small samples from otherwise inaccessible component geometries.

Details of the comparative Small Punch testing trials were published in 2014. The research paper can be found in Appendix 1.

CHAPTER 7

RECOMMENDATIONS FOR FUTURE ACADEMIC RESEARCH

7. Recommendations for Future Academic Research

Based upon the current level of knowledge associated with the metal injection moulding of 718 alloy, and in acceptance that the mechanical properties of injection moulded 718 alloy are unlikely to demonstrate equivalence with the conventional wrought aerospace equivalent 718 alloy, the following recommendations for future research are based upon consolidating the existing level of knowledge and expanding on the gaps that still exist within the process.

Powder and Processing

- Develop a specifically designed powdered alloy as a replacement for using powdered 718 alloy. The chemical composition of 718 alloy is tailored to meet elevated temperature applications in the wrought condition with close grain size control. The ideal alloy would provide good elevated temperature properties combined with good sintering properties.
- Establish the relationship between test piece sectional thickness, powder particle size and the removal of binder constituents during the sintering cycle in order to minimise the onset of internal micro cracking.
- Develop an understanding of the effects of sintering in a Hydrogen atmosphere on the bonding characteristics of the powdered 718 alloy.
- Examine the effects of consolidating the sintered 718 alloy material by incorporating a hot isostatic press (HIP) to further homogenise the sub surface microstructure and minimise sub surface discontinuities.
- Conduct a design of experiments to understand the relationship between powdered 718 alloy particle size and the resulting mechanical properties at elevated temperatures.
- Understand the effects of variable solids content and polymer molecular weight on the properties of the binder constituents and the subsequent feedstock moulding and debinding characteristics.
- Establish a measure which determines the homogeneity of injection moulding feedstock and understand the effects of incorporating recycled feedstock on the mechanical properties of the powdered 718 alloy.
- Modelling of the injection moulding process to understand mould die filling and solidification dynamics.

- Conduct a design of experiments which focuses specifically on the injection moulding process to understand the effects of the key process variables (including die temperatures) on the resulting structural integrity of green state mouldings.

Mechanical Testing

- Conduct a design of experiments to understand the effects of test piece surface finish on the mechanical properties of fully heat treated 718 alloy.
- Conduct a design of experiments to understand the relationship between powder particle size and resulting mechanical properties obtained from fully machined 718 alloy test pieces.
- Obtain mechanical test data from elevated temperature test pieces which are designed to incorporate an integral ‘shoulder’ from which the true extension can be measured and correlate the test results with non-contact methods of measurement.
- Conduct comparative aerofoil fatigue testing. The components manufactured from powdered 718 alloy could be compared to wrought 718 alloy component data in both 1^{st} flexural and 1^{st} torsional modes. Compare and contrast fatigue crack initiation and propagation modes.
- Understand the effects of dimensional and alignment influences on testing ‘as sintered’ mechanical test pieces.
- Conduct a ‘round robin’ comparison of mechanical test results obtained from aerospace and other testing standards to understand the variation in key mechanical test properties.
- Understand the effects on Small Punch Creep and Small Punch Tensile results from test discs removed from varying sample orientations and also varying sample thicknesses.

Examination Techniques

- Dark field Transmission Electron Microscope (TEM) analysis of injection moulded and fully heat treated 718 alloy in order to assess the volume fraction, morphology and distribution of the principal strengthening mechanism Ni_3Nb (gamma double prime).
- Understand the formation of undesirable products such a ‘Laves phase’ and confirm the absence of the phase in the microstructure of sintered and heat treated injection moulded 718 alloy.

Miscellaneous

- Understand the dimensional variability over a typical batch quantity of components. Relate the initial sectional thickness to the final fully heat treated dimensions.
- Understand the effects of variations in test piece sectional thicknesses on the resulting residual stress of fully processed test components.
- Establish a correlation between the test results obtained from conventional testing methods to the test results obtained from Small Punch Tensile and Small Punch Creep data specific to 718 alloy.

CHAPTER 8

REFERENCE LIST

8. Reference List

8.1 Published Papers

Davies, P.A., Dunstan, G.R., Hayward, A.C. and Howells, R.I.L. (2004). Metal Injection Moulding of Heat Treated Alloy 718 Master Alloy. *European Powder Metallurgy Association, 2004.*

Gulsoy, H.O., Ozbek, S., Gunay, V. and Baykara, T. (2011). Mechanical Properties of Powder Injection Molded Ni-based Superalloys. *Advanced Material Research,* **Volume 278,** page numbers 289-294, 2011.

Johnson, J.L., Tan, L.K., Suri, P. and German, R.M. (2004). Mechanical properties and corrosion resistance of MIM Ni-based Superalloys. *Proceeding of PM2Tec,* page numbers 89-101, 2004.

Ott, E.A. and Peretti, M.W. (2012). Metal Injection Molding of Alloy 718 for Aerospace applications. *JOM (Journal of Materials),* **Volume 64,** No. 2, 2012.

Sidambe, A.T., Derguti, F., Russell, A.D. and Todd, I. (2013). Influence of processing on the properties of IN718 parts produced via Metal Injection Moulding. *Powder Injection Moulding International, 2013.*

Sikorski, S., Kraus, M. and Müller, Dr. C. (2006). Metal Injection Molding for Superalloy jet engine components. *Cost effective manufacture via net-shape processing,* page numbers 9-1 - 9-12, 2006.

8.2 Published Patents

Andrees, G, Kranzeder, J, Kraus, M & Lackermeier, R 2007, *Method for manufacturing components*, US Patent Application Publication 2007/0202000 A1.

Behi, M, Duyckinck, R & Fanelli, A 2001, *Aqueous injection molding binder composition and molding process*, US Patent 6262150 B1.

Benard, J-P, Mengeling, V & Mottin J-P 2012, *Method for manufacturing an assembly including a plurality of blades mounted in a platform*, US Patent Application Publication 2012/0039738 A1.

Bohdal, R 2007, *Method for making gas turbine elements and corresponding element*, US Patent Application Publication 2007/0102572 A1.

Chen, W-H, Jiang, M-J, Lin, C-S, Weng, K-Y, Lai, M-S & Jeng, J-T 1995, *High performance binder/molder compounds for making precision metal part by powder injection molding*, US Patent 5421853.

Ciomek, MA 1991, *Feedstock and process for metal injection molding*, US Patent 5064463.

Duyckinck, RL, Snow, B, Sesny, S & Glandz G 2001, *Continuous compounding of aqueous injection molding feedstocks*, US Patent 6261496 B1.

Ferri, OM & Ebel, T 2011, *Process for producing components of titanium or titanium alloy by means of MIM technology*, US Patent Application Publication 2011/0033334 A1.

Gegal, GA & Ott, EA 2003, *Sinter bonding using a bonding agent*, US Patent 6551551 B1.

James, AW 2009, *Metal injection joining*, US Patent Application Publication 2009/0196761 A1.

Japka, JE 1995, *Carbonyl Iron powder premix composition*, US Patent 5401292.

Kelly, TJ 2006, *Microwave processing of MIM pRef.orms*, US Patent Application Publication 2006/0251536 A1.

Kelly, TJ & Parks, MJ 2007, *Method of making metallic composite foam components*, US Patent Application Publication 2007/0274854 A1.

Kelly, TJ, Meyer, MK, Parks, MJ & Ferrigno, SJ 2008, *Metal injection molding process for bimetallic applications and airfoil*, US Patent Application Publication 2008/0237403 A1.

Machado, R, Ristow Jr, W, Klein, AN, Muzart, JLR, Fredel, MS, Wendhausen, Par, Fusao, P, Alba, PR, da Silva, NFO & Mendes, LA 2007, *Industrial plasma reactor for plasma assisted thermal debinding of powder injection-molded parts*, US Patent Application Publication 2007/0292556 A1.

Nyberg, EA, Weil, KS & Simmons, KL 2005, *Feedstock composition and method of using same for powder metallurgy forming of reactive metals*, US Patent Application Publication 2005/0196312 A1.

Reiter Jr, FB, Beard, BD, Crump, Mw & Stuart TL 2003, *Metal injection molding multiple dissimilar materials to form composite electric machine rotor and rotor sense parts*, US Patent Application Publication 2003/0063993 A1.

Sagawa, M, Watanabe, T & Nagata, H 2002, *Powder compaction method*, US Patent Application Publication 2002/0098106 A1.

Scancarello, MJ 2003, *Powder metal scrolls*, US Patent Application Publication 2003/0138339 A1.

Schmidt, H, Nass, R, Aslan, M, Albayrak, S, Arpac, E, Konig, T & Fister D 1996, *Method for producing metal and ceramic sintered bodies and coatings*, US Patent 5590387.

Seyama, Y, Shimizu, Y & Iijima, S 2001, *Raw material for injection molding*, US Patent Application Publication 2001/0049412 A1.

Sikorski, S, Kraus, M, Hoffman, K & Niedersuss A 2010, *Vane ring, and the method for the production thereof*, US Patent Application Publication 2010/0074740 A1.

Stevenson, JF, Marsh, G, LaSalle, JC & Behi, M 2005, *Recycle methods for water based powder injection molding compounds*, US Patent Application Publication 2005/0046062 A1.

Suzuki, K & Fukushima, T 2001, *Binder for injection molding of metal powder or ceramic powder and molding composition and molding method wherein the same is used*, US Patent 6171360 B1.

Turner, NG 1982, *Products made by powder metallurgy and a method theRef.ore*, US Patent 4329175.

Voice, WE 2011, *Method of producing powder*, US Patent Application Publication 2011/0253815 A1.

Wilkinson, CE 2009, *Binderless metal injection molding apparatus and method*, US Patent Application Publication 2009/0208360 A1.

Yang, X & Petcavick, RJ 1999, *Powder and binder systems for use in metal and ceramic powder injection molding*, US Patent 5977230.

Zedalis, MS, Sherman, BC & LaSalle JC 1999, *Process for debinding and sintering metal injection molded parts made with an aqueous binder*, US Patent 5985208.

8.3 Published Standards and Specifications

AMS2750E, 2012, *Pyrometry*

ARP1917, Rev A, *Clarification of Terms Used in Aerospace Material Specifications*

ASTM E112, 2013, *Standard Test methods for Determining Average Grain Size*

ASTM B311, 2013, *Standard Test method for Density of Powder Metallurgy (PM) Materials Containing Less than two % Porosity*

ASTM E8/E8M, 2013, *Standard Test Methods for Tension Testing of Metallic material*

ASTM B883, 2010, *Standard Specification for Metal Injection Moulding (MIM) Ferrous Materials*

BS1407, 1970, Specification for High Carbon Steel (silver steel) - AMD 2157

BSEN ISO 6892-1, 2010, *Tensile testing- Part 1: Method of test at room temperature*

European CEN Workshop Agreement 15627:2007, *Small Punch Test Methods for Metallic Materials*

ISO 13320-1:1999 *(ISO 13320), 2009, Particle size Analysis - Laser diffraction Methods*

SAE Aerospace, 2009. AMS5662M, *Nickel Alloy, Corrosion and Heat-Resistant, Bars, Forging, and Rings 52.5Ni - 19Cr - 3.0Mo - 5.1Cb (Nb) - 0.90Ti - 0.50 Al - 18Fe. Consumable Electrode or Vacuum Induction Melted 1775 ºF (968 ºC) Solution Heat Treated, Precipitation-Hardenable*

SAE Aerospace, 2011. AMS5917, *Metal Injection Molded Nickel Based Alloy 718 Parts. Hot Isostatically Pressed, Solutioned and Aged*

SAE Aerospace, 2012. AMS2269*, Chemical Check Analysis Limits. Nickel, Nickel Alloys, and Cobalt Alloys*

SAE Aerospace, 2014. AMS2759/3, *Heat Treatment. Precipitation-Hardening Corrosion-Resistant and Managing Steel parts*

8.4 Published Images

Figure 1
http://www.flightglobal.com, accessed 2014

Figure 9
http://www.pharmacopeia.cn/v29240/usp29nf24s0_c429.html, accessed 2014

Figure 10-18
London and Scandanavian Metallurgical Co Ltd (Analytical Services (2011) Certificate Number 1101828

Figure 20-22
http://www.alcula.com/calculators/statistics/standard-deviation/, accessed 2014

Figure 23
http://www.essentialchemicalindustry.org/, accessed 2014

Figure 24-25
https://www.google.co.uk/#q=www.mpbio.com, accessed 2014

Figure 32-33
http://www.trescal.com/,accessed 2014

Figure 41
http://www.spaceflight.esa.int/impress/text/education/Glossary/Glossary_U.html

Figure 42
http://hsc.csu.edu.au/, accessed 2014

Figure 43
http://www.zwick.co.uk/en.html, accessed 2014

Figure 59
http://schools.wikia.com/wiki/Buoyancy_%26_Archimedes'_Principle, accessed 2014

Figure 60
http://www.oertling.com/ accessed 2014

Figure 61
http://hitachi-hta.com/library/low-voltage-transmission-imaging-hitachis-s-4800-fe-sem, accessed 2015

Figure 62-65
http://www.charfac.umn.edu/instruments/eds_on_sem_primer.pdf, accessed 2015

Figure 96
http://microscopegenius.com/, accessed 2015

Figure 97
https://www.google.co.uk/#q=zeiss+uk, accessed 2015

Figure 109
http://www.nde-ed.org, accessed 2015

Figure 113
http://www.instron.com/en-gb?region=United%20Kingdom, accessed 2015

Figure 114
http://www.struers.co.uk/default.asp?top_id=10&doc_id=1321, accessed 2015

Figure 118
http://www.instron.de/wa/home/default_de.aspx, accessed 2015

Figure 119
http://www.jtscorp.jp/product.eng.html, accessed 2015

Figure 122
http://www.spcforexcel.com/, accessed 2015

Figure 128-129
Deformation Process during disc bend loading SD Norris and JD Procter 1966, The Institute of Materials Manuscript

Figure 140
http://www.slideshare.net/Kashif_Hashmi/creep-of-metals, accessed 2015

CHAPTER 9

BIBLIOGRAPHY

9. Bibliography

9.1 Published Papers

Bricknell, R.H. and Woodford, D.A. (1981). The embrittlement of Nickel following high temperature air exposure. *American Society for Metals and the Metallurgical Society of AIME, 1981,* Metallurgical Transactions A, **Volume 12A,** page numbers 425-433, 1981.

Bricknell, R.H. and Woodford, D.A. (1984). Prevention and reversal of oxygen embrittlement in nickel. *Metal Science,* **Volume18**, 1984.

Cao, W-D. and Kennedy, R. (2004). Role of Chemistry in 718-Type alloys - Allvac® 718plus™ alloy development. *TMS (The Minerals, Metals & Material Society), 2004*.

Cao, W-D. and Kennedy, R.L. (2005). Application of direct aging to Allvac® 718plus™ alloy for improved performance. *TMS (The Minerals, Metals and Materials Society), 2005.*

Cihak, U., Stockinger, M., Staron, P., Tockner, J., and Clemens, H. (2005). Characterization of Residual Stesses in Compressor Discs for Aeroengines: Neutron Diffraction and Finite Element simulations. *TMS (The Minerals, Metals and Materials Society), 2005.*

Cone, F.P. (2001). Observations on the development of Delta Phase in IN718 Alloy. *TMS (The Minerals, Metals and Materials Society), 2001.*

Contreras, J.M., Jiménez-Morales, A. and Torralba, J.M. (2010). Influence of particle size distribution and chemical composition of the powder on final properties of Inconel 718 fabricated by Metal Injection Moulding (MIM). *Powder Injection Moulding International,* **Volume 4,** No. 1, page numbers 67-70, 2010.

Couturier, R., Burlet, H., Terzi, S., Guetaz, L. and Raisson, G. (2004). Process development and mechanical properties of Alloy U720LI for high temperature turbine disks. *TMS (The Minerals, Metals and Materials Society), 2004.*

Dahlén, M. and Fischmeister, H. (1980). Carbide Precipitation in Superalloys. *TMS (The Minerals, Metals and Materials Society), 1980.*

Davies, P.A., Dunstan, G.R., Hayward, A.C. and Howells, R.I.L. (2003). Development of Master Alloy powders, including nickel-based Superalloys, for Metal Injection Molding (MIM). *Advances in powder metallurgy and particulate material,* **Volume 8**, 2003: 8-1.

Dempster, I., Cao, W-D., Kennedy, R., Bond, B., Aurrecoecha, J. and Lipschutz, M. (2005). Structure and property comparison of Allvac® 718plus™ alloy and Waspaloy forgings. *TMS (The Minerals, Metals and Materials Society), 2005.*

Dye, D., Roder, B.A., Tin, DS., Rist, M.A., James, J.A. and Daymond, M.R. (2004). Modeling and measurement of residual stresses in a forged IN718 superalloy disc. *TMS (The Minerals, Metals and Materials Society), 2004.*

Gabb, T., Telesman, J., Kantzos, P.T., Bonacuse, P.J., Barrie, R.L. and Hornbach, D.J. (2004). Stress relaxation in powder metallurgy superalloy disks. *TMS Letters* **Volume 1** (Issue 5 - Processing, Microstructure and Properties of Powder-based Materials), Page numbers 115 and 116, 2004.

Gabb, T. (2012). Advances in Superalloys. *JOM (Journal of Materials),* **Volume 64,** No 2, 2012.

Garat, V., Cloue, J-M., Viguier, B. and Andrieu, E. (2005). Influence of Portevin-Le Chatelier effect on rupture mode of Alloy 718 specimens. *TMS (The Minerals, Metals and Materials Society), 2005.*

Gayda, J., Gabb, T.P. and Kantzos, P.T. (2004). The effect of dual microstructure heat treatment on an advanced nickel-base disk alloy. *TMS (The Minerals, Metals and Materials Society), 2004.*

Gu, Y.F., Cui, C., Harada, H., Fukado, T., Ping, D., Mitsuhashi, A., Kato, K., Kobayashi, T. and FGujioka, J. (2008). Development of Ni-Co base alloys for high temperature disk application. *TMS (The Minerals, Metals and Materials Society), 2008.*

Guest, R.P. and Tin, S. (2005). The dynamic and metadynamic recrystallization of IN 718. *TMS (The Minerals, Metals and Materials Society), 2005.*

Hamill, J., Schade, C. and Myers, N. (2001). Water atomized fine powder treatment. *Powder Metallurgy Science Technology Briefs,* **Volume 3** (no. 3), page numbers 10-13, 2001.

Holt, R.T. and Wallace, W. (1976). Impurities and trace elements in nickel-base superalloys. *International Metals Reviews* March 1976, **Review 203.**

Horvath, W., Zechner, W., Tockner, J., Berchthaler, M., Weber, G. and Werner, E.A. (2001). The effectiveness of direct aging on Inconel 718 forgings produced at high strain rates as obtained on a screw press. *TMS (The Minerals, Metals and Materials Society), 2001.*

Hu, J.P., Zhuang, J.Y., Zhong, Z.Y., Janchek, P. and Kramer, J. (2001). Study on constitutive equation of Alloy IN718 in hammer forging process. *TMS (The Minerals, Metals and Materials Society), 2001.*

Huron, E. (2012). Practical applications of modelling to be highlighted at Superalloys 2012. *Superalloys 2012,* **Volume 63,** No. 8.

Huron, E.S., Bain, K.R., Mourer, D.P., Schirra, J.J., Reynolds, P.L. and Montero, E.E. (2004). The influence of grain boundary elements on properties and microstructures of P/M Nickel base superalloys. *TMS (The Minerals, Metals and Materials Society), 2004.*

Huron, E.S., Bain, K.R., Mourer, D.P. and Gabb, T. (2008). Development of high temperature capability P/M disk superalloys. *TMS (The Minerals, Metals and Materials Society), 2008.*

Ibrahim, R., Azmirruddin, M., Jabir, M., Johari, N., Muhamad, M. and Talib, A.R.A. (2012). Injection Molding of Inconel 718 parts for Aerospace application using novel binder system based on palm oil derivatives. *World Academy of Science, Engineering and Technology 70, 2012.*

Jaeger, J de., Solas, D., Baudin, T., Fandeur, O., Schmitt, J-H. and Rey, C. (2012). Inconel 718 single and multipass modelling of hot forging. *TMS (The Minerals, Metals and Materials Society), 2012.*

Jena, A.K. and Chaturvedi, M.C. (1984). The role of alloying elements in the design of Nickel-base superalloys. *Journal of Materials Science 19*, pages numbers 3121-3139, 1984.

Jeniski, Jr., R.A. and Kennedy, R.L. (2006). *Stress, 807 (13), 15, 2006.*

Jillavenkatesa, A., Dapkunas, S.J. and Lum, L-H.H. (2001) NIST recommended practice guide. Particle Size and Characterization. *NIST (National Institute of Standards and Technology) Special Publication 960-1 (2001).*

Kennedy, R.L. (2005). Allvac ® 718plus™, superalloy for the next forty years. *TMS (The Minerals, Metals and Materials Society), 2005.*

Krempaszky, C., Werner, E.A. and Stockinger, M. (2005). Residual stress in IN718 turbine disks. *TMS (The Minerals, Metals and Materials Society), 2005.*

Krook, M., Recina, V. and Karlsson, B. (2005). Material properties affecting the machinability of Inconel 718. *TMS (The Minerals, Metals and Materials Society), 2005.*

Li, Y., Jiang, F., Zhao, L. and Huang, B. (2003). Critical thickness in binder removal process for injection molded compacts. *Materials Science and Engineering A 362,* page numbers 292-299, 2003.

Lindsley, B and Pierron, X. (2000). Sub-solvus recrystallization mechanisms in Udimet® Alloy 720LI. *TMS (The Minerals, Metals and Materials Society), 2000.*

Mannan, S, Hibner, E and Puckett, B 2012, *Physical Metallurgy of Alloys 718, 725, 725HS, 925 for service in aggressive corrosive environments,* US Patent Application 13/492951.

Menzies, R.G., Bricknell, R.H. and Craven, A.J. (1980). STEM microanalysis or precipitates and their nuclei in a nickel-base superalloy. *Philosophical Magazine A,* **41:4,** pages 493-508.

Mitchell, A. (2005). The precipitation of primary carbides in IN718 and its relation to solidification conditions. *TMS (The Minerals, Metals and Materials Society), 2005.*

Mitchell, A. and Wang, T. (2001). Solidification and precipitation in IN718. *TMS (The Minerals, Metals and Materials Society), 2001.*

Nakagawa, Y. (2004). Aero-engine business and material technologies in Japan. *TMS (The Minerals, Metals and Materials Society), 2004.*

Nathal, M.V. (2008). Nasa and superalloys: A customer, a participant, and a Referee. *TMS (The Minerals, Metals and Materials Society), 2008.*

Okada, I., Torigoe, T., Takahashi, K. and Izutsu, D. (2004). Development of Ni base superalloy for industrial gas turbine. *TMS (The Minerals, Metals and Materials Society), 2004.*

Ozgun, O., Gulsoy, H.O., Yilmaz, R. and Findik, F. (2013). Microstructural and mechanical characterization of injection molded 718 superalloy powders. Journal of Alloys and Compounds 576, page numbers 140-153, 2013.

Paulonis, D.F. and Schirra, J.J. (2001). Alloy 718 at Pratt & Whitney - Historical perspective and future challenges. *TMS (The Minerals, Metals and Materials Society), 2001.*

Qiu, C., Wu, X., Mei, J., Andrews, P. and Voice, W. (2013). Influence of heat treatment on microstructure and tensile behaviour of a hot isostatically pressed nickel-based superalloy. *Journal of Alloys and compounds,* 2013*.*

Radaick, J.F. and Carneiro, T. (2005). A microstructural study of Alloy 718plus™. *TMS (The Minerals, Metals and Materials Society), 2005.*

Rao, G.A., Kumar, M., Srinivas, M. and Sarma, D.S. (2003). Effect of standard heat treatment on the microstructure and mechanical properties of hot isostatically pressed superalloy Inconel 718. *Materials Science and Engineering A 355,* page numbers 114-125, 2003.

Rao, G.A., Srinivas, M. and Sarma, D.S. (2004). Effect of thermo-mechanical working on the microstructure and mechanical properties of hot isostatically pressed superalloy Inconel 718. *Materials Science and Engineering A 383,* page numbers 201-212, 2004.

Rao, G.A., Srinivas, M. and Sarma, D.S. (2006). Influence of modified processing on structure and properties of hot isostatically pressed superalloy Inconel 718. *Materials Science and Engineering A 418,* page numbers 282-291, 2006.

Rao, G.A., Srinivas, M. and Sarma, D.S. (2006). Effect of Oxygen content of powder on microstructure and mechanical properties of hot isostatically pressed superalloy Inconel 718. *Materials Science and Engineering A435-436,* page numbers 84-99, 2006.

Schafrik, R.E., Ward, D.D. and Groh, J.R. (2001). Application of Alloy 718 in GE aircraft engines: past, present and next five years. *TMS (The Minerals, Metals and Materials Society), 2001.*

Schafrik, R.E. and Walston, S. (2008). Challenges for high temperature materials in the new millennium. *TMS (The Minerals, Metals and Materials Society), 2008.*

Semiatin, S.L. and Bieler, T.R. (1999). Microstructural evolution during the hot working of superalloys. *1999 JOM (Journal of Materials).*

Seth, G.B. (2000). Superalloys - The utility gas turbine perspective. *TMS (The Minerals, Metals and Materials Society), 2000.*

Sjoberg, G., Antonsson, T., Azadian, S., Warren, R. and Fredriksson, H. (2005). Effect of δ-phase on the weldability and the hot ductility of Alloy 718. *TMS (The Minerals, Metals and Materials Society), 2005.*

Song, K. and Aindow, M. (2008). Grain growth and particle pinning in a model Ni-based superalloy. *Materials Science and Engineering* A 479 (2008), pages 365-372.

Stockinger, M. and Tockner, J. (2005). Optimizing the forging of critical aircraft parts by the use of finite element coupled microstructure modelling. *TMS (The Minerals, Metals and Materials Society), 2005.*

Thomas, J-P., Bauchet, E., Dumont, C. and Montheillet, F. (2004). EBSD investigation and modelling of the microstructural evolutions of Superalloy 718 during hot deformation. *TMS (The Minerals, Metals and Materials Society), 2004.*

Tien, J.K. and Nardone, V.C. (1984). The U.S. Superalloys Industry - status and outlook. *Journal of Metals,* September 1984.

Uginet, J.F. and Jackson, J.J. (2005). Alloy 718 forging development for large land-based gas turbines. *TMS (The Minerals, Metals and Materials Society), 2005.*

Woodford, D.A. and Bricknell, R.H. (1980). The effect of high temperature air exposure on the stress rupture life of Nickel and Cobalt base superalloys. *TMS (The Minerals, Metals and Materials Society), 1980.*

Woodford, D.A. and Bricknell, R.H. (1981). Grain boundary penetration of Oxygen in Nickel and the effect of Boron additions. *American Society for Metals and the Metallurgical Society of AIME, Metallurigical Transactions A,* **Volume 12A,** page numbers 1467-1475, 1981.

Xie, X., Dong, J., Wang, G. and You, W. (2005). The effect of NB, TI, AL on precipitation and stre ngthening behaviour of 718 type Superalloys. *TMS (The Minerals, Metals and Materials Society), 2005.*

Xie, X.,Wang, G., Dong, J., Xu, C., Cao, W-D. and Kennedy, R. (2005). Structure stability study of a newly developed Nickel-based superally - Allvac® 718plus™. *TMS (The Minerals, Metals and Materials Society), 2005.*

Xie, X., Xu, C., Wang, G., Dong, J., Cao, W-D. and Kennedy, R. (2005). TTT diagram of a newly developed Nickel-base superalloy - Allvac® 718plus™. *TMS (The Minerals, Metals and Materials Society), 2005.*

Youhua, H., Yimin, L., Hay, H., Jia, L. and Xiao, T. (2010). Preparation and mechanical properties of IUnconel 718 Alloy by Metal Injection Molding. *Rare Metal Materials and Engineering,* **Volume 39,** Issue 5, May 2010.

Zielińska, M., Tavorska, M., Poręba, M. and Sieniawski, J. (2010). Thermal properties of case nickel based superalloys. *Archives of Materials Science and Engineering* **Volume 44**, Issue 1, July 2010, pages 35-38.

9.2 Published Patents

Achikita, M & Ohtsuka, A 1992, *Compound for an injection molding*, US Patent 5080714.

Allen, JK & Brasel, GM 1998, *Molding process feedstock using a copper triflate catalyst*, US Patent 5840785.

Allroth, S, Engström, U & Bergman, O 2011, *A powder metallurgical composition and sintered component,* European Patent Application EP 2511031 A1.

Allroth, S & Bergman, O 2015, *A method for producing a sintered component,* World Intellectual Property Organization WO 2015/091366 A1.

Angus, JP 1989, *Method of making an integral bladed member*, US Patent 4826645.

Arai, T, Makino, I, Mimura, E & Kayano, H 2002, *Method of fabricating metal composite compact*, US Patent 6488887 B1.

Bayer, M & Nagl, I 1993, *Molding composition for the production of inorganic sintered products*, US Patent 5254613.

Barros, EL & Andreotti, ER 1999, *Method of forming cavities in ceramic or metal injection molded parts using a fugitive core*, US Patent 5972269.

Bartone, KJ & Das, SK 2003, *Densified sintered powder and method*, US Patent Application Publication 2003/0110887 A1.

Baum, LW & Wright M 1999, *Composition and process for metal injection molding*, US Patent 5993507.

Behi, M, Zedalis, M & Schoonover, JM 2000, *Rapid manufacture of metal and ceramic tooling*, US Patent 6056915.

Behi, M, LaSalle, JC & Glandz, A 2001, *Stable aqueous iron based feedstock formulation for injection molding*, US Patent 6261336 B1.

Benar, Z-P, Menzhelin, V & Motten, Z-B 2014, *Manufacturing method of system containing many blades installed in platform,* Russian Federation for Intellectual Property RU 2532783 C2.

Bihr, J-C & Bezin M 2004, *Making multi-component objects using metal injection moulding*, UK Patent Application GB2394724A.

Bloemacher, M, Weinand, D, Wohlfromm, H & ter Maat, JHH 2003, *Binding agent for inorganic material powders for producing metallic and ceramic moulded bodies*, US Patent Application Publication 2003/0091456 A1.

Boechat, J-M 2002, *Injection mouding tool and method for production thereof*, US Patent Application Publication 2002/0109260 A1.

Cartier, D 2014, *Binder for injection moulding composition,* World Intellectual Property Organization WO 2014/191304 A1.

Chung, CI & Cao MY 1997, *Solid polymer solution binders for shaping of finely-divided inert particles*, US Patent 5665289.

Czerwinski, F 2009, *Metal-molding conduit assembly of metal-molding system*, US Patent Application Publication 2009/0107646 A1.

Dasilva, PA & Kelly, TJ 2007, *MIM method for coating turbine shroud*, US Patent Application Publication 2007/0107216 A1.

Date, K, Kubo, Y & Morimoto, Y 2001, *Sintered Ti-system material product derived from injection molding of powder material and producing method thereof*, US Patent 6306196 B1.

Diaconu, V 2008, *Conduit connection of molding system*, US Patent Application Publication 2008/0199557 A1.

Durocher, E & Lefebvre, G 2013, *Gas turbine engine bosses,* Canadian Patent Application CA 2806365 A1.

Durocher E & Lefebvre, G 2014, *Turbine shroud segment with integrated impingement plate,* US Patent 8784037 B2.

Durocher E & Lefebvre, G 2014, *Turbine shroud segment,* US Patent 8784044 B2.

Durocher E & Lefebvre, G 2015, *Manufacturing of turbine shroud segment with internal cooling passages,* US Patent 9028744 B2.

Dwivedi, RK 2004, *Microporous metal parts*, US Patent Application Publication US 2004/0250653 A1.

Hayashi, J & Sakata, M 2002, *Metal sintered body and production method thereof*, US Patent 6428595 B1.

Hens, KF & Grohowski Jr, JA 1997, *Powder and binder systems for use in powder molding*, US Patent 5641920.

Hesse, W & Bittler, K 1999, *Process for producing granular material and shaped parts from hard metal materials or cermet material*, US Patent 5860055.

Hosamani, L, Endo, K, Meschke, A, Harmon, D, Encinia, S, Davenport, J & Sokol Jr, E 2006, *Method and composition for making a wire*, US Patent Application Publication 2006/0018780 A1.

Hullman, H-D, Schaer, U, Schuermaan, L & Wulf, B 2001, *Method for the production of an intermediate product which can be injection molded*, US Patent 6234660 B1.

Hwang, K-S & Lu, Y-C 2005, *Method for making sintered body with metal powder and sintered body prepared theRef.rom*, US Patent Application Publication 2005/0274222 A1.

Hwang, K-S & Chuand, K-H 2012, *Alloy steel powder and it's sintering body,* Deutsches Patent DE 10 2010 060 487 A1.

James, AW & Arrell, DJ 2010, *Injection molded component*, US Patent Application Publication 2010/0028163 A1.

Johnson, KP 1988, *Process for fabricating parts from particulate material*, US Patent 4765950.

Kankawa, Y 2000, *Metal powder injection moldable composition, and injection molding and sintering method using such composition*, US Patent 6051184.

Kasugai, SI & Mizuno, T 1988, *Method for producing ceramic parts*, US Patent 4783297.

Kawamoto, K & Osanaga, T 1994, *Moldable composition, process for producing sintered body theRef.rom and products from same*, US Patent 5280086.

Kelly, TJ 2006, *Preparation of filler-metal weld rod by injection molding of powder*, US Patent Application Publication 2006/0024190 A1.

Kinoshita, H Shiraiwa, T Uraoka, H & Ochiai, N 2000, *Powdered metal injection compacting composition*, US Patent 6159265.

Kruefer, DC 1996, *Process for improving the debinding rate of ceramic and metal injection molded products*, US Patent 5531958.

Larsson, A 2013, *Iron based powders for powder injection molding,* Canadian Patent Application CA2823267 A1.

LaSalle, JC & Sherman, BC 1999, *Net shape hastelloy X made by metal injection molding using an aqueous binder*, US Patent 5989493.

LaSalle, JC & Sherman, BC 2001, *Co-sintering of similar materials*, US Patent 6322746 B1.

Lavoie, LE, Moore, JC & Walker, DL 2009, *Metal injection molding methods and feedstocks*, US Patent Application Publication 2009/0129961 A1.

Liu, J & Ryneson ML 2004, *Blended powder solid-supersolidus liquid phase sintering*, US Patent Application Publication 2004/0009089 A1.

Liu, J 2007, *Processes for sintering aluminium and aluminium alloy components*, US Patent Application Publication 2007/0110608 A1.

Lu, J-WJ, Bartone, KJ, Olson, DM, Benson, DM & Tervo, JN 2002, *Sintering process and tools for use* in *metal injection molding of large parts*, US Patent Application Publication 2002/0168282 A1.

Lu, J-WJ, Bye, RL, Tervo, JN & LaSalle, JC 2007, *Advanced sintering process and tools for use in metal injection molding of large parts*, US Patent Application Publication 2007/0003426 A1.

Ludwig, DC 1991, *Composition suitable for injection molding or metal alloy, or metal carbide powders*, US Patent 5015294.

McCullough, KA 2008, *Screw design and method for metal injection molding*, US Patent Application Publication 2008/0217817 A1.

Meendering, DN, Malhotra, D, & Baltich, LK 1994, *Conditioning Metal Powder for Injection Moulding*, US Patent 5314658.

Meier, R, Mueller, C, Prieschl, F & Sikorski, S 2009, *Method for the production of a sealing segment, and sealing segment to be used in compressor and turbine components*, US Patent Application Publication 2009/0041607 A1.

Meier, R 2009, *Method for production of a honeycomb seal*, US Patent Application Publication 2009/0096138 A1.

Menke, K, Merz, L & Helfrich, M 1992, *Binder for metal or ceramic powder*, US Patent 5098942.

Milagres Ferri, O & Ebel, T 2012, *Method for producing components from titanium or titanium alloy using MIM technology,* European Patent EP 2292806 B1.

Nelles, H, Bader, V, Buchkremer, H-P, Ahmad-Khanlou, AM, Bram, M & Stover, D 2004, *Production of component parts by metal injection moulding (MIM)*, US Patent application Publication 2004/0146424 A1.

Nishimura, K & Yoshino, K 1995, *Binder system for use in the injection molding of sinterable powders and molding compound containing the binder system*, US Patent 5380179.

Noro, Y & Adachi, J 1999, *Sintered metal mould and method for producing the same*, US Patent 5997603.

Odenevall Wallinder, I, Hedberd, Y & Szakalos, P 2012, *Method of manufacturing a powder product, and use thereof,* World Intellectual Property Organization WO 2012/125113 A1.

Ono, H, Saitoh, K, Yagami, H, Saiki, T & Masuda, Y 1991, *Polyamide base binder for use in metal powder injection molding process*, US Patent 5002988.

Ott, EA, Woodfield, AP & Shamblen, CE 2004, *Production of injection-molded metallic articles using chemically reduced nonmetallic precursor compounds*, US Patent Application Publication 2004/0120841 A1.

Peiris, DDH & Zhang, JG 1995, *Injection-moldable metal feedstock and method of forming metal injection-molded article*, US Patent 5397531.

Rao, K, Grainger, L, Deane, J, Clifford, J & Mellor, I 2014, *Production of powder for powder metallurgy,* World Intellectual Property Organization WO 2014/068267.

Roth-Fagaraseanu, D & Schult, A 2012, *A method for near net shape manufacturing,* Deutsches Patent DE 10 2010 061 960 A1.

Roth-Fagaraseanu, D & Schrüfer, L 2013, *A method for producing a component by metal powder injection,* Deutsches Patent DE 10 2011 089 260 A1.

Saitoh, K & Hanamura, T 1992, *Metal binder and molding compositions*, US Patent 5159007.

Sakata, M & Shimodaira, K 2002, *Process for producing sintered product*, US Patent 6350407 B1.

Schofalvi, K-H, Hammond, DL & Philipp, WH 2003, *Binder system and method for particulate* material *cross-Ref.erence to related application*, US Patent Application Publication 2003/0220424 A1.

Scholl, R, Waag, U & Eiling, A 2010, *Metallic powder mixtures*, US Patent Application Publication 2010/0003157 A1.

Schoonover, J, Snow, B & Zedalis, MS 2001, *Low pressure injection molding of metal and ceramic threaded components*, US Patent 6328918 B1.

Schult, A & Roth-Fagaraseanu, D 2012, *A method for the production of engine components with geometrically complex structure,* Deutsches Patent DE 10 2010 061 958 A1.

Soda, Y & Aihara, M 2006, *Alloy steel powder for metal injection molding improved in sintering characteristics and sintered article*, US Patent Application Publication 2006/0162494 A1.

Sterzel, H-J 2000, *Injection-molding compositions containing metal oxides for the production of metal moldings*, US Patent 6080808.

Takayama, T, Miyake, M, Ohyama, Y, Saito, K & Ono, H 1997, *Binder for use in metal powder injection molding and debinding method for the use of the same*, US Patent 5627258.

Tanaka, S 2005, *Manufacturing method of a sintered powder molded body*, US Patent Application Publication 2005/0112016 A1.

Toda, T & Tsuda, M 1991, *Method of preparing a metal body by means of injection molding*, US Patent 5015289.

Truebenback, P 1997, *Production of sintered moldings*, US Patent 5611978.

Turenne, S & Mongeon P-E 1995, *Method of producing elements from powders*,US Patent 5445788.

Urevick, DJ 2010, *Method of producing composite materials through metal injection molding*, US Patent Application Publication 2010/0111745 A1.

Wiech Jr, RE 1987, *Method for rapidly removing binder from a green body*, US Patent 4661315.

Wohlfromm, H, Felder, R, ter Maat, JHH & Blomacher, M 2006, *Metal powder injection molding material and metal powder injection molding method*, US Patent Application Publication 2006/0099103 A1.

Yoshihiko, S & Tsutomu, I 1992, *Process for production of sintered body*, European Patent Application 0503966 A2.

Zedalis, MS, Duyckinck, R, Snow, B, Fanelli, A & Burlew, JV 2000, *Process for making stainless steel aqueous molding composition*, US Patent 6126873.

CHAPTER 10

APPENDIX

10. Appendix

Appendix 1

THE CHARACTERISATION OF CREEP PROPERTIES OF ADVANCED MANUFACTURED COMPONENTS THROUGH SMALL PUNCH TESTING

R. Banik, R.J. Lancaster, ***R.C. Hurst, M.R. Bache***[1]
[1] *Institute of Structural Materials, College of Engineering, Swansea University, United Kingdom*

G. Baxter[2]
[2] *Rolls-Royce plc., P.O. Box 31, Derby, DE24 8BJ, United Kingdom*

A.D. Russell[3],
[3] *Rolls-Royce plc., Inchinnan, Scotland, United Kingdom*